AD-A039 696 AIR FORCE INST OF TECH WRIGHT-PATTERSON AFB OHIO SCH--ETC F/G 20/5
MODEL FOR PREDICTING LASER SPECKLE PATTERNS RESULTING FROM ROUG--ETC(U)
MAR 77 W E LANDIS

UNCLASSIFIED AFIT/GEO/EE/77-1 NL

1 OF 3
AD A039696

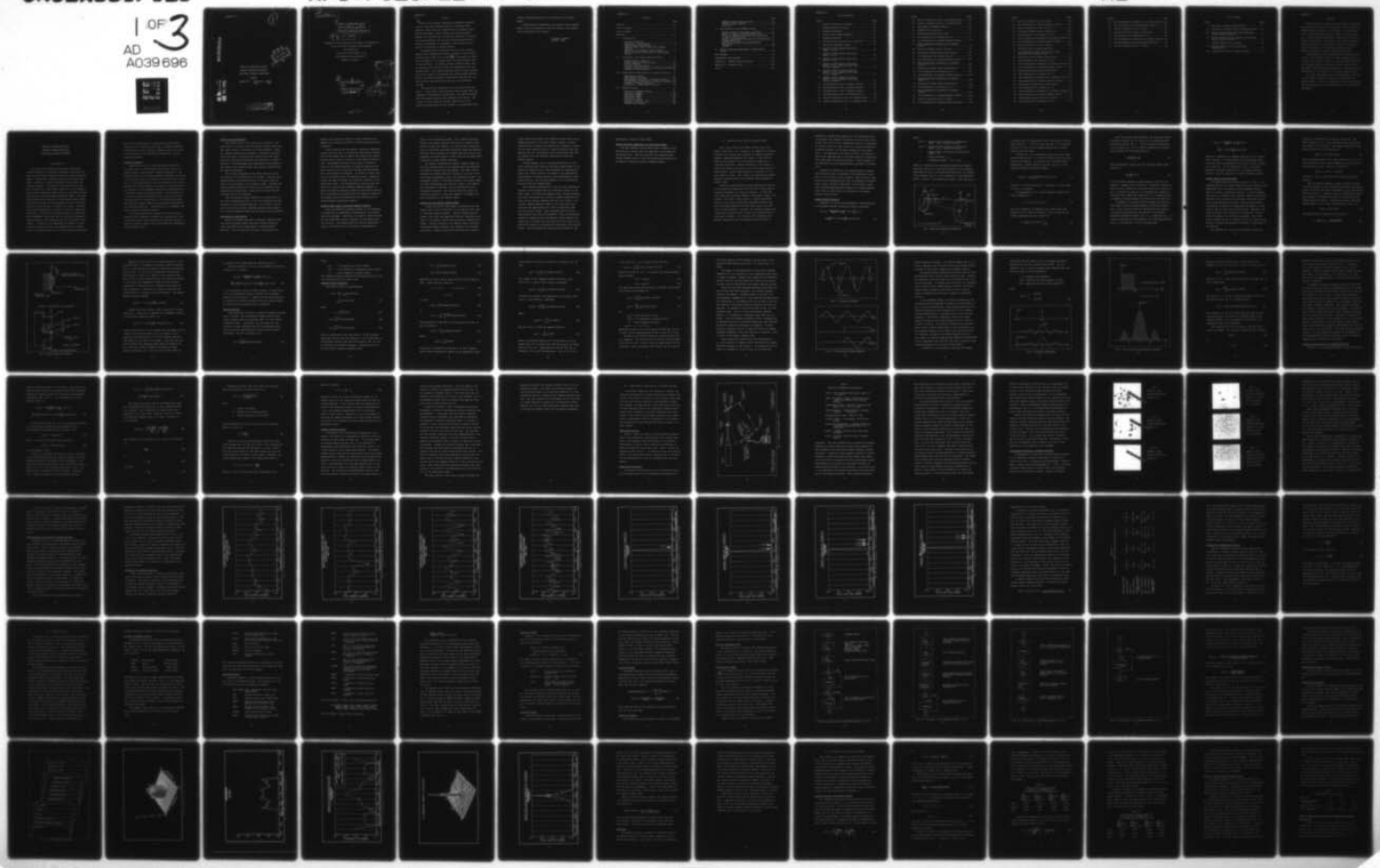


OF
3
9696

GEO/EE/77-1

(1)

B.S.

MODEL FOR PREDICTING LASER SPECKLE PATTERNS RESULTING FROM ROUGH SURFACE SCATTERING

THESIS

GEO/EE/77-1 William E. Landis
Capt. USAF

(14) AFIT/GEO/EE/77-1

(6) MODEL FOR PREDICTING LASER SPECKLE PATTERNS RESULTING FROM ROUGH SURFACE SCATTERING

(9) Master's THESIS

Presented to the Faculty of the School of Engineering

of the Air Force Institute of Technology

Air University

in Partial Fulfillment of the

Requirements for the Degree of

Master of Science

(10) by

William E. Landis B.S.

Capt. USAF

Graduate Electro-Optics

(11) March 1977

(12) 201 P.

012225

B

Preface

The Air Force Weapons Laboratory (AFWL/ALO) expressed a need to know what characteristics of reflected laser radiation could effect the operation of the Adaptive Laser Optical Techniques (ALOT) tracking and pointing system. Because the radiation that is used for tracking is reflected from rough surfaces, the far field intensity pattern has a complex distribution of irradiance. This complex distribution of irradiance is called speckle.

A computer model to calculate and plot laser speckle patterns was developed and tested. Because a rough surface scatters laser light in all directions, predicting the amplitude and phase of the electric field of the scattered light is very difficult. A complex aperture function model, used to describe this electric field, was incorporated into the speckle model. This complex aperture function model enables the user to input to the program the surface height measurements, the surface reflection coefficient distribution, and the incident laser radiation profile at the scattering surface.

The program was developed to run on the CDC 6600 computer. It was tested with simulated surface height data and compared to experimental observations. The results obtained from the program compared very favorably with theory. The results of this thesis and further application of the speckle program should be very valuable in understanding the

effects of speckle patterns on the operation of the ALOT system.

I appreciate the counseling of my advisor, Major Richard Potter, and the assistance of my wife, Karen, in the preparation and typing of this report.

William E. Landis
Captain, USAF

Contents

List of Figures

List of Tables

Abstract

Speckle patterns produced by laser radiation scattering from rough surfaces can be calculated and plotted using the SPECKLE program developed in this report. The scattering surface characteristics that are required by the program are; surface height measurements, surface reflection coefficient distribution, and incident laser radiation profile. These three inputs are required to calculate the complex aperture function at the scattering surface, which is Fourier transformed to produce the speckle pattern.

Through experimental investigation and program verification it was determined that the typical speckle width in a pattern is directly related to range and laser wavelength, and inversely related to scattering surface cross section. The highest spatial frequency present in a speckle pattern is proportional to the inverse of the typical speckle width.

The report also showed that the randomness of the scattering surface reflection coefficient also effects the speckle pattern. This is an important concept in camouflage and very important in the investigation of the ALOT system performance.

MODEL FOR PREDICTING LASER SPECKLE PATTERNS RESULTING FROM ROUGH SURFACE SCATTERING

I. Introduction

The design of an optimum laser weapon system must include provisions for pointing, focusing, and holding the laser beam on target accurately enough to provide sufficient damage. Conventional tracking and pointing systems using radar, infrared, or visual techniques do not provide the required accuracy. A concept for fine pointing and automatic focusing of a laser beam, referred to as the Adaptive Laser Optical Techniques (ALOT) system, is now being investigated at the Air Force Weapons Laboratory (AWFL). The ALOT system measures the intensity of the reflected laser radiation from the target and then generates a set of corrective pointing control signals to maximize the return. The ALOT system has performed well throughout a series of laboratory experiments. However, the experiments were run under near ideal atmospheric conditions, and the effects of absorption thermal blooming, and turbulence were not rigorously investigated. In addition, the phenomenon of speckle, a result of rough surface reflection, was observed but its overall effect on the ALOT system was not theoretically investigated.

The goal of this thesis is to investigate rough surface scattering of a reflected laser beam, excluding atmospheric deteriorations, and to develop a computer model that calculates and plots a far field speckle pattern for a given reflecting surface.

Origins of Speckle

Operation of the first continuous wave helium neon (CW HeNe) laser in 1960 revealed that objects viewed in a highly coherent light acquire a speckled appearance. The physical origin of the observed speckle phenomenon was quickly recognized by the early workers in the laser field (Ref.1; Ref.2). When monochromatic light is reflected from a rough surface the optical wavefront resulting at a distant point is the summation of many dephased wavefronts, each produced by a different surface scattering element. The distances traveled by the numerous wavefronts from a point on the scattering surface to a unique point in the observation plane, may differ by several integer and noninteger wavelengths of the reflected radiation. Interference of the dephased wavefronts produce the speckle pattern.

The random interference phenomenon of laser speckle parallels other branches of physics and engineering. Some of the more modern direct analogies are coherent imagery in synthetic aperture radar (Ref.3), and radio wave propagation (Ref.4:188-267, Ref.5).

Theoretical Investigation

The overall goal of this thesis was to develop a computer model to calculate and plot speckle patterns resulting when laser energy is reflected from rough surfaces. Before the computer program was developed, an extensive literature search was made to determine what theories have been hypothesized and developed concerning the prediction of speckle patterns. The bibliography and supplemental bibliography of this thesis lists numerous books and articles concerned with the speckle phenomenon.

The initial paragraphs of the theory section outline the history of the investigation of speckle. The well known Huygens-Fresnel diffraction formula is the basic equation used in the development of the computer model. Although the Huygens-Fresnel diffraction formula can be formulated from experimental observations, it can also be derived from the classical scalar wave equation.

From the Huygens-Fresnel equation it is shown that the far field diffraction pattern is the two dimensional Fourier transform of the scattering aperture. As a review, the last part of the theory section discusses discrete data processing, including sampling theory and the fast Fourier transform.

Experimental Investigation

Before any attempt was made to develop a computer model that would calculate speckle patterns, several laboratory laser experiments were accomplished to observe speckle patterns. The two properties that were investigated were

speckle size variations related to range variations and speckle size variations related to reflecting aperture size variations.

Direct observations and computer analysis of photomultiplier data were used to analyze the experimental results. The initial method used to observe and analyze the speckle patterns was to record a portion of each speckle pattern on film. Photographs provided an easy means of observing trends in the speckle patterns as range and aperture size were varied, but for statistical analysis the photographs were a poor medium of recording. To provide a higher resolution of contrast across the speckle pattern, a photomultiplier was used to measure the reflected intensity at the observation plane. The photomultiplier data was then analyzed, by a fast Fourier transform computer program, to obtain the spatial frequency content of the speckle pattern. This transformed data provided the best method of observing the speckle pattern characteristics as predicted by the Huygens-Fresnel diffraction formula.

Computer Model Used to Calculate Speckle Patterns

After an extensive literature search on the phenomenon of speckle and an experimental investigation, the computer model was developed. Basically, the computer model performs the two dimensional Fourier transform of the complex aperture function. The complex aperture function describes, in detail, the reflected field distribution immediately in

front of the reflecting surface. For a smooth reflection surface, the complex aperture function is a constant value across the aperture, however, for rough surface reflection there are amplitude and phase variations across the aperture. The model used to predict the complex aperture function was suggested by Goodman (Ref.6) in his study of the statistical properties of laser speckle patterns.

The chapter describing the speckle computer model details the formats used for the computer data and describes the possible outputs from the program. The input used to calculate the complex aperture function is an array of surface height measurements across the scattering surface. To accurately describe a scattering surface, an enormous number of height measurements are required, however, the computer core available to calculate the two dimensional Fourier transform is limited. This limited core size, which restricts the number of input data samples, is probably the major deficiency in the computer model.

Analysis of the Speckle Computer Model

A major portion of this thesis is devoted to the procedure used in the verification of the computer model used to calculate speckle patterns. Various complex aperture shapes, with known two dimensional Fourier transforms, were input to the speckle program and the results compared with theory. Without exception, the computer model calculated and plotted speckle patterns that compared very favorably with theory. When the apertures were modeled as randomly

rough reflecting surfaces, the speckle patterns could not be compared directly to the known results, however, several characteristic features were observed and compared to theory. The two major characteristics of speckle patterns that were observed and used for computer model verification were typical speckle size and intensity distribution across the speckle pattern.

Average speckle size is directly proportional to the laser wavelength and range and inversely proportional to the reflecting aperture size. This phenomenon is predicted by theory (see theory section), was shown in the experimental investigation of speckle patterns (see experimental investigation section), and was also observed in the calculations and plots from the speckle model.

The intensity distribution in the far field diffraction pattern is very complex when the reflecting surface is randomly rough. To verify the computer model, speckle patterns were first calculated for a series of smooth reflecting surfaces and the results compared very well with theory. For a square complex aperture function, the first minor lobe amplitude was approximately one order of magnitude lower than the central maxima. Each succeeding minor lobe was significantly less than the preceeding. When the scattering surface is randomly rough, the speckle pattern appears as a random array of bright and dark spots and minor lobes of the diffraction pattern can approach the amplitude of the central maxima. This phenomenon was observed and presented in the

experimental section of this thesis.

Thesis Conclusion Applicable to ALOT System Design

The last chapter of this thesis gives a summary of the thesis project results that are applicable to the ALOT system design study. The two areas that are summarized are average speckle size in a far field diffraction pattern and the spatial frequencies within a speckle pattern.

II. Diffraction and Fourier Analysis Theory

Laser light differs from common radiant light (sun, candle, light bulb, etc.) because it is composed of a single frequency and displays both temporal and spatial coherence. Temporal coherence expresses the length of time that the phase of the wavefront at a given point in space can be accurately predicted. Spatial coherence is the ability to predict the phase at one point in the laser beam relative to another point, either longitudinally or laterally, at the same instant of time. For a laser, the temporal and spatial coherence characteristics are extremely large compared to radiant light.

Finding an exact explanation and mathematical solution to the scattering process of light has been a major area of research throughout the history of physics. In 1678 the Dutch physicist, Christian Huygens, formulated a theory that stated: (Ref.7:60), "every point on a primary wavefront serves as the source of spherical secondary wavelets such that the primary wavefront at some later time is the envelope of these wavelets. Moreover, the wavelets advance with a speed and frequency equal to that of the primary wave at each point in space." In the early 1800's Augustin Jean Fresnel recognized that the huygens principle should be

modified to include the wavelength of the diffracted light. He corrected this apparent deficiency with his theory which stated (Ref.7:330), "every unobstructed point of a wavefront, at a given instant of time, serves as a source of spherical secondary wavelets (of the same frequency as the primary wave). The amplitude of the optical field at any point beyond is the superposition of all these wavelets (considering their amplitudes and relative phases)." This statement is now referred to as the Huygens-Fresnel principle of diffraction.

Although the phrases of the Huygens-Fresnel principle are relatively easy to understand, the mathematical statement of the principle is very complex. Many brilliant theoreticians and experimentalists such as Helmholtz, Kirchhoff, Green, Young, Rayleigh, Sommerfeld, and Fraunhofer formulated reliable approximations enabling the complex mathematical model of diffraction to be reduced to a solvable equation (Ref.8:30-54).

Huygens-Fresnel Equation

Equation 1 is one of many mathematical representations of the Huygens-Fresnel diffraction formula (Ref.8:60).

$$E_s(x,y) = \frac{\mathrm{Exp}(jkz)}{j\lambda z}\mathrm{Exp}\{\frac{jk}{2z}(x^2+y^2)\}\int_{-\infty}^{+\infty}\int E_a(u,v)$$

$$\mathrm{Exp}\{\frac{jk}{2z}(u^2+v^2)\}\mathrm{Exp}\{\frac{-j2\pi}{\lambda z}(ux+vy)\}dudv \qquad (1)$$

where:

$E_s(x,y)$ ≡ Electric field strength in observation plane (v/m) (complex envelope)

$E_a(u,v)$ ≡ Electric field strength in scattering plane (v/m) (complex envelope)

z ≡ Range between scattering and observation planes (m)

λ ≡ Laser wavelength (m)

k ≡ Propagation number = $2\pi/\lambda$ (1/m)

Equation 1 describes the relationship between the complex amplitude, $E_s(x,y)$, of the field strength of the scattered monochromatic wave in the observation plane due to a complex field strength, $E_a(u,v)$, over an aperture in the scattering plane. See Fig. 1 for geometrical layout. Note that $E_a(u,v)$

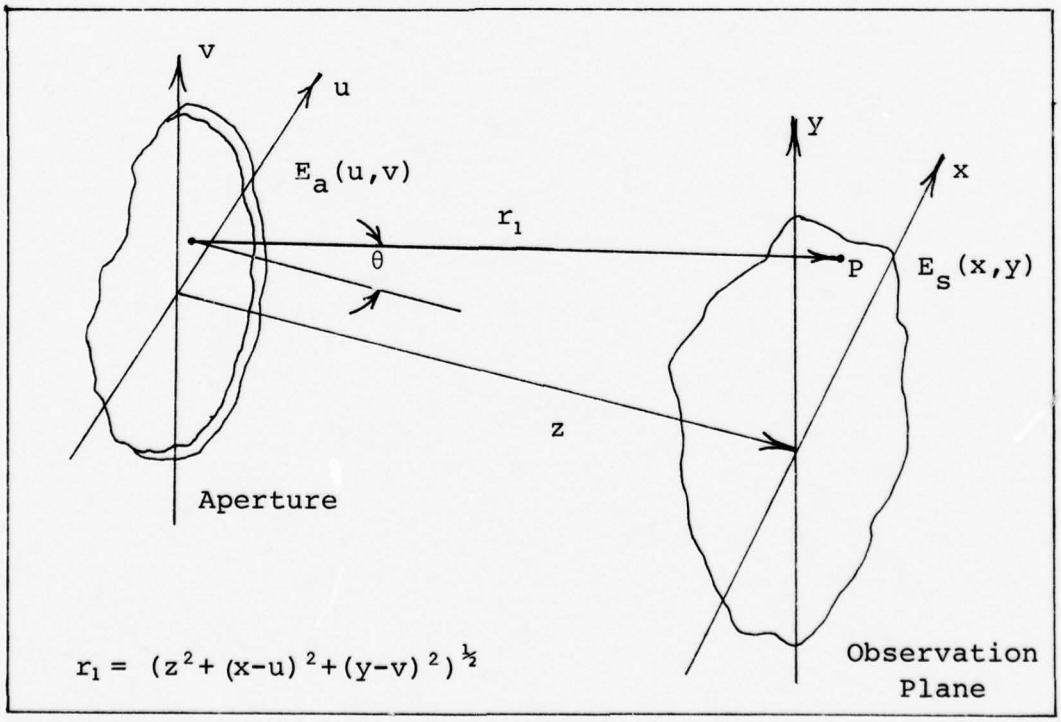

Fig. 1 Aperture Diffraction Geometry

is produced by the monochromatic wave illuminating the scattering aperture. It will be shown that Eq. 1 will simplify slightly by using far field approximations and a complex aperture function model.

Although Eq. 1 was formulated through the use of experimental observations, it can also be derived from the differential wave equation. An equation for a scattered field produced by a complex aperture function, $E_a(u,v)$, is the Fresnel-Kirchhoff diffraction formula

$$E_s(x,y) = \frac{1}{j\lambda}\iint_A \frac{1}{r_1}\mathrm{Exp}\{jkr_1\}E_a(u,v)\,dA \tag{2}$$

Equation 2 is valid for small θ's (see Fig. 1) in the range of zero to 15 degrees.

An approximation of r_1 can be obtained through the binomial expansion of

$$r_1 = (z^2+(x-u)^2+(y-v)^2)^{\frac{1}{2}} \tag{3}$$

When this expansion is completed, only those terms with powers of two or less are retained. This is known as the Fresnel approximation and is valid for

$$z^3 >> \frac{\pi}{4\lambda}\{(x-u)^2+(y-v)^2\}^2_{MAX} \tag{4}$$

With the previous approximations, the Fresnel-Kirchhoff diffraction formula (Eq. 2) reduces to the Huygens-Fresnel diffraction formula (Eq. 1). For the problems investigated in this thesis, Eq. 1 can be further simplified by envoking the Fraunhofer far field approximation

$$z >> \frac{k(u^2+v^2)}{2}\ \text{MAX} \tag{5}$$

This approximation insures that the quadratic phase factor, from Eq. 1,

$$\text{Exp}\{\frac{jk}{2z}(u^2+v^2)\} \tag{6}$$

of the incident radiation is approximately unity over the aperture. Goodman states (Ref.8:61), "Fraunhofer diffraction patterns can be observed at distances closer than implied by Eq. 5, provided the aperture is illuminated by a spherical wave converging toward the observer, or if a converging lens is properly situated between the observer and the aperture."

In summary, it has been stated (although not proven in this thesis) that the Huygens-Fresnel diffraction formula (Eq. 1) can be derived from the differential wave equation if realistic approximations are applied to the Fresnel-Kirchhoff diffraction formula (Eq. 2). In addition, Eq. 1 is further simplified by the Fraunhofer far field approximation (Eq. 5) to provide Eq. 7 on the following page.

$$E_s(x,y) = \frac{\text{Exp}(jkz)}{j\lambda z} \text{Exp}\{\frac{jk}{2z}(x^2+y^2)\}$$

$$\int_{-\infty}^{+\infty}\int E_a(u,v)\,\text{Exp}\{\frac{-j2\pi}{\lambda z}(ux+vy)\}\,dudv \qquad (7)$$

Equation 7 represents the complex amplitude of the electric field strength (v/m) distribution at an observation plane resulting from the backscatter of an electric field incident on an aperture. All the quantities in Eq. 7 are easily measured or defined except $E_a(u,v)$, the complex aperture function, when the aperture is a rough reflecting surface.

Complex Aperture Function Model

The complex aperture function, $E_a(u,v)$, in Eq. 7 is a representation of the complex amplitude of the electric field, immediately after the aperture, that propagates through space to produce a diffraction pattern. It can be assumed that $E_a(u,v)$ is produced by an infinite number of fictitious spherical point sources at the aperture, where each source has a unique amplitude and phase. Each of these sources contributes, by addition of amplitudes and phases, to every point on the far field diffraction pattern. Therefore, the relative phases of the sources, at the aperture, directly effect the shape of the diffraction pattern. The fundamental problem then is to construct an $E_a(u,v)$ function that properly describes the amplitude and phase of every point in the aperture.

The simplest case that can be discussed is when the

aperture is illuminated by a coherent laser beam. The upper drawing in Fig. 2 on the following page, illustrates the geometry of the problem. The complex amplitude of each spherical wavelet can be described by

$$E_a(u,v) = E_0(b)\,\mathrm{Exp}\{j(kb_n)\} \tag{8}$$

From the geometry shown in the upper drawing of Fig. 2 it is obvious that at b=0 all relative phases are zero and can be assumed equal to zero. Thus, Eq. 8 reduces to

$$E_a(u,v) = E_0(b=0) = \text{Constant} \tag{9}$$

and $E_a(u,v)$ in Eq. 7 can now be moved outside the double integral.

When the aperture becomes a rough reflecting surface, as in the operation of the ALOT pointing system, the surface height variations can cause a randomness in the phase distributions of $E_a(u,v)$. Rayleigh (Ref.9:9) suggested an elementary equation to determine the phase at each point of the complex aperture function. The path difference (AC+CD-AB) between waves 1 and 2 in the lower drawing of Fig. 2 is

$$\Delta\ \text{Path} = 2h(u,v)\cos\beta \tag{10}$$

The phase difference between the two waves is

$$\Delta\theta = \frac{2\pi}{\lambda}(\Delta\text{Path}) = \frac{4\pi h(u,v)\cos\beta}{\lambda} \tag{11}$$

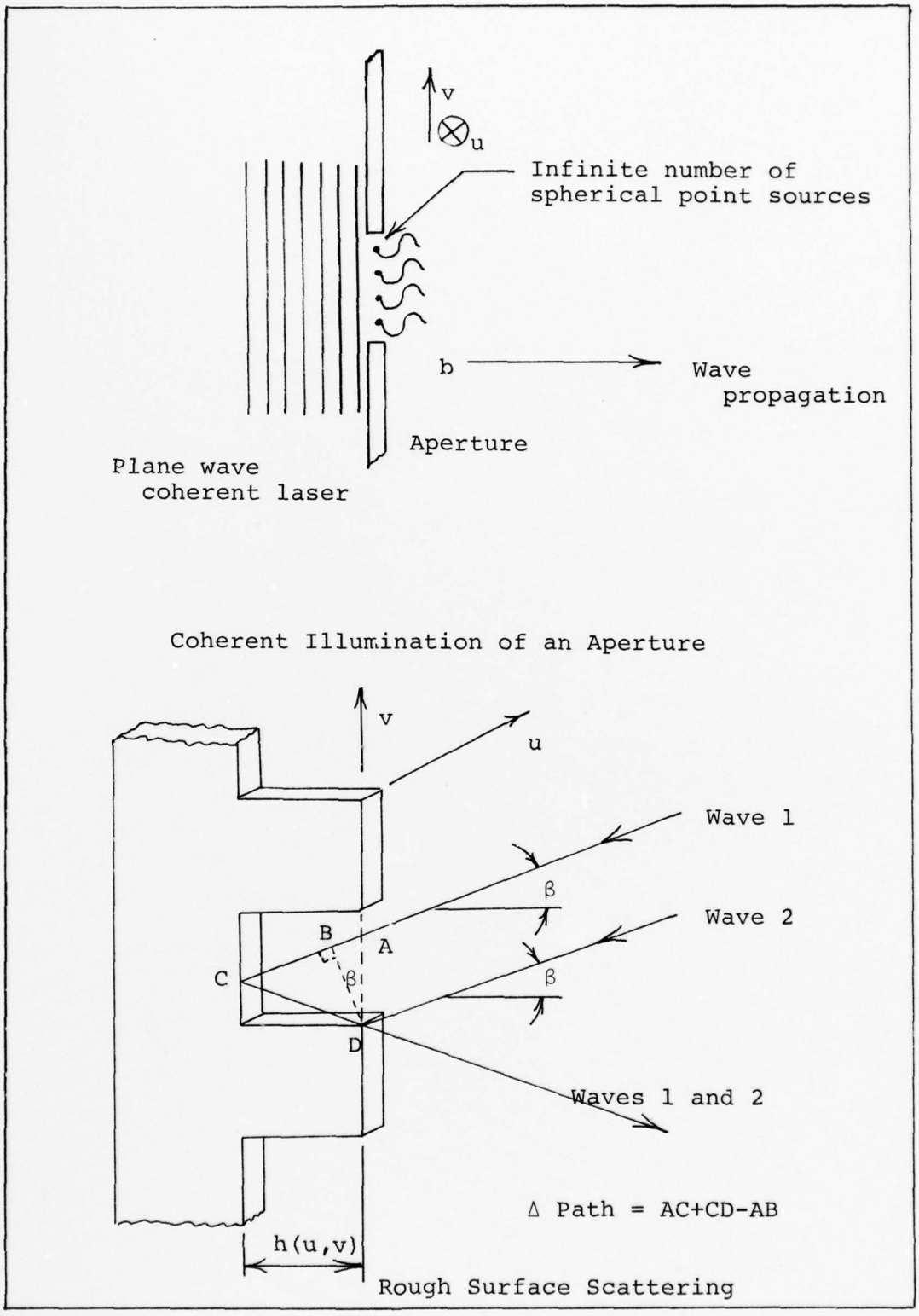

Fig. 2 Complex Aperture Geometry

Equation 11 can be used as the phase modulation of the reflected field. To complete the complex aperture function, $E_a(u,v)$, terms should be included to represent the amplitude of the field. Let $P(u,v)$ be the absolute field strength distribution at each (u,v) location of the incident radiation and let r be the reflectivity of the scattering surface. In this thesis the assumption is made that the incident radiation is a plane wave from a coherent laser where the field strength is a constant, E_0, across the beam and the reflectivity is a constant across the aperture. The complex aperture function becomes

$$E_a(u,v) = r\, E_0\, \mathrm{Exp}\{\frac{j4\pi}{\lambda} h(u,v)\mathrm{Cos}\beta\} \qquad (12)$$

Goodman (Ref.6:65) states, "that a simplistic relation (for $E_a(u,v)$) often used in analysis and reasonably accurate if the surface slopes are small." is

$$E_a(u,v) = r\, E_0\, \mathrm{Exp}\{\frac{j2\pi}{\lambda} (1+\mathrm{Cos}\beta)h(u,v)\} \qquad (13)$$

A quick check of Eq.s 12 and 13 shows that the phase of Eq.13 varies more slowly than that of Eq. 12, however, at 10 degrees or less inclination (β) of the incident radiation they differ by less than .033 radians. Since both are simplistic models and reasonably equal within 10 degrees and Eq. 13 has been used by Goodman in the study of laser speckle statistics, Eq. 13 will be used in this thesis as

the model of the complex aperture function, $E_a(u,v)$.

With the addition of Eq. 13, the Fraunhofer diffraction formula, Eq. 7, becomes

$$E_s(x,y) = \frac{\mathrm{Exp}(jkz)}{j\lambda z}\,\mathrm{Exp}\{\frac{jk}{2z}(x^2+y^2)\}r\,E_0$$

$$\int_{-\infty}^{+\infty}\int \mathrm{Exp}\{\frac{j2\pi}{\lambda}(1+\mathrm{Cos}\beta)h(u,v)\}\mathrm{Exp}\{\frac{-j2\pi}{\lambda z}(ux+vy)\}dudv \qquad (14)$$

It is recognizable that the double integral is proportional to the two dimensional Fourier transform of the complex aperture function, $E_a(u,v)$. Before any additional material is covered on diffraction patterns, Fourier analysis theory of discrete data processing must be discussed.

Fourier Analysis

This subsection of theory is devoted to Fourier analysis and, in general, the relationships between Fourier integrals, discrete Fourier transforms (DFT), and fast Fourier transforms (FFT). In addition, the provisions for the existence of each transform type will be discussed along with the pitfalls associated with discrete data Fourier transforms. The DFT is defined to be

$$g(r) = \frac{1}{N}\sum_{k=0}^{N-1} x(k)\,\mathrm{Exp}\{-j2\pi rk/N\} \qquad (15)$$

where:

$g(r)$ = r^{th} coefficient of DFT (sample)

$x(k)$ = k^{th} coefficient of spatial series (sample)

N = Total samples in spatial series

The connection between discrete and continuous Fourier transform representations are shown below.

Discrete Fourier Transform

The Fourier series is represented by

$$f(t) = \frac{a_0}{2} + \sum_{n=1}^{\infty} a_n \text{Cos}(n\pi t/p) + \sum_{n=1}^{\infty} b_n \text{ Sin}(n\pi t/p) \tag{16}$$

where

$$a_0 = \frac{1}{p} \int_0^{2p} f(t)dt \tag{17}$$

$$a_n = \frac{1}{p} \int_0^{2p} f(t)\text{Cos}(n\pi t/p)dt \tag{18}$$

$$b_n = \frac{1}{p} \int_0^{2p} f(t)\text{Sin}(n\pi t/p)dt \tag{19}$$

and p is the period of the time series. If the Dirichlet conditions are met plus the integral of $|f(t)|$ from minus to plus infinity exists, then the Fourier series (Eq. 16) can be replaced by the Fourier integral. Equations 20 and 21 are the Fourier integral transform pairs.

$$x(t) = \int_{-\infty}^{+\infty} g(f)\,\mathrm{Exp}\{j2\pi ft\}\,df \tag{20}$$

$$g(f) = \int_{-\infty}^{+\infty} x(t)\,\mathrm{Exp}\{-j2\pi ft\}\,dt \tag{21}$$

Equations 20 and 21 can be used to derive the DFT (Ref.10: 280). Start with Eq. 20 and let

$$t = t_i = i\Delta t \qquad i = 0,\pm 1,\pm 2,\cdots \tag{22}$$

$$F = 1/\Delta t \tag{23}$$

to yield

$$x(t_i) = \int_{-\infty}^{+\infty} g(f)\,\mathrm{Exp}\{j2\pi if/F\}\,df \tag{24}$$

or

$$x(t_i) = \sum_{k=-\infty}^{+\infty} \int_{kF}^{(k+1)F} g(f)\,\mathrm{Exp}\{j2\pi if/F\}\,df \tag{25}$$

The exponential is periodic in f with period F, so Eq. 25 can be written as

$$x(i\Delta t) = \int_{0}^{F} g_p(f)\,\mathrm{Exp}\{j2\pi if/F\}\,df \tag{26}$$

where

$$g_p(f) = \sum_{k=-\infty}^{+\infty} g(f+kF) \tag{27}$$

Since $g_p(f)$ is periodic with period F, it has a complex Fourier series expansion in powers of the exponential where

coefficients are given by $(1/F)X(i\Delta t)$, as shown in Eq. 26. Thus,

$$g_p(f) = \frac{1}{F} \sum_{i=-\infty}^{+\infty} x(i\Delta t)\,\mathrm{Exp}\{-j2\pi if/F\} \tag{28}$$

Now, sample in the frequency domain at points $f = n\Delta f$, $n=0,\pm1,\pm2,\cdots$, where $\Delta f = 1/T$, and Eq. 28 becomes

$$g_p(n\Delta f) = \frac{1}{F} \sum_{i=-\infty}^{+\infty} x(i\Delta t)\,\mathrm{Exp}\{-j2\pi in/TF\} \tag{29}$$

If $TF=N$ is an integer, the exponential is a periodic function of i with period N. Therefore

$$g_p(n\Delta f) = \frac{1}{F} \sum_{i=0}^{N-1} x_p(i\Delta t)\,\mathrm{Exp}\{-j2\pi in/N\} \tag{30}$$

where

$$x_p(i\Delta t) = \sum_{k=-\infty}^{+\infty} x((i+kN)\Delta t) \tag{31}$$

The sum in Eq. 31 gives the sampled values of

$$x_p(t) = \sum_{k=-\infty}^{+\infty} x(t+KT) \tag{32}$$

which is a periodic function of t, with period T, and is formed from x(t) in exactly the same way as $g_p(f)$ is formed from g(f) (Eq. 21). Substituting $\Delta t = T/N$ for $1/F$, Eq. 30 becomes Eq. 33 on the following page. Note if $x(t)=0$ for

$|t|>q$, $x_p(t)=x(t)$ (i.e.; space limited function).

$$g_p(n\Delta f) = \frac{1}{N}\sum_{i=0}^{N-1} Tx_p(i\Delta t)\,Exp\{-j2\pi in/N\} \tag{33}$$

which is the DFT (Eq. 15). In the DFT the following approximations apply:

$$x(i) = Tx_p(i\Delta t) \tag{34}$$

$$g(n) = g_p(n\Delta f) \tag{35}$$

This proof was extracted from Rabiner and Rader (Ref.10:280) and provides the DFT pairs of

$$g_p(n) = \frac{1}{N}\sum_{k=0}^{N-1} x_p(k)\,Exp\{-j2\pi nk/N\} \tag{36}$$

$$x_p(k) = \sum_{n=0}^{N-1} g_p(n)\,Exp\{j2\pi nk/N\} \tag{37}$$

and

$g_p(n)$ = n^{th} coefficient of DFT

$x_p(k)$ = k^{th} coefficient of spatial series

N = Total samples in series

k and n = 0, 1, 2$\cdots$N-1

Equations 36 and 37 are the DFT pairs provided Eqs. 20 and 21 exist and the approximations of Eqs. 34 and 35 are used.

The FFT is an efficient method for calculating the DFT on a computer. This thesis will not discuss the development of the FFT but Ref. 10 part 2 gives in depth details of the algorithm. There are several FFT routines that are used in

the signal analysis field, however, the one used in this thesis and most widely used is by J. W. Cooley and J. W. Tukey.

The number of multiplications for the FFT is $2N\text{Log}_2N$ compared to N^2 for the DFT for a one dimensional data array of length N samples. Besides this computational efficiency, the FFT uses only one data array for input to the routine, internal routine calculations, and output from the routine.

There are two major problems associated with using the DFT and FFT algorithms compared to the Fourier integral; aliasing and leakage. Aliasing refers to the fact that high frequency components of a time function can impersonate low frequencies if the sampling rate of the data is too low and therefore, two widely different functions can have the same DFT. An example of this can be seen in Fig. 3 on the following page. Curve A is the time function sampled, however, it is sampled at a frequency lower than its frequency. With data samples available, curve B frequency may be assumed since two or more data samples per time function period are required to determine a frequency. To avoid aliasing a sampling rate of at least two times the highest frequency component of the time function is required. This is known as the Nyquist sampling rate.

When working with systems that are band-limited it is a good practice to sample at more than twice the highest expected frequency of the function. An engineering rule of thumb is to sample at a rate of four to ten times the

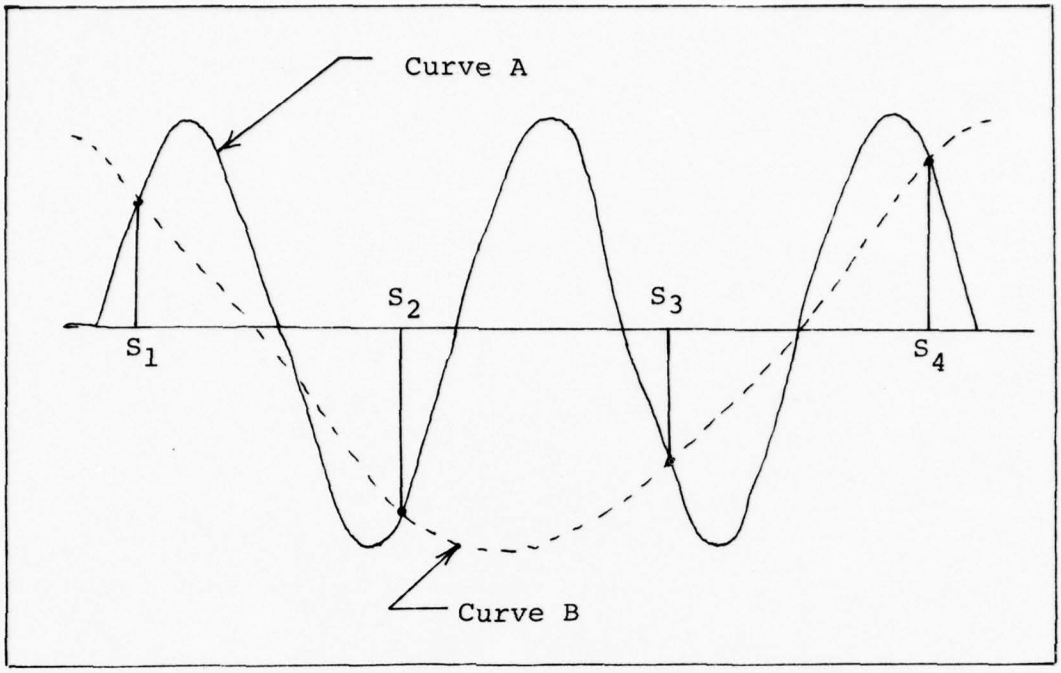

Fig. 3 Aliasing Phenomenon

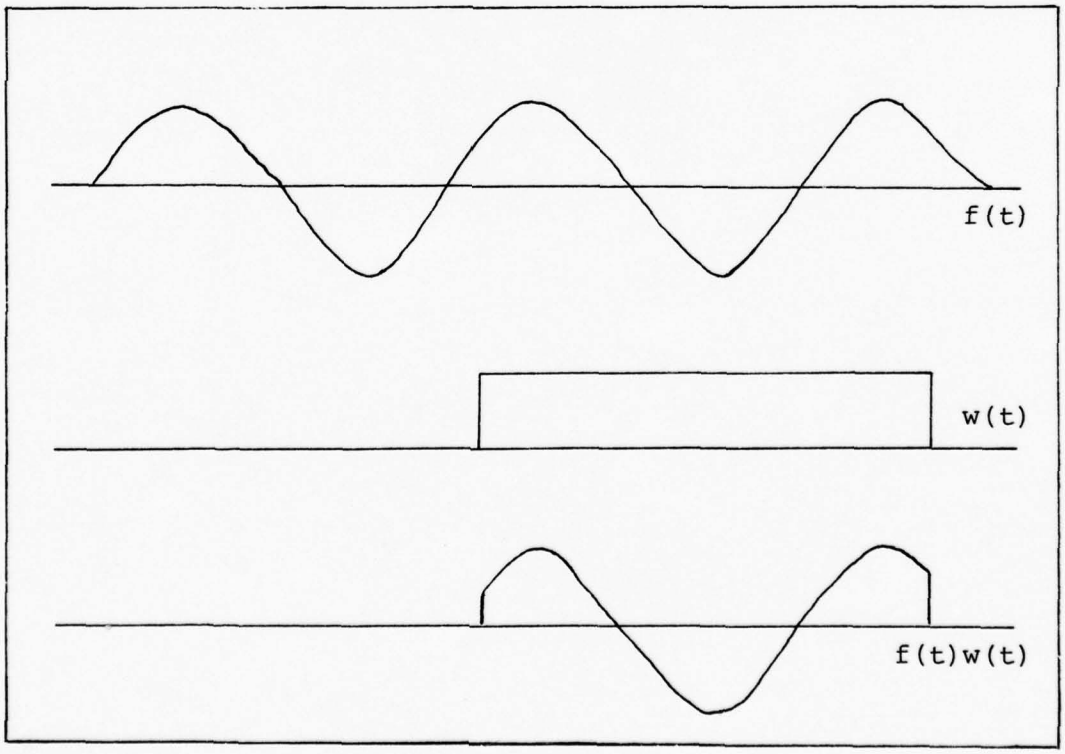

Fig. 4 Finite Buffer Length Sampling

highest expected frequency. The maximum sample rate is, of course, dependent upon the data handling and storage characteristics of the overall sampling and computer system.

The second problem associated with DFT is that of leakage resulting from a finite length record of data. Consider the continuous sine wave shown in the top part of Fig. 4 on the previous page. To analyze that sine wave, it is sampled until a finite record length buffer is filled. The finite length buffer is shown in the middle of Fig. 4 and the result of sampling the sine wave is shown in the bottom of Fig. 4.

In the frequency domain, the Fourier transform of the continuous sine wave appears as shown in the top drawing of Fig. 5 on the following page. This diagram shows only the positive frequency of the transform and it is an impulse function positioned at a frequency equal to the sine wave frequency. The Fourier transform of the finite length buffer is shown in the middle drawing of Fig. 5, which is a Sinc(x) function. The result of sampling the sine wave with a finite record length buffer is the convolution, in the frequency domain, of the impulse function and the Sinc (x) function, as shown in the bottom diagram of Fig. 5. This result is known as windowing and produces a maximum peak at the frequency of the sine wave and also a series of sidelobes associated with the finite buffer length.

In addition to the problems of aliasing and leakage

associated with DFT there is also a frequency resolution problem with the data returned from the FFT. The top drawing of Fig. 6 on the following page represents the common data array in the FFT subroutine

$$N \equiv \text{Maximum array dimension}$$

$$2q+1 \equiv \text{Total non zero data samples in array}$$

$$x(k) \equiv \text{Magnitude of data in array position } k$$

where

$$x(k) = \begin{cases} 1 & 1 \leq k \leq 2q+1 \\ 0 & 2q+1 < k \leq N \end{cases} \qquad (38)$$

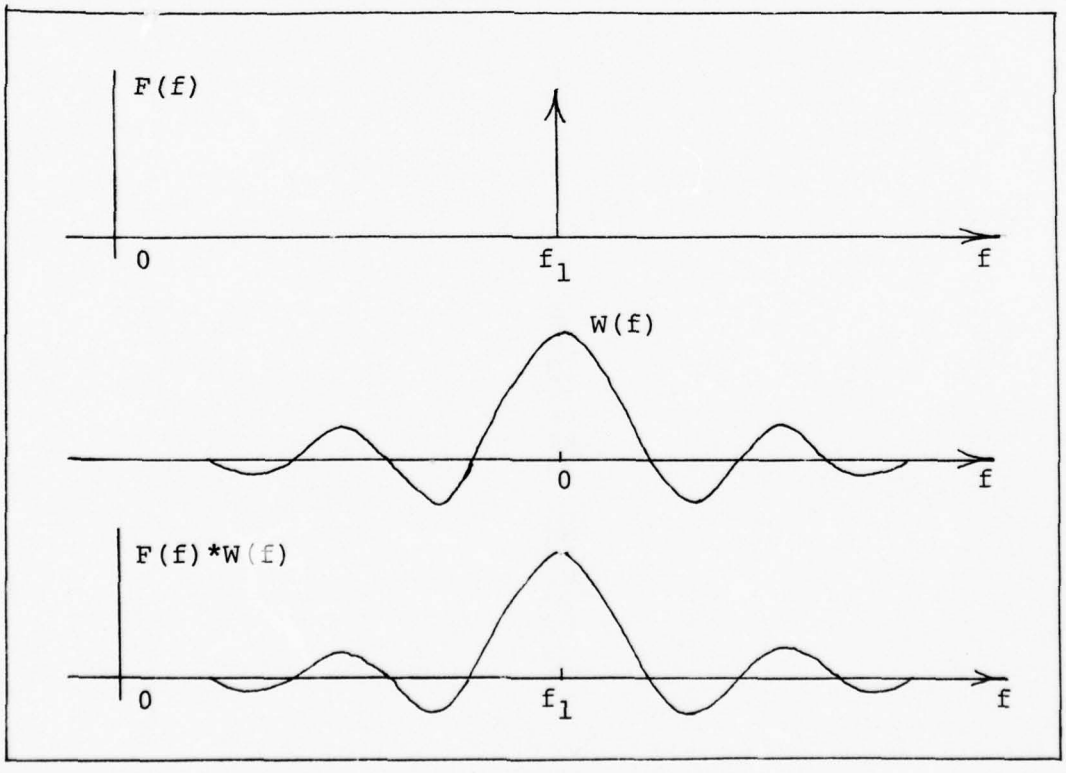

Fig. 5 Windowing Phenomenon

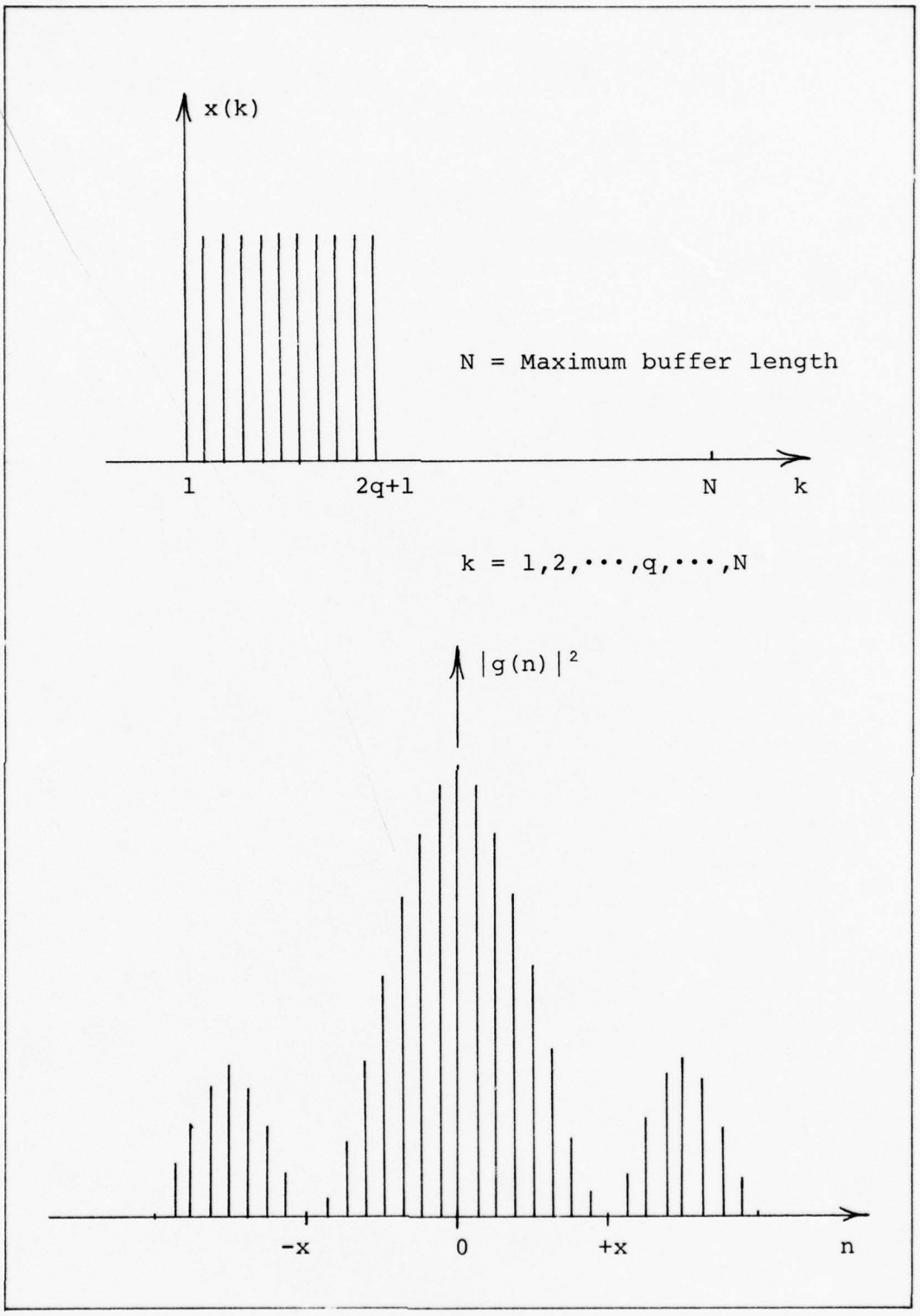

Fig. 6 FFT Data Array and $|\mathrm{Sinc}(x)|^2$ Function

Recalling the DFT equation (Eq. 36) and replacing the sequence k = 0,1,2,···N-1 with k = 1,2,3,···N, the result is

$$g_p(n) = \sum_{k=1}^{N} x_p(k)\,\mathrm{Exp}\{-j2\pi nk/N\} \tag{39}$$

where n=1,2,···N. Since x(k) equals zero for k>2q+1, Eq. 39 can be replaced by

$$g_p(n) = \sum_{k=1}^{2q+1} x_p(k)\,\mathrm{Exp}\{-j2\pi nk/N\} \tag{40}$$

and since x(k) = 1 for all $1 \leq k \leq 2q+1$, as shown in Fig. 6 on the previous page, Eq. 40 is approximated by

$$g(n) = 2q\,\mathrm{Sinc}\{2\pi nq/N\}\,\mathrm{Exp}\{-j2\pi n/N(1+q/2)\} \tag{41}$$

The exponential in Eq. 41 results from the pulse not centered around zero, and thus is a frequency shift in the frequency domain. For the analysis in this thesis, the exponential term can be neglected.

The function g(n) of Eq. 41 goes to zero when nq/N equals an integer. Let the first integer be one, therefore

$$nq/N = 1 \tag{42}$$

or

$$n = N/q \tag{43}$$

Equation 43 shows that there are N/q samples between 0 and x, as shown on the bottom diagram of Fig. 6. Therefore, to provide excellent resolution between 0 and x on the $|Sinc(x)|^2$ function returned from the FFT, N should be large and q small. As an example, if N = 128 and q = 8, there will be 16 data samples between 0 and the first null on the $|Sinc(x)|^2$ function.

In summary, the Fourier analysis review has shown that the DFT and FFT are excellent representations of the Fourier series and integrals if the Dirichlet conditions are met and the integral of $|f(t)|$ exists. To accurately represent a continuous time function with discrete sampling, the continuous function should be sampled at a rate greater than twice its highest frequency component. This sampling procedure will reduce or eliminate the aliasing problem. In addition finite record length buffers will cause leakage and corrupt the data returned from the FFT. Because it is desirable to have a high resolution of data between nulls of the function returned from the FFT, the actual number of data samples input to the FFT buffer should be considerably less than the total size of the input buffer. With this Fourier transform review, it is now possible to complete the development of the Huygens-Fresnel diffraction formula used to develop the computer model of speckle in this thesis.

Intensity Distribution at an Observation Plane

Equation 7 is the Huygens-Fresnel diffraction formula

used for speckle analysis in this thesis. This form of the Huygens-Fresnel equation is sometimes called the Fraunhofer diffraction equation because of the Fresnel and Fraunhofer assumptions (Eqs. 4 and 5). For convenience, Eq. 14 is repeated in Eq. 44.

$$E_s(x,y) = \frac{Exp(jkz)}{j\lambda z} Exp\{\frac{jk}{2z}(x^2+y^2)\} r\ E_0$$

$$\int_{-\infty}^{+\infty}\int Exp\{\frac{j2\pi}{\lambda}(1+Cos\beta)h(u,v)\} Exp\{\frac{-j2\pi}{\lambda z}(ux+vy)\} dudv \qquad (44)$$

Although not evident, Eq. 44 is a time varying function and the intensity distribution can be obtained from $E_s(x,y)Exp\{jwt\}$ by taking the time average. Thus

$$I(x,y) = <(R_e E(x,y))^2> \qquad (45)$$

where $< >$ denotes time average which reduces to

$$I(x,y) = \tfrac{1}{2}E(x,y)E^*(x,y) \qquad (46)$$

for monochromatic light.

Since Eq. 46 contains the electric field at the observation plane multiplied by its complex conjugate, the exponentials outside the integrals of Eq. 44 disappear. The resulting intensity distribution at the observation plane is given by Eq. 47 on the following page, where I(x,y) is in WATTS/m^2 and is sometimes called irradiance. Recalling Fig. 1 shows the geometry of the diffraction problem.

$$I(x,y) = \tfrac{1}{2} \left| \frac{rE_0}{\lambda z} \{ \int\int_{-\infty}^{+\infty} \mathrm{Exp}\{ \frac{j2\pi}{\lambda} (1+\mathrm{Cos}\beta) h(u,v) \} \right.$$

$$\left. \mathrm{Exp}\{ \frac{-j2\pi}{\lambda z} (ux+vy) \} \} du dv \right|^2 \qquad (47)$$

The proper scaling per unit at the observation plane can be determined by solving Eq. 47 for a simplified aperture function. Let the aperture be square with linear dimension b the total width. Also let r and h(u,v) equal one across the aperture with a β of zero. From Eq. 47, I(x,y) becomes

$$I(x,y)/I_0 = \left(\frac{\mathrm{Sin}(\frac{\pi bx}{\lambda z})}{\frac{\pi bx}{\lambda z}} \right)^2 \left(\frac{\mathrm{Sin}(\frac{\pi by}{\lambda z})}{\frac{\pi by}{\lambda z}} \right)^2 \qquad (48)$$

The distance out to the first null in I(x,y) is determined by

$$\frac{\pi bx}{\lambda z} = \pi \qquad (49)$$

or

$$x = \frac{\lambda z}{b} \qquad (50)$$

and also

$$y = \frac{\lambda z}{b} \qquad (51)$$

Although not proven here (Ref.7:352) the intensity pattern produced by a circular aperture is

$$I(R)/I_0 = \left[\frac{J_1(2\pi rR/\lambda z)}{\pi rR/\lambda z}\right]^2 \tag{52}$$

where

$r \equiv$ Radius of aperture

$R \equiv$ Radius out in intensity plane

$J_1 \equiv$ Bessel function of first order

and the distance out to the first null of the intensity pattern is given by

$$R = \frac{1.22\lambda z}{2r} \tag{53}$$

From Eq. 43 of the FFT discussion, there are n data values between zero and the first null in the intensity pattern returned from the FFT subroutine (n = N/q). Recall N was the total samples in the input buffer and q was the total samples of real data in that buffer. Therefore, the linear distance per sample at the observation plane is

$$\Delta x = \Delta y = x/n = y/n = \frac{\lambda z/b}{N/q} \tag{54}$$

However, b was the total pulse width subdivided into q

samples, therefore

$$\Delta x = \Delta y = \frac{\lambda z}{N} \cdot \frac{q}{b} \tag{55}$$

Equation 55 gives the linear distance per sample of the speckle pattern in the observation plane when the input is a square aperture. It is obvious that the resolution distance at the observation plane is directly proportional to λ and z and inversely proportional to N (total record length of data buffer). Equation 47 will be programmed to calculate the speckle phenomenon for rough surface scattering and Eq. 55 to determine the unit sample distance at the observation plane.

Summary of Theory Section

As revealed in the introductory paragraphs of this chapter, the search for a mathematical solution to the diffraction of light began 300 years ago. In the early 1800's the Huygens-Fresnel equation (Eq. 1) was developed as hypothesized from experimental data and later proven to be a valid solution of the scalar wave equation. The general Huygens-Fresnel equation was simplified by using the Fresnel approximation to replace the spherical waves by plane waves. Equation 4 gives the conditions when the approximation is valid. The Fraunhofer far field approximation (Eq. 5) was also utilized to remove the quadratic phase factors at the aperture. The generalized Huygens-Fresnel equation (also called Fraunhofer diffraction equation) was then revised to

include rough surface scattering. The term added to the equation is called the complex aperture function (Eq. 13) as suggested by Goodman (Ref.6). The final result was an equation that predicted the electric field strength (v/m) at an observation plane when an incident laser beam was scattered from a rough surface (Eq. 14).

Before the intensity field (irradiance) formula was developed, a detailed investigation of Fourier analysis was accomplished. It was shown that the Fourier integrals, discrete Fourier transforms, and fast Fourier transforms are analogous if several conditions exist. As stated, to represent a time function by the Fourier integral instead of the series, the Dirichlet conditions must be met and the integral of $|f(t)|$ must exist for all time. The discrete and fast Fourier transforms are valid approximations to the integral transform, however, the time function must be sampled at the Nyquist rate or greater to remove the aliasing problem. Leakage was covered in detail and it was shown that discrete and fast Fourier transformed data are corrupted by the use of finite record length data buffers. The Fourier analysis section was concluded by proving that the input array to the fast Fourier transform should be large and the actual data samples should fill only a portion of the array. This restriction was required to provide high resolution of the $|\mathrm{Sinc}(x)|^2$ envelope between zero and the first null at the observation plane.

The final section of the theory chapter developed the

equation to predict the intensity pattern (Eq. 47) at an observation plane. As stated, the intensity pattern is actually proportional to the magnitude squared of the two dimensional Fourier transform of the complex aperture function. The last equation to be developed (Eq. 55) provided the proper scaling of distance at the observation plane. Equation 47, the far field diffraction equation, was used to develop the computer model for the speckle phenomenon.

III. Experimental Investigation of Speckle Patterns

A laboratory experiment was conducted to measure the intensity distribution in speckle patterns and identify the trends, from pattern to pattern, as the incident laser beam size and range between scattering and observation planes were changed. By observing and tabulating these quantities and then comparing them to the theoretical computer model, a qualitative estimate of the model "goodness" was established. This section of the thesis covers only the experimental investigation, while the comparison of the computer model patterns with the experimental data is covered in a later chapter.

Experimental Set-Up

Figure 7 shows the layout of the laboratory equipment used in the experimental investigation of the speckle patterns. The equipment used was available in the physics laboratories of the Air Force Institute of Technology at Wright-Patterson Air Force Base, Ohio. Table I, lists the equipment shown in Fig. 7. It should be noted that measurements of the reflecting surface roughness were not obtained and the consequences of this are discussed later in this chapter.

Experimental Procedure

To provide an understanding of the diffraction properties of speckle patterns two experimental procedures were

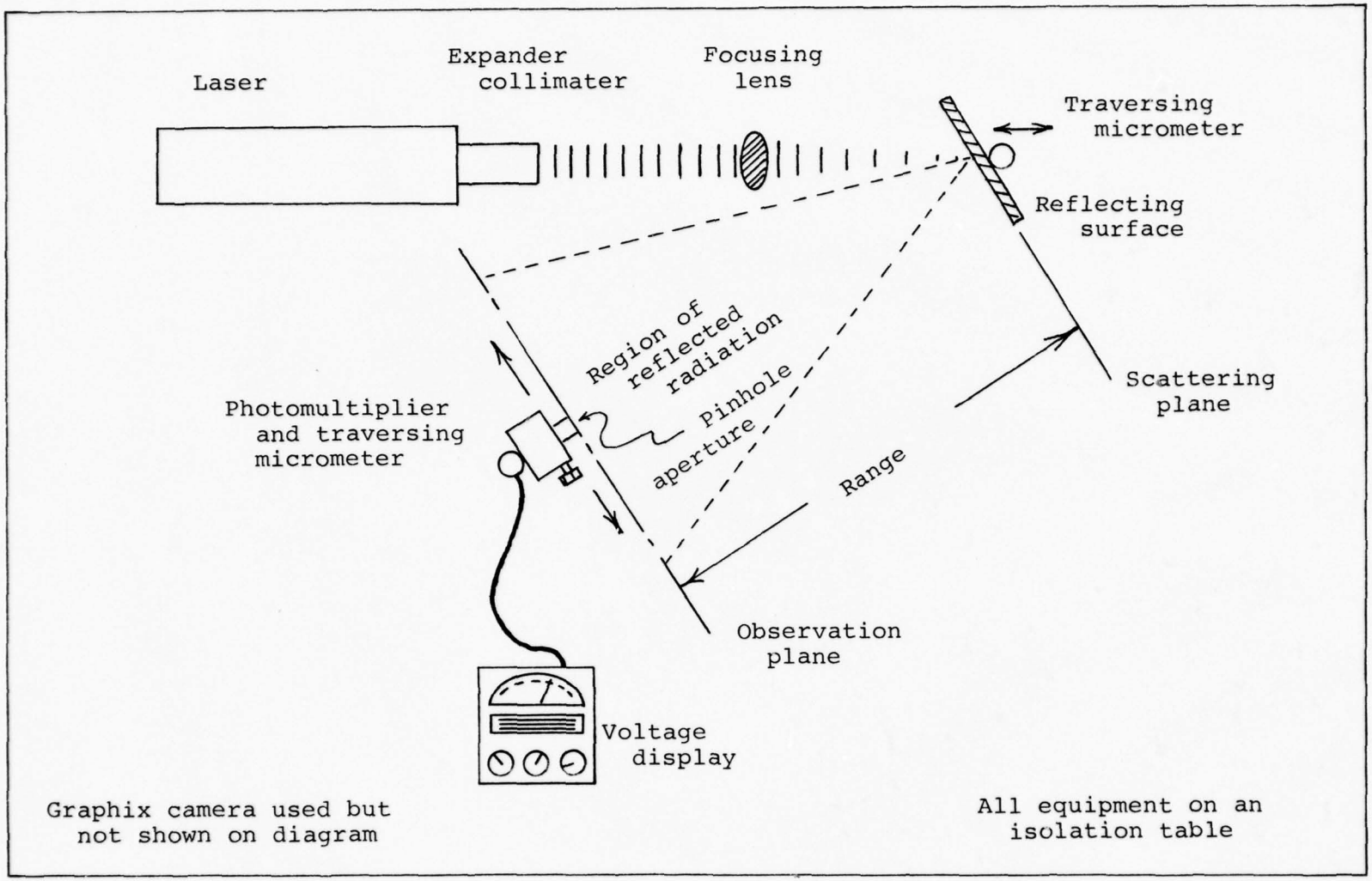

Fig. 7 Laboratory Equipment Layout

Table I

Laboratory Equipment Nomenclature

Laser: HeNe 50 mW spectra physics model 125
λ = 6328 Å

Laser collimator: Model 336 multiple wavelength collimating lens, spectra physics

Reflecting surface: Oxidized aluminum scrap metal (7.5 x 7.5 x 0.5 cm)

Photomultiplier: Photomultiplier microphotometer No. 10-213

Photomultiplier tube: Type "S", EMI

Focusing lens: 4 cm diameter, 20 cm focal length

Traversing micrometers: Standard laboratory traversing micrometer with 1 μm. resolution

Camera: Graphix, aperture and focal plane shutters

Film: Polaroid, black and white, Polapan/ type 52

developed. The first procedure was to observe the speckle patterns at various observation planes while keeping the beam focused on the reflecting surface (smallest incident beam spot). Features of these speckle patterns (a pattern formed by a series of bright and dark spots) were identified and could be recognized at several observation planes. Photographs of one section of each speckle pattern, at three observation planes, were obtained. For the next part of the experiment the scattering plane was traversed parallel to the incident radiation. This operation defocused

the radiation on the scattering surface which increased the spot size, however, a constant distance between the scattering and observation planes was maintained. Three scattering plane locations were used and a photograph of a section of each speckle pattern was obtained.

The second procedure was similar to the first except a photomultiplier was used to measure the speckle pattern intensities (irradiance). Use of the photomultiplier presented some problems that had to be solved. The first problem was the enormous area of the input aperture (approximately 25 sq. cm.) of the photomultiplier. Since this area encompassed many bright and dark spots of the speckle pattern, speckle intensity (actually a measurement of the electric field strength) resolution was very poor and, in fact, an average was obtained. This problem was solved by decreasing the aperture of the photomultiplier tube with a piece of metal that contained a 2.50 ± 0.05 mm. diameter hole. Tin foil was then taped over the metal and a pin hole (0.75 ± 0.05 mm. diameter) was made to coincide with the hole in the metal plate. Because of the reduction in the aperture area of the photomultiplier, intensity measurements obtained were relative and not calibrated. The second major problem with using the photomultiplier to measure relative intensity strengths of the speckle patterns was the large amount of data samples required to characterize a pattern. The solution to this problem was to search the speckle pattern, at the observation plane, for the maximum

reflected radiation and then obtain a one dimensional set of data values (parallel to the isolation table and perpendicular to the scattering plane) through this point. Through trial and error investigation, it was determined that sample points equally spaced 0.5 mm. apart would characterize the speckle pattern and provide enough resolution for analysis. This one dimensional sampling approach was used by McKechnie (Ref.11) in his experimental measurements of second order statistical properties of speckle patterns.

Speckle patterns were compared when the range was held constant and the reflecting aperture size was changed. The smallest incident radiation spot size was obtained when the scattering surface was placed at the focal plane of the focusing lens. The spot size increased when the scattering surface was moved 5 mm. from focus condition and also at 10 mm. off focus. In all cases, the incident radiation spot size was not accurately measured. The object of this part of the experiment was to observe the trend in the speckle size as the aperture size increased.

Photographic Evaluation of Speckle Patterns

Photographs are an easy way to record speckle patterns in the laboratory, however, measurement of contrast is usually very hard to accomplish from photographs. Figure 8 shows a speckle pattern photographed 0.5 ± 0.005 m. from the scattering plane with the incident laser beam radiation focused on the scattering surface. Areas of intensity

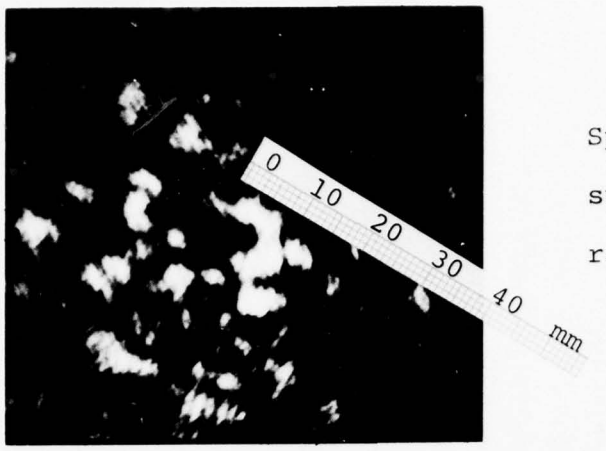

Fig. 8

Speckle, rough surface scattering, range=0.5 m

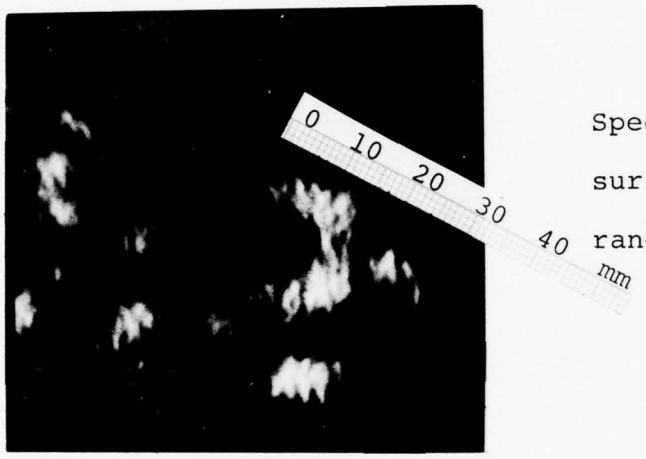

Fig. 9

Speckle, rough surface scattering, range=1.0 m

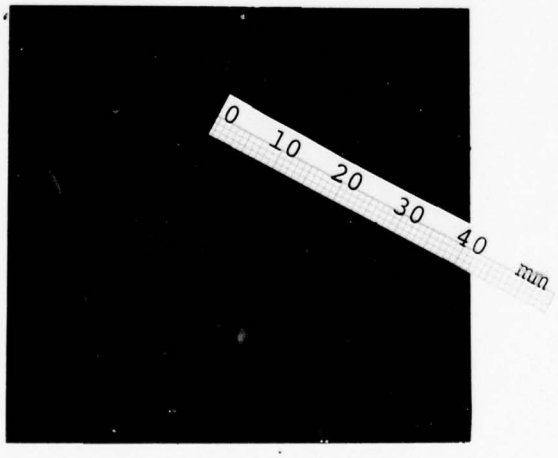

Fig. 10

Speckle, rough surface scattering, range=1.5 m

Fig. 11
Speckle, rough surface scattering, range=0.5 m, aperture less than 0.2 mm diameter

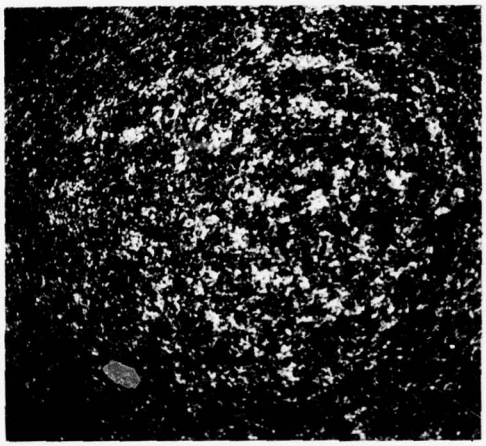

Fig. 12
Speckle, rough surface scattering, range=0.5 m, aperture less than 0.5 mm diameter

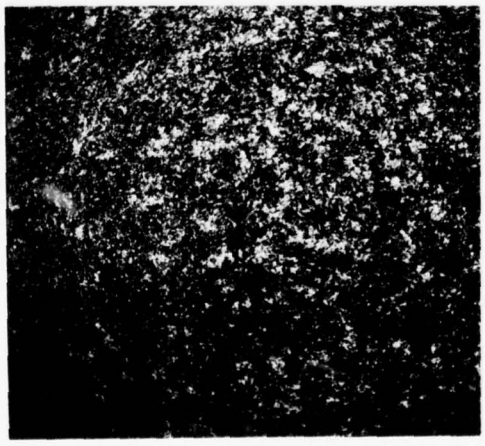

Fig. 13
Speckle, rough surface scattering, range=0.5 m, aperture less than 0.8 mm diameter

enhancement and cancellation are readily apparent, and in addition, areas with unique speckle shapes can be located. The centimeter scale overlay on Fig. 8 highlights a speckle and shows its length to be 14.5 ± 0.5 mm. Figure 9 is a photograph of the same speckle pattern area with the observation plane at 1.0 ± 0.005 m. The speckle is now 29.5 ± 0.5 mm. long. Figure 10 is a photograph of the same area at 1.5 ± 0.005 m. with the speckle now 43.5 ± 0.5 mm. long.

These three photographs illustrate one of the principles of diffraction theory. Recalling from the theory section, (Eqs. 52 and 53) the linear extent of a typical speckle lobe is directly proportional to the range between the scattering and observation planes. The measurement values from the three figures support the diffraction theory, i.e., when the range is doubled or tripled so does the speckle spot diameter.

For the next experimental investigation, the range from observation plane to scattering plane was held constant at 0.5 ± 0.005 m. Figure 11 is a photograph of a section of the speckle pattern when the incident laser beam radiation was focused on the scattering surface. Although an accurate measurement of the scattering spot size was not obtained, it was less than 0.2 mm. diameter. Figures 12 and 13 are photographs of the same speckle pattern area as in Fig. 11 with the scattering plane moved 5.0 and 10.0 ± 0.5 mm. from the focus position. The incident radiation diameters at these locations were less than 0.5 and 0.8 mm. respectively.

It is very difficult to make any quantitative statement about the characteristics shown in Figs. 11 through 13, however, qualitatively the speckle sizes were reduced as the aperture size increased. To obtain more quantitative information about the speckle phenomenon, increased resolution of intensity contrast in the speckle pattern was required. A photomultiplier was used to provide the increase in resolution.

Photomultiplier Evaluation of Speckle Patterns

As shown in Fig. 7, the photomultiplier entrance (pin hole) aperture was positioned at the speckle pattern observation plane. After a maximum intensity in the speckle pattern was located, the photomultiplier apparatus was aligned to traverse parallel to the scattering surface through the maximum intensity. As stated earlier, the photomultiplier aperture position was incremented in 0.5 mm. steps. After each increment, an indicated voltage (proportional to the intensity of the speckle pattern over by pin hole was recorded in the laboratory notebook. This procedure was repeated for four speckle patterns: 1.) Range one meter, scattering surface at focus plane, 2.) Range two meters, scattering surface at focus plane, 3.) Range two meters, scattering surface five millimeters from focus plane, and 4.) Range two meters, scattering surface ten millimeters from focus plane.

To aid in surveying the intensity data, a computer

program was written to normalize the data and provide plots. Figures 14 through 17 show the normalized speckle patterns for the four cases described in the previous paragraph. To obtain the frequency content of each speckle pattern a program was written to perform the Fourier transform on each recorded speckle pattern and to produce a frequency plot for analysis. Figures 18 through 21 show the Fourier transformed data for the four speckle patterns recorded.

The speckle patterns were sampled every 0.5 mm. or at a rate of 2 cycles/mm. Recalling from the theory section that a sample rate of twice the highest frequency content of the data is required to prevent aliasing, the sample rate used provided valid frequency information below 1 cycle/mm. Inspection of the Fourier transform plots (Figs. 18 through 21) reveal that the frequency content of the speckle patterns was far below the Nyquist rate. Thus, the sample rate was much greater than required to characterize the speckle patterns.

Analysis of the Speckle Patterns

A FFT routine was used to calculate the Fourier transform of the speckle pattern data collected with the photomultiplier. The Fourier transform of this intensity data provided the spatial frequency content of the segment of each speckle pattern sampled. Although each speckle pattern segment was only a small portion of the total speckle pattern, the spatial frequencies obtained should be

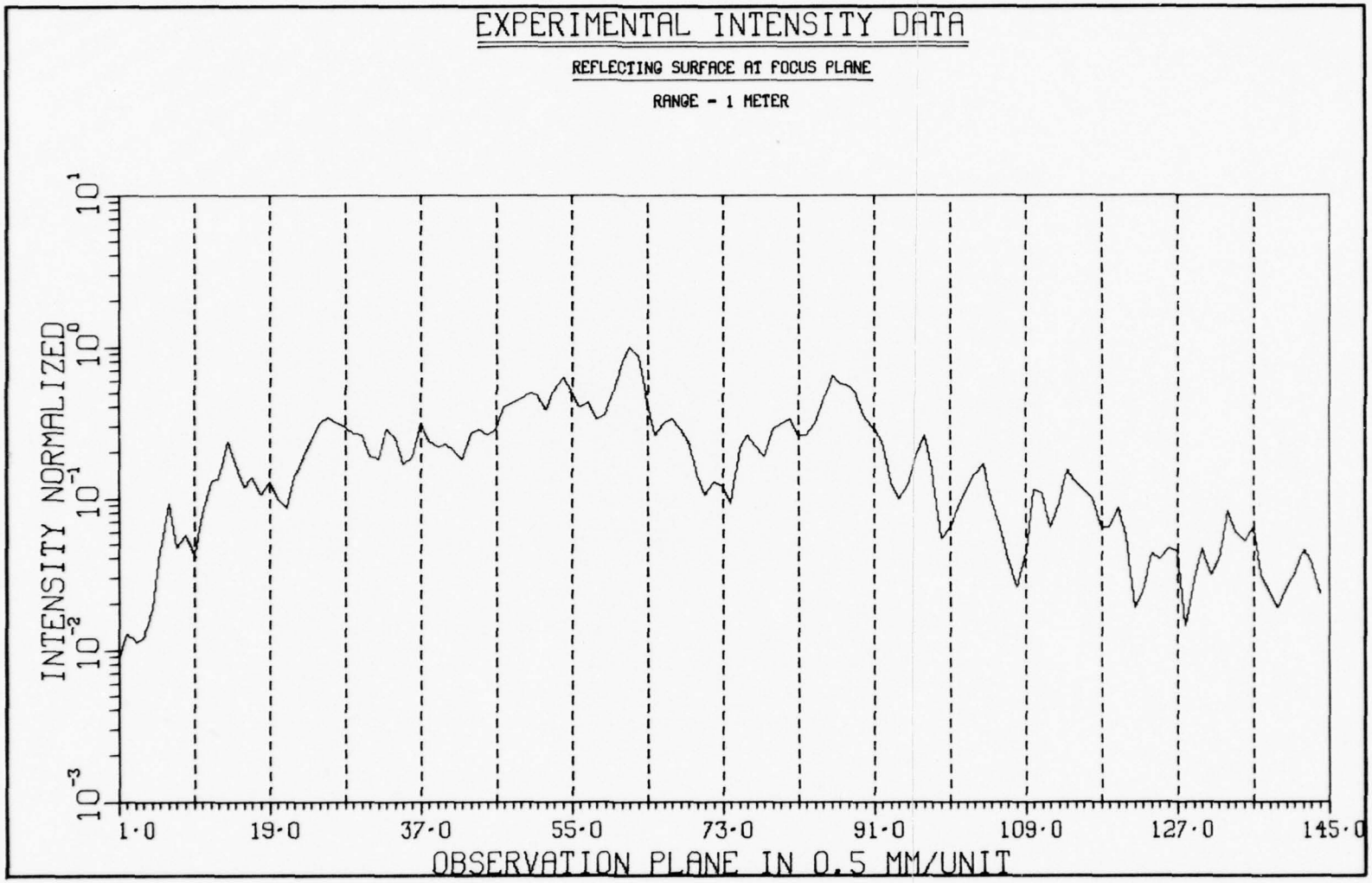

Fig. 14 Photomultiplier Data of Speckle Pattern

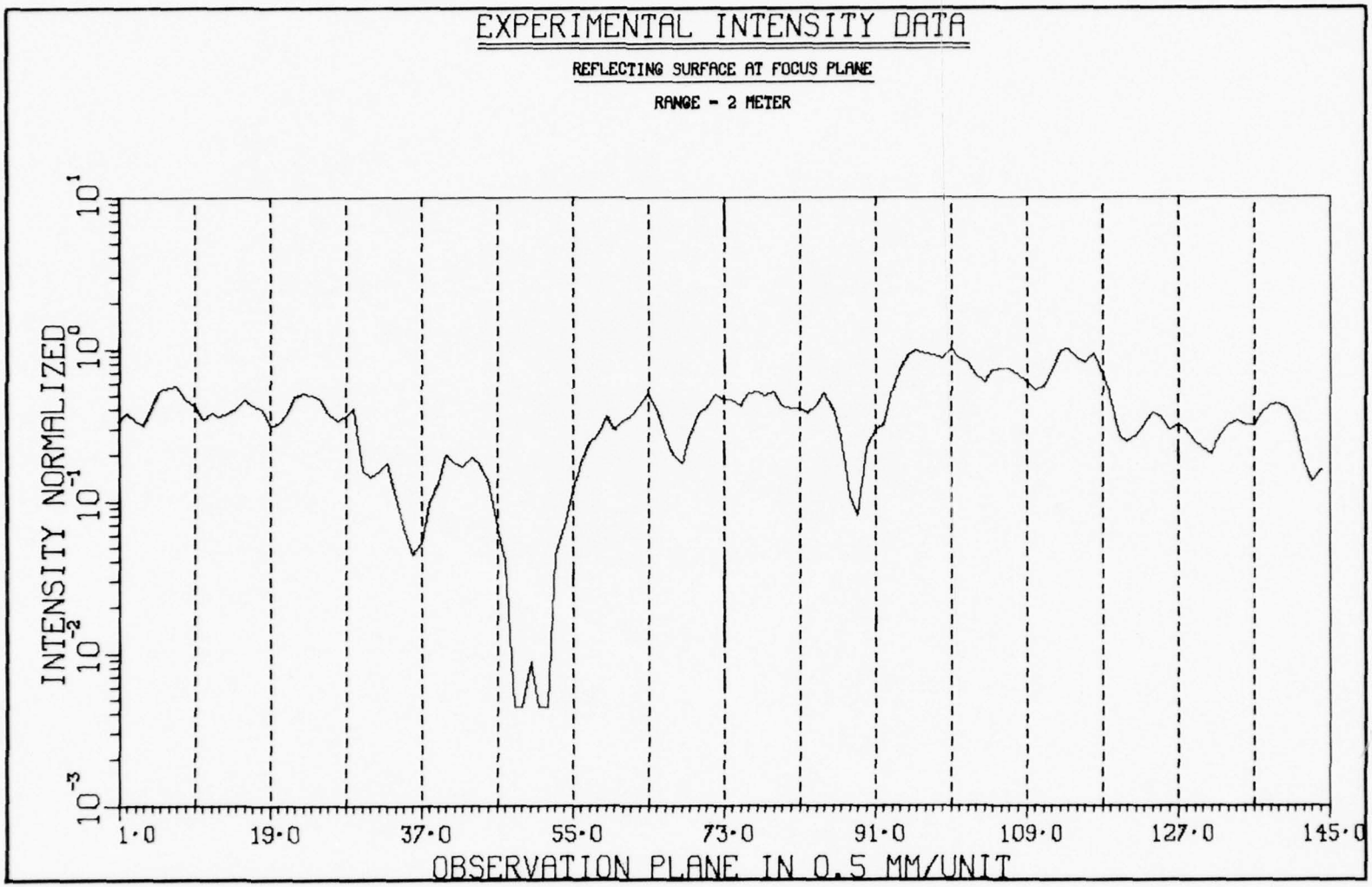

Fig. 15 Photomultiplier Data of Speckle Pattern

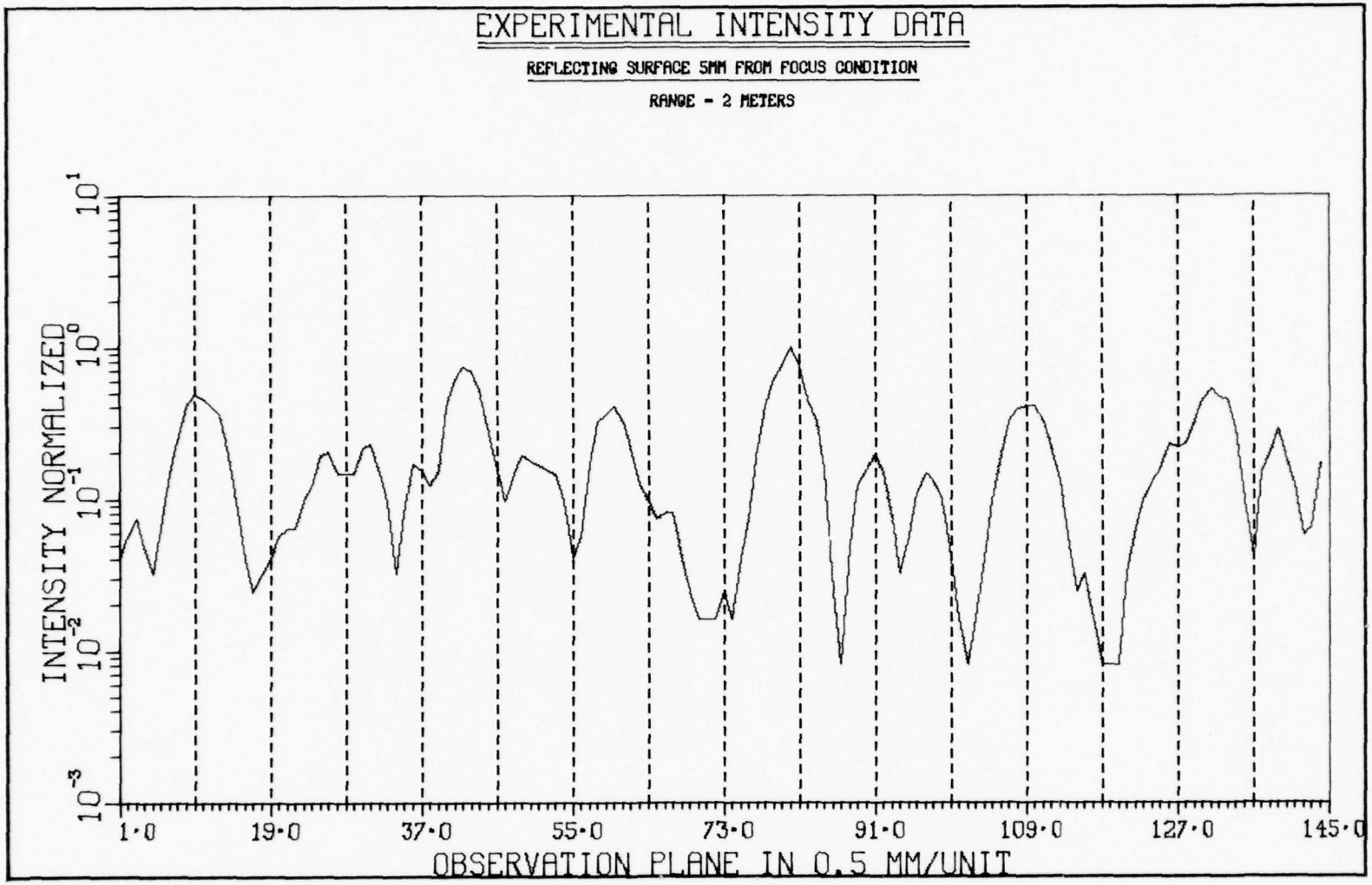

Fig. 16 Photomultiplier Data of Speckle Pattern

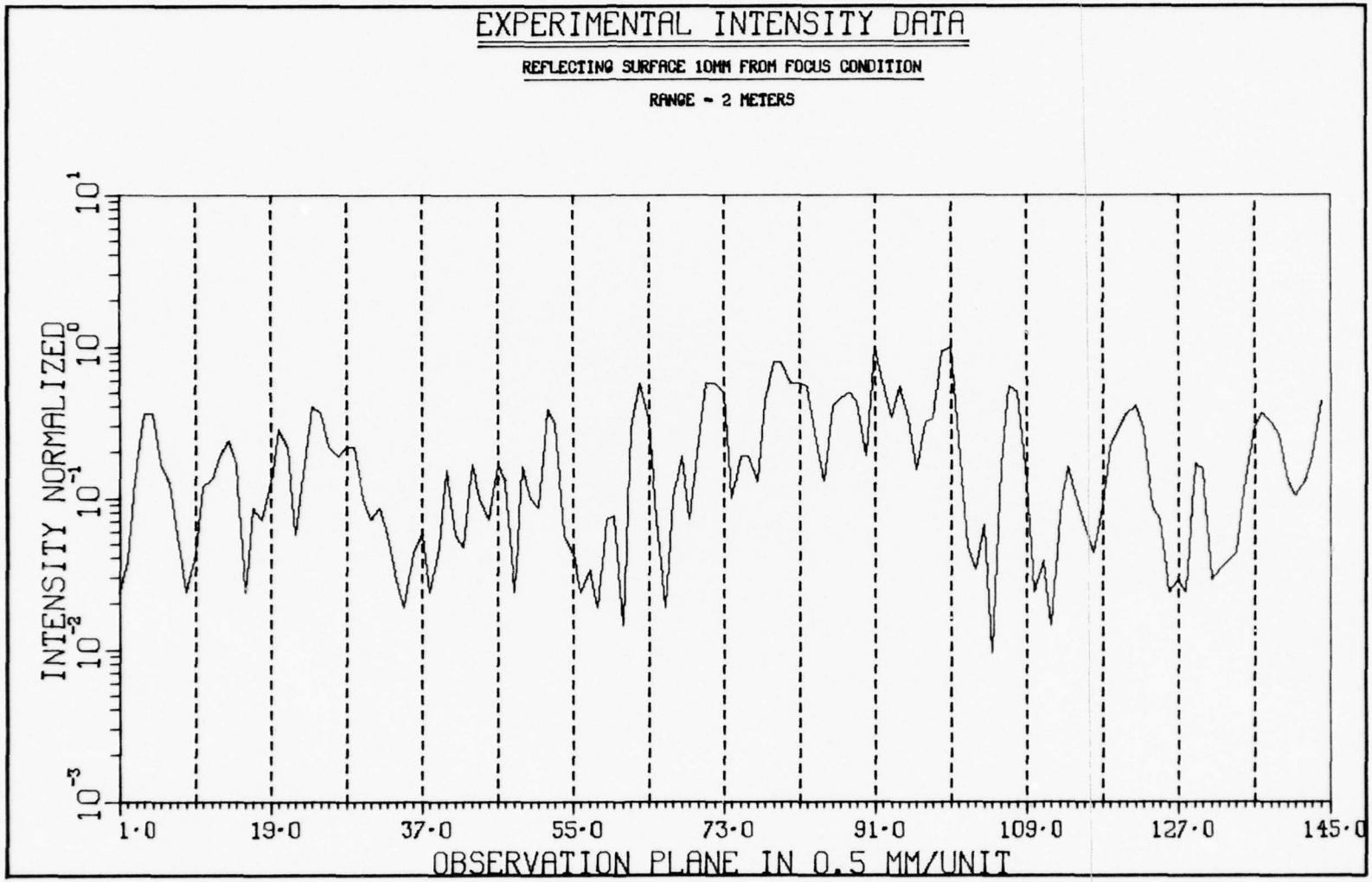

Fig. 17 Photomultiplier Data of Speckle Pattern

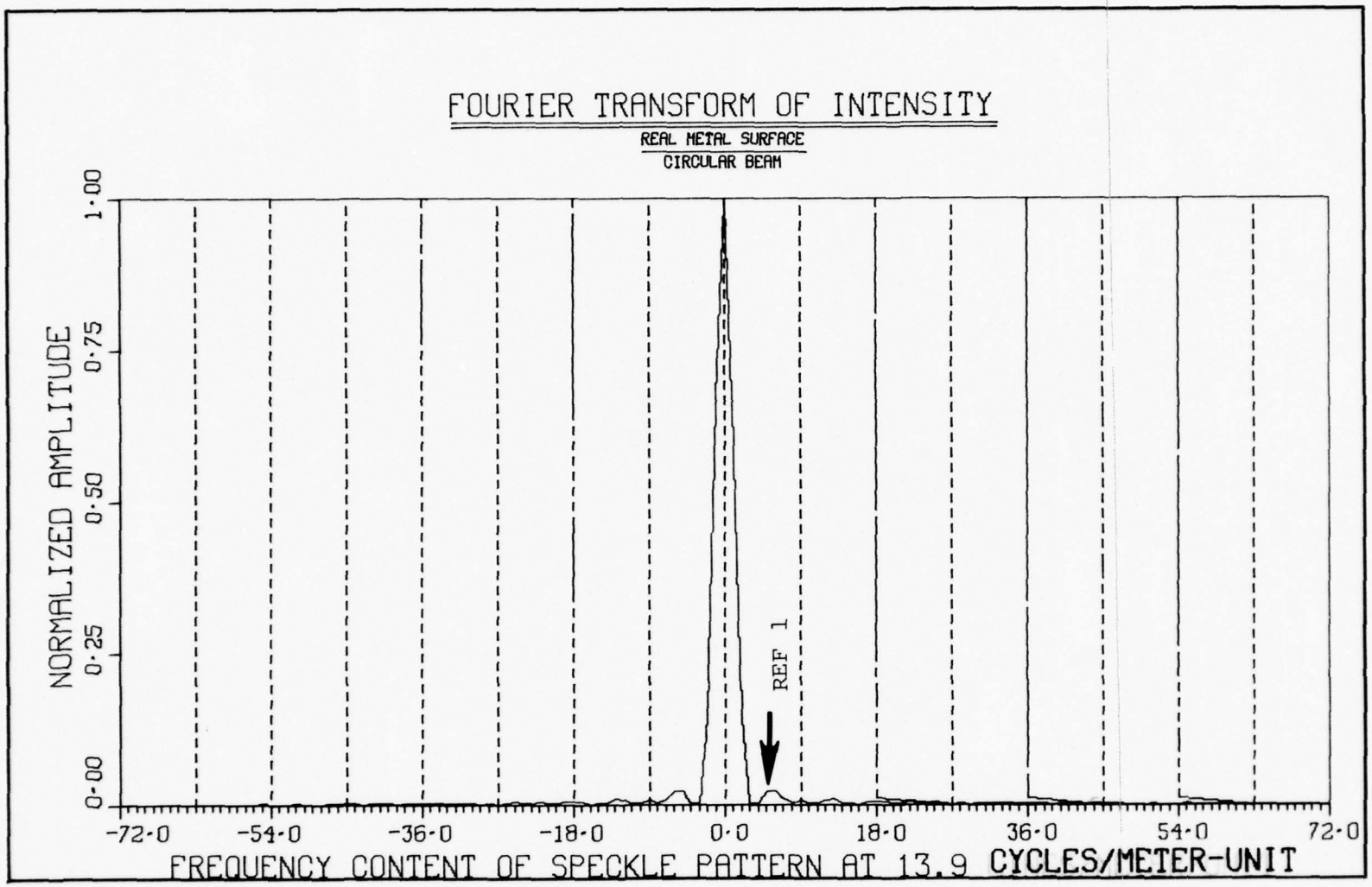

Fig. 18 Fourier Transform of Fig. 14 Intensity Data

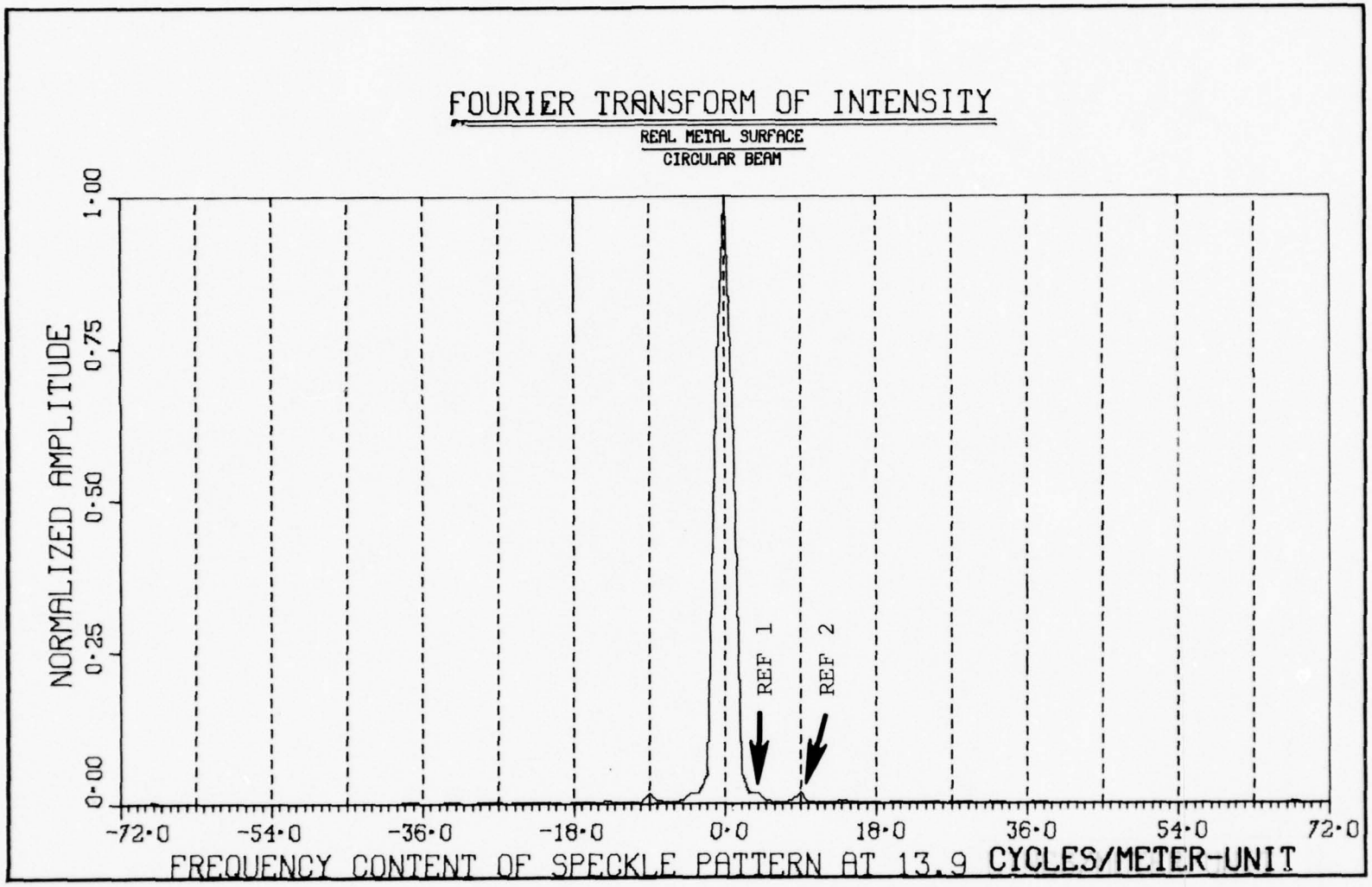

Fig. 19 Fourier Transform of Fig. 15 Intensity Data

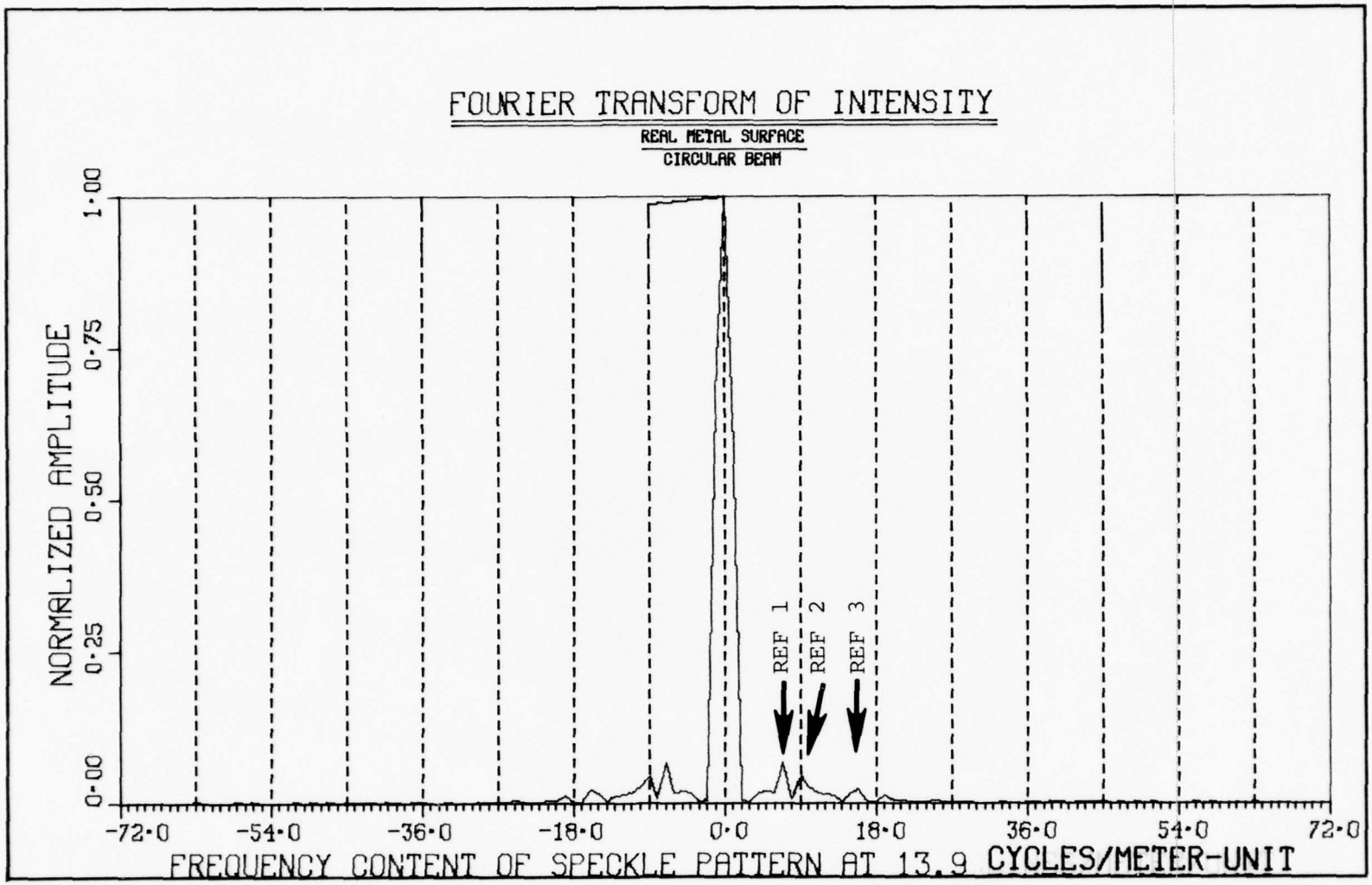

Fig. 20 Fourier Transform of Fig. 16 Intensity Data

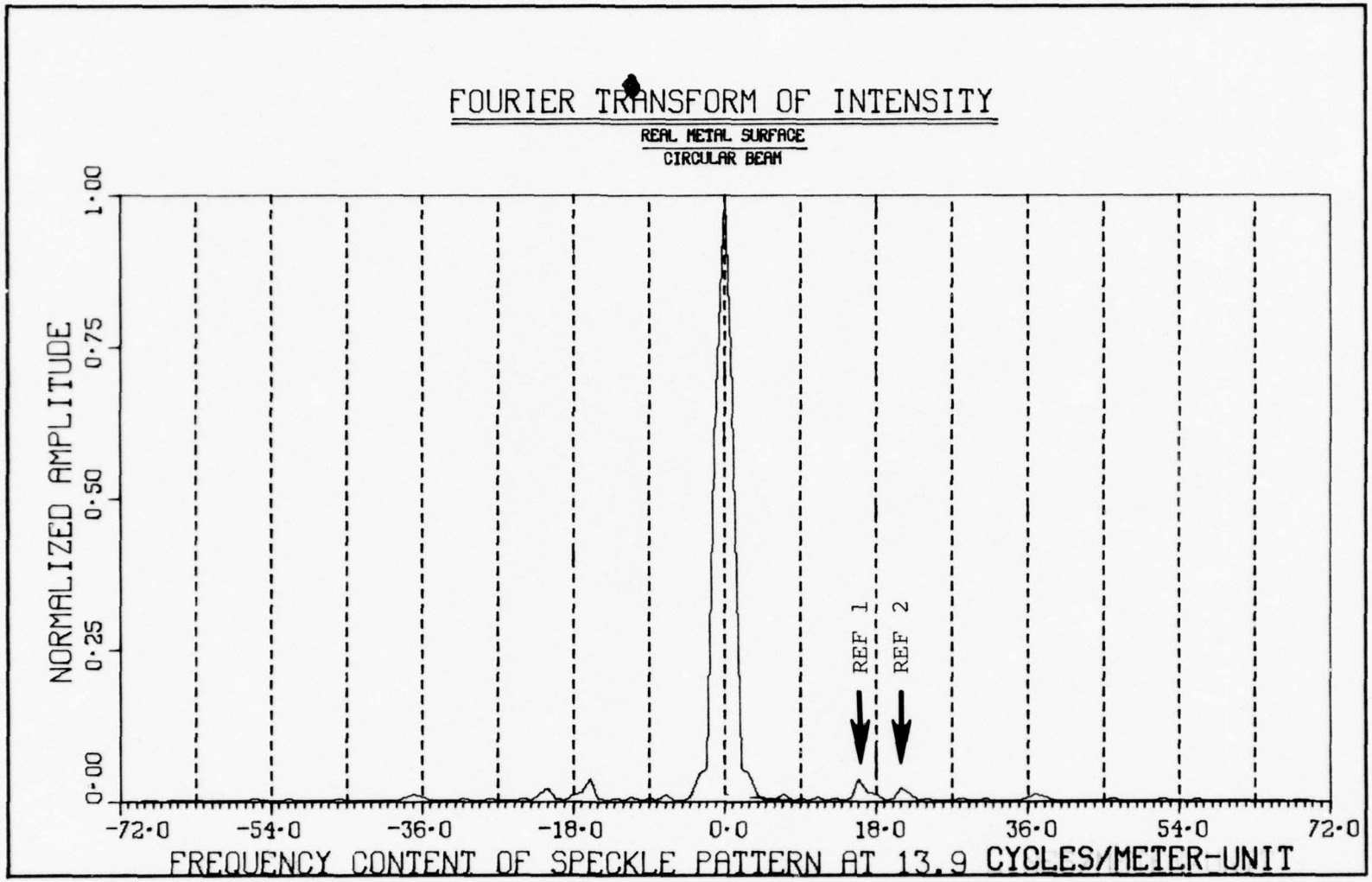

Fig. 21 Fourier Transform of Fig. 16 Intensity Data

representative of the total pattern.

To explain the analysis procedure, Fig. 17 (intensity data) and Fig. 21 (Fourier transform of the data on Fig. 17) will be used. Note that on the Fourier transform plot, Fig. 21, there is a high spatial frequency content around zero cycles/m. This amplitude at zero frequency results from the Fourier transform of the zero frequency level of the input intensity data, Fig. 17. The three REF marks on the spatial frequency plot, Fig. 21, highlight three dominant frequencies that were present in the segment of the speckle pattern sampled. Note that there was a frequency peak at ± 37 units on Fig. 21 that was not highlighted. That frequency was not highlighted because its normalized amplitude was less than 0.01, and only peaks greater than 0.01 were referenced. Since the amplitude and spread of a frequency peak, on the Fourier transform plot, are a measure of the dominance of that frequency in the spatial data, the 0.01 value is an analyst benchmark. Since the Fourier transform plots do not provide the resolution necessary to pick the frequency amplitudes which are greater than 0.01, the tabulated frequency/amplitude data from the program was used.

A typical speckle width was also calculated for each speckle pattern segment analyzed. To obtain the typical speckle width, Eq. 56 was used.

$$\text{Typical speckle width} = \frac{1}{\text{Highest REF frequency}} \qquad (56)$$

Table II

Tabulation of Speckle Pattern Characteristics

Experiment number	1	2	3	4
Figure numbers	14 and 18	15 and 19	16 and 20	17 and 21
Range (m.)	1	2	2	2
Focus condition	focus	focus	5 mm. off	10 mm. off
Incident radiation diameter (mm.)	<0.2	<0.2	>0.2 <0.5	>0.4 <0.8
REF 1 (cycles/m.)	69.5 ± 3.0	41.7 ± 3.0	83.4 ± 3.0	222.4 ± 3.0
REF 2 (cycles/m.)	none	132.0 ± 3.0	125.1 ± 3.0	291.9 ± 3.0
REF 3 (cycles/m.)	none	none	222.4 ± 3.0	none
Typical speckle width (mm.)	14.3 ± 0.5	7.6 ± 0.5	4.5 ± 0.5	3.4 ± 0.5

Since the highest REF frequency was an analyst choice based on normalized amplitudes, the typical speckle width may be subject to error and should be verified. As an example use Figs. 16 and 20. The REF frequency on Fig. 20 is 16 units or 222.4 cycles/m. Using Eq. 56 this gives a typical speckle width of 4.5 ± 0.1 mm. or 9.0 ± 0.2 units on Fig. 16. A close inspection of the intensity data shown on Fig. 16 reveals that 9 units is a good typical speckle width for the data. Figures 17 and 21 also reveal that Eq. 56 is a good evaluation of the intensity data. Table II summarizes the photomultiplier data analysis.

Discussion of Experimental Results

The most tangible conclusion from the experimental investigation of speckle patterns was that when the range from scattering to observation planes was doubled or tripled so did the typical speckle size. This phenomenon was supported by theory (Eqs. 52 and 53), Figs. 8, 9, 10, and the results shown in Table II. Theory also predicts that speckle size should decrease as the reflecting aperture size increases. Although accurate measurements of the scattering spot sizes were not obtained, the experimental results support the theory. This phenomenon can be seen in Figs. 11, 12, 13, and the results shown in Table II.

Although the surface roughness of the scattering plane was not measured, it was obvious that the height variations were greater than the laser wavelength. Recalling from the

theory section, when the reflecting aperture is smooth, the far field diffraction pattern is an Airy pattern where the minor lobes are more than an order of magnitude below the central major lobe. When the scattering surface is rough, height variations greater than the laser wavelength, the secondary lobes can approach the amplitude of the central peak. This characteristic is observed in Fig. 16 where it is very easy to pick out the diffraction lobes. From Eq. 53, of the theory section, the linear dimension of a speckle produced by a circular aperture is

$$R = \frac{1.22\lambda z}{2r} \tag{57}$$

or the diameter of the aperture is

$$D = 2r = \frac{1.22\lambda z}{R} \tag{58}$$

From Table II, experiment 3, if we use the typical speckle size (R) of 4.5 mm., range (z) of 2 m., and wavelength (λ) of 6328 Å, and Eq. 58, the aperture diameter should be approximately 0.3 mm. Note that this value is in the range of the estimated spot size. Rough surface diffraction will be discussed in greater detail in the computer model verification chapter.

IV. SPECKLE Program

A principle part of the time allotted to the completion of this thesis was devoted toward the development of a reliable and accurate computer code to calculate and display speckle (diffraction) patterns. This program was written to satify two requirements: 1.) to provide a simulation tool for the systems control engineers involved in the ALOT system investigation and 2.) to provide visual aids on Fourier optics and diffraction theory for the electro-optics systems engineer.

The SPECKLE program was designed to calculate and plot the far field diffraction pattern resulting from the rough surface scattering of a laser beam. The user of this program must supply two subroutines. The first subroutine, HEIGHS, provides the SPECKLE program with input data including an array, DATA, that contains the scattering surface height measurements normalized by the laser wavelength. The arrangement of the normalized height data, in the array DATA, defines the aperture cross section. The second subroutine, COMAPE, calculates the complex aperture function and returns the result to the SPECKLE program through the array DATA. In the COMAPE subroutine, the normalized surface height data is modified by the complex aperture function model which includes the incident radiation field distribution, AIFIEL (u,v), and the surface reflection coefficient, REF (u,v). These subroutines along with the

SPECKLE program are explained in detail in this chapter

Overview of SPECKLE Program

The SPECKLE program was coded in Extended Fortran and designed to run on the CD 6600 computer at Wright-Patterson AFB, Dayton, Ohio. The core requirements are large, 245,000 (octal) words, with the following approximate assignment for major routines:

SPECKLE	Main program	$75{,}000_8$ words
DATA	Array	$100{,}000_8$ words
FOURT	FFT subroutine	$2{,}000_8$ words
DISSPLA	Plotting package	$67{,}000_8$ words

The DATA array is used for input, common storage for FOURT and DISSPLA, and output routines. This is a two dimensional complex array, thus requiring two consecutive core locations (real and imaginary parts) for every data value. The overall dimensions of this array determines the frequency resolution of the data returned from the FOURT subroutine (see theory section of this thesis). The DISSPLA package is a library program available on the CD 6600 computer at Wright-Patterson AFB.

The computer code consists of a main program (SPECKLE) and six subroutines which are listed on the following page.

HEIGHS	User supplied subroutine to input surface height data
COMAPE	User supplied subroutine to calculate the complex aperture function
FOURT	FFT subroutine
SHIFT	Moves data in array DATA
DISSPLA	Plotting package
VALU	Function subroutine to assist DISSPLA

The following paragraphs describe the operations of the subroutines, the input data descriptions, and finally the flow chart and operation of the main program.

Subroutine HEIGHS

Subroutine HEIGHS is a user supplied routine that inputs data to the SPECKLE program. The following is a list of variables that must be supplied by HEIGHS:

DATA (IROW, ICOL)	Normalized surface height measurements
IROW	Maximum row size of DATA array
ICOL	Maximum column size of DATA array
MRDAT	Maximum number of height data samples in u direction (row)
MCDAT	Maximum number of height data samples in v direction (column)
ALAMBA	Laser wavelength in meters
RANGE	Distance from scattering to observation plane in meters

AMESC	Linear distance between surface height samples in meters
IN2D	Set to 1 if a two dimensional plot of surface height data is desired, 0 otherwise
IN3D	Set to 1 if a three dimensional plot of surface height data is desired, 0 otherwise
INT2D	Set to 1 if a two dimensional plot of speckle pattern is desired, 0 otherwise
INT3D	Set to 1 if a three dimensional plot of speckle pattern is desired, 0 otherwise
ISFREQ	Set to 1 if a plot of the Fourier transform of the two dimensional speckle pattern is desired, 0 otherwise
ISQAP	1 signifies a square aperture shape
ICRAP	1 signifies a circular aperture shape
ICOAP	1 signifies a complex aperture shape
ISMSU	1 signifies a smooth scattering surface
IROSU	1 signifies a rough scattering surface

Subroutine HEIGHS is called from the SPECKLE program by

```
CALL HEIGHS (IROW, ICOL, MRDAT, MCDAT, ALAMBA,
    RANGE, AMESC, IN2D, IN3D, INT2D, INT3D,
    ISFREQ, ISQAP, ICRAP, ICOAP, ISMSU, IROSU)
```

The array DATA is passed through common by

```
COMPLEX DATA
COMMON /A/ DATA (128, 128)
```

The information that is transferred to the SPECKLE program through DATA is the normalized surface height measurements, i.e., actual surface height measurements divided by the laser wavelength. In addition, the normalized height data is centered in the DATA array and the data arrangement describes the aperture cross section. The array DATA is complex, however, the surface height measurements are real, therefore, the data must be entered into the real part of each DATA location. As an example, if the size of the DATA array was 128x128 and a square aperture cross section 15x15 samples was to be represented, only the central 15x15 samples of the DATA array would contain normalized surface height data. All other locations in DATA will be filled with zeros.

The maximum size of DATA must be specified by IROW and ICOL at 128x128, 64x64, 32x32, or 16x16. The maximum number of data samples across the aperture cross section is provided to the main program by MRDAT and MCDAT. MRDAT and MCDAT must be less than IROW and ICOL, and to provide good resolution in the data returned from the fast Fourier transform, the ratios of IROW to MRDAT and ICOL to MCDAT should be large. As an example, let IROW and ICOL equal 128 and MRDAT and MCDAT equal 15 or 31.

Subroutine COMAPE

COMAPE is a user supplied subroutine that transforms the normalized surface height data into the complex aperture function distribution

$$\begin{aligned} &ADATA(I,J) = REF(I,J)*AIFIEL(I,J)* \\ &\quad Exp\{j2\pi*DATA(I,J)*(1.-Cos(GLAZ))\} \\ &ADATA(I,J) = 0 \quad \text{if} \quad DATA(I,J) \text{ is zero} \end{aligned} \tag{59}$$

The complex aperture function distribution is returned to the SPECKLE program through the array DATA(I,J). The input variables to the complex aperture function are as follows:

REF(I,J)	Surface reflection coefficient distribution
AIFIEL(I,J)	Incident field radiation distribution (v/m)
GLAZ	Angle between incident field normal and scattering surface normal ($\leq$0.26 radians)

The variables REF and AIFIEL permits the user to vary the reflection coefficient across the aperture and provide an incident field profile other than a plane wave. For the examples seen in this thesis, REF(I,J) and AIFIEL(I,J) were set to constant, REF and AIFIEL, to reduce the core requirements.

Subroutine SHIFT

Subroutine SHIFT was designed to rearrange data in the complex two dimensional array DATA. The data returned from

the FOURT subroutine (FFT) has the zero frequency magnitude of the Fourier transform positioned in DATA (1,1). Recalling that IROW and ICOL define the maximum dimensions of the array DATA, the highest frequency of the transform is positioned in DATA (1, ICOL/2) in one direction and DATA (IROW/2, 1) in the other direction. The remaining three-fourths of the array DATA contain redundant information. SHIFT rearranges the data to position the zero frequency component in the center of the array and provide a symmetrical Fourier transform function around DATA (IROW/2,ICOL/2).

Subroutine FOURT

The FOURT subroutine (multi-dimensional FFT) used in this program was obtained from the Electrical Engineering Department of the Air Force Institute of Technology, Wright-Patterson AFB, Ohio. The subroutine performs the Cooley-Tukey fast Fourier transform

$$\text{TRANSFORM}\{\text{DATA}(x,y)\} = \sum_{u=1}^{\text{IROW}} \sum_{v=1}^{\text{ICOL}} \text{DATA}(u,v)$$

$$\text{Exp}\{-j2\pi\{\frac{(x-1)(u-1)}{\text{IROW}} + \frac{(y-1)(v-1)}{\text{ICOL}}\}\} \qquad (60)$$

where IROW and ICOL are the maximum row and column dimensions of the array DATA.

Subroutine DISSPLA

The DISSPLA subroutine package is present on the CD6600

computer user library at Wright-Patterson AFB, Ohio. This display package was used because it contained the three dimensional plotting routines used in this thesis.

Function Subroutine VALU

The VALU function is called by the DISSPLA package when a three dimensional plot is desired. The complex aperture function and intensity data are always stored in the complex array DATA, however, DISSPLA plots only real data. VALU assists DISSPLA by providing a real array of data.

SPECKLE Main Program

This section covers the flow of data through the SPECKLE program as outlined in Fig. 22. The operations of the subroutines and the input data formats have been discussed in previous paragraphs and will not be covered in detail in this section of the thesis.

The first operation performed by SPECKLE is to call subroutine HEIGHS which will input the normalized surface height measurements and the other program variables. Control returns to the main program where the normalized surface height data is output on the line printer to provide a numerical record of the input data. The program then checks the plotting option flags (IN2D and IN3D) and determines if one and/or three dimensional plots of the normalized surface height data are requested.

SPECKLE then calls COMAPE to calculate the complex

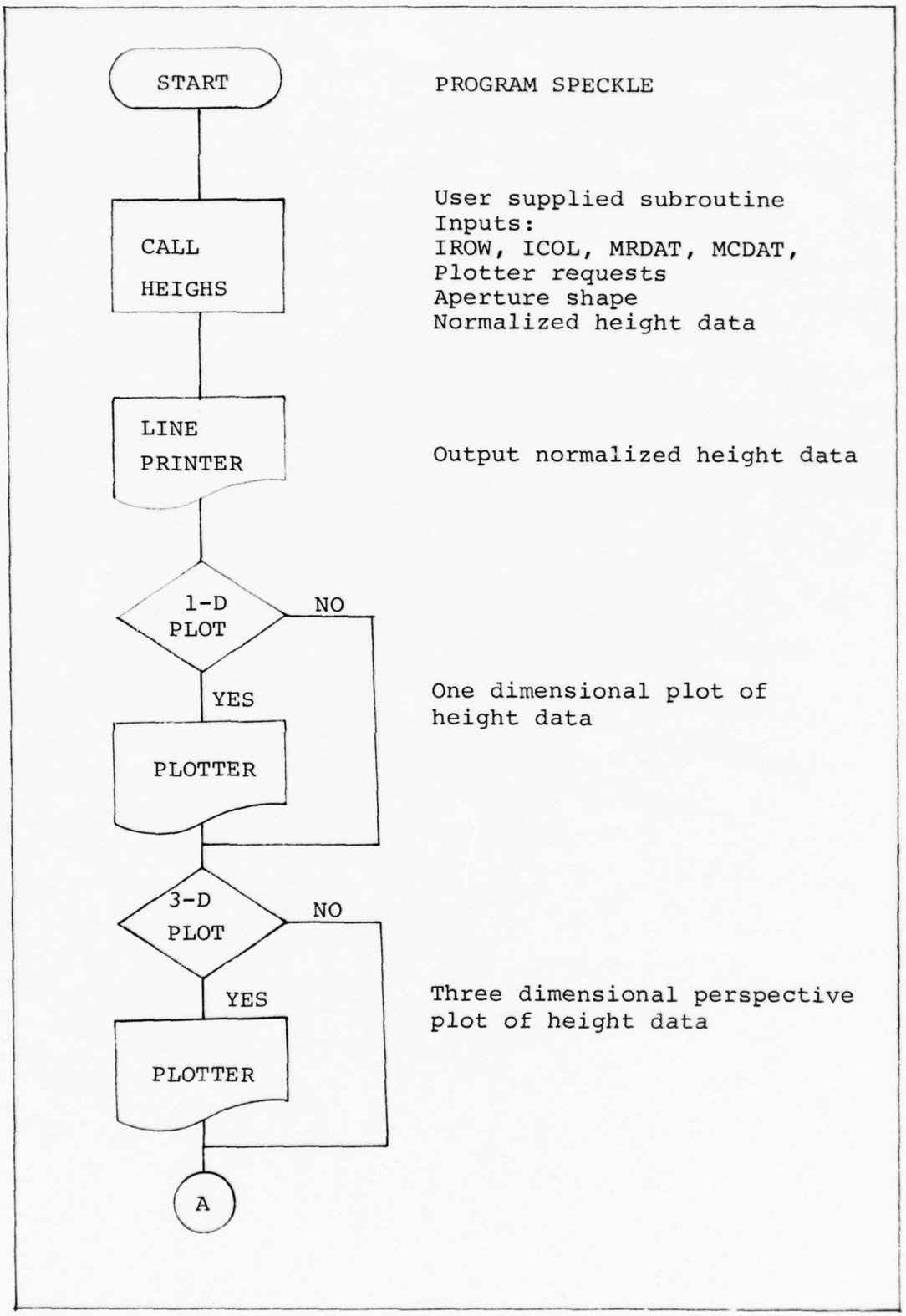

Fig. 22 Flow Chart of the SPECKLE Program (1 of 4)

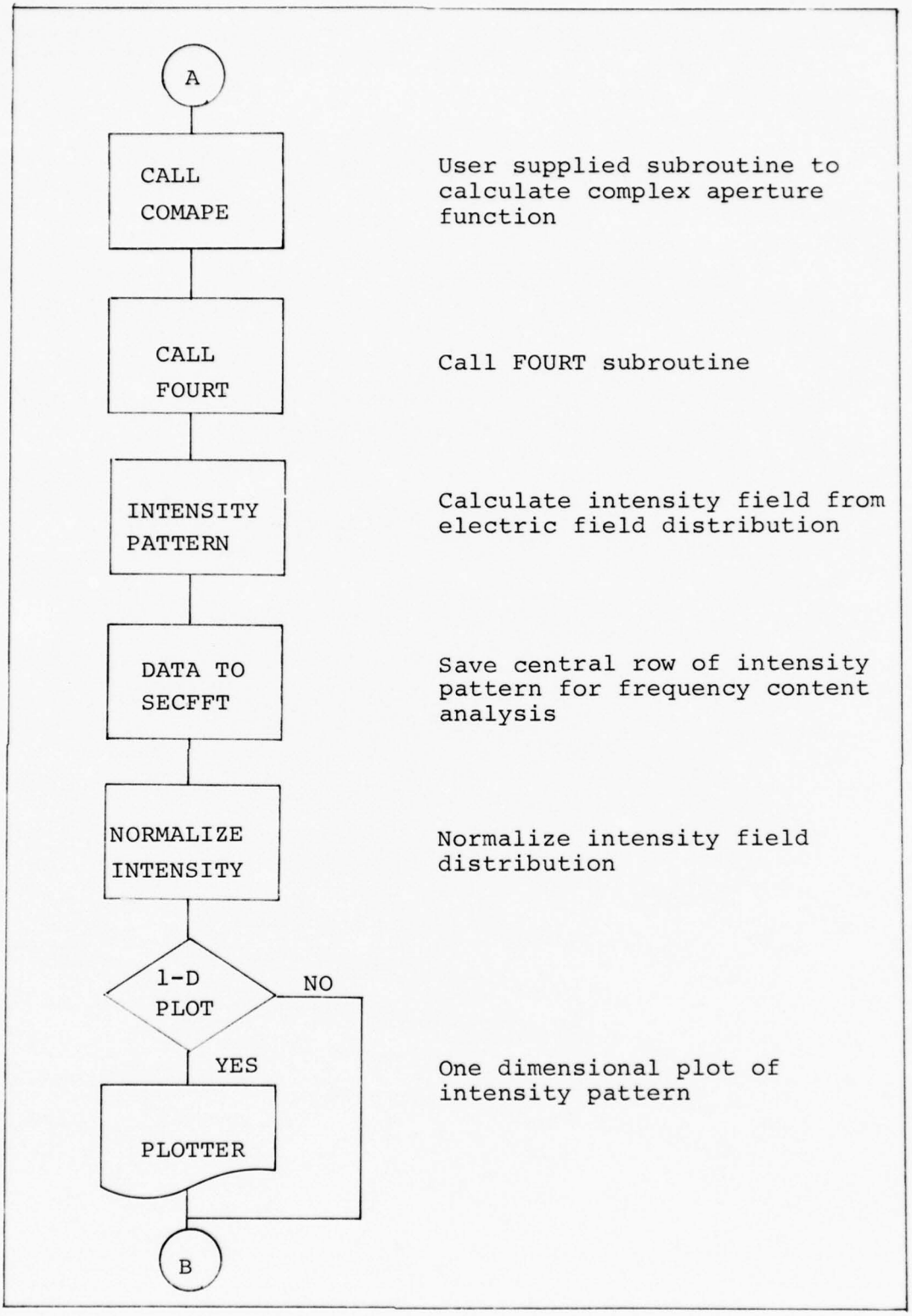

Fig. 22 Flow Chart of the SPECKLE Program (2 of 4)

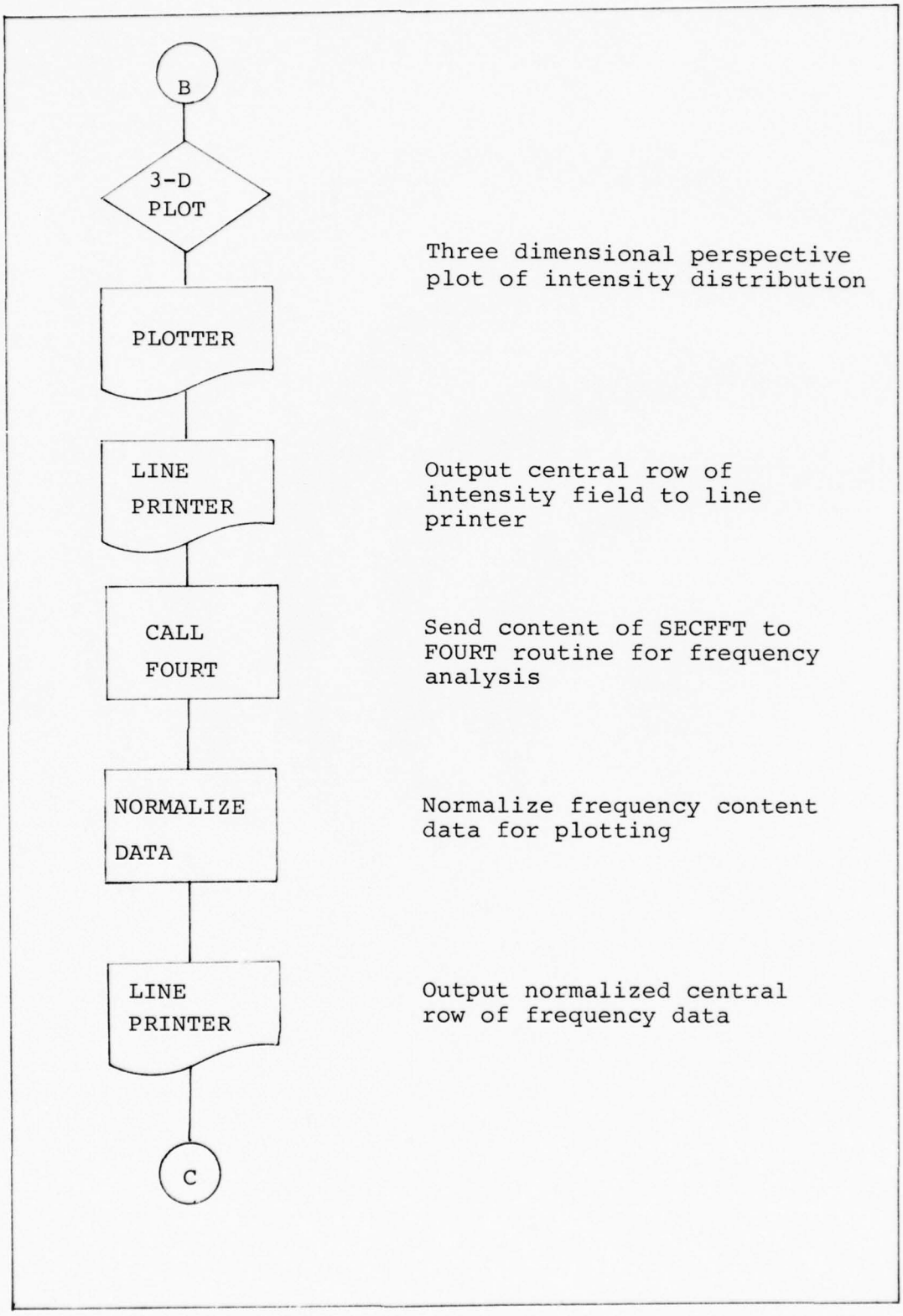

Fig. 22 Flow Chart of the SPECKLE Program (3 of 4)

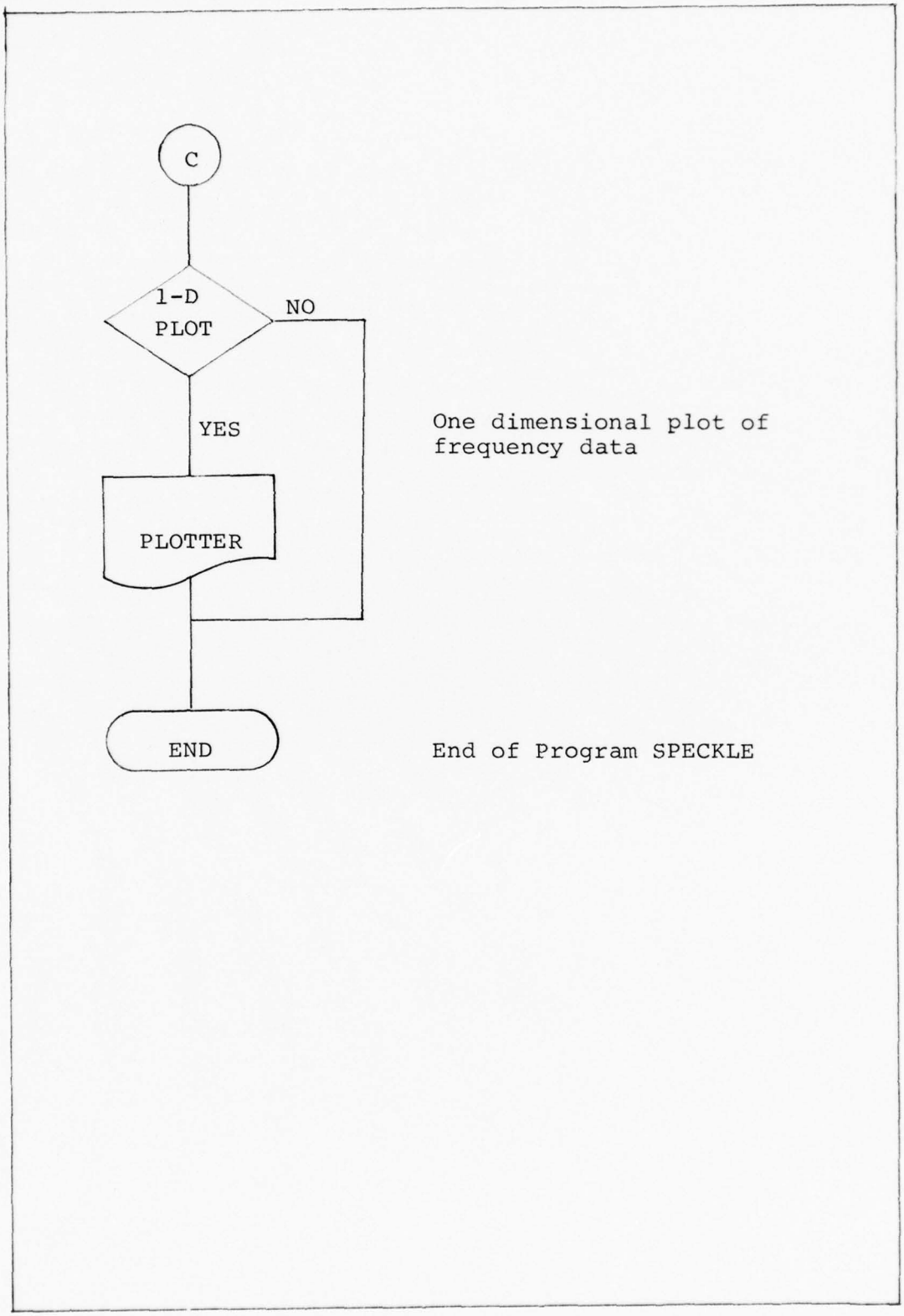

Fig. 22 Flow Chart of the SPECKLE Program (4 of 4)

aperture function. The resulting data is passed to the FOURT subroutine, which returns the two dimensional fast FOURIER transform. The SHIFT subroutine then completes the symmetrical rearrangement on the data to obtain the zero frequency magnitude at the center of the DATA array. The far field idffraction pattern is finally obtained by

$$\text{DATA(I,J)} = \frac{\text{DATA(I,J)(Complex Conjugate DATA(I,J))}}{(2)(\text{ALAMBA})^2(\text{RANGE})^2} \qquad (61)$$

where the distance between samples of the intensity pattern in the observation plane is

$$\text{AMEOB} = \frac{(\text{ALAMBA})(\text{RANGE})}{(\text{IROW})(\text{AMESC})} \qquad (62)$$

This completes the calculation of the intensity speckle (diffraction) pattern, in the far field, as given by Eq. 47 from the theory chapter.

The maximum value of the speckle pattern is located and used to normalize the intensity data in the DATA array. The results of this normalization is an intensity pattern with a maximum of one. Plotter flags (INT2D and INT3D) are checked to see if one dimensional and/or three dimensional plots of the speckle pattern are desired. In addition, the intensity data along row IROW/2 of the array DATA is stored in array SECFFT for future use and is also printed out on the line printer for a numerical record and

to obtain better resolution than provided on the plots.

The remaining portion of the program computes the frequency content and proper scaling factors for the center row of the two dimensional speckle pattern. This is accomplished by first sending the data previously saved in array SECFFT to FOURT for a one dimensional Fourier transform and then performing a single row shift operation (recalling that SHIFT is used on two dimensional arrays). The pattern is normalized, plotted if requested, and a listing of the amplitudes is provided on the line printer. The program is then terminated.

SPECKLE Program Deck Structure

Figure 23 shows the deck structure required to run the SPECKLE program on the CDC 6600 computer at Wright-Patterson, AFB.

SPECKLE Program Example

For this example, the normalized surface height data was an 15x15 array (square aperture shape) and the DATA array was dimensioned at 128x128. The laser wavelength was 6328 Å, range was 1000 meters, and the distance between surface height measurements was 0.1 millimeters. All output plots were requested.

Figures 24 through 28 are the five plots produced by the SPECKLE program. Figures 24 and 25 show the normalized scattering surface height distribution for the rough surface, a one dimensional cut and a three dimensional perspective.

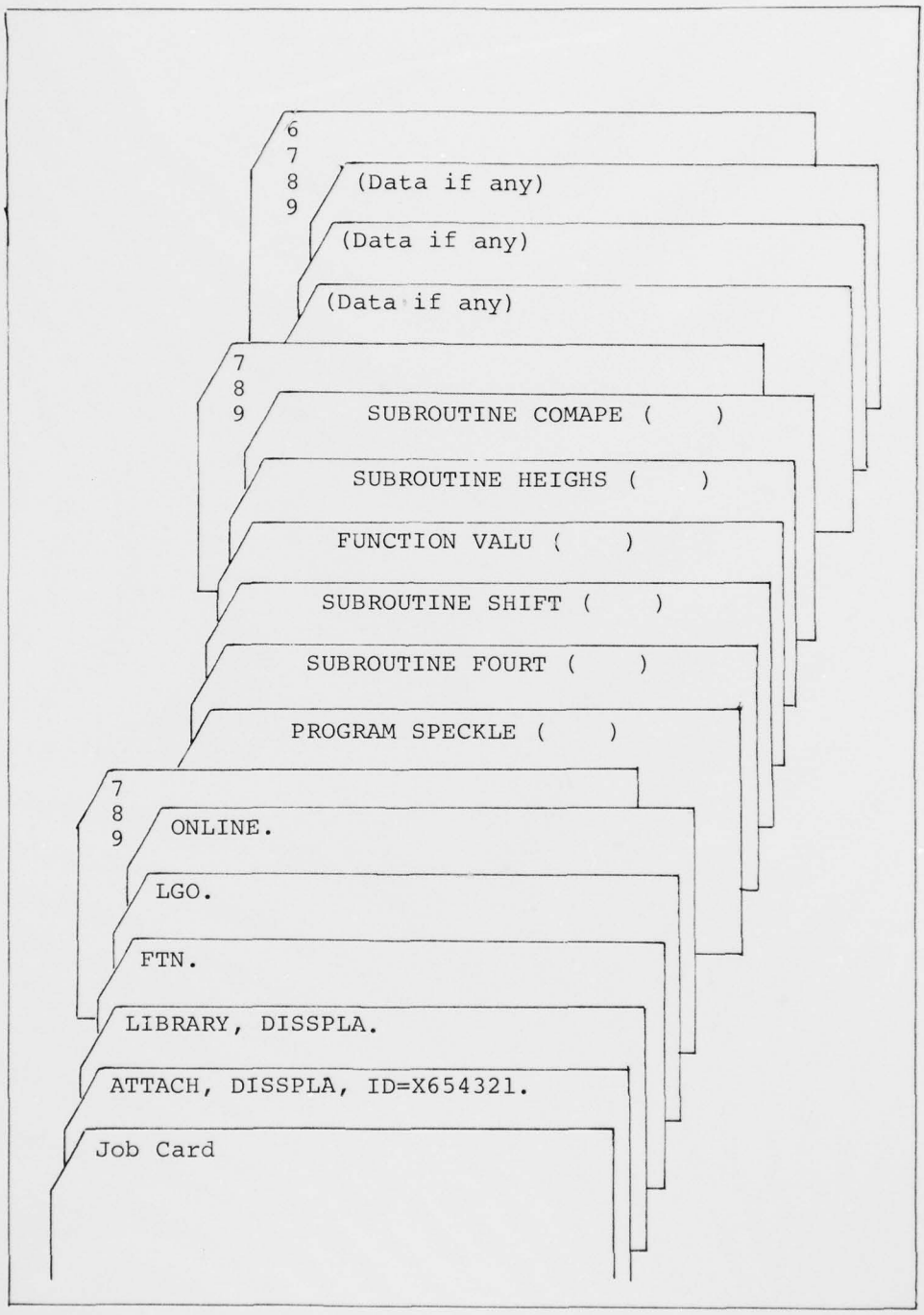

Fig. 23 SPECKLE Deck Structure

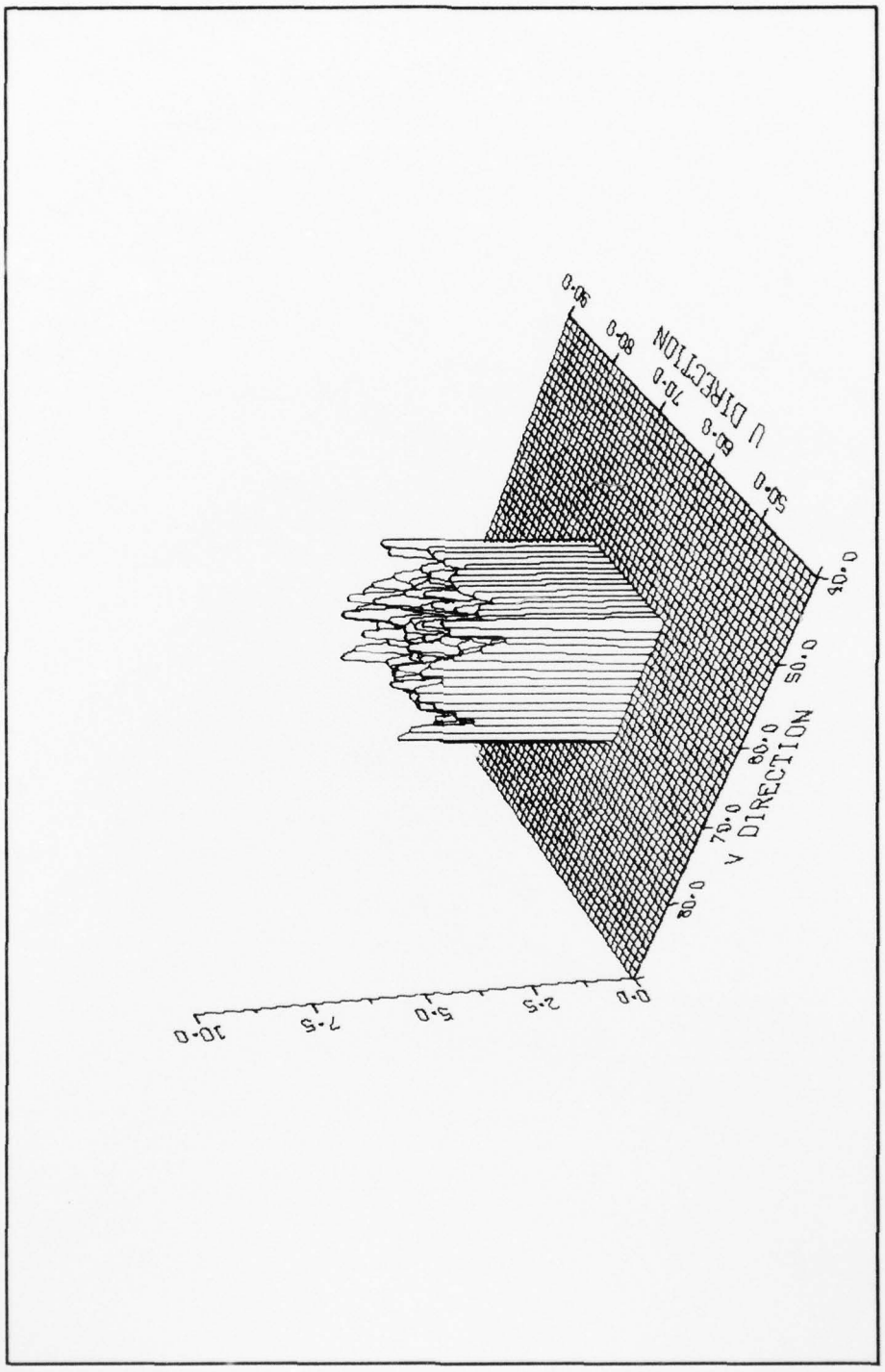

Fig. 24 Normalized Surface Height Data

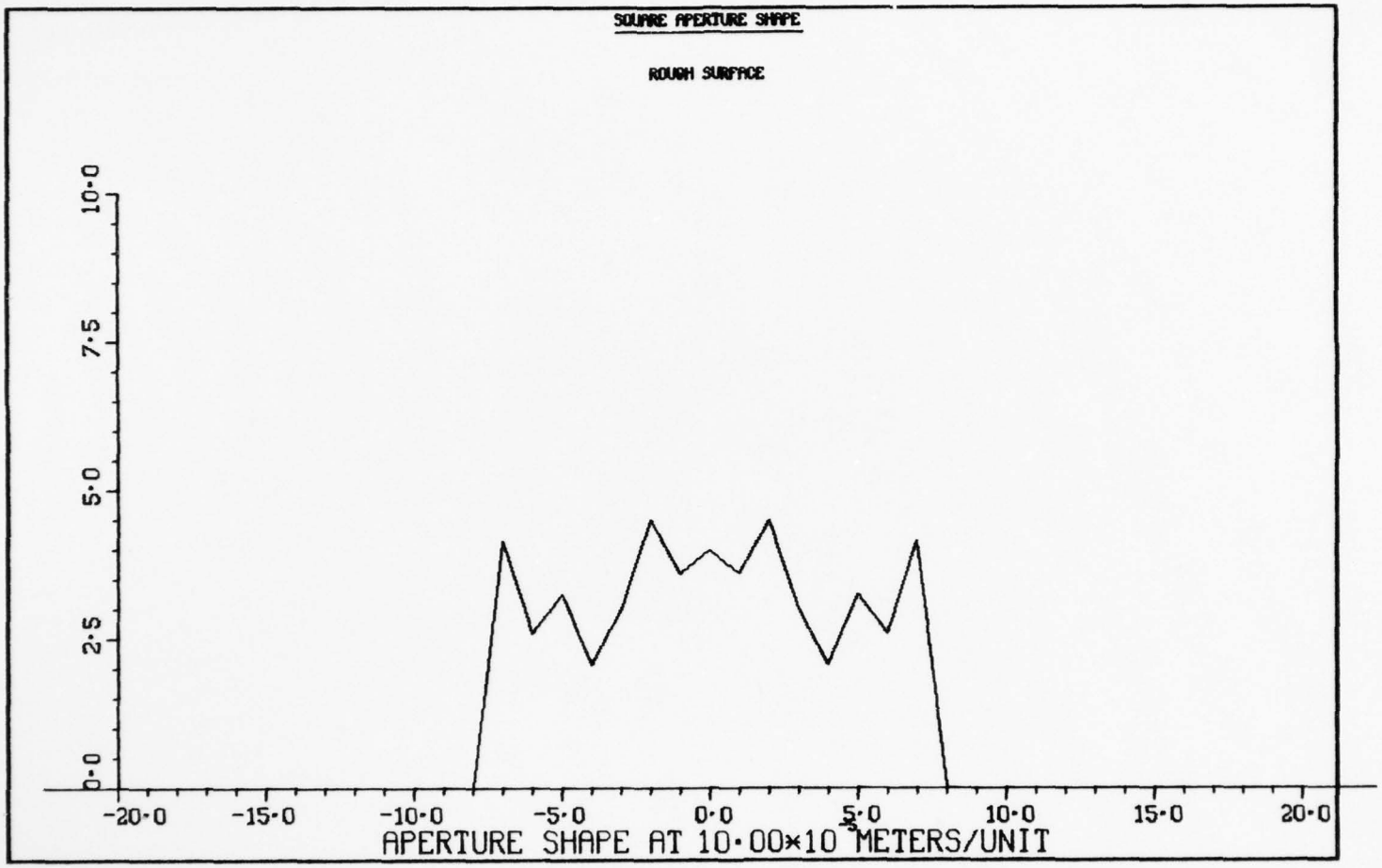

Fig. 25 One Dimensional Cut Through Fig. 24

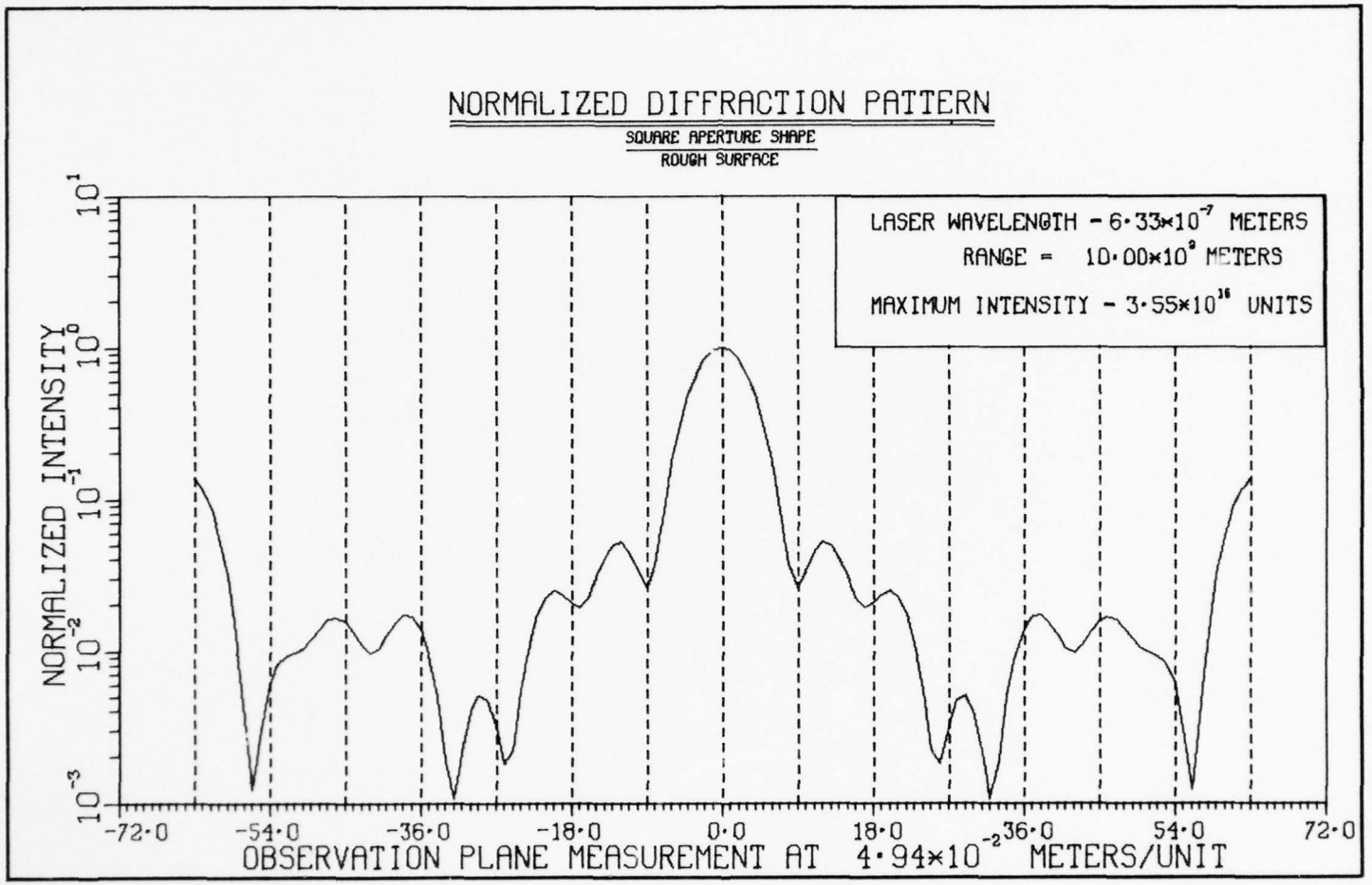

Fig. 26 One Dimensional Cut Through Speckle Pattern

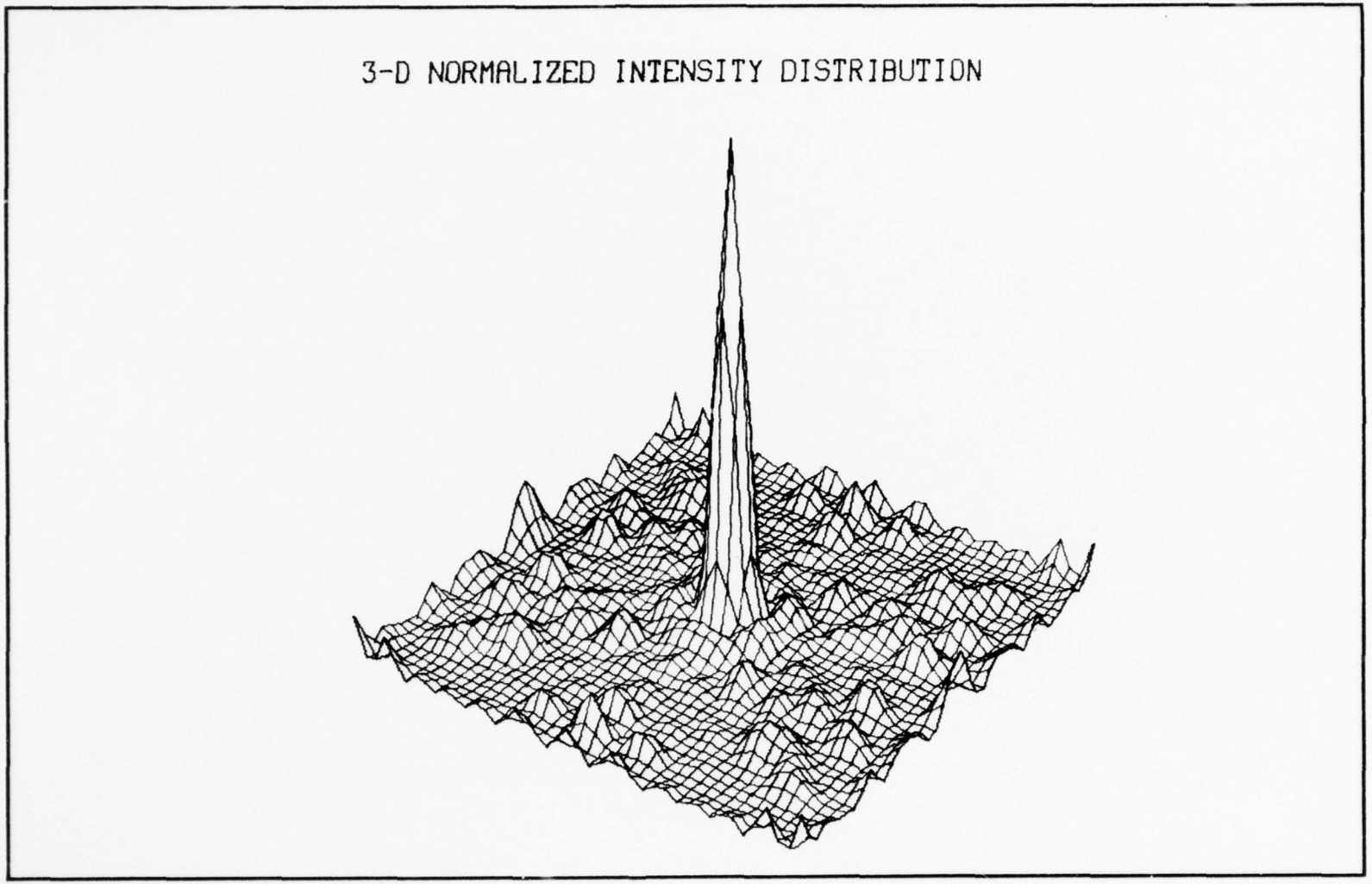

Fig. 27 Three Dimensional Perspective of Speckle Pattern

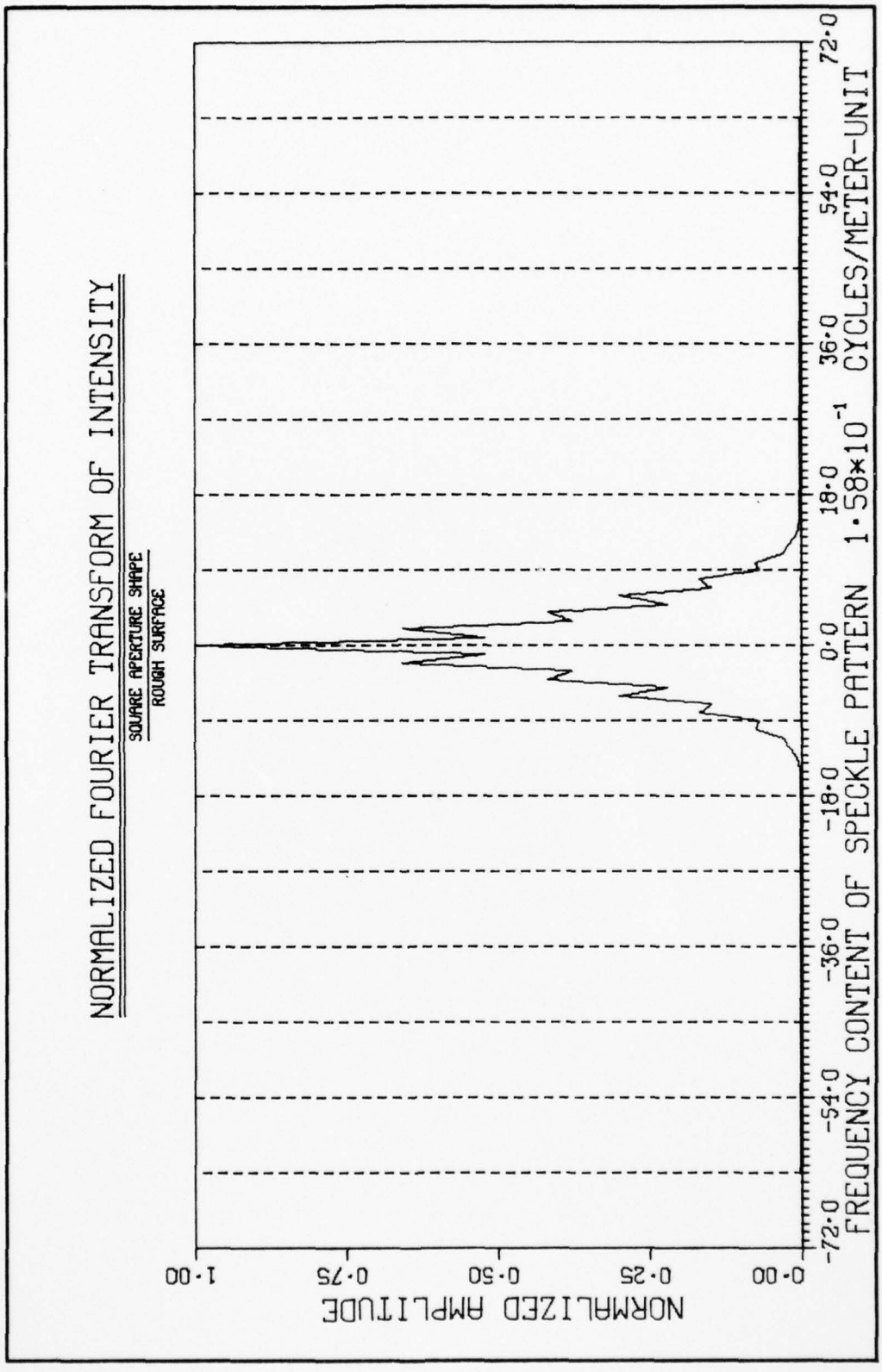

Fig. 28 Fourier Transform of Fig. 26 Data

Figures 26 and 27 show the speckle (diffraction) pattern at the observation plane. Figure 26 shows a one dimensional cut through the center of the intensity pattern, plotted on a log-linear graph. Figure 27 is a three dimensional perspective of the intensity pattern, plotted with three linear axis. Figure 28 is a one dimensional plot of the Fourier transform of Fig. 26. By noting on Fig. 28 that the normalized frequency content goes to zero at 15.0 units or 2.37 cycles/meter (15.0 units x .158 scale factor), the typical width of the intensity lobes in the intensity pattern should be 0.422 meters (1/frequency). On Fig. 26, 0.422 meters is equivalent to 8.54 units (0.422/4.94E-2), which is the width of a typical speckle lobe.

Recalling from the theory chapter, the typical diffraction (speckle) lobe width is related to the linear size of the aperture by

$$\text{Aperture Width} = \frac{\lambda z}{\text{Typical Lobe Width}} \tag{63}$$

From the previous paragraph, the typical lobe width was 0.422 meters. Using Eq. 63 the aperture width should be 15E-3 meters. This was the size of the reflecting area.

Conclusion

The SPECKLE program is designed to calculate and plot the speckle pattern, in the far plane, produced by rough surface scattering of a laser beam. The user is required to

provide two subroutines, one which inputs the normalized surface height measurements to the program and one which calculates the complex aperture function model. The scattering aperture cross section is described by the arrangement of the normalized surface height measurements in the array DATA through the subroutine HEIGHS. The profile of the incident radiation field and the distribution of the surface reflection coefficients can be modeled in the complex aperture function subroutine COMAPE. One model for the complex aperture function, as described by Goodman (REF.6), has been described and used in this thesis, however, COMAPE enables the user to use a different model if desired.

This chapter was written to describe in detail the operation of the program and the significance of each variable. Appendix A contains a listing of the SPECKLE program and the two user supplied subroutines used by this author to analyze speckle patterns produced by rough surface (simulated data) scattering of a laser beam.

V. Verification of the Speckle Program

This chapter will address the validity of the computer model used to generate speckle patterns produced by rough surface scattering by comparing the computer simulations with theory and experimental results. The speckle pattern phenomena that will be discussed are the affects on typical speckle size from range and scattering surface size variations and the changes in speckle pattern distributions caused by variations in scattering surface roughness and surface reflectivity. Because of the numerous computer plots required to completely describe the various characteristics, all data plots appear in Appendix B.

Speckle Patterns from Smooth Surfaces

The simplest diffraction patterns result when the scattering surface is smooth, i.e., no phase variations across the reflecting area. The two smooth diffracting apertures that are always discussed and analyzed in optics text books (Refs.7 and 12) are those with square (rectangular) and circular cross sections. The square aperture produces the well known $|\mathrm{Sinc}(x)|^2$ normalized intensity distribution in the far field, which was given by Eq. 48 and repeated here as

$$I(x,y) = \left[\frac{\mathrm{Sin}(\frac{\pi bx}{\lambda z})}{\frac{\pi bx}{\lambda z}}\right]^2 \left[\frac{\mathrm{Sin}(\frac{\pi by}{\lambda z})}{\frac{\pi by}{\lambda z}}\right]^2 \qquad (64)$$

or

$$I(x,y) = \left(\frac{\text{Sin } \beta}{\beta}\right)^2 \left(\frac{\text{Sin } \gamma}{\gamma}\right)^2 \tag{65}$$

where β and γ represent the arguments of the sine functions in Eq. 64. Recalling from the theory section that λ = laser wavelength, Z = range, and b = aperture width.

The extrema of I(x,y) can be found by taking the derivative of Eq. 65 and setting it equal to zero. In one dimension the derivative is

$$\frac{dI(x)}{d\beta} = \frac{2 \text{ Sin } \beta \ (\beta \text{Cos}\beta - \text{Sin}\beta)}{\beta^3} \tag{66}$$

From Eq. 66 the irradiance is zero (nulls) when $\beta = n\pi$, where $n = 1, 2, \cdots\infty$. The maxima are found from the solutions of the transcendental function

$$\beta \text{ Cos } \beta - \text{Sin } \beta = 0 \tag{67}$$

which reduces to

$$\text{Tan } \beta = \beta \tag{68}$$

From Eqs. 66 and 68 the first three nulls occur at $\beta = \pi$, 2π, and 3π and the first three maxima occur at $\beta = 1.4303\pi$, 2.4590π, and 3.4707π.

Figures 29 through 32 of Appendix B are plots produced by the speckle model program for a square aperture, simulated by discrete data, where λ = 6328 Å, Z = 1000 m., and

b=1.5 millimeters. Table III lists the values of the normalized peaks and locations of the nulls as predicted by theory and calculated by the program as shown in Fig. 31. The computer listing provided when Fig. 31 was plotted was used to obtain the resolution of the normalized peaks reported in Table III. It should be noted that the first null of Fig. 31 does not go to zero. The reason for this unexpected result is that the zero value did not fall on a discrete data sample.

Table III

Smooth Surface Square Aperture
Figure 31 (Appendix B)
Diffraction Pattern Characteristics

	Null Location from Theory (m)	Null Location from Program (m)	Peak Amplitude from Theory	Peak Amplitude from Program
First	0.422	0.420	0.0472	0.0448
Second	0.844	0.840	0.0164	0.0167
Third	1.266	1.260	0.0083	0.0091

Although not developed in the theory section, the normalized intensity pattern, in the far field, for circular aperture reflection (Ref.7:352) is

$$I(x) = \left[\frac{2\ J_1\left(\frac{2\pi bx}{\lambda z}\right)}{\frac{2\pi bx}{\lambda z}}\right]^2 = \left[\frac{2\ J_1(2\beta)}{2\beta}\right]^2 \qquad (69)$$

In Eq. 69, b is the radius of the aperture, x is the radius in the observation plane, J_1 is a first order Bessel function of the first kind, and β, λ, and Z are defined as before. Equation 69, when plotted, is the well known Airy function. The first three nulls are obtained when J_1 equals zero, i.e., β = 3.831, 7.016, and 10.17 (Ref.13:250). From the equation of β, the x values can be calculated if λ, b, and Z are given. The derivative of Eq. 69 can be set equal to zero to obtain the maxima values, where $d\,J_1(2\beta)/d\beta = J_2(2\beta)$. The first three secondary peaks occur at β = 5.135, 8.417, and 11.619 (Ref.13:250).

Figures 33 through 36 of Appendix B are plots provided by the speckle program for a simulated discrete circular aperture where λ = 6328 Å, Z = 1000 m., and b = 1.5 millimeters. Table IV lists the values of the null locations and normalized secondary peak amplitudes for the data shown in Fig. 35 and as predicted from theory.

Table IV

Smooth Surface Circular Aperture
Figure 35 (Appendix B)
Diffraction Pattern Characteristics

	Null Location from Theory (m)	Null Location from Program (m)	Peak Amplitude from Theory	Peak Amplitude from Program
First	0.248	0.247	0.0175	0.0140
Second	0.456	0.454	0.0042	0.0037
Third	0.661	0.667	0.0016	0.0012

Figures 29 through 36 and Tables III and IV are data, for smooth scattering surfaces (square and circular), calculated from theory and by program SPECKLE. With the data already analyzed there is a good correlation between theory prediction and computer model results. The small differences in results observed in Tables III and IV, can be contributed to discrete data processing.

Effect of Range on Typical Speckle Size

The typical speckle size is directly proportional to range as predicted by theory and as shown by the experimental investigation of speckle. The chapter on the experimental investigation of speckle patterns shows photographic and photomultiplier data that supported the theory.

Figures 37 through 45 of Appendix B are plots provided by the SPECKLE program to aid in the analysis of the effect of range variations on typical speckle size. Figures 37 and 38 are plots of the normalized scattering surface height variations and Fig. 39 is a three dimensional perspective plot of the intensity pattern at the observation plane. Although these plots show a rough scattering surface, the effect of the rough surface on the speckle pattern will not be discussed in this subsection of the chapter. Figures 40 through 45 show one dimensional cuts through each of the three dimensional perspective plots of the intensity patterns and Fourier transform plots of the respective one dimensional cuts. For these calculations, observation planes

were located at 500 m., 1000 m., and 1500 m. from the scattering surfaces as indicated on the one dimensional intensity plots.

On Figs. 41, 43, and 45 the reference (REF) marks indicate where the normalized Fourier transform plot goes to zero. The inverse of each reference spatial frequency provides a measure of the typical speckle width on the respective one dimensional intensity plot. Table V lists the reference spatial frequencies and typical speckle sizes for the three ranges indicated. From the data in Table V it is apparent that the speckle model accurately calculated the effect of range variations on typical speckle size.

Table V

Typical Speckle Size vs Range

Range (m.)	500	1000	1500
Reference Frequency (Cycles/m.)	4.74	2.37	1.57
Typical Speckle Size (m.)	0.211	0.422	0.633
Plots (Appendix A)	40 and 41	42 and 43	44 and 45

Effect of Reflecting Surface Size Variations on Typical Speckle Size

In the theory section it was shown that the typical speckle size is inversely proportional to the reflecting surface size. The experimental analysis of speckle patterns produced by rough surface scattering supported the theory through photographic and photomultiplier data analysis.

AD-A039 696 AIR FORCE INST OF TECH WRIGHT-PATTERSON AFB OHIO SCH--ETC F/G 20/5
MODEL FOR PREDICTING LASER SPECKLE PATTERNS RESULTING FROM ROUG--ETC(U)
MAR 77 W E LANDIS

UNCLASSIFIED AFIT/GEO/EE/77-1 NL

2 OF 3
AD
A039696

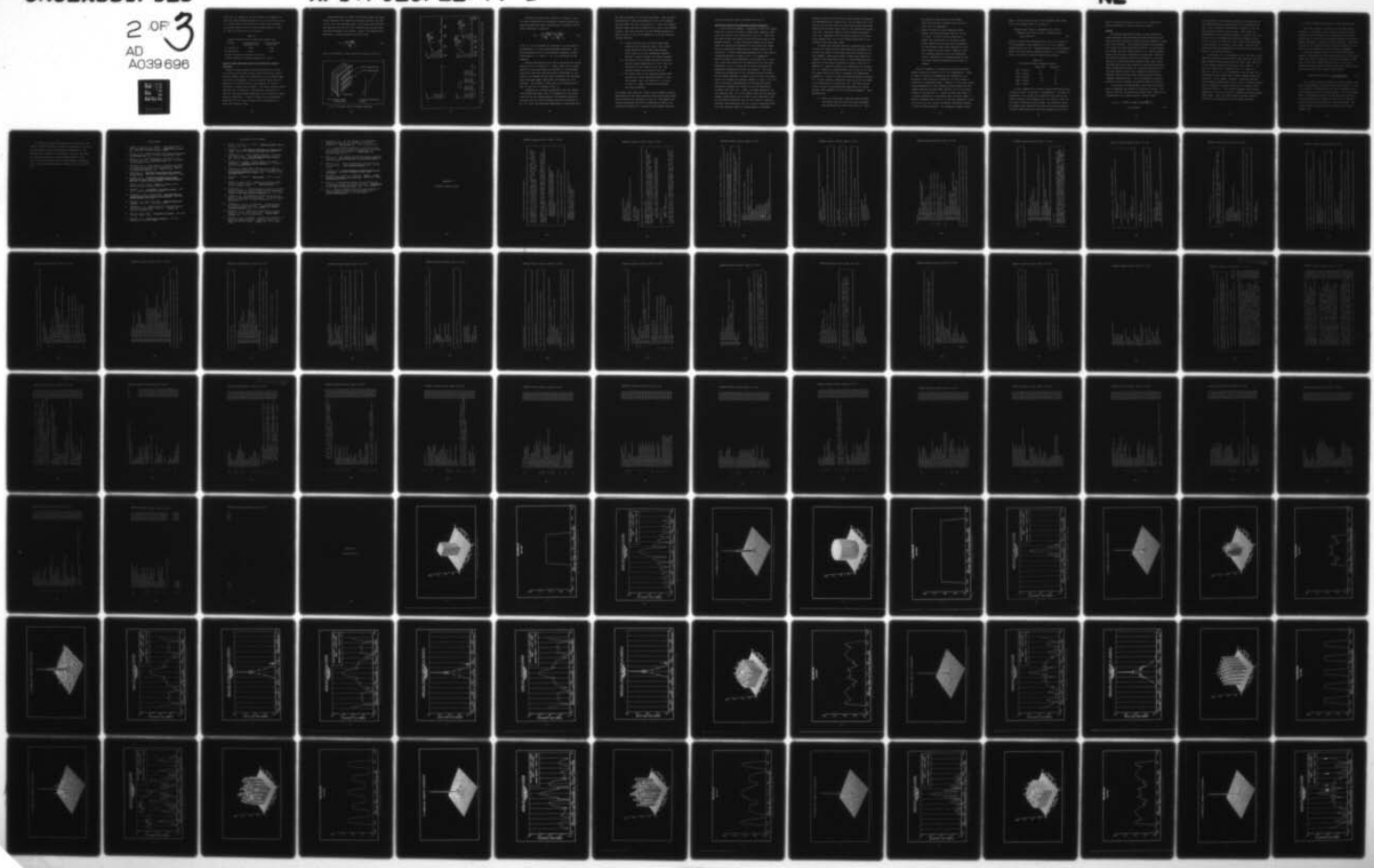

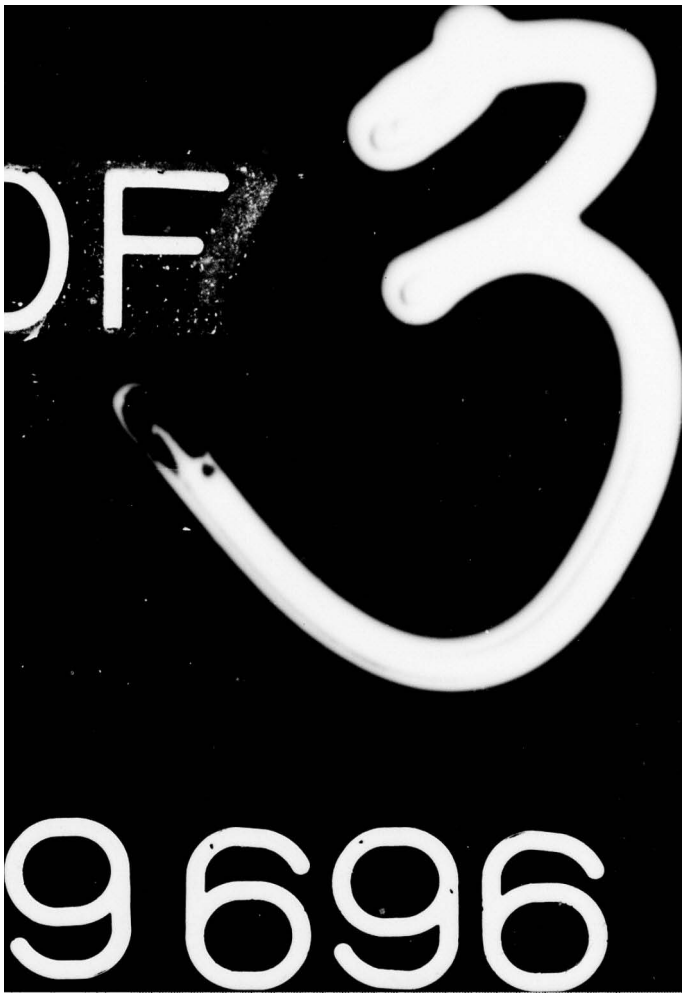
OF
3
9696

From Figs. 37 through 41, and 46 through 50 of Appendix B, using the same analysis procedure as in the previous section, it is shown that as the reflecting surface size increases the typical speckle size is reduced proportionally. Table VI lists the results from the analysis.

Table VI

Typical Speckle Size vs Scattering Surface Size

Figures	Surface Linear Measurement (m.)	Typical Speckle Size (m.)
37 through 41	15E-4	0.422
46 through 50	31E-4	0.204

Percent increase in surface size +106.7

Percent decrease in typical speckle size -106.8

Equally Spaced Apertures with Zero Reflectivity Between Apertures

Before discussing speckle patterns produced by scattering surfaces with random surface height variations, pulsed aperture shapes, where the reflectivity is zero between apertures will be discussed. The term "pulsed" means that the aperture is a periodic array of rectangular or circular reflecting (transmitting) surfaces. The areas for each unique aperture have a reflection (transmission) coefficient of 100% and the areas between apertures a zero reflection (transmission) coefficient. Figure 51 shows a three dimensional perspective of an array of square holes illuminated by a plane wave coherent laser.

Representations for single and multiple pulse one dimensional apertures and respective intensity patterns are shown on Fig. 52 on the following page. The single pulse discrete data aperture and its far field intensity pattern have been discussed throughout this thesis. Recall the normalized one dimensional intensity pattern has the form of

$$I/I_0 = \left[\frac{\mathrm{Sin}(\frac{\pi qx}{\lambda z})}{\frac{\pi qx}{\lambda z}}\right]^2 \qquad (70)$$

where the meanings of each variable are given on Fig. 52.

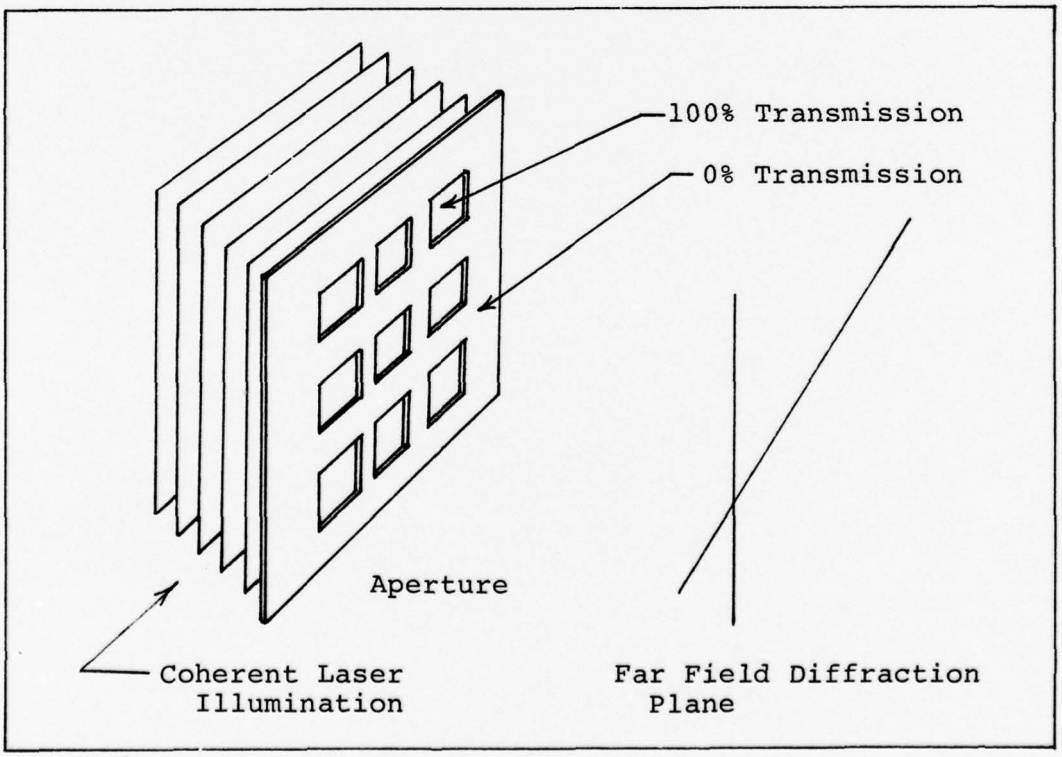

Fig. 51 Periodic Array of Square Apertures

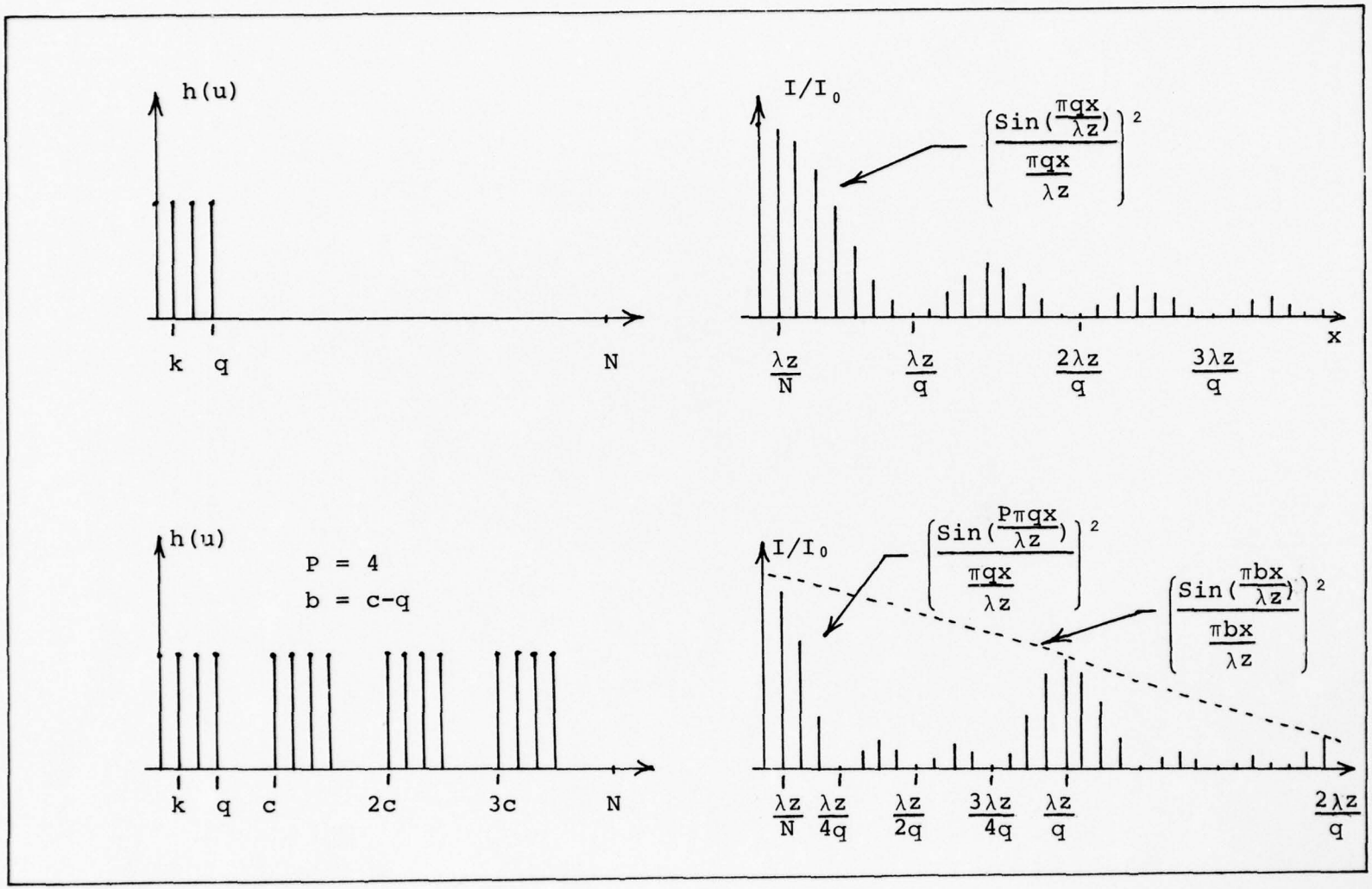

Fig. 52 One Dimensional Single and Multiple Pulse Apertures and Intensity Plots

Although not proven here (see Ref.7 or Ref.12), the far field normalized one dimensional intensity pattern produced by plane wave laser illumination on a periodic set of square apertures is given by

$$I/I_0 = \left[\frac{\mathrm{Sin}(\frac{P\pi qx}{\lambda z})}{\frac{\pi qx}{\lambda z}}\right]^2 \left[\frac{\mathrm{Sin}(\frac{\pi bx}{\lambda z})}{\frac{\pi bx}{\lambda z}}\right]^2 \qquad (71)$$

In Eq. 71, P is the number of apertures, q is the width of the apertures, b is the interval between apertures. The bottom drawing of Fig. 52 illustrates a sequence of apertures where P = 4. Note, c = q + b is the period of the sequence.

Several conclusions can be made by analyzing the bottom drawing of Fig. 52 and Eq. 71. First, there are P-2 minor lobes with nulls positioned at multiples of $\lambda z/Pq$ between each major lobe which are positioned at multiples of $\lambda z/q$. Second, as b becomes smaller and q increases, the secondary major lobe amplitudes, positioned at multiples of $\lambda z/q$, decrease. And finally, in the limit as q increases and b goes to zero, Eq. 71 reduces to Eq. 70.

A sequence of reflecting apertures, with zero reflection between apertures, Fig. 53 of Appendix B, was formulated to test the effectiveness of the speckle program to calculate the far field intensity pattern as predicted by Eq. 71. Note, the normalized amplitudes of the pulses were

not made a constant of the laser wavelength. This was done intentionally to keep the exponential term in the complex aperture model (Eq. 59) from going to 1. Thus, the complex aperture model returned a complex set of data to the SPECKLE program. The plots returned from the SPECKLE program are shown in Figs. 53 and 56 of Appendix B, with the following analysis results:

a.) Figure 54 shows there are five pulses separated by zero reflection areas. From theory there should be three minor lobes between major lobes in the one dimensional intensity pattern. Figure 56 shows the correct results.

b.) The nulls in the intensity pattern associated with the pulse separation of 0.3 mm. (Fig. 54) should be at ±42.7 units on Fig. 56. The correct results are obvious on Fig. 56.

c.) The first nulls in the intensity pattern associated with a total aperture width of 3.2 mm., five pulses, (Fig. 54) should be at ±4 units on Fig. 56. Again, the program calculated the nulls correctly.

For clarity, the $|\mathrm{Sinc}(x)|^2$ curves on the intensity pattern associated with the total aperture width and the pulse separation interval are indicated on Fig. 56. The program calculated and plotted the DFT, as predicted by theory, the diffraction pattern for a series of pulse shaped apertures

and zero reflection areas as depicted in Fig. 51.

Reflecting Surfaces with Arbitrary Height Variations

In the previous example, a scattering surface was represented by a series of pulses of equal width, spacing, amplitude, and areas of zero reflectivity (Fig. 53). That data was used to show the effect of zero reflection areas on the speckle pattern. A rough reflecting surface can be represented by varying the amplitudes of the pulses that represent the scattering surface and not include areas of zero reflection. A three dimensional perspective of this type of reflecting aperture is shown in Fig. 57 of Appendix B. Figure 58 shows a one dimensional cut through Fig. 57, however, since the pulses over the aperture do not have equal amplitudes, Fig. 57 is only one of several different one dimensional perspectives across the aperture. The three dimensional perspective of the intensity pattern produced by the complex aperture is shown in Fig. 59 and a one dimensional cut through the intensity pattern is shown in Fig. 60. Some of the basic characteristics of diffraction theory previously discussed are evident in the two dimensional intensity plot (Fig. 60). First, the pulse repetition for this aperture (Fig. 57) is the same as that for the previous example (except there are no areas of zero reflection) and the intensity diffraction null at ±42.7 units is retained. Secondly, the diffraction null at ±4 units, associated with the total aperture width of 3.2 millimeters is retained.

Finally, there are five distinct pulses across the aperture, one representation is shown in Fig. 58, and again as in the previous set of data there are three minor lobes positioned between each secondary major lobe in the diffraction pattern (Fig. 60). The major change in this diffraction pattern (Fig. 60), compared to the diffraction pattern of the previous example (Fig. 56), is the reduced amplitudes of the secondary major and minor lobes.

To extend the simulated aperture representation closer to that of a rough surface, three additional parameter variations were added to the pulsed scattering surface of the last example; random pulse width, random pulse repetition interval, and sloped pulse edges. A three dimensional perspective of this type of aperture is shown in Fig. 61 of Appendix B. Figure 62 shows a one dimensional cut through Fig. 61, however, as stated before this is only one of many cuts where each would reveal a different one dimensional perspective. Figure 63 shows the three dimensional perspective of the intensity diffraction pattern and Fig. 64 shows a one dimensional cut through Fig. 63. The most obvious result is that all secondary peak amplitudes are greatly reduced, when compared to the two previous examples. Other phenomena are:

a.) There are three minor lobes positioned between the central lobe and the first major secondary lobe positioned at ±18 units on Fig. 64. This

was expected since there are five pulses across the aperture, although they are not of equal width or separation.

b.) Figure 64 shows one minor lobe positioned between two major secondary lobes at ±18 and ±27 units. A first intuition would be to assume that some portion of the three dimensional complex aperture was being represented as three pulses, which would produce one minor lobe between two major lobes. However, since the intensity pattern is the two dimensional Fourier transform of the complex aperture function this simplified generalization cannot be assumed.

The next example is a scattering surface with random height variations as shown in Fig. 65 of Appendix B. Figure 66 shows a typical one dimensional cut through Fig. 65. Obviously, each unique cut through Fig. 65 will produce a different one dimensional plot. Figure 67 is the three dimensional persepctive of the intensity pattern produced by the complex aperture function model and Fig. 60 is a one dimensional cut through Fig. 67. Figure 68 shows that there is a random distribution of secondary major and minor peaks. A Fourier transform plot, Fig. 69, of the one dimensional intensity plot, Fig. 68, reveals the spatial frequencies present in the diffraction pattern. The frequency reference marks

(REF) on Fig. 68 are related to the reference (REF) marks on Fig. 69 through Table VII and Eq. 72.

$$\text{Intensity plot units} = (\text{Frequency plot units} \times \text{Frequency plot scale factor} \times \text{Intensity plot scale factor})^{-1} \quad (72)$$

Since 31 units on the frequency plot, Fig. 69, is equal to 4.9 cycles/meter, this converts to 0.2 m. for a typical speckle width, Fig. 68. Transforming back to the scattering plane, this data gives an aperture width of 3.1 milimeters. This is the correct result as predicted by theory.

Table VII

Diffraction Pattern Frequency Content

	Figure 69	Figure 68
REF 1 (units)	31	4.1
REF 2 (units)	18	7
REF 3 (units)	8.2	15
REF 4 (units)	3.7	35
REF 5 (units)	2	64

A final example for a circular rough scattering surface is shown in Figs. 70 through 74 of Appendix B. Although not discussed in this thesis, the analysis of the spatial frequency content of the intensity plot is similar to that for the square reflecting surface shape. The important factor to remember when analyzing diffraction patterns produced by circular cross sections is that the intensity nulls do not

occur at integer multiples as they do for a diffraction pattern produced by a square scattering surface.

Summary

The SPECKLE program was tested by first simulating simple apertures that produced well known diffraction patterns and then by making the apertures more complex to represent rough surfaces. The program calculated and displayed the correct far field diffraction patterns for those aperture shapes with well known results, i.e., smooth surfaces, square, and circular reflecting cross sections. Although the intensity patterns could not be compared to text book results for rough scattering surfaces, there were certain characteristics that were checked for program verification. These characteristics were null locations associated with the total aperture width and a complex distribution of secondary major and minor lobes associated with surface roughness characteristics. For all examples the program provided correct displays and accurate numerical results.

It was shown, through example, that there are several ways to represent the profile of scattering surface. The electric field at the scattering surface after reflection is represented by the complex aperture function model

$$E_a(u,v) = \text{AIFIEL}(u,v)\,\text{REF}(u,v)\,\text{Exp}\left(\frac{j2\pi}{\lambda}h(u,v)\right.$$

$$\left.1.+\text{Cos}(\text{GLAZ})\right) \qquad (73)$$

If the profile of the incident radiation is represented by the normalized height distributions of the scattering surface, h(u,v), phase variations will be present in the complex aperture function, $E_a(u,v)$ data. When pulses are represented in the reflecting aperture, a value of zero for h(u,v) will not represent zero reflection between pulses. As seen in Eq. 73, a zero for h(u,v) forces the exponential to one and $E_a(u,v)$ will have a real value. Areas of zero reflection must be represented by the reflection coefficient, REF(u,v), for correct results.

By using Eq. 73 it is possible to fill the entire array DATA with normalized surface height data and model the incident radiation cross section with the field term, AIFIEL(u,v) or the surface reflection coefficient term, REF(u,v). By using the three major variables in Eq. 73, AIFIEL(u,v), REF(u,v), and h(u,v), it is possible to use the same set of normalized surface height data to model complex reflecting scenarios. As an example, consider a reflecting surface with normalized height data, h(u,v), that is randomly pointed with an absorption material resulting in a complex distribution for REF(u,v). The incident radiation distribution, AIFIEL(u,v), can now be varied to represent different shaped laser beams. Thus, the speckle model provides numerous options for investigating far field speckle patterns.

VI. Thesis Conclusion Applicable to ALOT System Design

This final chapter is provided for the ALOT systems engineers, at the AFWL, who initiated this thesis project. The major areas that were to be investigated were typical speckle size in a far field diffraction pattern and induced spatial frequencies caused by a speckle pattern. These characteristics for speckle patterns have been answered in the thesis and are summarized in the following paragraphs.

The typical speckle size in a far field diffraction pattern is determined by the cross section of the laser beam, range from target to detector, and laser wavelength. Equation 74 gives the typical speckle size, at a far field observation plane, produced when a plane wave coherent laser beam is reflected from a square rough surface,

$$\text{Typical speckle size} = \frac{\lambda z}{\text{Reflecting width}} \tag{74}$$

For a circular aperture shape, the typical speckle size will be approximately 1.22 times value given by Eq. 74. The 1.22 factor is a characteristic of the Airy pattern distribution produced by the circular aperture. The term "approximate" is appropriate because the intensity lobe widths in an Airy pattern are not equal as they are in a $|\text{Sinc}(x)|^2$ pattern distribution produced by a square aperture. The highest spatial frequency is the inverse of the typical speckle size.

It should be noted that variations in reflectivity and surface roughness introduce secondary frequencies in the diffraction pattern which are inversely proportional to the characteristic length of the variation. That is, the highest spatial frequency is inversely proportional to the total reflecting surface size but lower spatial frequencies result from unique characteristic lengths of the reflecting area.

Bibliography

1. Rigden, J. D. and E. I. Gordon. "The Granularity of Scattered Optical Maser Light." Proceedings I. R. E., 50: 2367-2368 (October-December 1962)

2. Oliver, B. M. "Sparkling Spots and Random Diffraction." Proceedings IEEE, 51: 220-221 (January-March 1963)

3. Leith, E. N. "Quasi-Holographic Techniques in the Microwave Region." Proceedings IEEE, 59: 1305-1318 (July-December 1971)

4. Ratcliffe, J. A. "Some Aspects of Diffraction Theory and Their Applications to the Ionosphere." Reports on Progress in Physics, 19: 188-267 (1956).

5. Middleton, D. Introduction to Statistical Communication Theory. New York: McGraw-Hill Book Co., 1968.

6. Goodman, J. W. Statistical Properties of Laser Speckle Patterns, Vol. 9, Topics in Applied Physics. New York: Springer-Verlag, 1975.

7. Hecht, E. and A. Zajac. OPTICS. Reading, Mass.: Addison-Wesley Publishing Co., 1975.

8. Goodman, J. W. Introduction to Fourier Optics. New York: McGraw-Hill Book Co., 1968.

9. Beckmann, P. and A. Spizzichino. The Scattering of Electromagnetic Waves from Rough Surfaces. New York: MacMillan Book Co., 1963.

10. Rabiner, L. R. and C. M. Rader. Digital Signal Processing. New York: IEEE Press, 1972.

11. McKechnie, T. S. "Measurements of Some Second Order Statistical Properties of Speckle." OPTICS, 39: 258-267 (January 1974).

12. Born, M. and E. Wolf. Principles of Optics. New York: Perganon Press, 1975.

13. Spiegel, M. R. Mathematical Handbook. New York: McGraw-Hill Book Co., 1968.

Supplemental Bibliography

1. Allen, L. and D. G. C. Jones. Physics Letters, Vol. 7, No. 5: 321 (1963).

2. Bracewell, R. The Fourier Transform and Its Applications. New York: McGraw Hill Book Co., 1965.

3. Burkhard, C. B. "Laser Speckle Patterns - A Narrow-band Noise Model." Bell Systems Technical Journal, 49: 309-316 (January-April 1970).

4. Dainty, J. C., et al. "Laser Speckle and Related Phenomena." Topics in Applied Physics, 9, New York: Springer-Verlag, 1975.

5. Enloe, L.H. "Noise-Like Structure in the Image of Diffusely Reflecting Optics in Coherent Illumination." Bell Systems Technical Journal, 46: 1479-1489 (July-December 1967).

6. George, N. "Speckle." Optics News: 14-20 (January 1976).

7. George, N. and A. Jain. "Space and Wavelength Dependence of Speckle Intensity." Applied Physics, 4: 201-212 (August 1974).

8. Goldfischer, L. I. "Autocorrelation Function and Power Spectral Density of Laser Produced Speckle Patterns." Journal of Optical Society of America, 55: 247 (1965).

9. Leader, J. C. "Bidirectional Scattering of Electromagnetic Waves from Rough Surfaces." Printed at Spring Meeting of USNC/URSI of IEEE, Washington, D. C.: (16 April 1970).

10. Lowenthal, S. and H. H. Arsenault. "Image Formation for Coherent Diffuse Objects." Journal of Optical Society of America, 60: 1478 (1970).

11. McKechnie, T. S. "Reduction of Speckle by a Moving Aperture - First Order Statistics." Optics Communication, 13: 35-39 (January 1975).

12. Ohtsubo, J. and T. Asakura. "Statistical Properties of Speckle Patterns Produced by Coherent Light at the Image and Defocus Planes." OPTIK, 45: 65-72 (April 1976).

13. Pedersen, H. M. "On the Contrast of Polychromatic Speckle Patterns and Its Dependence on Surface Roughness." OPTICA ACTA, 22: 15-24 (January 1975).

14. -----. "Second Order Statistics of Light Diffracted from Gaussian Rough Surfaces with Application to Roughness Dependence of Speckles." OPTICA ACTA, 22: 523-535 (June 1975).

15. Reed, I. S. "On a Moment Thereom for Complex Gaussian Processes." IRE Transactions on Information Theory, 8: 194-195 (1962).

16. Shmelev, A. B. "Wave Scattering by Statistically Uneven Surfaces." Soviet Physics-Uspekhi, 15: 173-183 (1972).

17. Stroke, G. W. An Introduction to Coherent Optics and Holography. New York: Academic Press, 1969.

18. Williams, C. S. and O. A. Becklund. Optics: A Short Course for Engineers and Scientists. New York: Wiley-Interscience, 1972.

19. Wolf, E. "A Macroscopic Theory of Interference and Diffraction of Light from Finite Sources." Proceedings of the Royal Society of London, 225: 96-111(1954).

20. -----. "Three Dimensional Structure Determination of Semi-Transparent Objects from Holographic Data." Optical Communication, 1: 153-156 (1969).

Appendix A

SPECKLE Program Listing

```
      PROGRAM SPEKLE(INPUT=/80,OUTPUT,PLFILE=0)

*****************************************************************************
*                                                                           *
*  THIS PROGRAM WAS DEVELOPED BY WILLIAM E LANDIS, CAPT. USAF..  THE THESIS  *
*  WAS REQUIRED TO MEET GRADUATION REQUIREMENTS AT THE AIR FORCE INSTITUTE   *
*  OF TECHNOLOGY AT WRIGHT-PATTERSON AFB, OHIO.  COPIES OF THE THESIS CAN    *
*  BE VIEWED AT AFIT OR OBTAINED THROUGH DDC...       24 JAN 77              *
*                                                                           *
*                                                                           *
*  THIS PROGRAM WILL CALCULATE THE INTENSITY DISTRIBUTION PATTERN AT AN      *
*  OBSERVATION PLANE FOR MONOCHROMATIC LASER LIGHT SCATTERED FROM A ROUGH    *
*  SURFACE.  THE EQUATION FOR THE FIELD DISTRIBUTION AT THE OBSERVATION PLANE*
*  IS AS FOLLOWS.....                                                       *
*                                                                           *
*        A(I,J)=(1./(WAVELENGTH*RANGE))*SUM*SUM((AIFIEL*REF                 *
*        *EXP(SQRT(-1)*2.*PIE*DATA(U,V)*(1.+COS(GLAZ)))                     *
*        *EXP(((-SQRT(-1)*2.*PIE)/(WAVELENGTH*RANGE))                       *
*        *(UX+VY))DUDV                                                      *
*                                                                           *
*  THE INTENSITY DISTRIBUTION IS THEN OBTAINED THROUGH...                   *
*                                                                           *
*        INTENSITY(X,Y)=(1./2.)*(A(X,Y)*CONG A(X,Y))                        *
*                                                                           *
*****************************************************************************

      COMPLEX A, B, C, AA, AC, CC, DATA, SECFFT, W, DD
      DIMENSION  II(1), NN(2), SECFFT(128)
      DIMENSION HELP(128), OUTS(128)
      DIMENSION YES(1000), IPAK(400)
```

```
      COMMON /A/DATA(128,128)
      EXTERNAL VALU
      DATA PIE/3.14159/
      DATA NN,II/ 128,128/
      DATA A,CC,DD/(0.0,1.0),(0.0,0.0),(1.0,0.0)/

      DO 105 I=1,128
      DO 105 J=1,128
      SECFFT(I)=CC
  105 DATA(I,J)=CC

*****************************************************************
*                                                               *
*  CALL SUBROUTINE HEIGHS                                       *
*  SUBROUTINE HEIGHS IS A USER SUPPLIED ROUTINE THAT WILL INPUT THE SCATTER-*
*  ING SURFACE HEIGHT DATA, NORMALIZED BY THE INCIDENT LASER WAVELENGTH.*
*  THIS DATA IS TRANSFERED TO THE MAIN PROGRAM THROUGH ARRAY -DATA- IN A*
*  COMMON STATEMENT.  THE SUBROUTINE MUST BE TITLED....         *
*                                                               *
*      SUBROUTINE HEIGHS(IROW,ICOL,MRDAT,MCDAT,ALAMDA,RANGE,AMESC,*
*     IN2D,IN3D,INT2D,INT3D,ISFREQ,ISCAP,ICRAP,ICOAP,ISMSU,IROSU)*
*                                                               *
*  FOLLOWED BY....                                              *
*                                                               *
*      COMPLEX DATA                                             *
*      COMMON /A/DATA(128,128)                                  *
*                                                               *
*  THE USER MUST SUPLY THE PROGRAM VARIABLES LISTED IN -HEIGHS- AND EXPLAIN-*
*  ED IN THE THESIS CHAPTER ON THE PROGRAM OPERATION.  NOTE IN THE THESIS *
*  THAT THE POSITION OF THE DATA IN THE ARRAY -DATA- DEFINES THE PROFILE OF *
```

```
*  THE REFLECTING APERTURE,  SUCH AS SQUARE, CIRCULAR, OR COMPLEX...          *
*                                                                             *
*******************************************************************************

      CALL HEIGHS(IROW,ICOL,MRDAT,MCDAT,ALAMBA,RANGE,AMESC,IN2D,IN3D,INT
     12D,INT3D,ISFREQ,ISOAP,ICRAP,ICOAP,ISMSU,IROSU)
*******************************************************************************
*                                                                             *
*  FIRST SETUP THE HEADINGS, THEN CALCULATE DUMMY VARIABLES, AND FINALLY      *
*  PRINT OUT THE APERTURE HEIGHT DATA.  COLUMNS VARRING FASTEST....           *
*                                                                             *
*******************************************************************************

      PRINT 3
    3 FORMAT(////,35X,"INPUT APERTURE DATA")
      PRINT 4
    4 FORMAT(27X,"COLUMNS VARRING FASTEST, ROWS SLOWEST"//)
      PRINT 8, AMESC
    8 FORMAT(26X,"INCREMENT OF SAMPLES = ",E10.3," METERS."//)
      NROW=IROW/2
      NCOL=ICOL/2
      LKR=(MRDAT+1)/2
      LKC=(MCDAT+1)/2
      LKROW=NROW-LKR+1
      LKCOL=NCOL-LKC+1
      KKROW=NROW+LKR-1
      KKCOL=NCOL+LKC-1
      DO 5 I=LKROW,KKROW
      PRINT 6, I,LKCOL,KKCOL
    6 FORMAT(/,4X,"*********************************" /4X,"* ROW",I3,"
```

```
C  COLUMNS ",I3," THROUGH ",I3," *"/4X,"**********************************
     $*********"/)
    5 PRINT 7,((DATA(I,J),J=LKCOL,KKCOL)
    7 FORMAT(4(6X,E9.3,2X,E9.3))
C
C**********************************************************************
C                                                                      *
C  CALL DISSPLA PLOTTING PACKAGE...                                    *
C                                                                      *
C**********************************************************************
      CALL COMPRS
C**********************************************************************
C                                                                      *
C  CHECK TO SEE IF A 2-D PLOT OF THE INPUT SURFACE HEIGHT DATA WAS REQUESTED. *
C                                                                      *
C**********************************************************************
      IF(IN2D.LE.0) GO TO 25
C**********************************************************************
C                                                                      *
C  SET UP PLOT BUFFERS AND CALL 2-D PLOT ROUTINE                       *
C                                                                      *
C**********************************************************************
      S=(-(FLOAT(NROW)-1.))
      DO 804 J=1,ICOL
  804 OUTS(J)=REAL(DATA(NROW,J))
      DO 803 J=1,ICOL
      HELP(J)=S
```

```
 803 S=S+1.
     CALL BGNPL(1)
     CALL TITLE(1H ,-1," ",+1," ",+1,8.0,4.0)
     CALL RLNK1(-0.75,8.25,-.500,5.25,2)
     CALL RESET(5HRLNK1)
     IF(ISOAP.EQ.1) GO TO 32
     IF(ICRA.EQ.1) GO TO 33
     IF(ICOAP.EQ.1) GO TO 134
  32 CALL HEADIN("SQUARE APERTURE SHAPE$",-100,1,2)
     GO TO 35
  33 CALL HEADIN("CIRCULAR APERTURE SHAPE$",-100,1,2)
     GO TO 35
 134 CALL HEADIN("COMPLEX APERTURE SHAPE$",-100,1,2)
  35 IF(ISMSU.EQ.1) GO TO 36
     CALL HEADIN("ROUGH SURFACE$",100,1,2)
     GO TO 37
  36 CALL HEADIN("SMOOTH SURFACE$",100,1,2)
  37 CALL XTICKS(5)
     CALL YTICKS(5)
     CALL GRAPH(-20.,5.0,0.0,2.5)
     CALL CURVE(HELP,OUTS,128,0)
     CALL RLMESS("APERTURE SHAPE AT",+17,-11.,-1.093)
     CALL RLREAL(AMESC,-2,-1.0,-1.093)
     CALL RLMESS("METERS/UNIT",+11,5.,-1.093)
     CALL ENDPL(0)
*************************************************************
*                                                           *
*  CHECK TO SEE IF A 3-D PLOT OF THE INPUT SURFACE HEIGHT DATA WAS REQUESTED.  *
*                                                           *
*************************************************************
```

```
 25   IF(IN3D.EQ.0) GO TO 28
*****************************************************************
*                                                               *
*  CALL 3-D PLOT ROUTINE.                                       *
*                                                               *
*****************************************************************

      CALL BGNPL(2)
      CALL PHYSOR(1.75,1.50)
      CALL TITL3D(1H ,-1,8.0,6.0)
      CALL RLNK1(-0.75,8.25,0.0,5.75,2)
      CALL RESET(5HBLNK1)
      CALL VUABS(-3.,-2.,3.)
      CALL AXES3D(12HU DIRECTION$,100,12HV DIRECTION$,100,2H $,100,1.,1.
     1,1.)
      CALL ZTICKS(2)
      CALL GRAF3D(46.,5HSCALE,82.,46.,5HSCALE,82.,0.,2.5,10.)
      CALL SURFUN(VALU,2,1.,2,1.,YES)
      CALL RESET(6HPHYSOP)
      CALL ENDPL(0)
*****************************************************************
*                                                               *
*  CALL COMAPE                                                  *
*                                                               *
*  SUBROUTINE COMAPE IS A USER SUPPLIED SUBROUTINE THAT WILL CALCULATE THE  *
*  COMPLEX APERTURE FUNCTION FROM THE NORMALIZED SURFACE HEIGHT DATA IN THE  *
*  ARRAY -DATA- AND VARIABLES -GLAZ,REF(U,V),AND AIFIEL(U,V). THE VARIABLES  *
*  ARE EXPLAINED IN THE THESIS CHAPTER ON THE SPECKLE PROGRAM. THE USER  *
*  PROGRAM SHOULD INCLUDE THIS MODEL ( REF. APPLIED PHYSICS VOL. 9, PAGE 63)  *
```

```
*                                                                     *
*  IN HIS SUBROUTINE , FOR THE COMPLEX APERTURE FUNCTION....          *
*                                                                     *
*       DATA(I,J)=REF(I,J)*AIFIEL(I,J)*EXP(SQRT(-1)*2.*PIE*DATA(I,J)  *
*      *(1.+COS(GLAZ))                                                *
*                                                                     *
*  THE SUBROUTINE MUST BE TITLED.....                                 *
*                                                                     *
*       SUBROUTINE COMAPE(IROW,ICOL)                                  *
*                                                                     *
*  FOLLOWED BY....                                                    *
*                                                                     *
*       COMPLEX DATA                                                  *
*       COMMON /A/DATA(128,128)                                       *
*                                                                     *
***********************************************************************

   28  CONTINUE
       CALL COMAPE(IROW,ICOL)

***********************************************************************
*                                                                     *
*  PROCESS THE SCALING FACTOR FOR THE OBSERVATION PLANE.  CALL 2-D FFT.*
*                                                                     *
***********************************************************************

       SS=FLOAT(IROW)
       AMEOB=(ALAMBA*RANGE)/(SS*AMESC)
       CALL FOURT(DATA,NN,2,-1,+1,0)
       CALL SHIFT(ICOL,IROW)
***********************************************************************
```

```
*                                                                     *
*  INTENSITY IS OBTAINED BY.....                                      *
*                                                                     *
*       AINT(I,J)=(1./2.)*DATA(I,J)*(CONJUGATE DATA(I,J))             *
*                                                                     *
*  SEE HECHT AND ZAJAC OPTICS PAGE 352.  SINCE THES DIFFRACTION PATTERN IS *
*  FROM A MONOCHROMATIC LASER BEAM, INTENSITY IS EQUAL TO REAL PART SQUARED *
*  PLUS THE IMAG PART SQUARED TIMES ONEHALF...                        *
*                                                                     *
***********************************************************************

      JROW=IROW-1
      JCOL=ICOL-1
      DO 52 I=1,JROW
      DO 52 J=1,JCOL
      W=DATA(I,J)*((1./(ALAMDA*RANGE))**2)
      X=REAL(W)
      Y=AIMAG(W)
      B=((X**2+Y**2)*(1./2.))*DD
   52 DATA(I,J)=B

***********************************************************************
*                                                                     *
*  SAVE CENTRAL ROW OF INTENSITY PLOT TO BE USED IN THE FREQUENCY ANALYSIS *
*  OF THE SPECKLE PATTERN...                                          *
*                                                                     *
***********************************************************************

      DO 82 J=1,JCOL
   82 SECFFT(J)=DATA(NROW,J)
```

```
C*************************************************************
C*                                                           *
C*  SAVE MAXIMUM VALUE OF THE SPECKLE PATTERN FOR PRINT OUT.. *
C*                                                           *
C*************************************************************

      YY=REAL(DATA(NROW,NCOL))
      PRINT 409, YY
  409 FORMAT(///"MAXIMUM VALUE OF INTENSITY VALUE BEFORE NORMALIZING"///
     1 14X,E10.4,/////)

C*************************************************************
C*                                                           *
C*  NORMALIZE THE SPECKLE PATTERN FOR A MAXIMUM OF 1....     *
C*                                                           *
C*************************************************************

      X=REAL(DATA(NROW,NCOL))
      DO 404 I=1,JROW
      DO 404 J=1,JCOL
  404 DATA(I,J)=(REAL(DATA(I,J))/X)*DD
C*************************************************************
C*                                                           *
C*  CHECK IF A 2-D PLOT OF THE SPECKLE PATTERN WAS REQUESTED.. *
C*                                                           *
C*************************************************************

      IF(INT2D.LE.0) GO TO 26
C*************************************************************
```

```
*                                                                       *
*  SET UP THE 2-D PLOT BUFFERS AND CALL THE 2-D PLOT ROUTINE...         *
*                                                                       *
*************************************************************************

      S=(-(FLOAT(NROW)-1.))
      DO 800 J=1,JCOL
      HELP(J)=S
  800 S=S+1.
      DO 801 J=1,JCOL
  801 OUTS(J)=REAL(DATA(NROW,J))
      CALL BGNPL(3)
      CALL TITLE(1H ,-1," ",+1,"NORMALIZED INTENSITY",+20,8.,4.)
      CALL BLNK1(-0.75,8.25,-.500,5.25,2)
      CALL BLNK2(4.75,8.0,3.0,4.0,1)
      CALL RESET(SHBLNK1)
      CALL HEADIN("NORMALIZED DIFFRACTION PATTERN$",-100,-2,3)
      IF(ISQAP.EQ.1) GO TO 38
      IF(ICRAP.EQ.1) GO TO 39
      IF(ICQAP.EQ.1) GO TO 40
   38 CALL HEADIN("SQUARE APERTURE SHAPE$",-100,1,3)
      GO TO 41
   39 CALL HEADIN("CIRCULAR APERTURE SHAPE$",-100,1,3)
      GO TO 41
   40 CALL HEADIN("COMPLEX APERTURE SHAPE$",-100,1,3)
   41 IF(ISMSU.EQ.1) GO TO 42
      CALL HEADIN("ROUGH SURFACE$",100,1,3)
      GO TO 43
   42 CALL HEADIN("SMOOTH SURFACE$",100,1,3)
   43 CALL DASH
```

```
      CALL XTICKS(18)
      CALL YLOG(-72.,18.,1.0E-3,1.)
      CALL GRID(2,0)
      CALL RESET(4HDASH)
      CALL BLNK3(-.5,8.0,-1.96,0.0,0)
      CALL CURVE(HELP,OUTS,127,0)
      CALL RESET(5HBLNK2)
      CALL RESET(5HBLNK3)
      CALL HEIGHT(0.10)
      CALL RLMESS("LASER WAVELENGTH =",+18,18.,.6E1)
      CALL RLREAL(ALAMDA,-2,45.0,0.6E1)
      CALL RLMESS("METERS",5,61.,0.6E1)
      CALL RLMESS("RANGE =",7,29.,0.35E1)
      CALL RLREAL(RANGE,-2,42.,0.35E1)
      CALL RLMESS("METERS",5,58.,0.35E1)
      CALL RLMESS("MAXIMUM INTENSITY =",19,18.,0.17E1)
      CALL RLREAL(YY,-2,47.2,0.17E1)
      CALL RLMESS("UNITS",5,63.0,0.17E1)
      CALL RESET(6HHEIGHT)
      CALL RLMESS("OBSERVATION PLANE MEASUREMENT AT",32,-57.,0.380E-3)
      CALL RLREAL(AMEOB,-2,14.,0.380E-3)
      CALL RLMESS("METERS/UNIT",11,37.,0.380E-3)
      CALL ENDPL(0)
C*****************************************************************
C*                                                               *
C*  CHECK TO SEE IF A 3-D PLOT OF THE SPECKLE PATTERN WAS REQUESTED.. *
C*                                                               *
C*****************************************************************
      IF(INT3D.EQ.0) GO TO 126
```

```
C*****************************************************************
C*                                                               *
C*  CALL 3-D PLOT ROUTINE                                        *
C*                                                               *
C*****************************************************************

      CALL BGNPL(4)
      CALL PHYSOR(1.75,1.50)
      CALL TITL3D(1H ,-1,8.0,5.0)
      CALL BLNK1(-0.75,8.25,0.0,5.75,2)
      CALL RESET(5HBLNK1)
      CALL VUABS(-3.,-2.,3.)
      CALL AXES3D(0.0,0.0,0.0,1.,1.,1.)
      CALL GRAF3D(1.,32.,123.,1.,32.,128.,0.1E-3,1.E0,1.E0)
      CALL SURFUN(VALU,1,3.,1,3.,YES)
      CALL LINES("3-D NORMALIZED INTENSITY DISTRIBUTION$",IPAK,1)
      CALL STORY(IPAK,1,1.625,5.25)
      CALL RESET(6HPHYSOR)
      CALL ENDPL(0)
C*****************************************************************
C*                                                               *
C*  PRINT OUT CENTRAL ROW OF NORMALIZED SPECKLE PATTERN WITH HEADINGS...  *
C*                                                               *
C*****************************************************************

  126 PRINT 75
   75 FORMAT(////,35X,"3-D DATA OF INTENSITY PATTERN"//)
      PRINT 4
      PRINT 34, AMEO3
   34 FORMAT(27X,"INCREMENT OF DATA =",E10.3,"  METERS."//)
```

```
      PRINT 64, ALAMDA,RANGE
   64 FORMAT(31X,"LASERWAVELENGTH =",E12.5," METERS."/42X,"RANGE = ",E12
     $.5," METERS."//)
      INN=1
      PRINT 6, NROW,INN,JCOL
      DO 405 J=1,JCOL
      X=REAL(DATA(NROW,J))
  405 PRINT 7,X
C*****************************************************************
C                                                                 *
C  TAKE FFT OF CENTRAL ROW OF SPECKLE PATTERN, PREVIOUSLY SAVED TO OBTAIN  *
C  DATA FOR FREQUENCY ANALYSIS OF PATTERN...                      *
C                                                                 *
C*****************************************************************
      CALL FOURT(SECFFT,II,1,-1,0,0)
C*****************************************************************
C                                                                 *
C  CALCULATE MAGNITUDE OF TRANSFORMED DATA...                     *
C                                                                 *
C*****************************************************************
      DO 152 I=1,JROW
      W=SECFFT(I)
      X=REAL(W)
      Y=AIMAG(W)
      Z=(X**2+Y**2)*(1./2.)
  152 SECFFT(I)=Z*DD
C*****************************************************************
C                                                                 *
```

```
C  SHIFT DATA TO OBTAIN MAXIMUM VALUE OF PATTERN AT CENTER OF BUFFER..
C
C**********************************************************************
      M=0
      DO 184 I=1,NROW
      K=JROW-M
      L=NROW-M
      SECFFT(K)=SECFFT(L)
  184 M=M+1
      M=0
      DO 185 I=NROW,JROW
      K=I-2*M
      SECFFT(K)=SECFFT(I)
  185 M=M+1
C**********************************************************************
C
C  NORMALIZE FREQUENCY DATA....
C
C**********************************************************************
      X=REAL(SECFFT(1))
      DO 186 I=1,IROW
      Y=REAL(SECFFT(I))
      IF(Y.LE.X) GO TO 186
      X=Y
  186 CONTINUE
      DO 1186 I=1,IROW
      Y=REAL(SECFFT(I))
```

```
 1186 SECFFT(I)=(Y/X)*DD
*****************************************************************************
*                                                                           *
*  CALCULATE SCALE FACTOR FOR FREQUENCY DATA...                             *
*                                                                           *
*****************************************************************************

      DFRIOP=1./(IROW*AMEOB)
*****************************************************************************
*                                                                           *
*  PRINT OUT NORMALIZED FREQUENCY DATA AND PAGE HEADINGS..                  *
*                                                                           *
*****************************************************************************

      PRINT 83
   83 FORMAT(////,26X,"FFT OF INTENSITY IN OBSERVATION PLANE"/26X,"ONLY
     $ROW WITH CENTRAL MAXIMUM USED"/////)
      PRINT 187, DFRIOP
  187 FORMAT(26X,"FREQUENCY PER UNIT = ",E10.3///)
      DO 153 I=1,IROW
      Y=REAL(SECFFT(I))
  153 PRINT 7, Y
*****************************************************************************
*                                                                           *
*  CHECK TO SEE IF A 2-D PLOT OF THE FREQUENCY ANALYSIS DATA WAS REQUESTED..*
*                                                                           *
*****************************************************************************

      IF(ISFREQ.LE.0) GO TO 27
*****************************************************************************
```

```
C*********************************************************************
C*                                                                   *
C*  SET UP 2-D PLOT BUFFERS AND CALL 2-D PLOT ROUTINE.               *
C*                                                                   *
C*********************************************************************
      S=(-(FLOAT(NROW)-1.))
      DO 188 J=1,IROW
      HELP(J)=S
  188 S=S+1.
      DO 189 J=1,IROW
  189 OUTS(J)=REAL(SECOFT(J))
      CALL PGNPL(5)
      CALL TITLE(1H ,-1," ",+1,"NORMALIZED AMPLITUDE",+20,8.,4.)
      CALL BLNK1(-0.75,8.25,-.500,5.25,2)
      CALL RESET(5HBLNK1)
      CALL HEADIN("NORMALIZED FOURIER TRANSFORM OF INTENSITY$",-100,-2,3
     1)
      IF(ISQAP.EQ.1) GO TO 44
      IF(ICRAP.EQ.1) GO TO 45
      IF(ICOAP.EQ.1) GO TO 46
   44 CALL HEADIN("SQUARE APERTURE SHAPE$",-100,1,3)
      GO TO 47
   45 CALL HEADIN("CIRCULAR APERTURE SHAPE$",-100,1,3)
      GO TO 47
   46 CALL HEADIN("COMPLEX APERTURE SHAPE$",-100,1,3)
   47 IF(ISMSU.EQ.1) GO TO 48
      CALL HEADIN("ROUGH SURFACE$",100,1,3)
      GO TO 49
   48 CALL HEADIN("SMOOTH SURFACE$",100,1,3)
   49 CALL DASH
```

```
      CALL XTICKS(18)
      CALL GRAPH(-72.,18.,0.0,.25)
      CALL GRID(2,0)
      CALL RESET(4HDASH)
      CALL CURVE(HELP,OUTS,127,0)
      CALL PLMESS("FREQUENCY CONTENT OF SPECKLE PATTERN",36,-70.,-.109)
      CALL PLREAL(DFRIQP,-2,10.,-.109)
      CALL PLMESS("CYCLES/METER-UNIT",17,33.,-.109)
      CALL ENDPL(0)
   27 CONTINUE
      CALL DONEPL(1)
      END

      SUBROUTINE HEIGHS(IROW,ICOL,MRDAT,MCDAT,ALAMDA,RANGE,AMESC,IN2D,IN
     13D,INT2D,INT3D,ISFREQ,ISDAP,ICPAP,ICOAP,ISMSU,IPOSU)
C*************************************************************************
C                                                                        *
C  THIS IS A USER SUPPLIED SUBROUTINE TO INPUT THE NORMALIZED SURFACE HEIGHT *
C  DATA TO THE MAIN PROGRAM.  ALL VARIABLES ARE EXPLAINED IN THE THESIS  *
C  REPORT.  NOTE, THIS EXAMPLE OF -HEIGHS- READS DATA FROM CARDS.. THIS IS *
C  NOT A REQUIREMENT BUT LEFT TO THE USERS DESIRE...                     *
C                                                                        *
C*************************************************************************
```

```
      COMPLEX DATA
      COMMON /A/DATA(128,123)
      READ 20, IROW, ICOL, MRDAT, MCDAT
   20 FORMAT(4(I10))
      READ 22, ALAMBA, RANGE, AMESC
   22 FORMAT(3(E10.0))
      READ 23, IN2D, IN3D, INT2D, INT3D, ISPEC
   23 FORMAT(5(I5))
      READ 31, ISCAP,ICRAP,ICCAP,ISMSU,IRSU
   31 FORMAT(5(I5))
C*****************************************************************
C                                                                 *
C  READ IN DATA FOR THE APERTURE WHICH IS THE HEIGHT DISTRIBUTIONS IN *
C  DECIMAL PERCENTAGES OF THE LASER WAVELENGTH.  THIS DATA IS REAL BUT *
C  STORED IN A COMPLEX ARRAY.  THE FIRST FIELD OF THE ARRAY CONTAINS THE *
C  REAL PART AND THE SECOND FIELD CONTAINS THE IMAGINARY PART. WHICH IS *
C  ZERO.                                                          *
C                                                                 *
C*****************************************************************
      LKR=(MRDAT+1)/2
      LKC=(MCDAT+1)/2
      READ 2, ((DATA(I,J),J=1,LKC),I=1,LKR)
    2 FORMAT(8(2E5.2))
      CALL SHIFT(IROW,ICOL)
      RETURN
      END
```

```
      SUBROUTINE COMAPE(IROW,ICOL)
*********************************************************************
*                                                                   *
*  THIS IS A USER SUPPLIED SUBROUTINE TO CALCULATE THE COMPLEX APERTURE *
*  FUNCTION AS EXPLAINED IN THE MAIN PROGRAM OR THE THESIS REPORT.  *
*                                                                   *
*********************************************************************
      COMPLEX DATA,A,B,C,AA,AC,CC
      COMMON /A/DATA(128,128)
      DATA PIE/3.14159/
      DATA A,CC/(0.0,1.0),(0.0,0.0)/
      READ 21,GLAZ,REF,AIFIEL
   21 FORMAT(3(F10.1))
      DO 12 I=1,IROW
      DO 12 J=1,ICOL
      C=2.*PIE*DATA(I,J)*(1.+COS(GLAZ))
      B=A*C
      AA=CEXP(B)
      AC=AA*REF*AIFIEL
      IF(B.EQ.CC) GO TO 665
      GO TO 666
  665 AC=CC
  666 CONTINUE
   12 DATA(I,J)=AC
      RETURN
      END
```

```
      FUNCTION VALU(XVAL,YVAL)
C*****************************************************************
C*                                                               *
C*  THIS FUNCTION ROUTINE ATDS THE 3-D PLOT ROUTINE IN THE DISSPLA PACKAGE.  *
C*                                                               *
C*****************************************************************
      COMPLEX DATA(128,128), AA
      COMMON/A/DATA
      AA=DATA(XVAL,YVAL)
      VALU=REAL(AA)
      RETURN
      END

      SUBROUTINE SHIFT(IROW,ICOL)
C*****************************************************************
C*                                                               *
C*  THIS SECTION WILL SHIFT THE INTENSITY DISTRIBUTION INTO A SYMETRIC PLANE  *
C*  WITH THE MAXIMUM VALUE IN THE CENTER OF THE PLANE.           *
C*                                                               *
C*****************************************************************
      COMPLEX DATA
```

```
      COMMON /A/DATA(128,128)
      NROW=IROW/2
      NCOL=ICOL/2
      LROW=NROW-1
      LCOL=NCOL-1
      JROW=IROW-1
      JCOL=ICOL-1
      M=0
      DO 72 I=NROW,JROW
      IX=I-2*M
      IW=JROW-M
      M=M+1
      MM=0
      DO 72 J=NCOL,JCOL
      JX=J-2*MM
      JW=JCOL-MM
      MM=MM+1
   72 DATA(IW,JW)=DATA(IX,JX)
      DO 73 I=NROW,JROW
      M=0
      DO 73 J=NCOL,JCOL
      K=J-2*M
      DATA(I,K)=DATA(I,J)
   73 M=M+1
      DO 74 I=1,NROW
      K=IROW-I
      DO 74 J=1,JCOL
   74 DATA(I,J)=DATA(K,J)
      RETURN
      END
```

```
      SUBROUTINE FOURT(DATA,NN,NDIM,ISIGN,IFORM,WORK)                   FFT00000
C*****************************************************************
C*                                                               *
C*  THE FFT SUBROUTINE WAS NOT DEVELOPED IN CONJUNCTION WITH THE SPECKLE *
C*  PROGRAM BUT WAS OBTAINED FROM THE ELECTRICAL ENGINEERING BRANCH OF AFIT. *
C*  REFERENCES TO THE PROGRAM AUTHOR ARE FOUND ON THE FOLLOWING CARDS.... *
C*                                                               *
C*****************************************************************
C
C     FOR INFORMATION CONTACT MR. MARK HALLER 4950/ADDS/56248       FFT00010
C
C     THE COOLEY-TUKEY FAST FOURIER TRANSFORM IN USASI BASIC FORTRAN FFT00020
C
C                                                                   FFT00030
C     TRANSFORM(K1,K2,...) = SUM(DATA(J1,J2,...)*EXP(ISIGN*2*PI*SQRT(-1)FFT00040
C    *((J1-1)*(K1-1)/NN(1)+(J2-1)*(K2-1)/NN(2)+...)), SUMMED FOR ALL  FFT00050
C     J1, K1 BETWEEN 1 AND NN(1), J2, K2 BETWEEN 1 AND NN(2), ETC.    FFT00060
C     THERE IS NO LIMIT TO THE NUMBER OF SUBSCRIPTS.  DATA IS A       FFT00070
C     MULTIDIMENSIONAL COMPLEX ARRAY WHOSE REAL AND IMAGINARY         FFT00080
C     PARTS ARE ADJACENT IN STORAGE, SUCH AS FORTRAN IV PLACES THEM.  FFT00090
C     IF ALL IMAGINARY PARTS ARE ZERO (DATA ARE DISGUISED REAL), SET  FFT00100
C     IFORM TO ZERO TO CUT THE RUNNING TIME BY UP TO FORTY PERCENT.   FFT00110
C     OTHERWISE, IFORM = +1.  THE LENGTHS OF ALL DIMENSIONS ARE       FFT00120
C     STORED IN ARRAY NN, OF LENGTH NDIM.  THEY MAY BE ANY POSITIVE   FFT00130
C     INTEGERS, THO THE PROGRAM RUNS FASTER ON COMPOSITE INTEGERS, AND FFT00140
C     ESPECIALLY FAST ON NUMBERS RICH IN FACTORS OF TWO.  ISIGN IS +1 FFT00150
C     OR -1.  IF A -1 TRANSFORM IS FOLLOWED BY A +1 ONE (OR A +1      FFT00160
```

```
C     BY A -1) THE ORIGINAL DATA REAPPEAR, MULTIPLIED BY NTOT (=NN(1)*  FFTT0170
C     NN(2)*...).  TRANSFORM VALUES ARE ALWAYS COMPLEX, AND ARE RETURNEDFFTT0180
C     IN ARRAY DATA, REPLACING THE INPUT.  IN ADDITION, IF ALL          FFTT0190
C     DIMENSIONS ARE NOT POWERS OF TWO, ARRAY WORK MUST BE SUPPLIED,    FFTT0200
C     COMPLEX OF LENGTH EQUAL TO THE LARGEST NON 2**K DIMENSION.        FFTT0210
C     OTHERWISE, REPLACE WORK BY ZERO IN THE CALLING SEQUENCE.          FFTT0220
C     NORMAL FORTRAN DATA ORDERING IS EXPECTED, FIRST SUBSCRIPT VARYING FFTT0230
C     FASTEST.  ALL SUBSCRIPTS BEGIN AT ONE.                            FFTT0240
C                                                                       FFTT0250
C     RUNNING TIME IS MUCH SHORTER THAN THE NAIVE NTOT**2, BEING        FFTT0260
C     GIVEN BY THE FOLLOWING FORMULA.  DECOMPOSE NTOT INTO              FFTT0270
C     2**K2 * 3**K3 * 5**K5 * ....  LET SUM2 = 2*K2, SUMF = 3*K3 + 5*K5 FFTT0280
C     + ... AND NF = K3 + K5 + ....  THE TIME TAKEN BY A MULTI-         FFTT0290
C     DIMENSIONAL TRANSFORM ON THESE NTOT DATA IS T = T0 + NTOT*(T1+    FFTT0300
C     T2*SUM2+T3*SUMF+T4*NF).  ON THE CDC 3300 (FLOATING POINT ADD TIME FFTT0310
C     OF SIX MICROSECONDS), T = 3000 + NTOT*(500+43*SUM2+68*SUMF+       FFTT0320
C     320*NF) MICROSECONDS ON COMPLEX DATA.  IN ADDITION, THE           FFTT0330
C     ACCURACY IS GREATLY IMPROVED, AS THE RMS RELATIVE ERROR IS        FFTT0340
C     BOUNDED BY 3*2**(-B)*SUM(FACTOR(J)**1.5), WHERE B IS THE NUMBER   FFTT0350
C     OF BITS IN THE FLOATING POINT FRACTION AND FACTOR(J) ARE THE      FFTT0360
C     PRIME FACTORS OF NTOT.                                            FFTT0370
C                                                                       FFTT0380
C     PROGRAM BY NORMAN BRENNER FROM THE BASIC PROGRAM BY CHARLES       FFTT0390
C     RADER.  RALPH ALTER SUGGESTED THE IDEA FOR THE DIGIT REVERSAL.    FFTT0400
C     MIT LINCOLN LABORATORY, AUGUST 1967.  THIS IS THE FASTEST AND MOSTFFTT0410
C     VERSATILE VERSION OF THE FFT KNOWN TO THE AUTHOR.  SHORTER PRO-   FFTT0420
C     GRAMS FOUR1 AND FOUR2 RESTRICT DIMENSION LENGTHS TO POWERS OF TWO.FFTT0430
C     SEE-- IEEE AUDIO TRANSACTIONS (JUNE 1967), SPECIAL ISSUE ON FFT.  FFTT0440
C                                                                       FFTT0450
C     THE DISCRETE FOURIER TRANSFORM PLACES THREE RESTRICTIONS UPON THE FFTT0460
```

```
C                                                                       FFTT0470
C     DATA.                                                             FFTT0480
C     1.  THE NUMBER OF INPUT DATA AND THE NUMBER OF TRANSFORM VALUES   FFTT0490
C     MUST BE THE SAME.                                                 FFTT0500
C     2.  BOTH THE INPUT DATA AND THE TRANSFORM VALUES MUST REPRESENT   FFTT0510
C     EQUISPACED POINTS IN THEIR RESPECTIVE DOMAINS OF TIME AND         FFTT0520
C     FREQUENCY.  CALLING THESE SPACINGS DELTAT AND DELTAF, IT MUST BE  FFTT0530
C     TRUE THAT DELTAF=2*PI/(NN(I)*DELTAT).  OF COURSE, DELTAT NEED NOT FFTT0540
C     BE THE SAME FOR EVERY DIMENSION.                                  FFTT0550
C     3.  CONCEPTUALLY AT LEAST, THE INPUT DATA AND THE TRANSFORM OUTPUTFFTT0560
C     REPRESENT SINGLE CYCLES OF PERIODIC FUNCTIONS.                    FFTT0570
C                                                                       FFTT0580
C     EXAMPLE 1.  THREE-DIMENSIONAL FORWARD FOURIER TRANSFORM OF A      FFTT0590
C     COMPLEX ARRAY DIMENSIONED 32 BY 25 BY 13 IN FORTRAN IV.           FFTT0600
      DIMENSION DATA(32,25,13),WORK(60),NN(3)                           FFTT0610
      COMPLEX DATA                                                      FFTT0620
      DATA NN/32,25,13/                                                 FFTT0630
      DO 1 I=1,32                                                       FFTT0640
      DO 1 J=1,25                                                       FFTT0650
      DO 1 K=1,13                                                       FFTT0660
    1 DATA(I,J,K)=COMPLEX VALUE                                         FFTT0670
      CALL FOURT(DATA,NN,3,-1,1,WORK)                                   FFTT0680
C                                                                       FFTT0690
C     EXAMPLE 2.  ONE-DIMENSIONAL FORWARD TRANSFORM OF A REAL ARRAY OF  FFTT0700
C     LENGTH 64 IN FORTRAN II.                                          FFTT0710
      DIMENSION DATA(2,64)                                              FFTT0720
      DO 2 I=1,64                                                       FFTT0730
      DATA(1,I)=REAL PART                                               FFTT0740
    2 DATA(2,I)=0.                                                      FFTT0750
      CALL FOURT(DATA,64,1,-1,0,0)                                      FFTT0760
C
```

```
      DIMENSION DATA(1),NN(1),IFACT(32),WORK(1)                          FFTT0770
C     CDC 6600 INITIALIZATION
      WR=0.
      WI=0.
      WSTPR=0.
      WSTPI=0.
      TWOPI=6.283185307                                                  FFTT0780
      IF(NDIM-1)920,1,1                                                  FFTT0790
1     NTOT=2                                                             FFTT0800
      DO 2 IDIM=1,NDIM                                                   FFTT0810
      IF(NN(IDIM))920,920,2                                              FFTT0820
2     NTOT=NTOT*NN(IDIM)                                                 FFTT0830
C                                                                        FFTT0840
C     MAIN LOOP FOR EACH DIMENSION                                       FFTT0850
C                                                                        FFTT0860
      NP1=2                                                              FFTT0870
      DO 910 IDIM=1,NDIM                                                 FFTT0880
      N=NN(IDIM)                                                         FFTT0890
      NP2=NP1*N                                                          FFTT0900
      IF(N-1)920,900,5                                                   FFTT0910
C                                                                        FFTT0920
C     FACTOR N                                                           FFTT0930
C                                                                        FFTT0940
5     M=N                                                                FFTT0950
      NTWO=NP1                                                           FFTT0960
      IF=1                                                               FFTT0970
      IDIV=2                                                             FFTT0980
10    IQUOT=M/IDIV                                                       FFTT0990
      IREM=M-IDIV*IQUOT                                                  FFTT1000
      IF(IQUOT-IDIV)50,11,11                                             FFTT1010
```

```
11    IF(IREM)20,12,20                                                  FFTT1020
12    NTWO=NTWO+NTWO                                                    FFTT1030
      M=IQUOT                                                           FFTT1040
      GO TO 10                                                          FFTT1050
20    IDIV=3                                                            FFTT1060
30    IQUOT=M/IDIV                                                      FFTT1070
      IREM=M-IDIV*IQUOT                                                 FFTT1080
      IF(IQUOT-IDIV)60,31,31                                            FFTT1090
31    IF(IREM)40,32,40                                                  FFTT1100
32    IFACT(IF)=IDIV                                                    FFTT1110
      IF=IF+1                                                           FFTT1120
      M=IQUOT                                                           FFTT1130
      GO TO 30                                                          FFTT1140
40    IDIV=IDIV+2                                                       FFTT1150
      GO TO 30                                                          FFTT1160
50    IF(IREM)60,51,60                                                  FFTT1170
51    NTWO=NTWO+NTWO                                                    FFTT1180
      GO TO 70                                                          FFTT1190
60    IFACT(IF)=M                                                       FFTT1200
C                                                                       FFTT1210
C     SEPARATE FOUR CASES--                                             FFTT1220
C        1. COMPLEX TRANSFORM OR REAL TRANSFORM FOR THE 4TH, 5TH,ETC.   FFTT1230
C           DIMENSIONS.                                                 FFTT1240
C        2. REAL TRANSFORM FOR THE 2ND OR 3RD DIMENSION.  METHOD--      FFTT1250
C           TRANSFORM HALF THE DATA, SUPPLYING THE OTHER HALF BY CON-   FFTT1260
C           JUGATE SYMMETRY.                                            FFTT1270
C        3. REAL TRANSFORM FOR THE 1ST DIMENSION, N ODD.  METHOD--      FFTT1280
C           TRANSFORM HALF THE DATA AT EACH STAGE, SUPPLYING THE OTHER  FFTT1290
C           HALF BY CONJUGATE SYMMETRY.                                 FFTT1300
C        4. REAL TRANSFORM FOR THE 1ST DIMENSION, N EVEN.  METHOD--     FFTT1310
```

```
C     TRANSFORM A COMPLEX ARRAY OF LENGTH N/2 WHOSE REAL PARTS      FFT1320
C       ARE THE EVEN NUMBERED REAL VALUES AND WHOSE IMAGINARY PARTS FFT1330
C       ARE THE ODD NUMBERED REAL VALUES.  SEPARATE AND SUPPLY     FFT1340
C       THE SECOND HALF BY CONJUGATE SYMMETRY.                     FFT1350
C                                                                  FFT1360
   70 NON2=NP1*(NP2/NTWO)                                          FFT1370
      ICASE=1                                                     FFT1380
      IF(IDIM-4)71,90,90                                          FFT1390
   71 IF(IFORM)72,72,90                                           FFT1400
   72 ICASE=2                                                     FFT1410
      IF(IDIM-1)73,73,90                                          FFT1420
   73 ICASE=3                                                     FFT1430
      IF(NTWO-NP1)90,90,74                                        FFT1440
   74 ICASE=4                                                     FFT1450
      NTWO=NTWO/2                                                 FFT1460
      N=N/2                                                       FFT1470
      NP2=NP2/2                                                   FFT1480
      NTOT=NTOT/2                                                 FFT1490
      I=3                                                         FFT1500
      DO 80 J=2,NTOT                                              FFT1510
      DATA(J)=DATA(I)                                             FFT1520
      I=I+2                                                       FFT1530
   80 I1RNG=NP1                                                   FFT1540
      IF(ICASE-2)100,95,100                                       FFT1550
   95 I1RNG=NP1*(1+NPREV/2)                                       FFT1560
C                                                                  FFT1570
C     SHUFFLE ON THE FACTORS OF TWO IN V.  AS THE SHUFFLING       FFT1580
C     CAN BE DONE BY SIMPLE INTERCHANGE, NO WORKING ARRAY IS NEEDED FFT1590
C                                                                  FFT1600
  100 IF(NTWO-NP1)600,600,110                                     FFT1610
```

```
  110   NP2HF=NP2/2                                                    FFTT1620
        J=1                                                            FFTT1630
        DO 150 I2=1,NP2,NON2                                           FFTT1640
        IF(J-I2)120,130,130                                            FFTT1650
  120   I1MAX=I2+NON2-2                                                FFTT1660
        DO 125 I1=I2,I1MAX,2                                           FFTT1670
        DO 125 I3=I1,NTOT,NP2                                          FFTT1680
        J3=J+I3-I2                                                     FFTT1690
        TEMPR=DATA(I3)                                                 FFTT1700
        TEMPI=DATA(I3+1)                                               FFTT1710
        DATA(I3)=DATA(J3)                                              FFTT1720
        DATA(I3+1)=DATA(J3+1)                                          FFTT1730
        DATA(J3)=TEMPR                                                 FFTT1740
  125   DATA(J3+1)=TEMPI                                               FFTT1750
  130   M=NP2HF                                                        FFTT1760
  140   IF(J-M)150,150,145                                             FFTT1770
  145   J=J-M                                                          FFTT1780
        M=M/2                                                          FFTT1790
        IF(M-NON2)150,140,140                                          FFTT1800
  150   J=J+M                                                          FFTT1810
C                                                                      FFTT1820
C     MAIN LOOP FOR FACTORS OF TWO.  PERFORM FOURIER TRANSFORMS OF     FFTT1830
C     LENGTH FOUR, WITH ONE OF LENGTH TWO IF NEEDED.  THE TWIDDLE FACTORFFTT1840
C     W=EXP(ISIGN*2*PI*SQRT(-1)*M/(4*MMAX)).  CHECK FOR W=ISIGN*SQRT(-1)FFTT1850
C     AND REPEAT FOR W=ISIGN*SQRT(-1)*CONJUGATE(W).                    FFTT1860
C                                                                      FFTT1870
        NON2T=NON2+NON2                                                FFTT1880
        IPAR=NTWO/NP1                                                  FFTT1890
  310   IF(IPAR-2)350,330,320                                          FFTT1900
  320   IPAR=IPAR/4                                                    FFTT1910
```

```
      GO TO 310                                                         FFT1920
  330 DO 340 I1=1,I1RNG,2                                               FFT1930
      DO 340 J3=I1,NON2,NP1                                             FFT1940
      DO 340 K1=J3,NTOT,NON2T                                           FFT1950
      K2=K1+NON2                                                        FFT1960
      TEMPR=DATA(K2)                                                    FFT1970
      TEMPI=DATA(K2+1)                                                  FFT1980
      DATA(K2)=DATA(K1)-TEMPR                                           FFT1990
      DATA(K2+1)=DATA(K1+1)-TEMPI                                       FFT2000
      DATA(K1)=DATA(K1)+TEMPR                                           FFT2010
  340 DATA(K1+1)=DATA(K1+1)+TEMPI                                       FFT2020
  350 MMAX=NON2                                                         FFT2030
  360 IF(MMAX-NPREF)370,600,600                                         FFT2040
  370 LMAX=MAX0(NON2T,MMAX/2)                                           FFT2050
      IF(MMAX-NON2)405,405,330                                          FFT2060
  380 THETA=-TWOPI*FLOAT(NON2)/FLOAT(4*MMAX)                            FFT2070
      IF(ISIGN)400,390,390                                              FFT2080
  390 THETA=-THETA                                                      FFT2090
  400 WR=COS(THETA)                                                     FFT2100
      WI=SIN(THETA)                                                     FFT2110
      WSTPR=-2.*WI*WI                                                   FFT2120
      WSTPI=2.*WR*WI                                                    FFT2130
  405 DO 570 L=NON2,LMAX,NON2T                                          FFT2140
      M=L                                                               FFT2150
      IF(MMAX-NON2)420,420,410                                          FFT2160
  410 W2R=WR*WR-WI*WI                                                   FFT2170
      W2I=2.*WR*WI                                                      FFT2180
      W3R=W2R*WR-W2I*WI                                                 FFT2190
      W3I=W2R*WI+W2I*WR                                                 FFT2200
  420 DO 530 I1=1,I1RNG,2                                               FFT2210
```

```
      DO 530 J3=I1,NON2,NP1                                             FFTT2220
      KMIN=J3+IPAR*M                                                    FFTT2230
      IF(MMAX-NON2)430,430,440                                          FFTT2240
  430 KMIN=J3                                                           FFTT2250
  440 KDIF=IPAR*MMAX                                                    FFTT2260
  450 KSTEP=4*KDIF                                                      FFTT2270
      DO 520 K1=KMIN,NTOT,KSTEP                                         FFTT2280
      K2=K1+KDIF                                                        FFTT2290
      K3=K2+KDIF                                                        FFTT2300
      K4=K3+KDIF                                                        FFTT2310
      IF(MMAX-NON2)460,460,480                                          FFTT2320
  460 U1R=DATA(K1)+DATA(K2)                                             FFTT2330
      U1I=DATA(K1+1)+DATA(K2+1)                                         FFTT2340
      U2R=DATA(K3)+DATA(K4)                                             FFTT2350
      U2I=DATA(K3+1)+DATA(K4+1)                                         FFTT2360
      U3R=DATA(K1)-DATA(K2)                                             FFTT2370
      U3I=DATA(K1+1)-DATA(K2+1)                                         FFTT2380
      IF(TSIGN)470,475,475                                              FFTT2390
  470 U4R=DATA(K3+1)-DATA(K4+1)                                         FFTT2400
      U4I=DATA(K4)-DATA(K3)                                             FFTT2410
      GO TO 510                                                         FFTT2420
  475 U4R=DATA(K4+1)-DATA(K3+1)                                         FFTT2430
      U4I=DATA(K3)-DATA(K4)                                             FFTT2440
      GO TO 510                                                         FFTT2450
  480 T2R=W2R*DATA(K2)-W2I*DATA(K2+1)                                   FFTT2460
      T2I=W2R*DATA(K2+1)+W2I*DATA(K2)                                   FFTT2470
      T3R=WR*DATA(K3)-WI*DATA(K3+1)                                     FFTT2480
      T3I=WR*DATA(K3+1)+WI*DATA(K3)                                     FFTT2490
      T4R=W3R*DATA(K4)-W3I*DATA(K4+1)                                   FFTT2500
      T4I=W3R*DATA(K4+1)+W3I*DATA(K4)                                   FFTT2510
```

```
      U1R=DATA(K1)+T2R                                          FFTT2520
      U1I=DATA(K1+1)+T2I                                        FFTT2530
      U2R=T3R+T4R                                               FFTT2540
      U2I=T3I+T4I                                               FFTT2550
      U3R=DATA(K1)-T2R                                          FFTT2560
      U3I=DATA(K1+1)-T2I                                        FFTT2570
      IF(ISIGN)490,500,500                                      FFTT2580
  490 U4R=T3I-T4I                                               FFTT2590
      U4I=T4R-T3R                                               FFTT2600
      GO TO 510                                                 FFTT2610
  500 U4R=T4I-T3I                                               FFTT2620
      U4I=T3R-T4R                                               FFTT2630
  510 DATA(K1)=U1R+U2R                                          FFTT2640
      DATA(K1+1)=U1I+U2I                                        FFTT2650
      DATA(K2)=U3R+U4R                                          FFTT2660
      DATA(K2+1)=U3I+U4I                                        FFTT2670
      DATA(K3)=U1R-U2R                                          FFTT2680
      DATA(K3+1)=U1I-U2I                                        FFTT2690
      DATA(K4)=U3R-U4R                                          FFTT2700
      DATA(K4+1)=U3I-U4I                                        FFTT2710
  520 KMIN=4*(KMIN-J3)+J2                                       FFTT2720
      KDIF=KSTEP                                                FFTT2730
      IF(KDIF-NP2)450,530,530                                   FFTT2740
  530 CONTINUE                                                  FFTT2750
      M=MMAX-M                                                  FFTT2760
      IF(ISIGN)540,550,550                                      FFTT2770
  540 TEMPR=WR                                                  FFTT2780
      WR=-WI                                                    FFTT2790
      WI=-TEMPR                                                 FFTT2800
      GO TO 560                                                 FFTT2810
```

```
  550  TEMPR=WR                                                      FFTT2820
       WR=WI                                                         FFTT2830
       WI=TEMPR                                                      FFTT2840
  560  IF(M-LMAX)565,565,410                                         FFTT2850
  565  TEMPR=WR                                                      FFTT2860
       WR=WR*WSTPR-WI*WSTPI+WR                                       FFTT2870
  570  WI=WI*WSTPR+TEMPR*WSTPI+WI                                    FFTT2880
       IPAR=3-IPAR                                                   FFTT2890
       MMAX=MMAX+MMAX                                                FFTT2900
       GO TO 360                                                     FFTT2910
C                                                                    FFTT2920
C      MAIN LOOP FOR FACTORS NOT EQUAL TO TWO.  APPLY THE TWIDDLE FACTOR FFTT2930
C      W=EXP(ISIGN*2*PI*SQRT(-1)*(J2-1)*(J1-J2)/(NP2*IFP1)), THEN     FFTT2940
C      PERFORM A FOURIER TRANSFORM OF LENGTH IFACT(IF), MAKING USE OF FFTT2950
C      CONJUGATE SYMMETRIES.                                         FFTT2960
C                                                                    FFTT2970
  600  IF(NTWO-NP2)605,700,700                                       FFTT2980
  605  IFP1=NON2                                                     FFTT2990
       IF=1                                                          FFTT3000
       NP1HF=NP1/2                                                   FFTT3010
  610  IFP2=IFP1/IFACT(IF)                                           FFTT3020
       J1RNG=NP2                                                     FFTT3030
       IF(ICASE-3)612,611,612                                        FFTT3040
  611  J1RNG=(NP2+IFP1)/2                                            FFTT3050
       J2STP=NP2/IFACT(IF)                                           FFTT3060
       J1RG2=(J2STP+IFP2)/2                                          FFTT3070
  612  J2MIN=1+IFP2                                                  FFTT3080
       IF(IFP1-NP2)615,640,640                                       FFTT3090
  615  DO 635 J2=J2MIN,IFP1,IFP2                                     FFTT3100
       THETA=-TWOPI*FLOAT(J2-1)/FLOAT(NP2)                           FFTT3110
```

```
      IF(ISIGN)625,620,620                                          FFTT3120
620   THETA=-THETA                                                  FFTT3130
625   SINTH=SIN(THETA/2.)                                           FFTT3140
      WSTPR=-2.*SINTH*SINTH                                         FFTT3150
      WSTPI=SIN(THETA)                                              FFTT3160
      WR=WSTPR+1.                                                   FFTT3170
      WI=WSTPI                                                      FFTT3180
      J1MIN=J2+IFP1                                                 FFTT3190
      DO 635 J1=J1MIN,J1RNG,IFP1                                    FFTT3200
      I1MAX=J1+I1RNG-2                                              FFTT3210
      DO 630 I1=J1,I1MAX,2                                          FFTT3220
      DO 630 I3=I1,NTOT,NP2                                         FFTT3230
      J3MAX=I3+IFP2-NP1                                             FFTT3240
      DO 630 J3=I3,J3MAX,NP1                                        FFTT3250
      TEMPR=DATA(J3)                                                FFTT3260
      DATA(J3)=DATA(J3)*WR-DATA(J3+1)*WI                            FFTT3270
630   DATA(J3+1)=TEMPR*WI+DATA(J3+1)*WR                             FFTT3280
      TEMPR=WR                                                      FFTT3290
      WR=WR*WSTPR-WI*WSTPI+WR                                       FFTT3300
635   WI=TEMPR*WSTPI+WI*WSTPR+WI                                    FFTT3310
640   THETA=-TWOPI/FLOAT(IFACT(IF))                                 FFTT3320
      IF(ISIGN)650,645,645                                          FFTT3330
645   THETA=-THETA                                                  FFTT3340
650   SINTH=SIN(THETA/2.)                                           FFTT3350
      WSTPR=-2.*SINTH*SINTH                                         FFTT3360
      WSTPI=SIN(THETA)                                              FFTT3370
      KSTEP=2*N/IFACT(IF)                                           FFTT3380
      KRANG=KSTEP*(IFACT(IF)/2)+1                                   FFTT3390
      DO 698 I1=1,I1RNG,2                                           FFTT3400
      DO 698 I3=I1,NTOT,NP2                                         FFTT3410
```

```
      DO 690 KMIN=1,KRANG,KSTEP                                         FFTT3420
      J1MAX=I3+J1RNG-IFP1                                               FFTT3430
      DO 680 J1=I3,J1MAX,IFP1                                           FFTT3440
      J3MAX=J1+IFP2-NP1                                                 FFTT3450
      DO 680 J3=J1,J3MAX,NP1                                            FFTT3460
      J2MAX=J3+IFP1-IFP2                                                FFTT3470
      K=KMIN+(J3-J1+(J1-I3)/IFACT(IF))/NP1HF                            FFTT3480
      IF(KMIN-1)655,655,665                                             FFTT3490
  655 SUMR=0.                                                           FFTT3500
      SUMI=0.                                                           FFTT3510
      DO 660 J2=J3,J2MAX,IFP2                                           FFTT3520
      SUMR=SUMR+DATA(J2)                                                FFTT3530
  660 SUMI=SUMI+DATA(J2+1)                                              FFTT3540
      WORK(K)=SUMR                                                      FFTT3550
      WORK(K+1)=SUMI                                                    FFTT3560
      GO TO 680                                                         FFTT3570
  665 KCONJ=K+2*(N-KMIN+1)                                              FFTT3580
      J2=J2MAX                                                          FFTT3590
      SUMR=DATA(J2)                                                     FFTT3600
      SUMI=DATA(J2+1)                                                   FFTT3610
      OLDSR=0.                                                          FFTT3620
      OLDSI=0.                                                          FFTT3630
      J2=J2-IFP2                                                        FFTT3640
  670 TEMPR=SUMR                                                        FFTT3650
      TEMPI=SUMI                                                        FFTT3660
      SUMR=TWOWR*SUMR-OLDSR+DATA(J2)                                    FFTT3670
      SUMI=TWOWR*SUMI-OLDSI+DATA(J2+1)                                  FFTT3680
      OLDSR=TEMPR                                                       FFTT3690
      OLDSI=TEMPI                                                       FFTT3700
      J2=J2-IFP2                                                        FFTT3710
```

```
      IF(J2-J3)675,675,670                                              FFTT3720
  670 TEMPR=WR*SUMR-OLDSI*DATA(J2)                                      FFTT3730
      TEMPI=WI*SUMI                                                     FFTT3740
      WORK(K)=TEMPR-TEMPI                                               FFTT3750
      WORK(KCONJ)=TEMPR+TEMPI                                           FFTT3760
      TEMPR=WR*SUMI-OLDSI*DATA(J2+1)                                    FFTT3770
      TEMPI=WI*SUMR                                                     FFTT3780
      WORK(K+1)=TEMPR+TEMPI                                             FFTT3790
      WORK(KCONJ+1)=TEMPR-TEMPI                                         FFTT3800
  680 CONTINUE                                                          FFTT3810
      IF(KMIN-1)685,685,686                                             FFTT3820
  685 WR=WSTPR+1.                                                       FFTT3830
      WI=WSTPI                                                          FFTT3840
      GO TO 690                                                         FFTT3850
  686 TEMPR=WR                                                          FFTT3860
      WR=WR*WSTPR-WI*WSTPI+WR                                           FFTT3870
      WI=TEMPR*WSTPI+WI*WSTPR+WI                                        FFTT3880
  690 TWOWR=WR+WR                                                       FFTT3890
      IF(ICASE-3)692,691,692                                            FFTT3900
  691 IF(IFP1-NP2)695,692,692                                           FFTT3910
  692 K=1                                                               FFTT3920
      I2MAX=I3+NP2-NP1                                                  FFTT3930
      DO 693 I2=I3,I2MAX,NP1                                            FFTT3940
      DATA(I2)=WORK(K)                                                  FFTT3950
      DATA(I2+1)=WORK(K+1)                                              FFTT3960
  693 K=K+2                                                             FFTT3970
      GO TO 698                                                         FFTT3980
C                                                                       FFTT3990
C     COMPLETE A REAL TRANSFORM IN THE 1ST DIMENSION, N ODD, BY CON-    FFTT4000
C     JUGATE SYMMETRIES AT EACH STAGE.                                  FFTT4010
```

```
C
695   J3MAX=I3+IFP2-NP1                                                 FFTT+020
      DO 697 J3=I3,J3MAX,NP1                                            FFTT+030
      J2MAX=J3+NP2-J2STP                                                FFTT+040
      DO 697 J2=J3,J2MAX,J2STP                                          FFTT+050
      J1MAX=J2+J1RG2-IFP2                                               FFTT4060
      J1CNJ=J3+J2MAX+J2STP-J2                                           FFTT+070
      DO 697 J1=J2,J1MAX,IFP2                                           FFTT+080
      K=1+J1-I3                                                         FFTT4090
      DATA(J1)=WORK(K)                                                  FFTT4100
      DATA(J1+1)=WORK(K+1)                                              FFTT4110
      IF(J1-J2)637,697,696                                              FFTT+120
696   DATA(J1CNJ)=WORK(K)                                               FFTT4130
      DATA(J1CNJ+1)=-WORK(K+1)                                          FFTT4140
697   J1CNJ=J1CNJ-IFP2                                                  FFTT4150
698   CONTINUE                                                          FFTT+160
      IF=IF+1                                                           FFTT+170
      IFP1=IFP2                                                         FFTT+180
      IF(IFP1-NP1)700,700,610                                           FFTT+190
C                                                                       FFTT+200
C     JUGATE SYMMETRIES.                                                FFTT+210
C     COMPLETE A REAL TRANSFORM IN THE 1ST DIMENSION, N EVEN, BY CON-   FFTT+220
C                                                                       FFTT+230
700   GO TO (900,800,900,701),ICASE                                     FFTT+240
701   NHALF=N                                                           FFTT+250
      N=N+N                                                             FFTT+260
      THETA=-TWOPI/FLOAT(N)                                             FFTT+270
      IF(ISIGN)702,702,702                                              FFTT+280
702   THETA=-THETA                                                      FFTT+290
707   SINTH=SIN(THETA/2.)                                               FFTT+300
                                                                        FFTT+310
```

```
      WSTPR=-2.*SINTH*SINTH                                             FFTT4320
      WSTPI=SIN(THETA)                                                  FFTT4330
      WR=WSTPR+1.                                                       FFTT4340
      WI=WSTPI                                                          FFTT4350
      IMIN=3                                                            FFTT4360
      JMIN=2*NHALF-1                                                    FFTT4370
      GO TO 725                                                         FFTT4380
  710 J=JMIN                                                            FFTT4390
      DO 720 I=IMIN,NTOT,NP2                                            FFTT4400
      SUMR=(DATA(I)+DATA(J))/2.                                         FFTT4410
      SUMI=(DATA(I+1)+DATA(J+1))/2.                                     FFTT4420
      DIFR=(DATA(I)-DATA(J))/2.                                         FFTT4430
      DIFI=(DATA(I+1)-DATA(J+1))/2.                                     FFTT4440
      TEMPR=WR*SUMI+WI*DIFR                                             FFTT4450
      TEMPI=WI*SUMI-WR*DIFR                                             FFTT4460
      DATA(I)=SUMR+TEMPR                                                FFTT4470
      DATA(I+1)=DIFI+TEMPI                                              FFTT4480
      DATA(J)=SUMR-TEMPR                                                FFTT4490
      DATA(J+1)=-DIFI+TEMPI                                             FFTT4500
  720 J=J+NP2                                                           FFTT4510
      IMIN=IMIN+2                                                       FFTT4520
      JMIN=JMIN-2                                                       FFTT4530
      TEMPR=WR                                                          FFTT4540
      WR=WR*WSTPR-WI*WSTPI+WR                                           FFTT4550
      WI=TEMPR*WSTPI+WI*WSTPR+WI                                        FFTT4560
  725 IF(IMIN-JMIN)710,730,740                                          FFTT4570
  730 IF(ISIGN)731,740,740                                              FFTT4580
  731 DO 735 I=IMIN,NTOT,NP2                                            FFTT4590
  735 DATA(I+1)=-DATA(I+1)                                              FFTT4600
  740 NP2=NP2+NP2                                                       FFTT4610
```

```
      NTOT=NTOT+NTOT                                                    FFTT4620
      J=NTOT+1                                                          FFTT4630
      IMAX=NTOT/2+1                                                     FFTT4640
  745 IMIN=IMAX-2*NHALF                                                 FFTT4650
      I=IMIN                                                            FFTT4660
      GO TO 755                                                         FFTT4670
  750 DATA(J)=DATA(I)                                                   FFTT4680
      DATA(J+1)=-DATA(I+1)                                              FFTT4690
  755 I=I+2                                                             FFTT4700
      J=J-2                                                             FFTT4710
      IF(I-IMAX)750,760,760                                             FFTT4720
  760 DATA(J)=DATA(IMIN)-DATA(IMIN+1)                                   FFTT4730
      DATA(J+1)=0.                                                      FFTT4740
      IF(I-J)770,780,780                                                FFTT4750
  765 DATA(J)=DATA(I)                                                   FFTT4760
      DATA(J+1)=DATA(I+1)                                               FFTT4770
  770 I=I-2                                                             FFTT4780
      J=J-2                                                             FFTT4790
      IF(I-IMIN)775,775,765                                             FFTT4800
  775 DATA(J)=DATA(IMIN)+DATA(IMIN+1)                                   FFTT4810
      DATA(J+1)=0.                                                      FFTT4820
      IMAX=IMIN                                                         FFTT4830
      GO TO 745                                                         FFTT4840
  780 DATA(1)=DATA(1)+DATA(2)                                           FFTT4850
      DATA(2)=0.                                                        FFTT4860
      GO TO 900                                                         FFTT4870
C                                                                       FFTT4880
C     COMPLETE A REAL TRANSFORM FOR THE 2ND OR 3RD DIMENSION BY         FFTT4890
C     CONJUGATE SYMMETRIES.                                             FFTT4900
C                                                                       FFTT4910
```

```
      IF(I1RNG-NP1)805,900,900                                  FFTT4920
805   DO 860 I3=1,NTOT,NP2                                      FFTT4930
      I2MAX=I3+NP2-NP1                                          FFTT4940
      DO 860 I2=I3,I2MAX,NP1                                    FFTT4950
      IMIN=I2+I1RNG                                             FFTT4960
      IMAX=I2+NP1-2                                             FFTT4970
      JMAX=2*I3+NP1-IMIN                                        FFTT4980
      IF(I2-I3)820,820,810                                      FFTT4990
810   JMAX=JMAX+NP2                                             FFTT5000
820   IF(IDIM-2)850,850,830                                     FFTT5010
830   J=JMAX+NP0                                                FFTT5020
      DO 840 I=IMIN,IMAX,2                                      FFTT5030
      DATA(I)=DATA(J)                                           FFTT5040
      DATA(I+1)=-DATA(J+1)                                      FFTT5050
840   J=J-2                                                     FFTT5060
850   J=JMAX                                                    FFTT5070
      DO 860 I=IMIN,IMAX,NP0                                    FFTT5080
      DATA(I)=DATA(J)                                           FFTT5090
      DATA(I+1)=-DATA(J+1)                                      FFTT5100
860   J=J-NP0                                                   FFTT5110
C                                                               FFTT5120
C     END OF LOOP ON EACH DIMENSION                             FFTT5130
C                                                               FFTT5140
900   NP0=NP1                                                   FFTT5150
      NP1=NP2                                                   FFTT5160
910   NPREV=N                                                   FFTT5170
```

```
FFTT5180
FFTT5190
```

```
920   RETURN
      END
```

Appendix B

Computer Plots

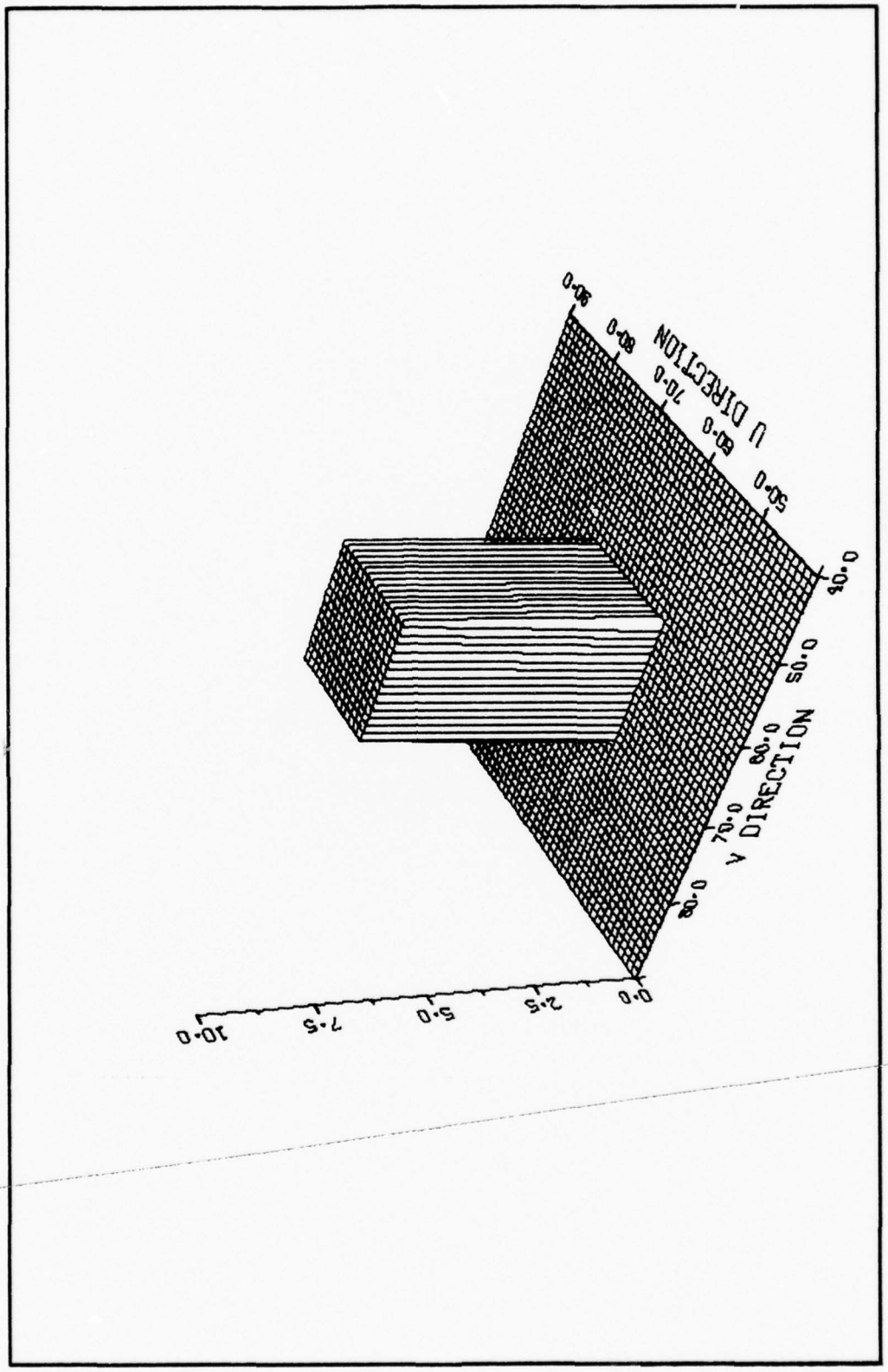

Fig. 29 Normalized Surface Height Distribution

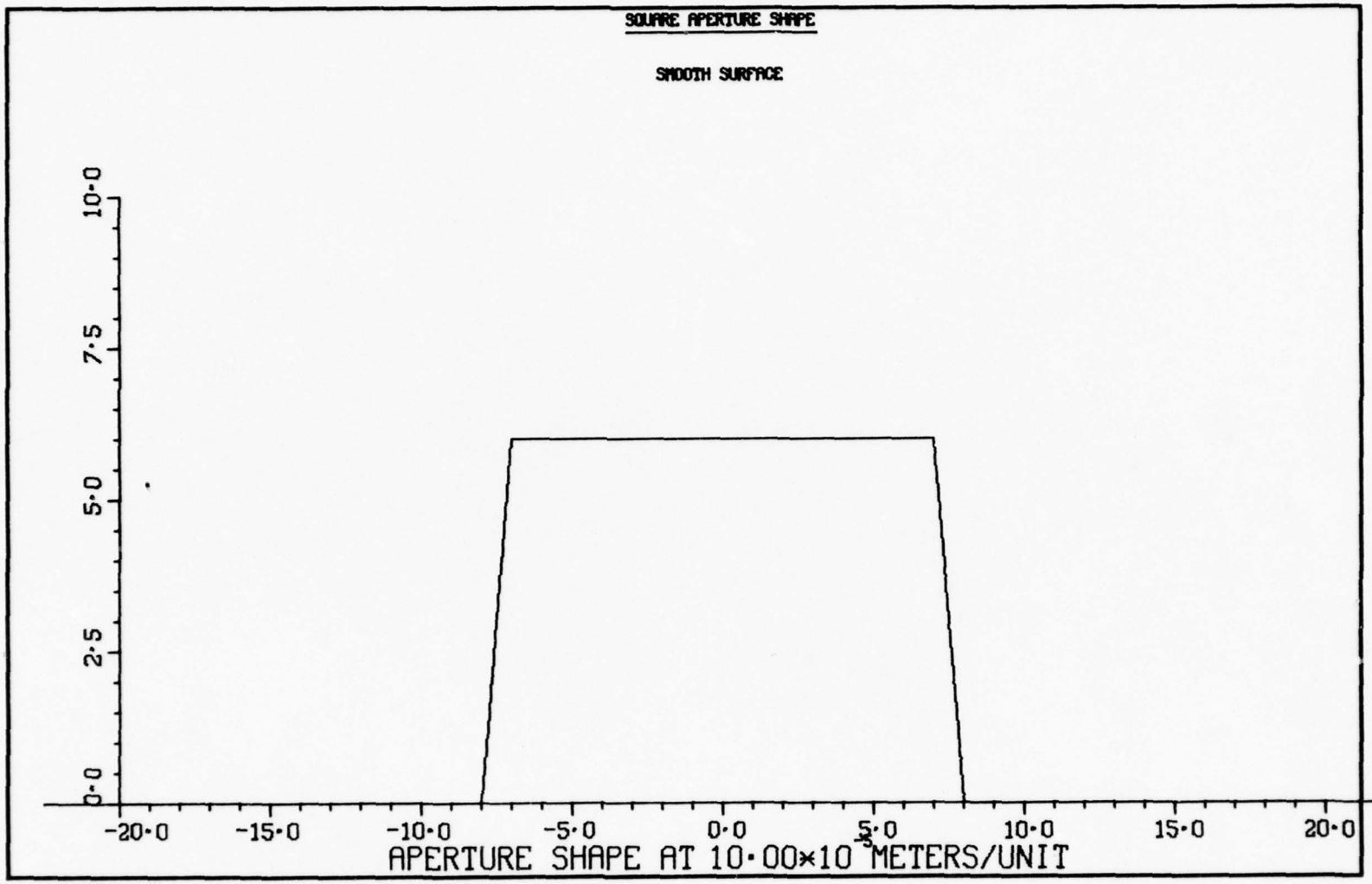

Fig. 30 One Dimensional Cut Through Fig. 29

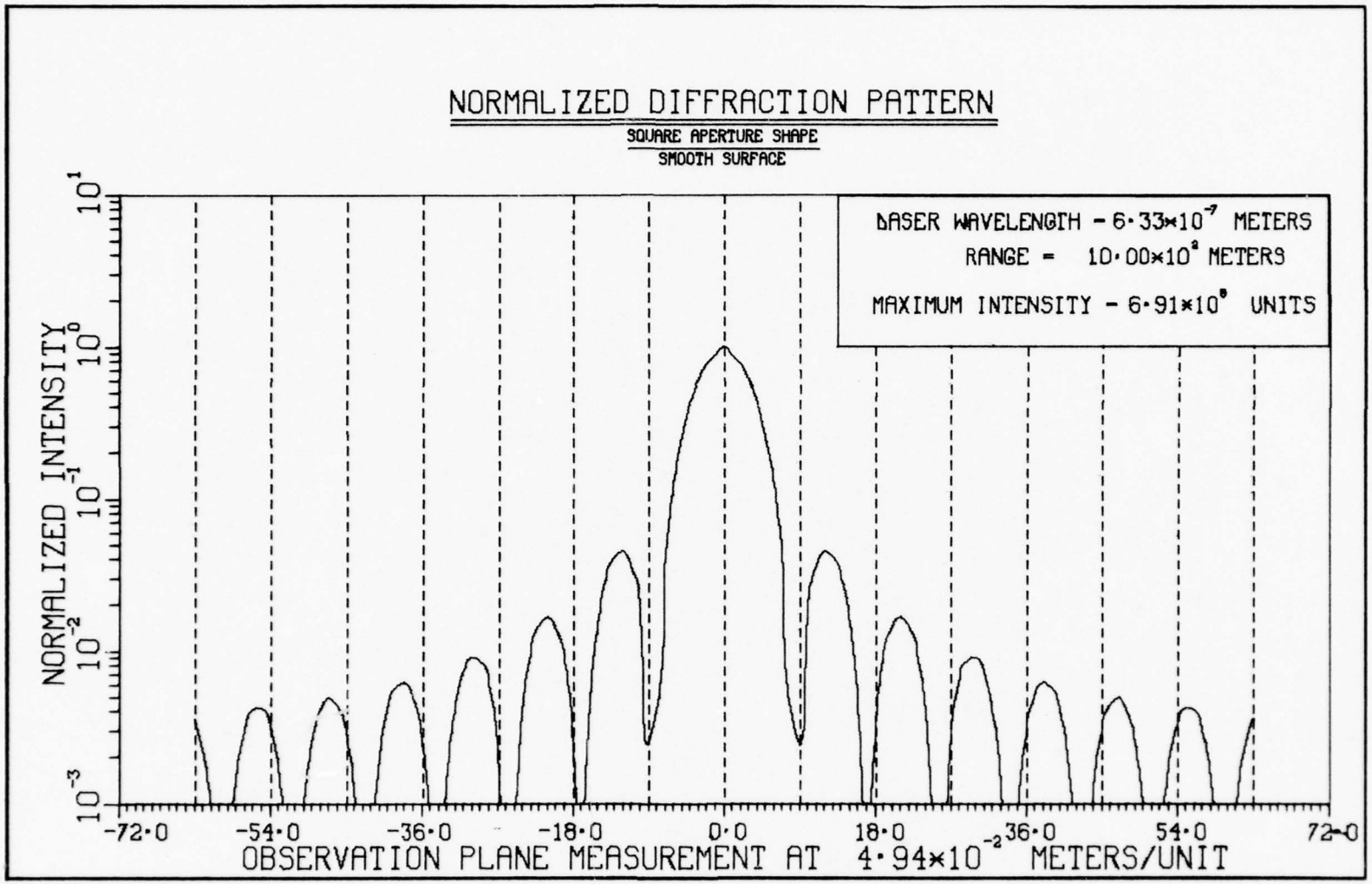

Fig. 31 One Dimensional Cut Through Speckle Pattern

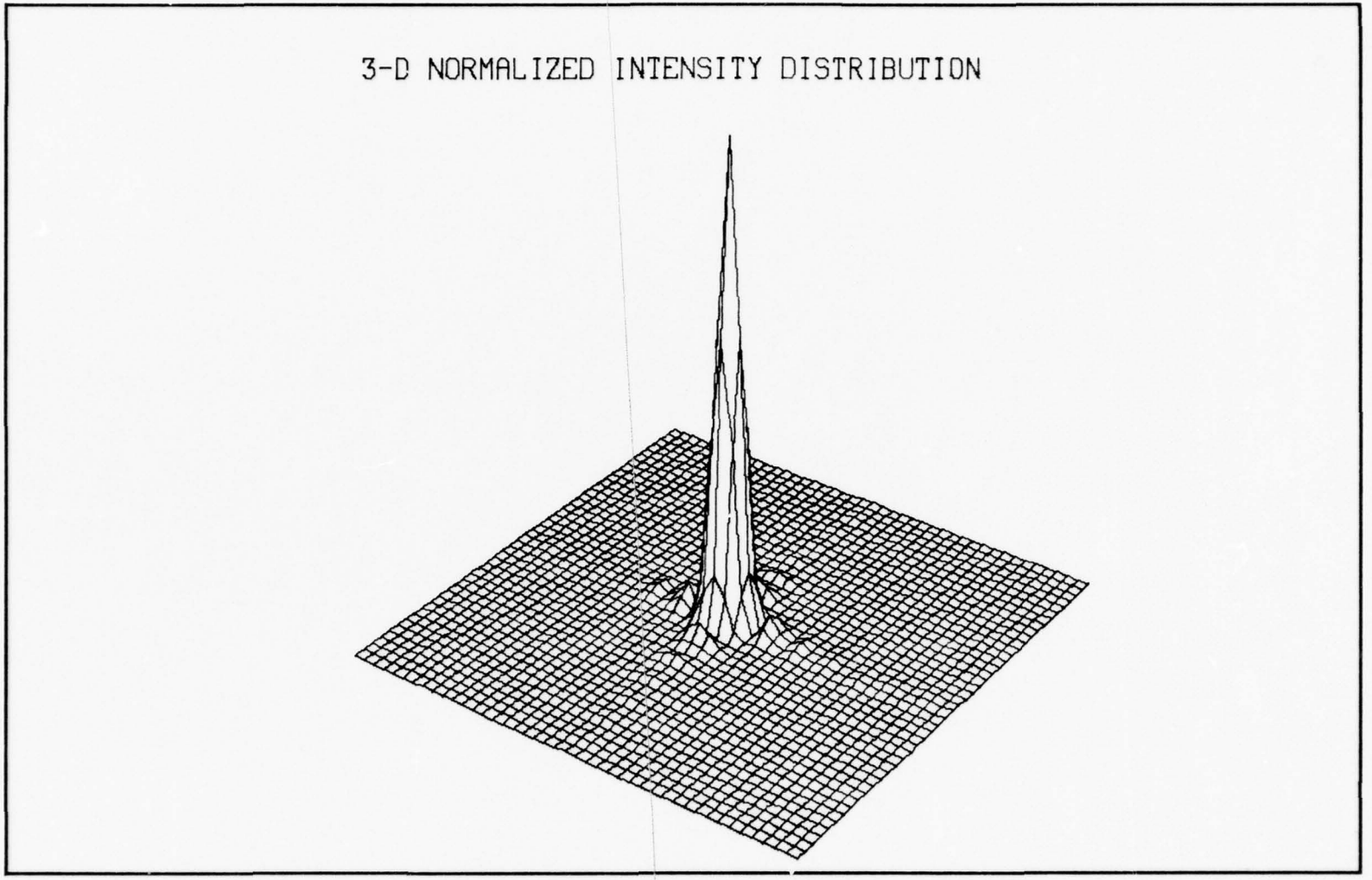

Fig. 32 Three Dimensional Perspective of Speckle Pattern

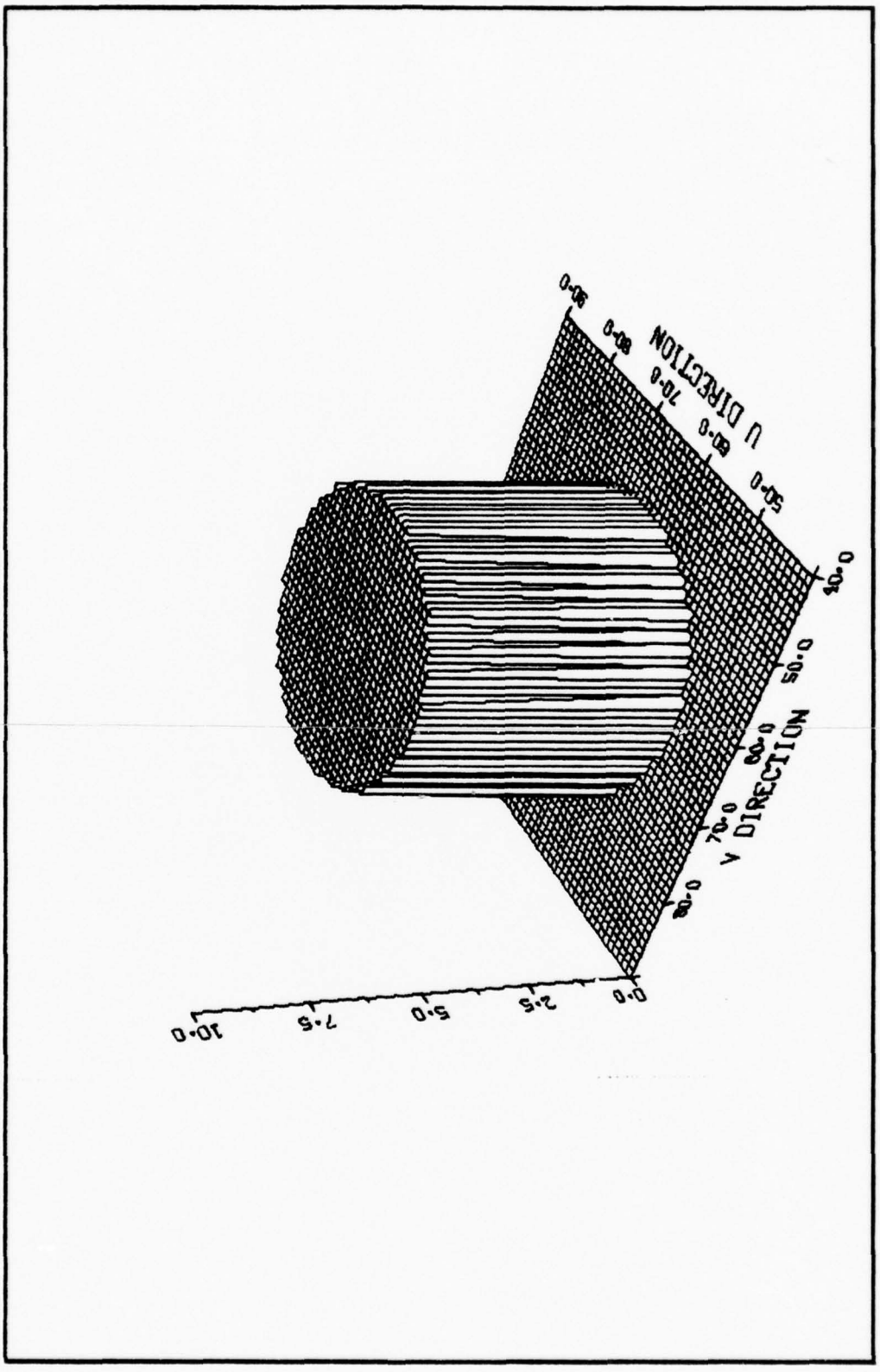

Fig. 33 Normalized Surface Height Distribution

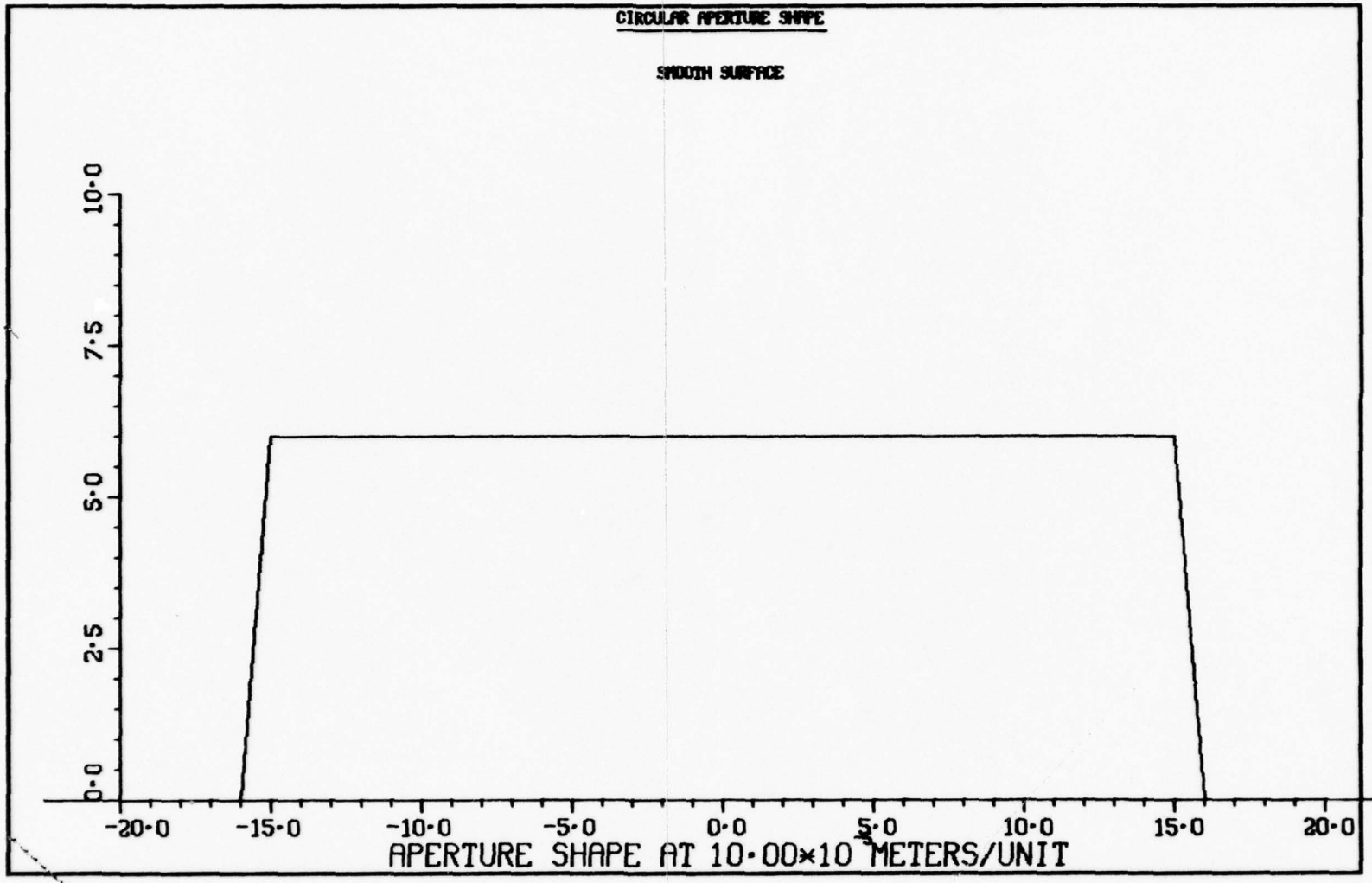

Fig. 34 One Dimensional Cut Through Fig. 33

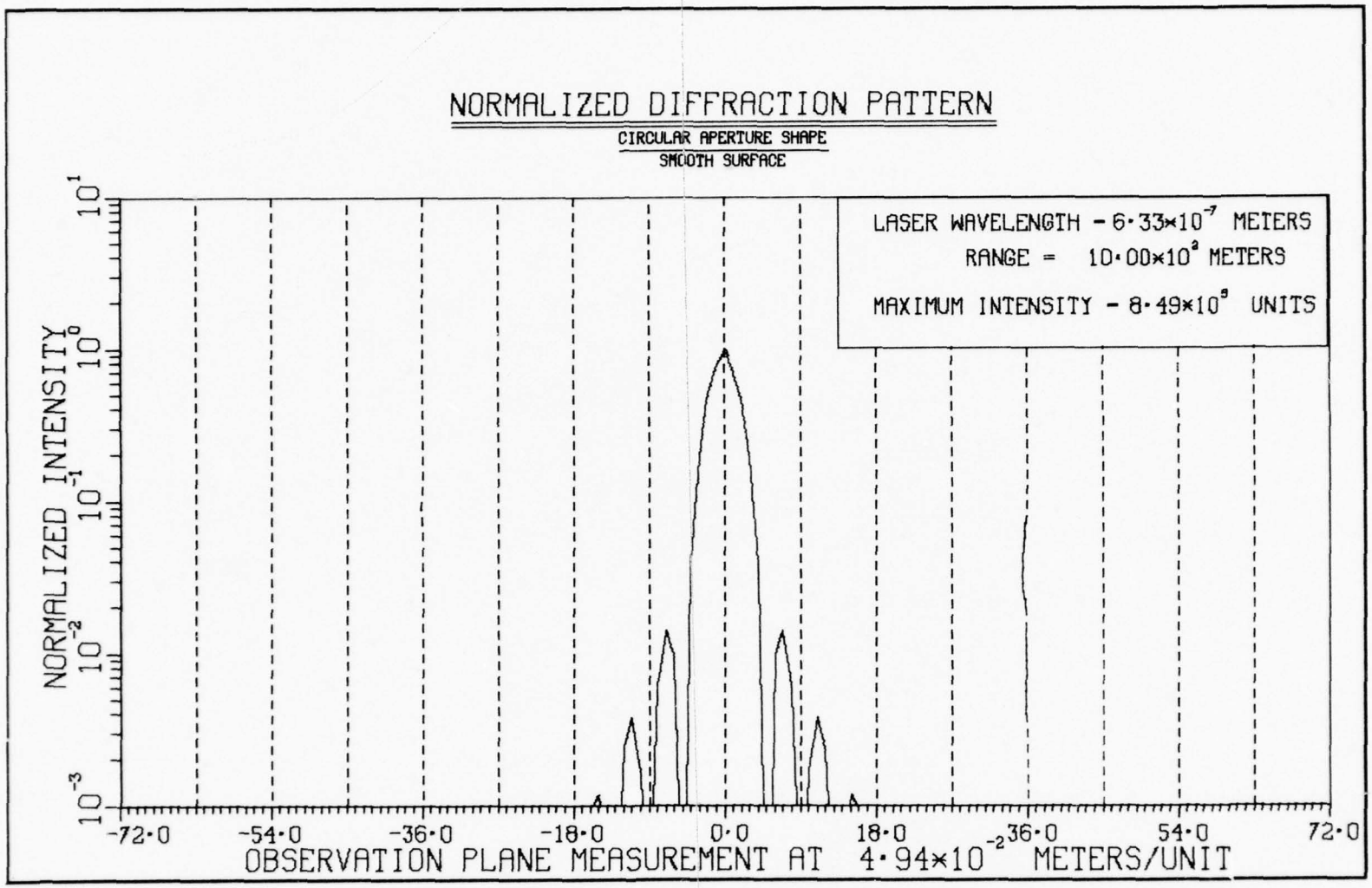

Fig. 35 One Dimensional Cut Through Speckle Pattern

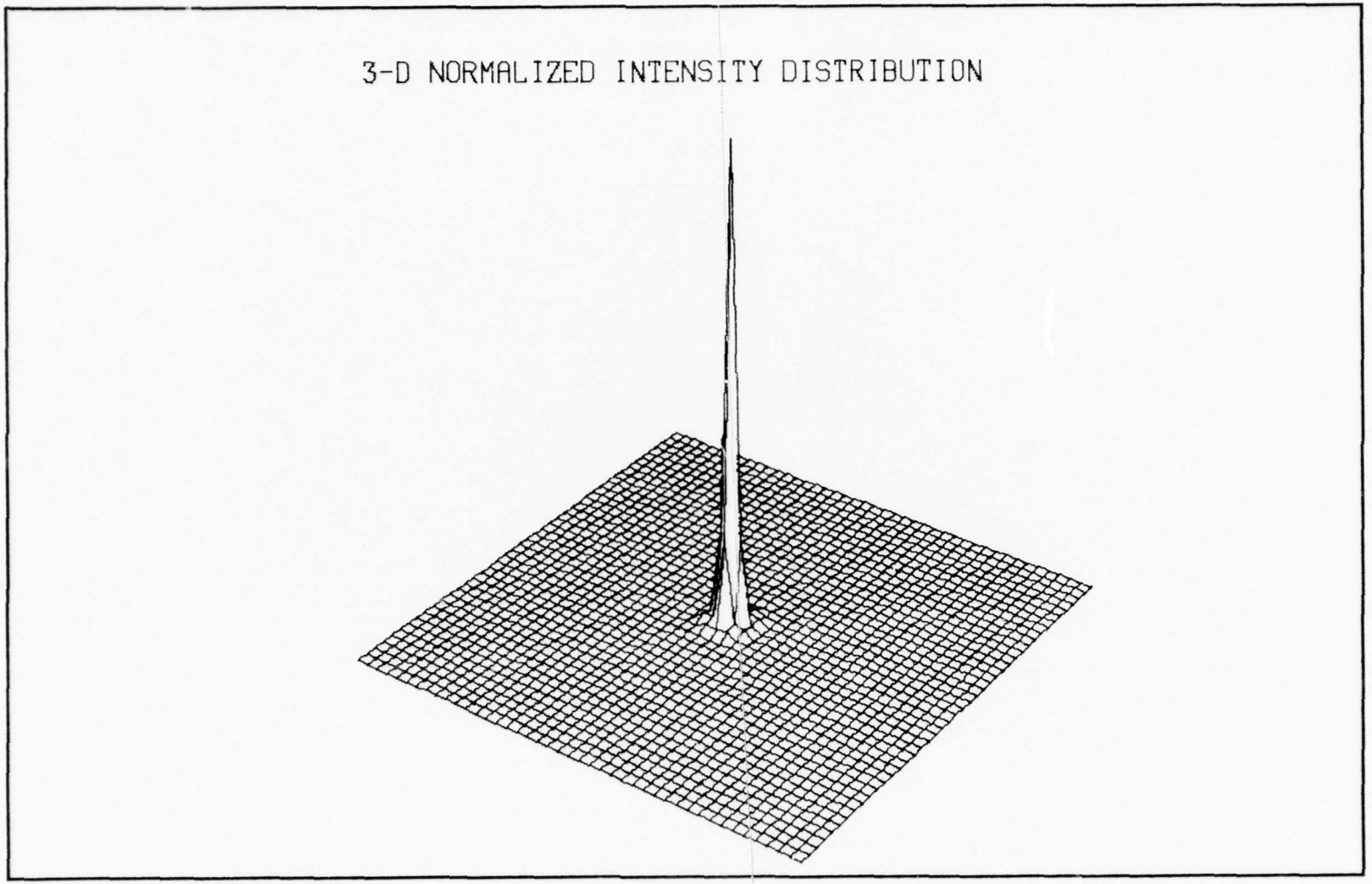

Fig. 36 Three Dimensional Perspective of Speckle Pattern

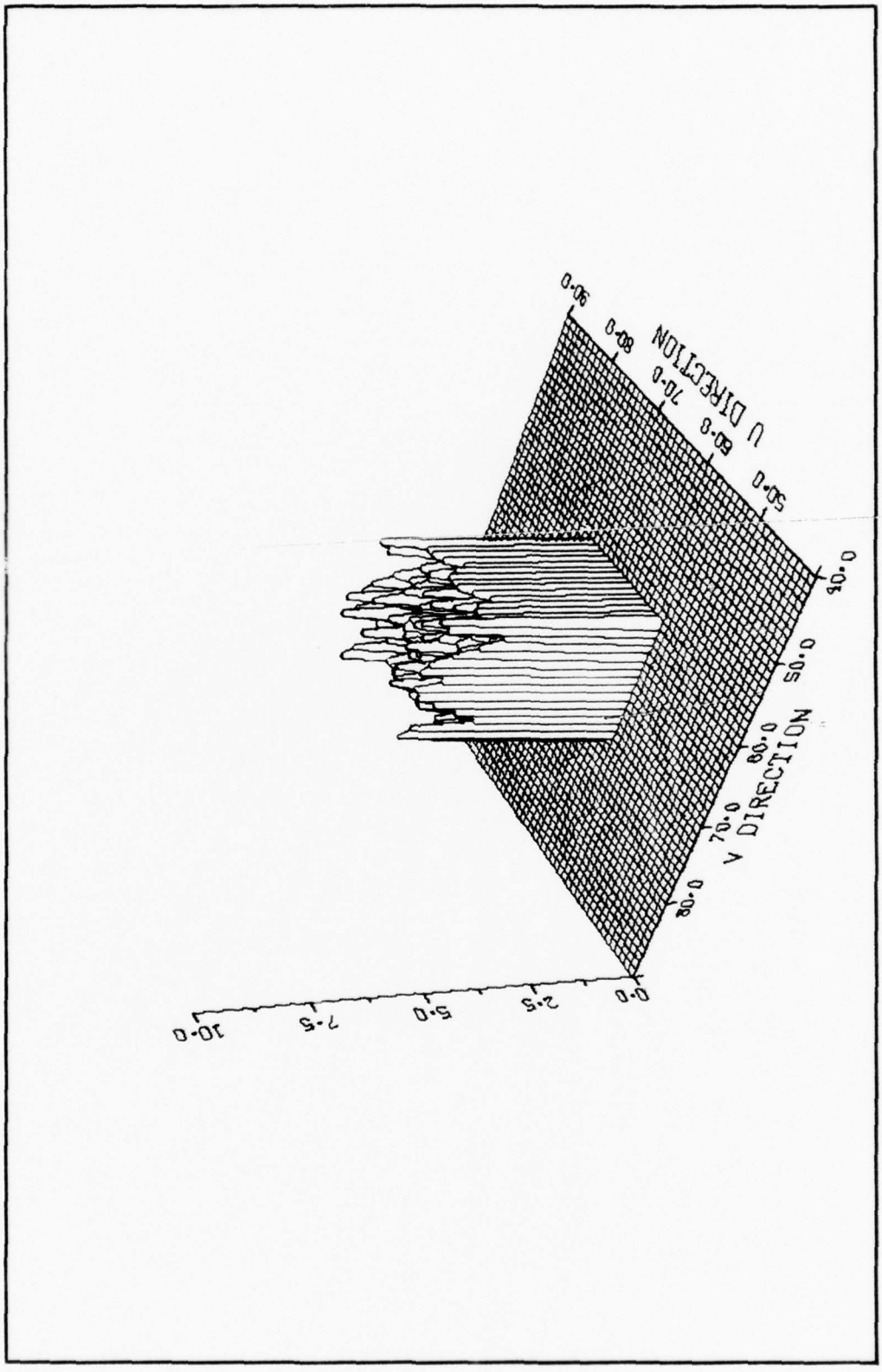

Fig. 37 Normalized Surface Height Distribution

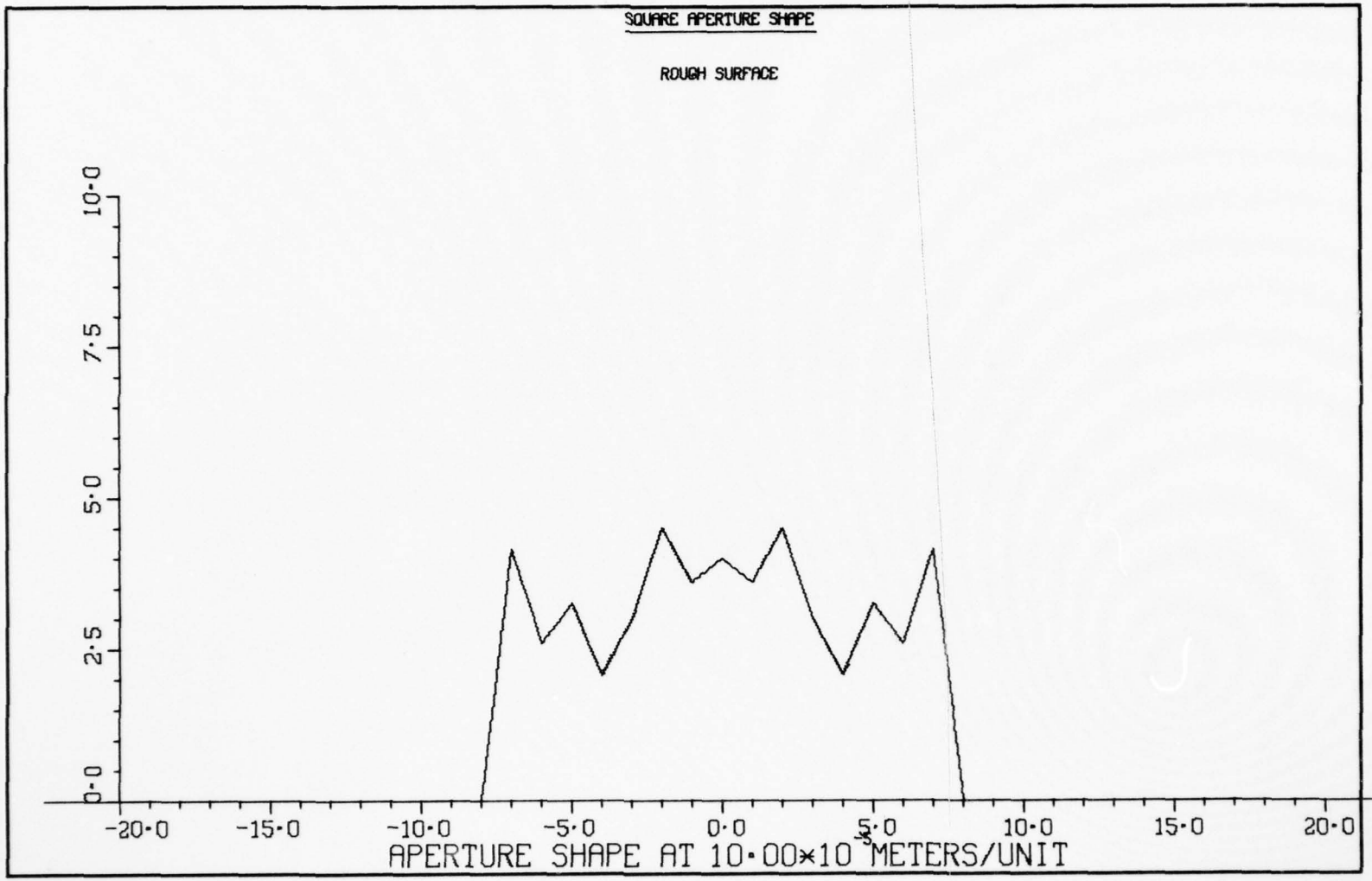

Fig. 38 One Dimensional Cut Through Fig. 37

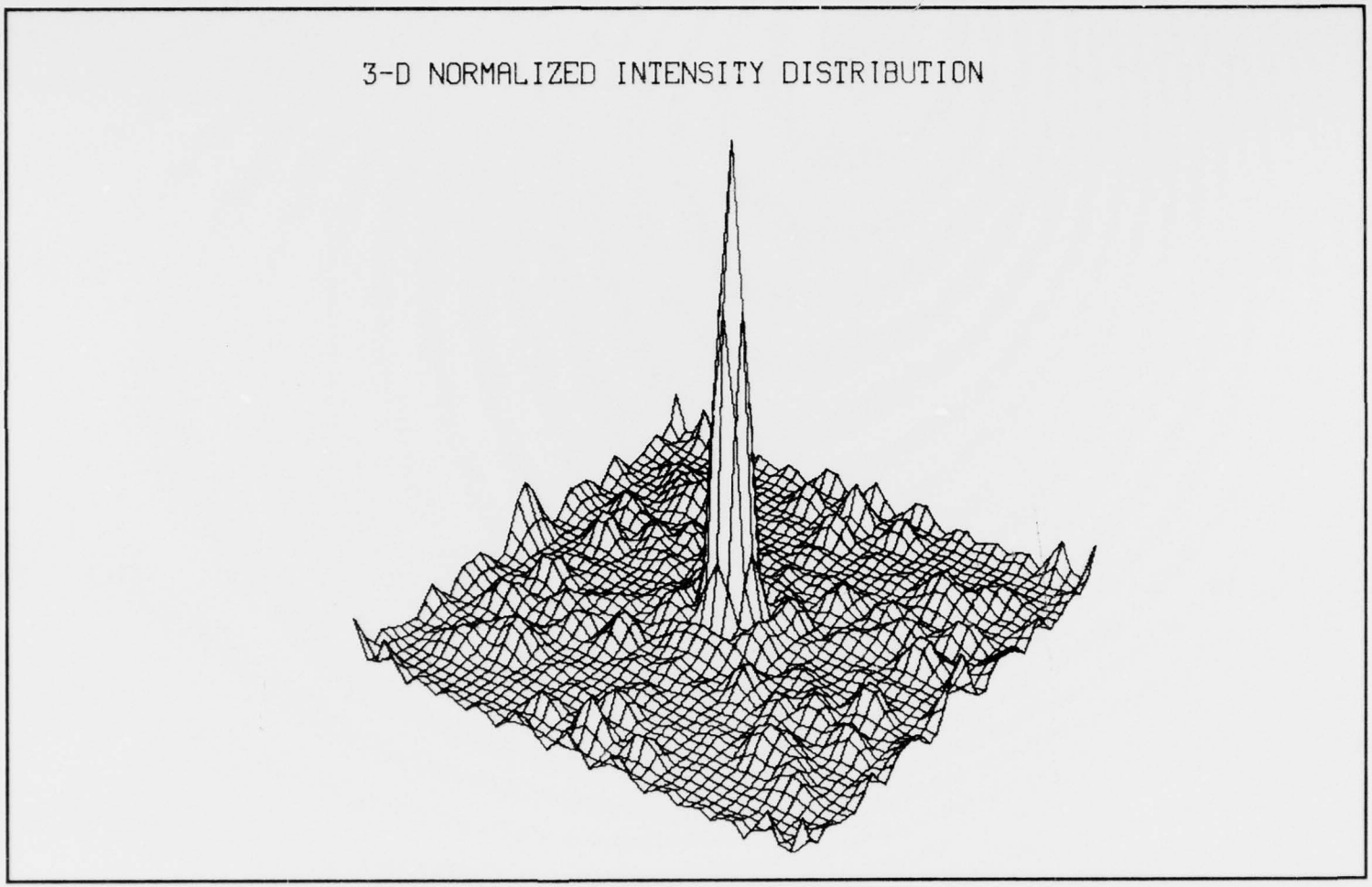

Fig. 39 Three Dimensional Perspective of Speckle Pattern

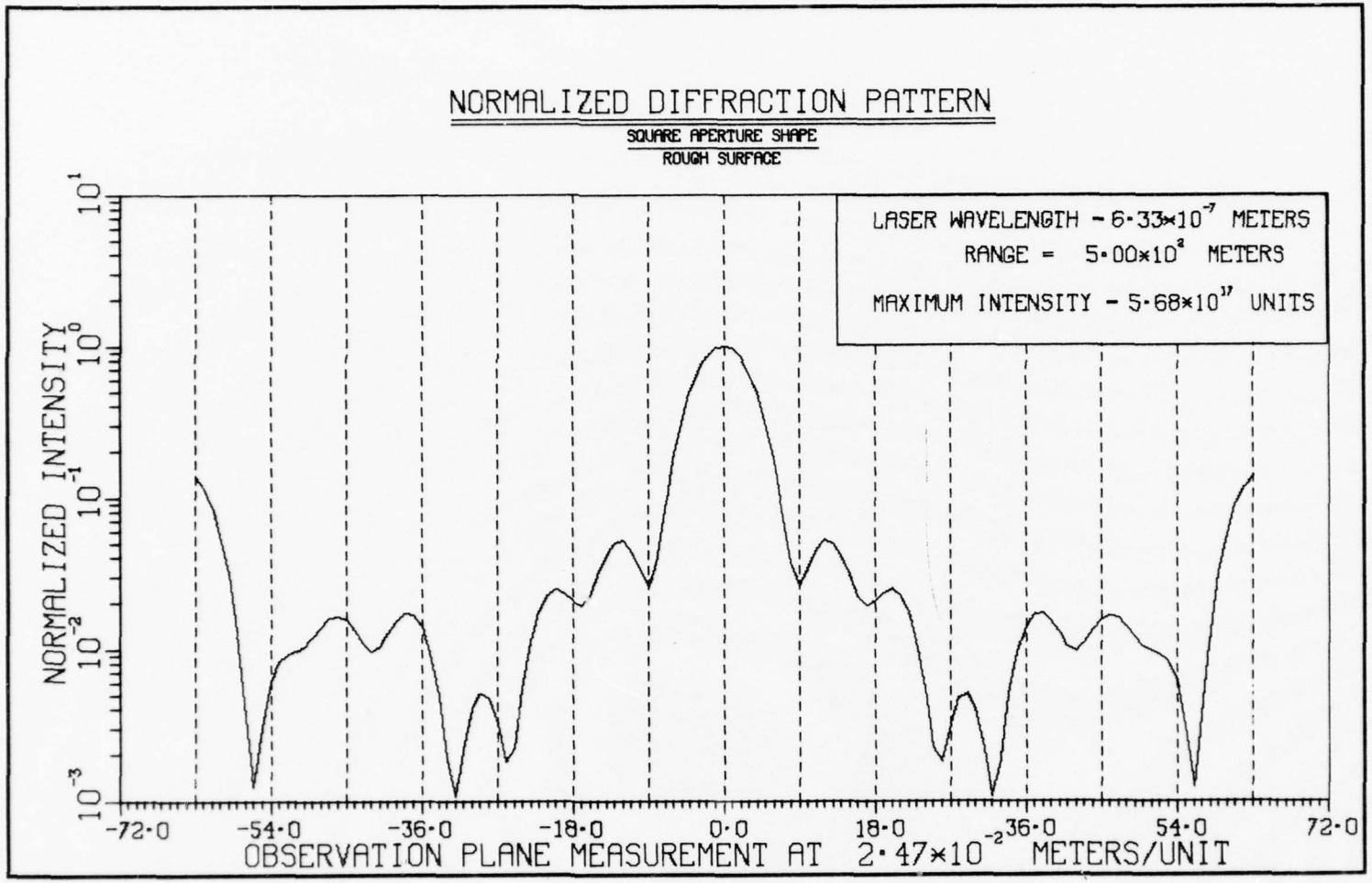

Fig. 40 One Dimensional Cut Through Speckle Pattern

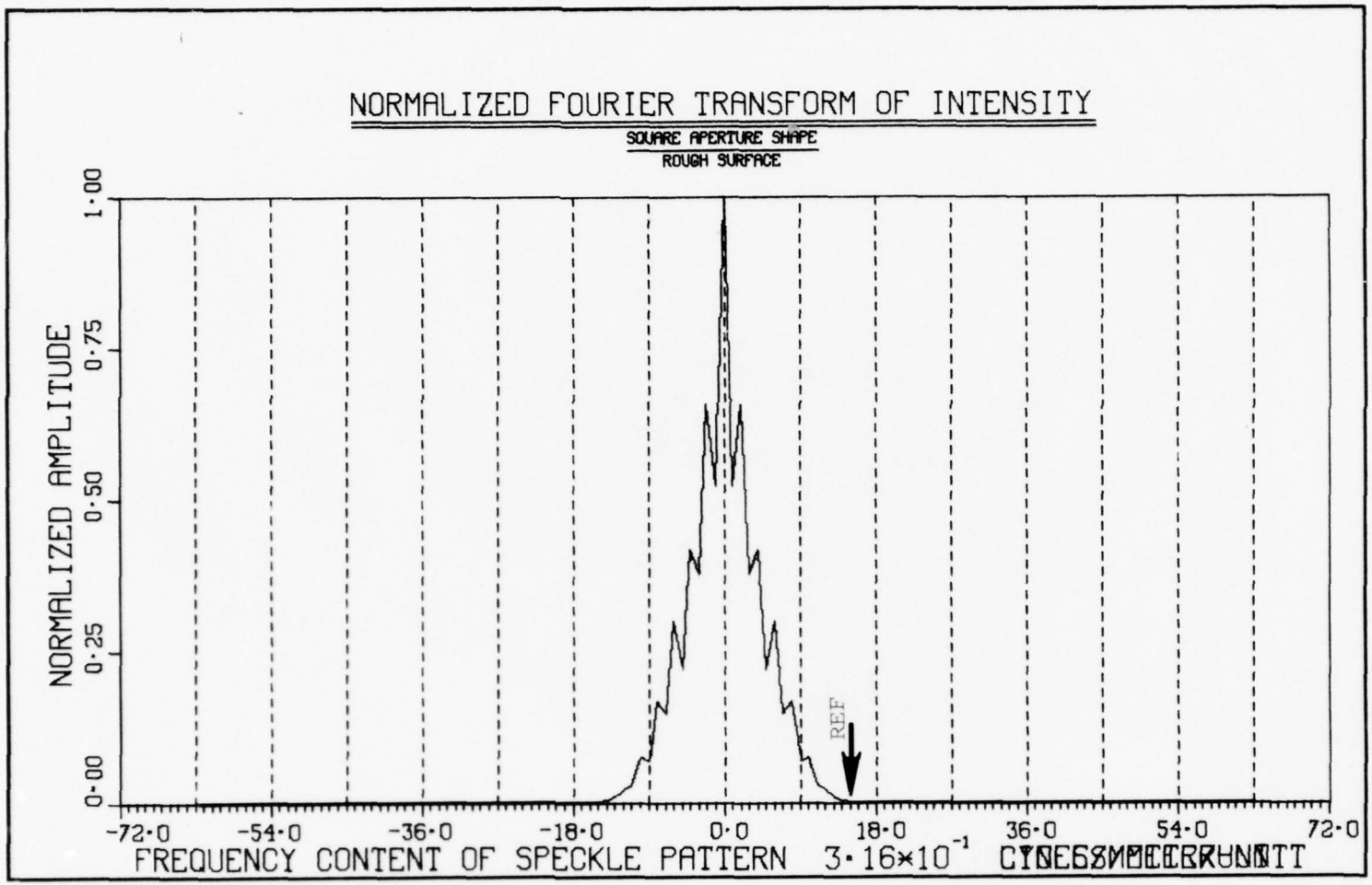

Fig. 41 Fourier Transform of Fig. 40 Data

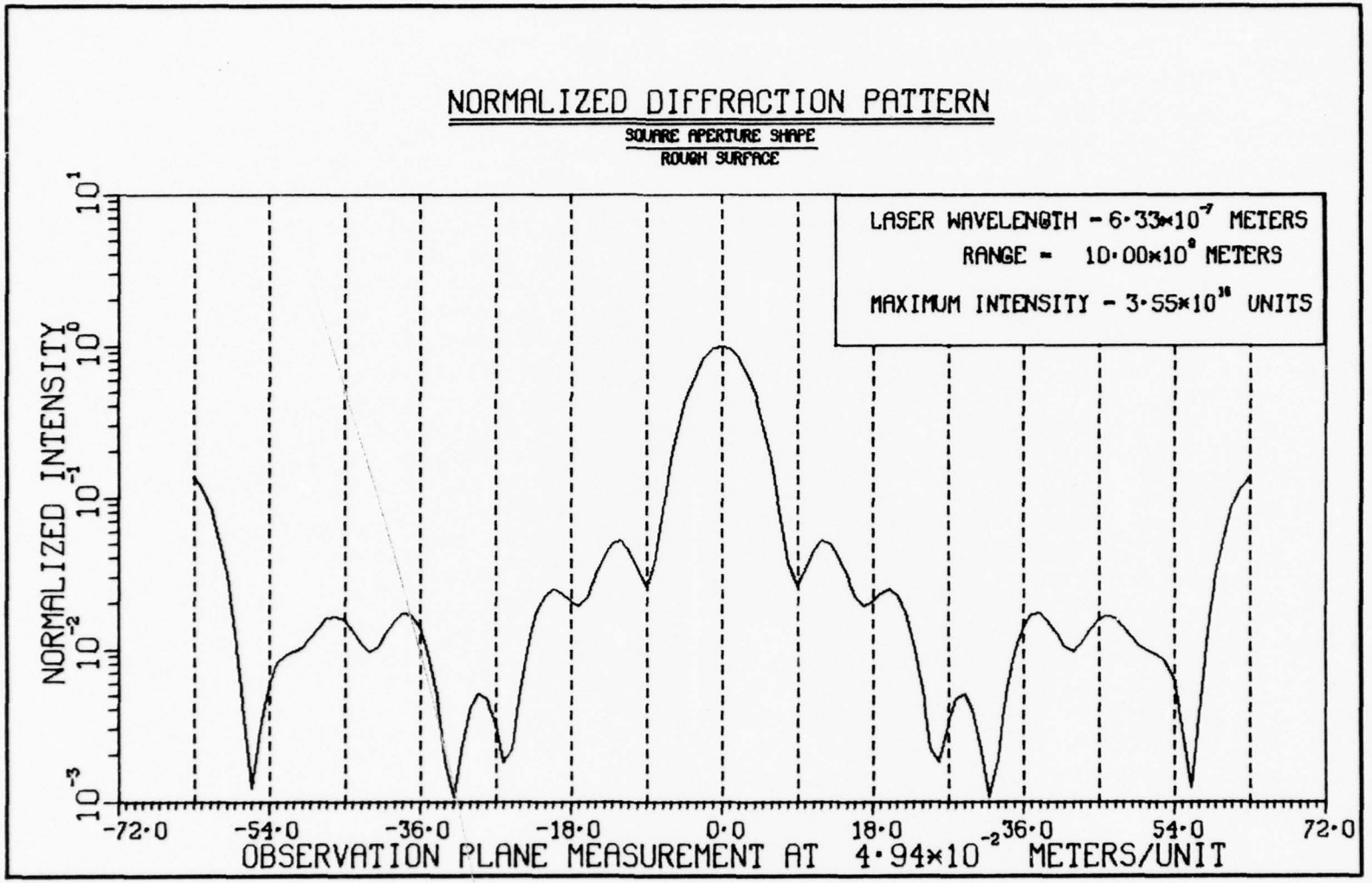

Fig. 42 One Dimensional Cut Through Speckle Pattern

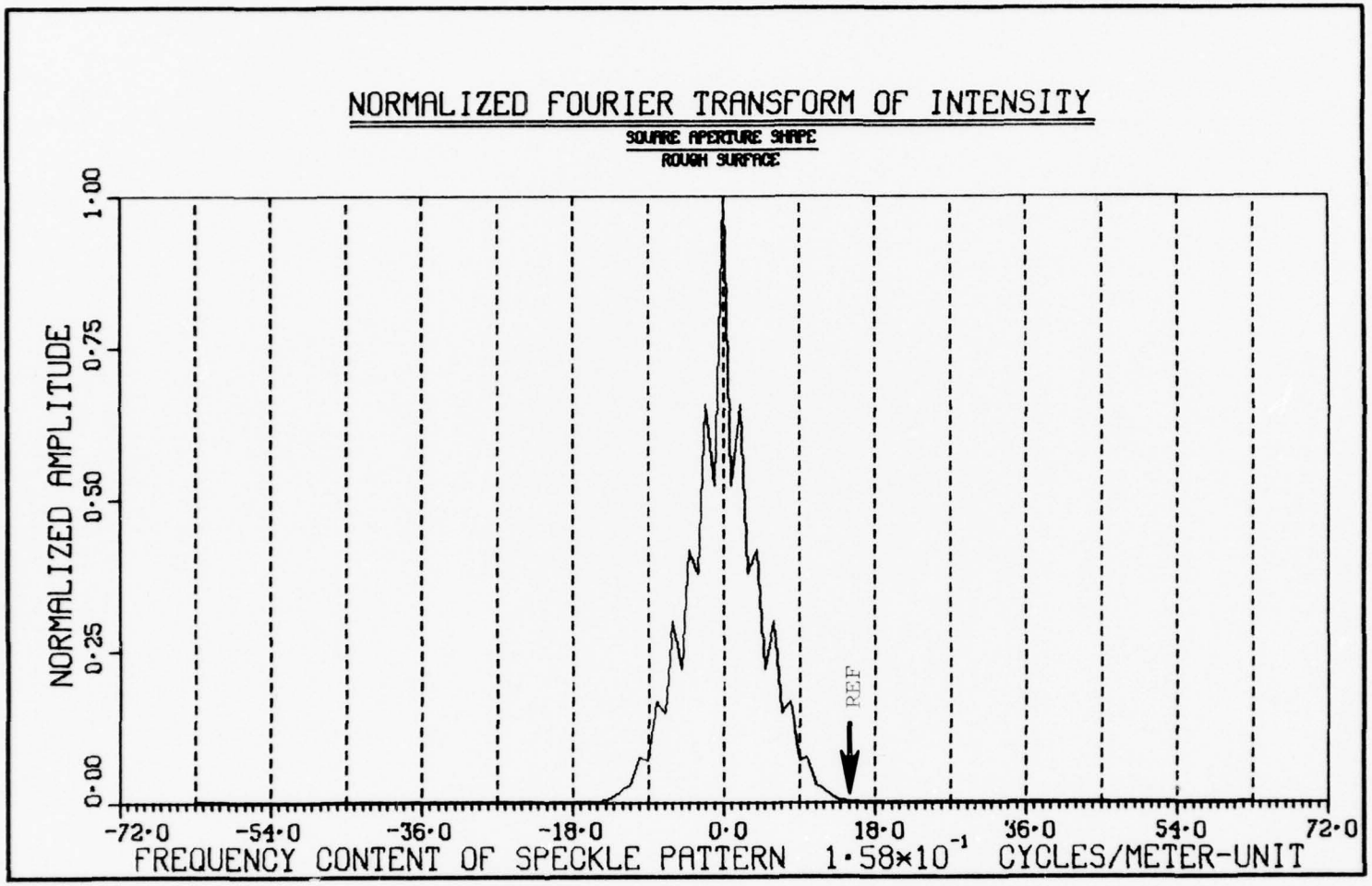

Fig. 43 Fourier Transform of Fig. 42 Data

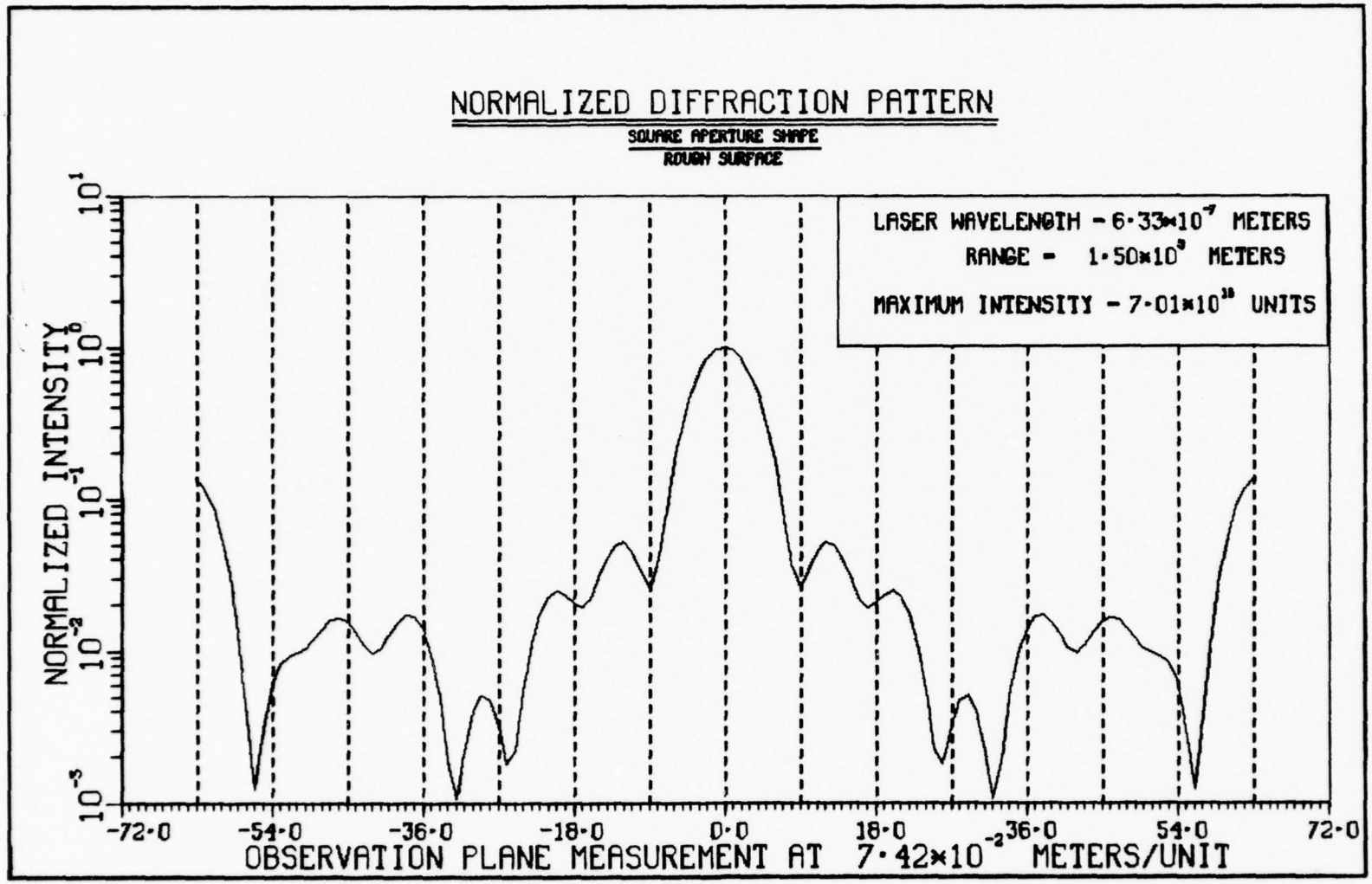

Fig. 44 One Dimensional Cut Through Speckle Pattern

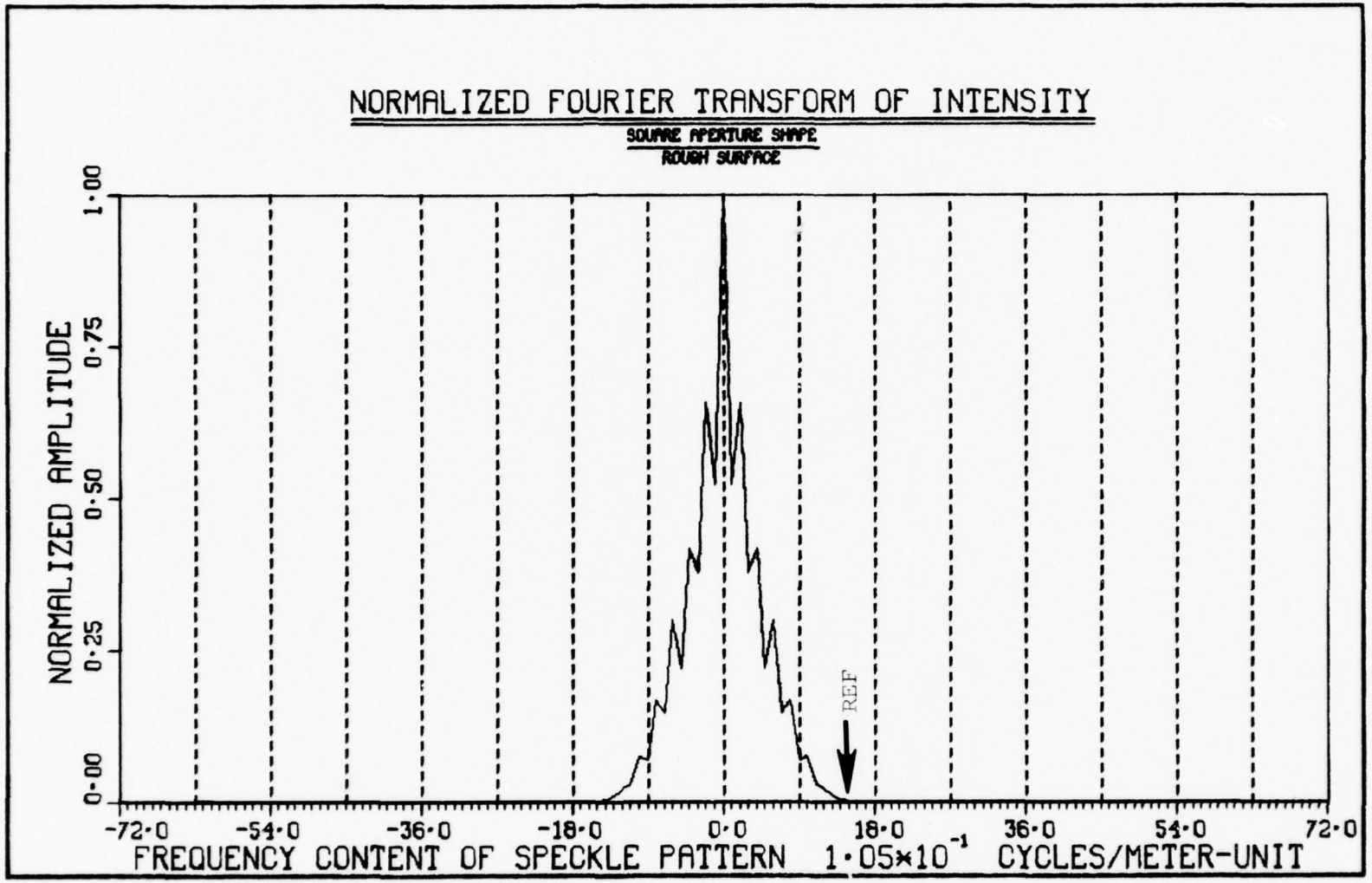

Fig. 45 Fourier Transform of Fig. 44 Data

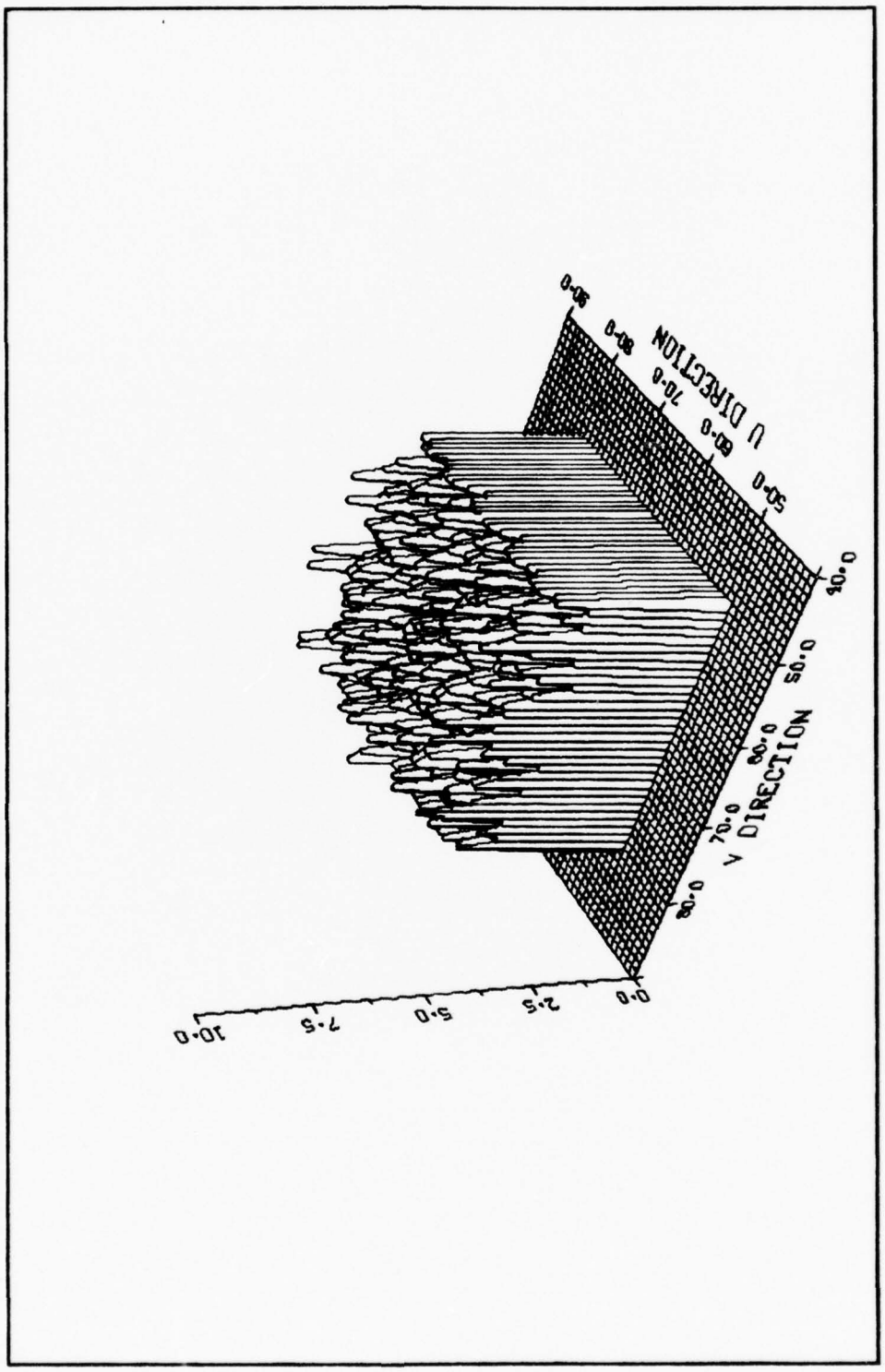

Fig. 46 Normalized Surface Height Distribution

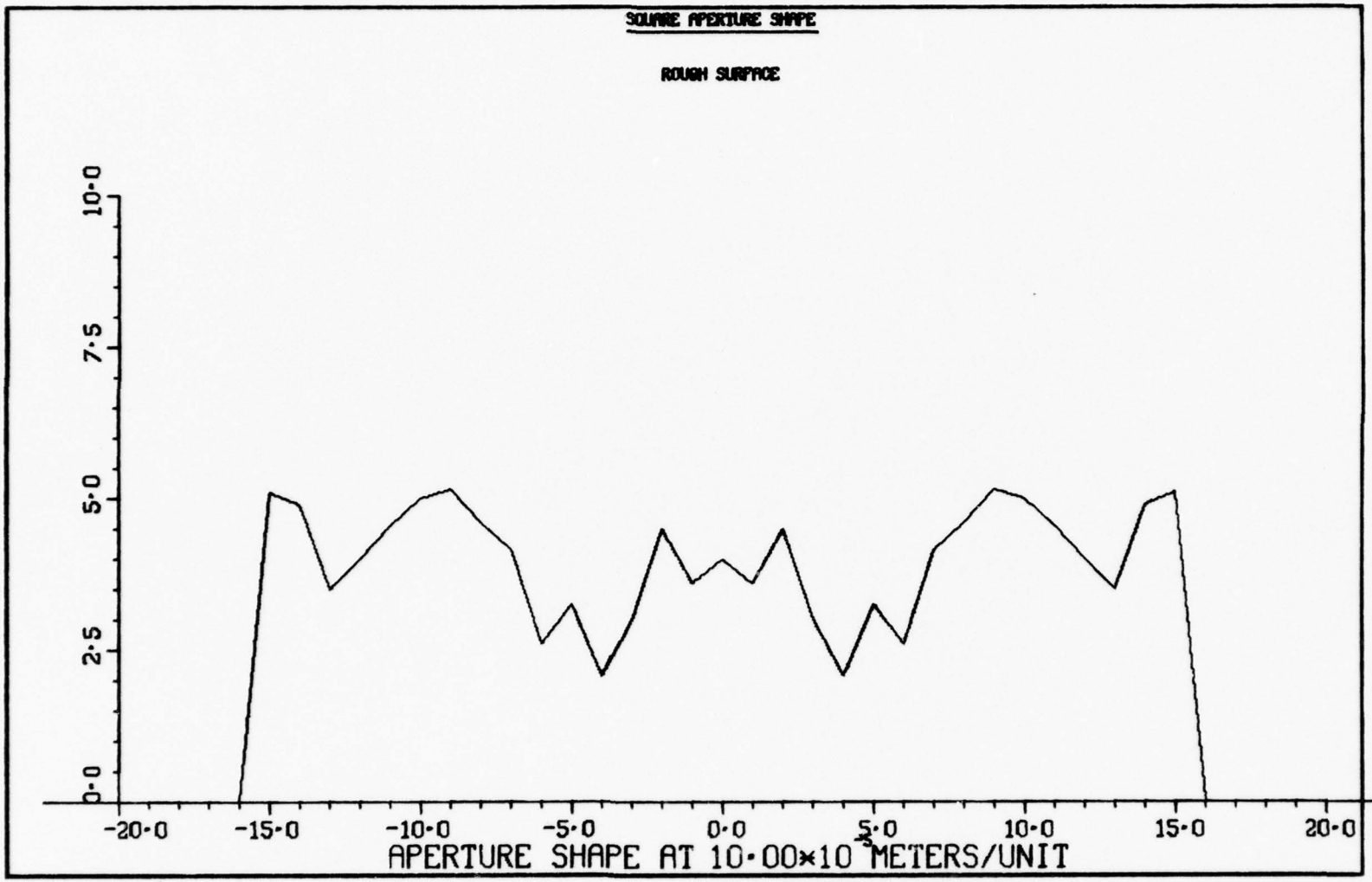

Fig. 47 One Dimensional Cut Through Fig. 46

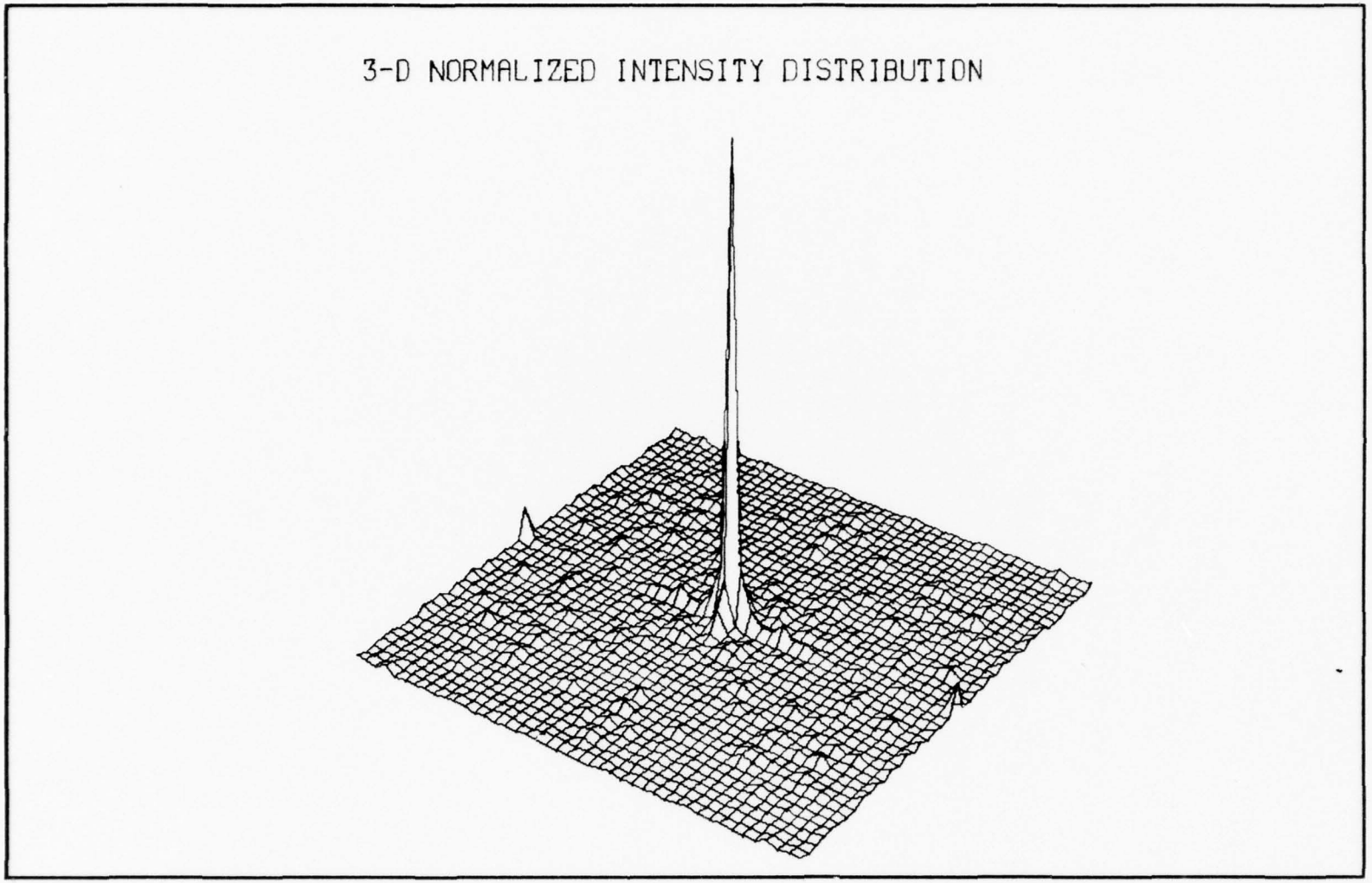

Fig. 48 Three Dimensional Perspective of Speckle Pattern

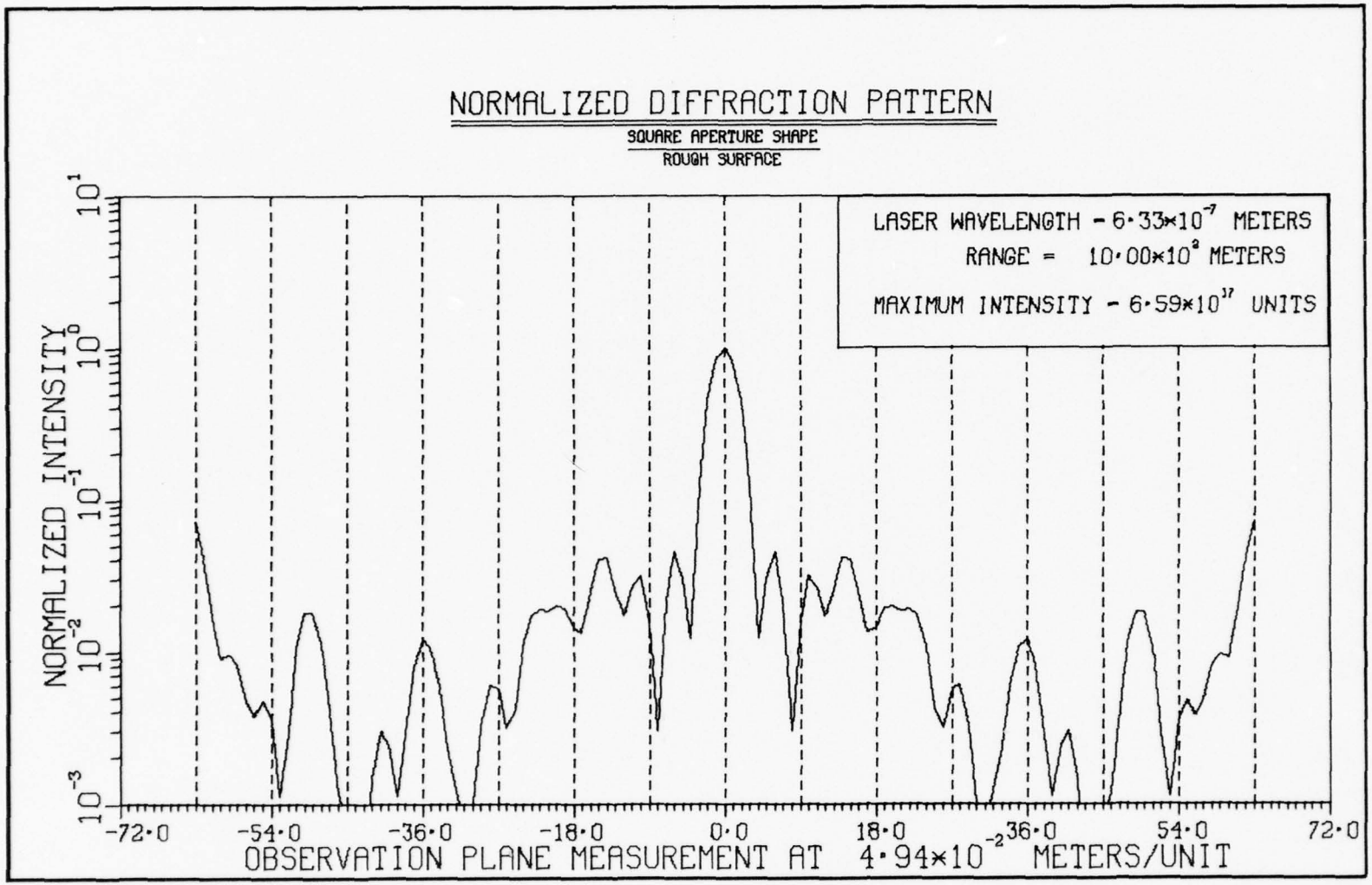

Fig. 49 One Dimensional Cut Through Speckle Pattern

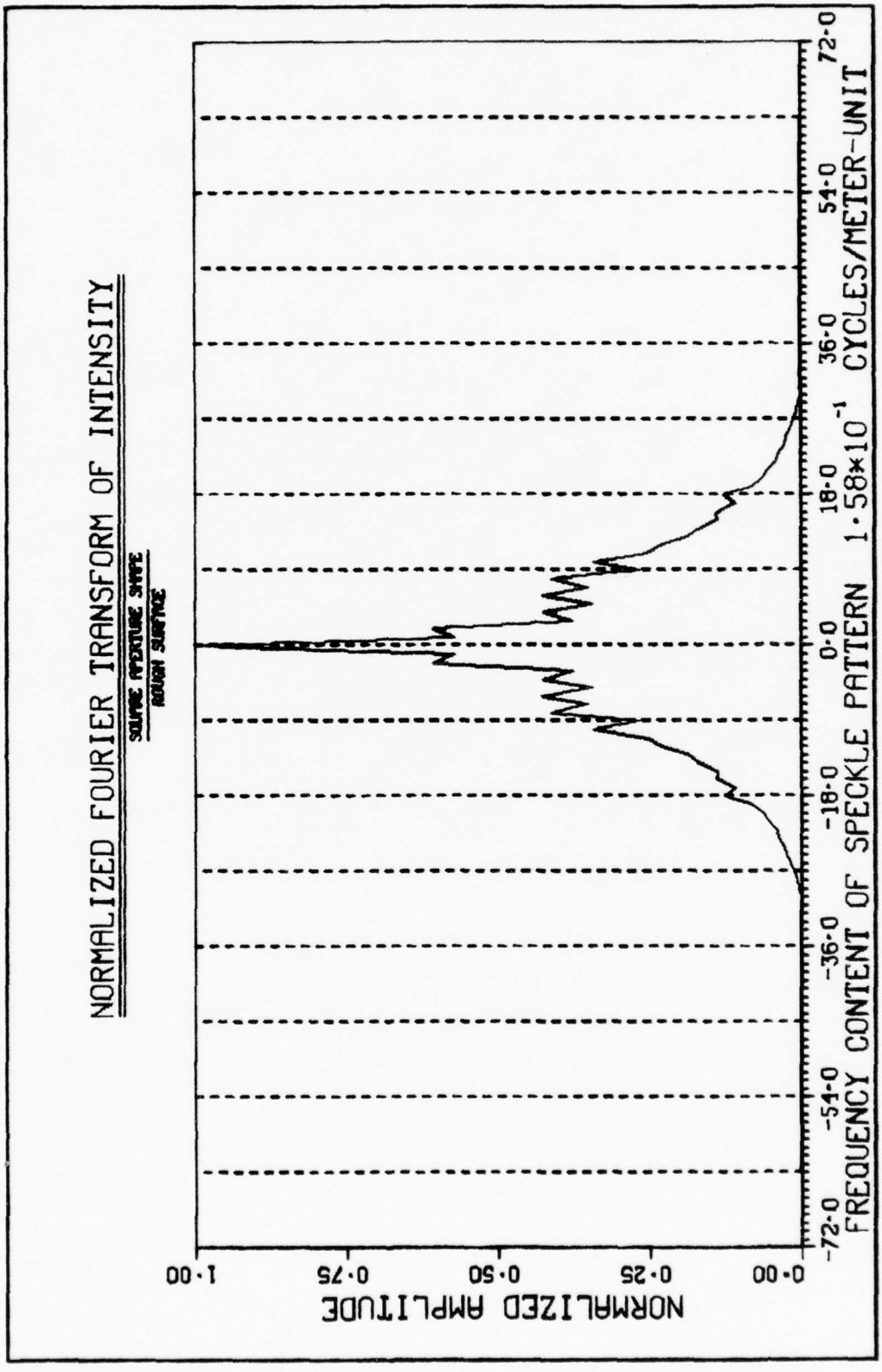

Fig. 50 Fourier Transform of Fig. 49 Data

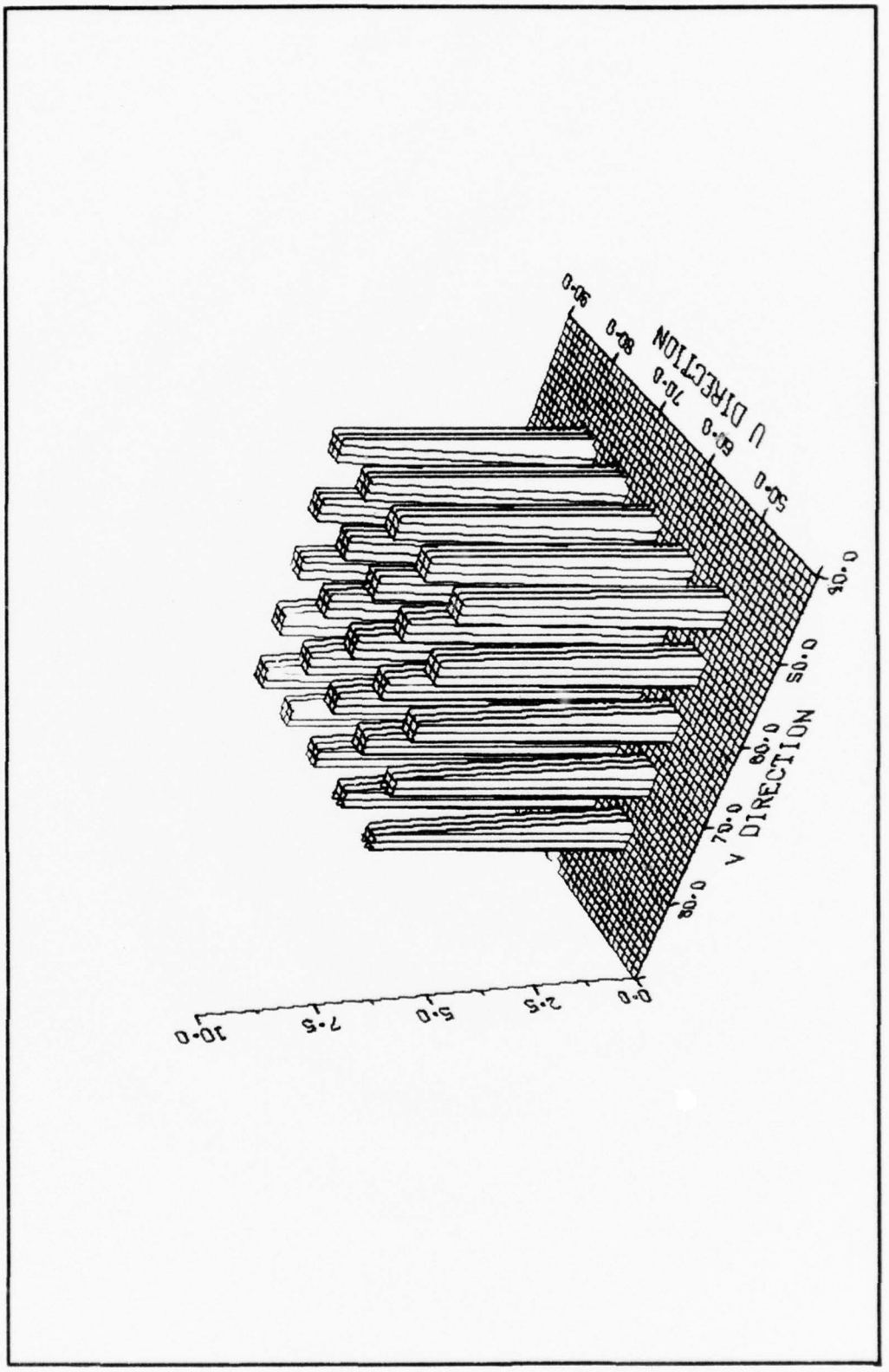

Fig. 53 Normalized Surface Height Distribution

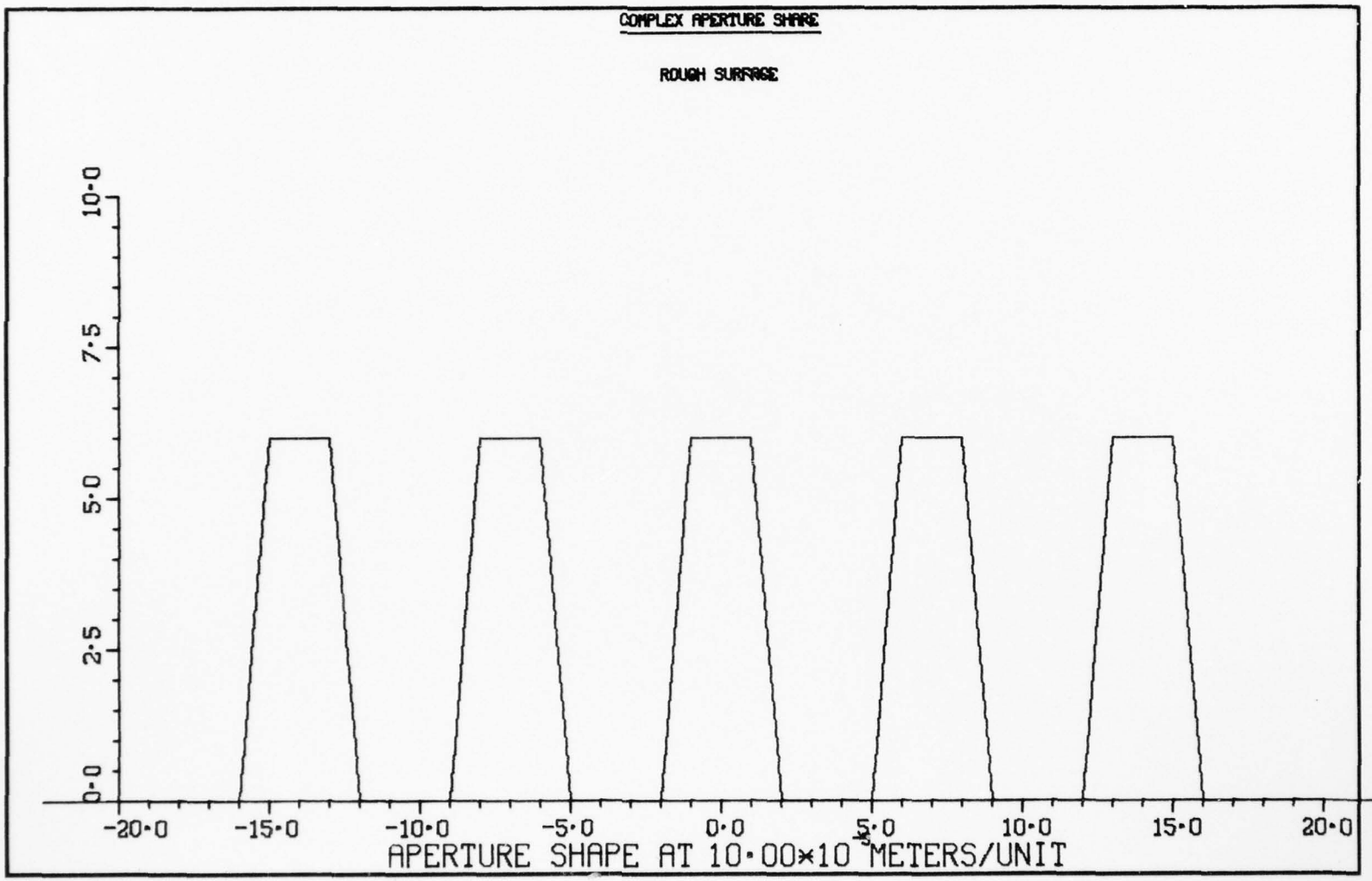

Fig. 54 One Dimensional Cut Through Fig. 53

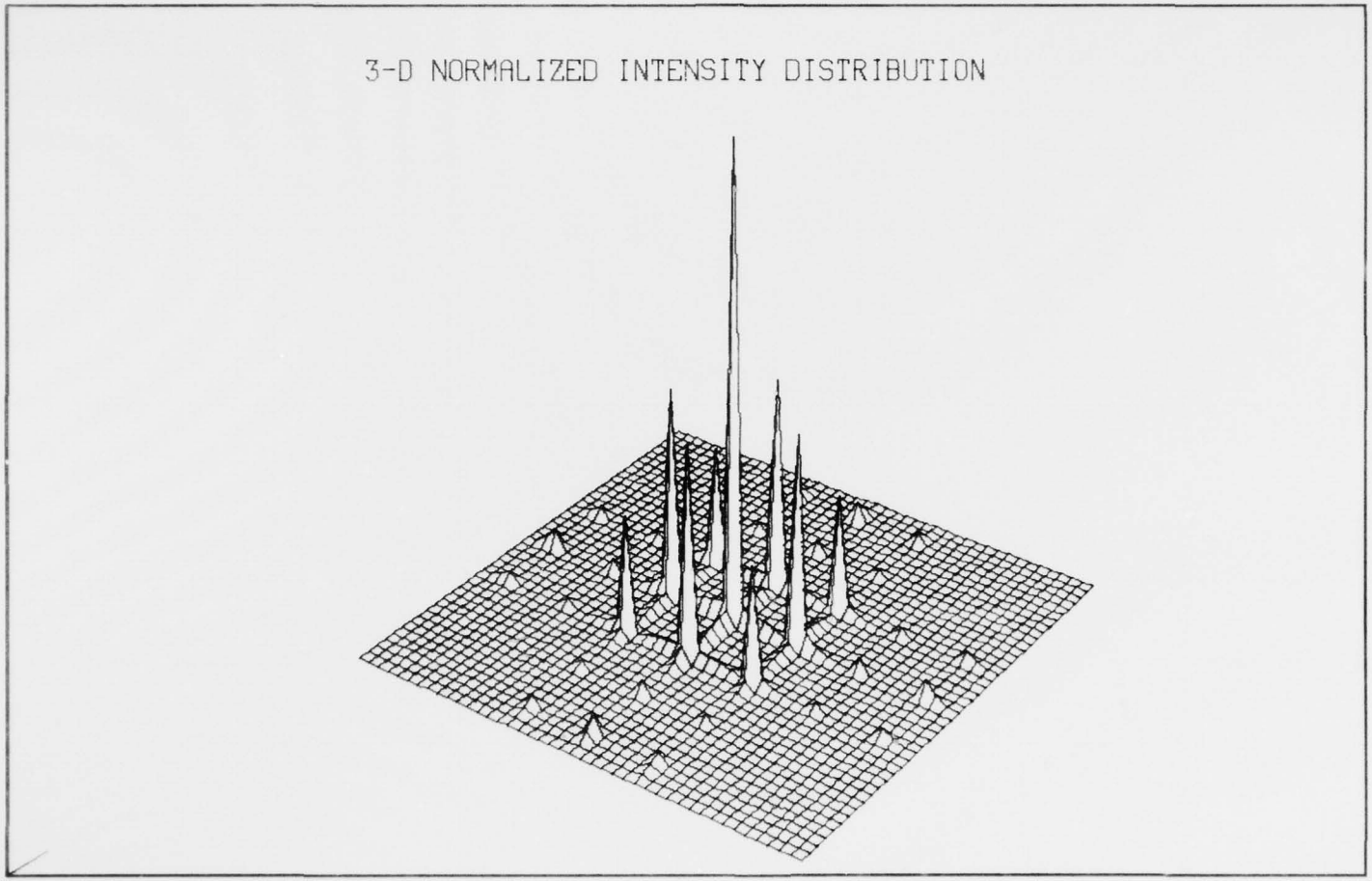

Fig. 55 Three Dimensional Perspective of Speckle Pattern

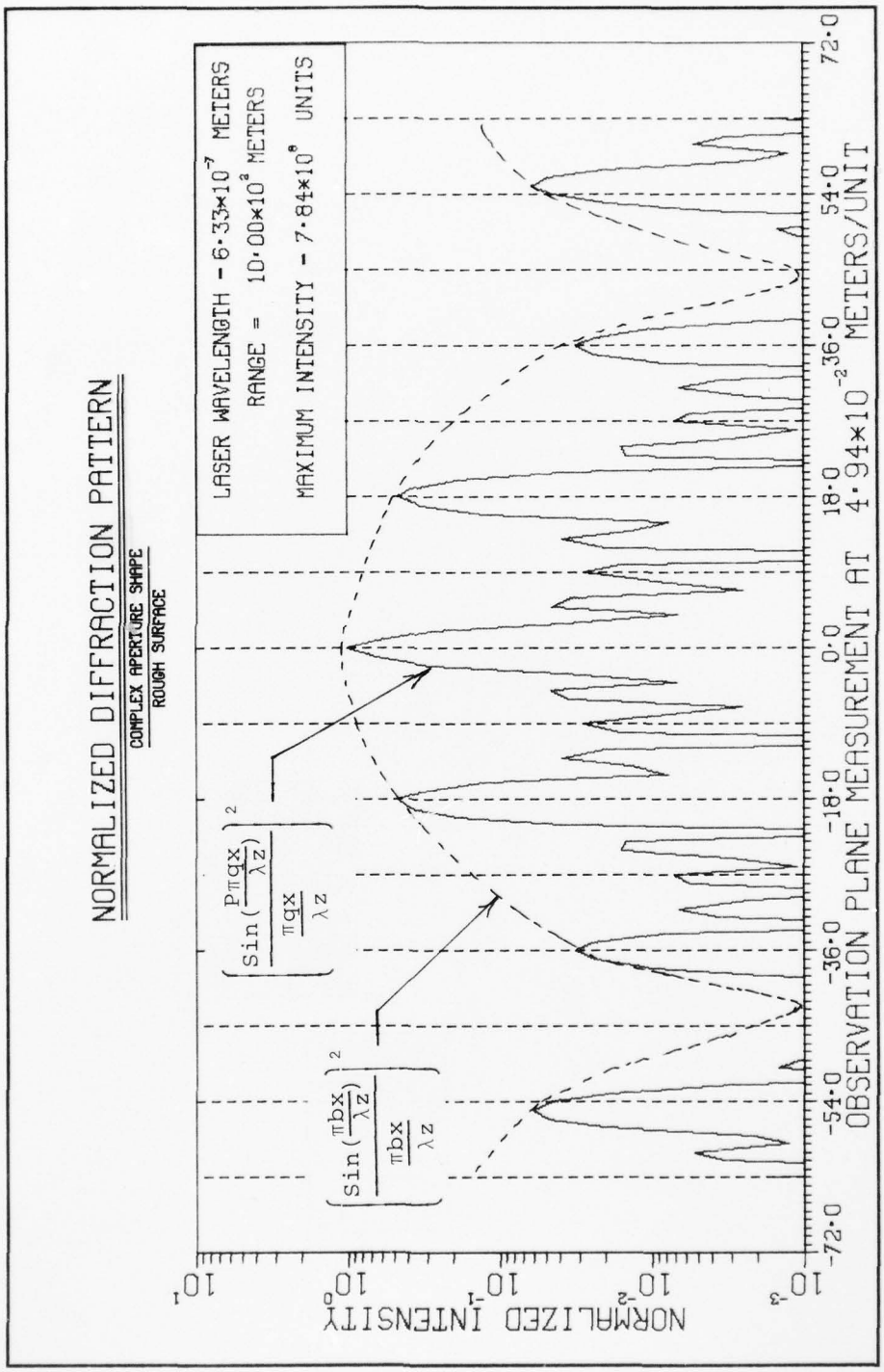

Fig. 56 One Dimensional Cut Through Speckle Pattern

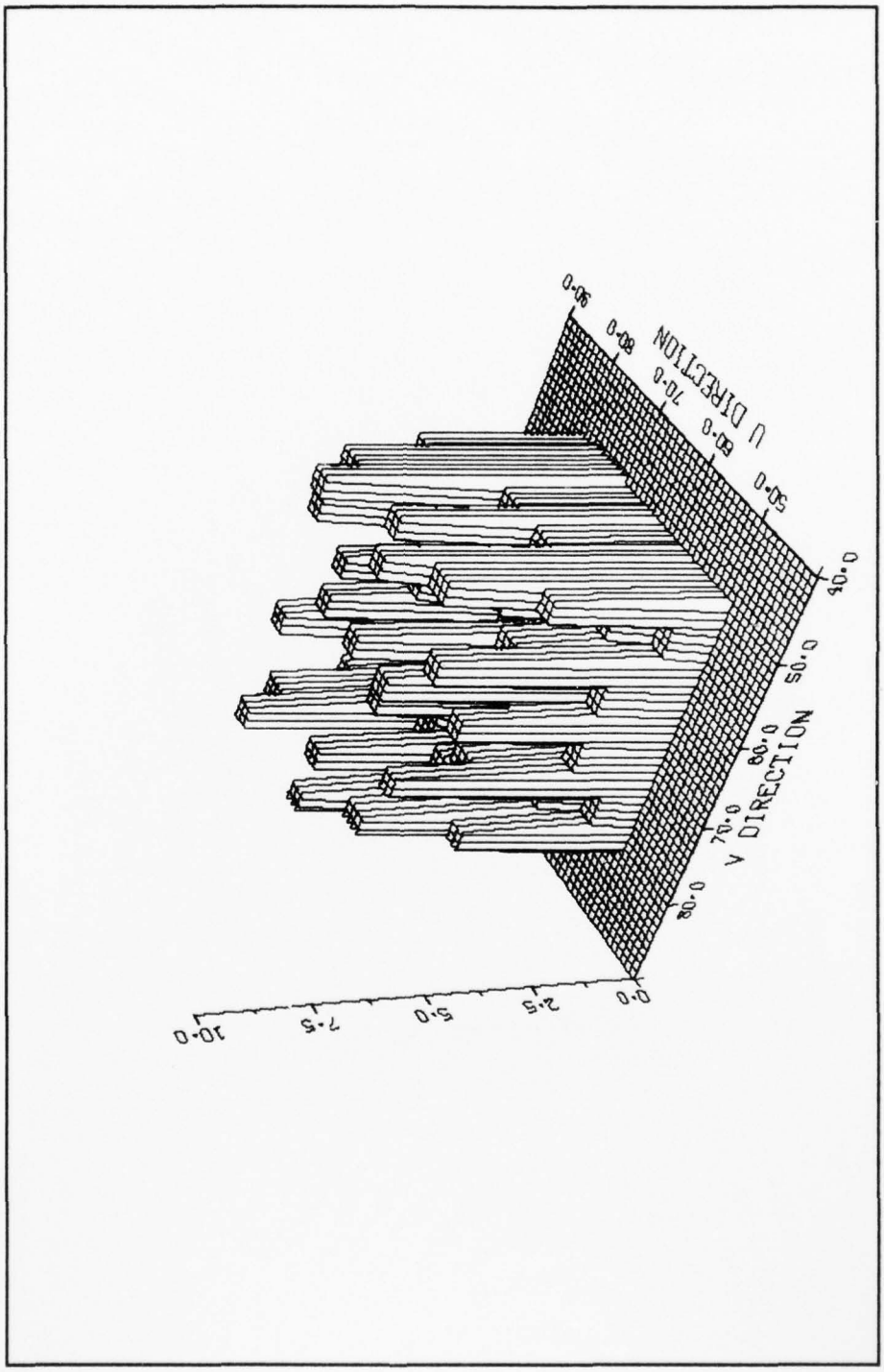

Fig. 57 Normalized Surface Height Distribution

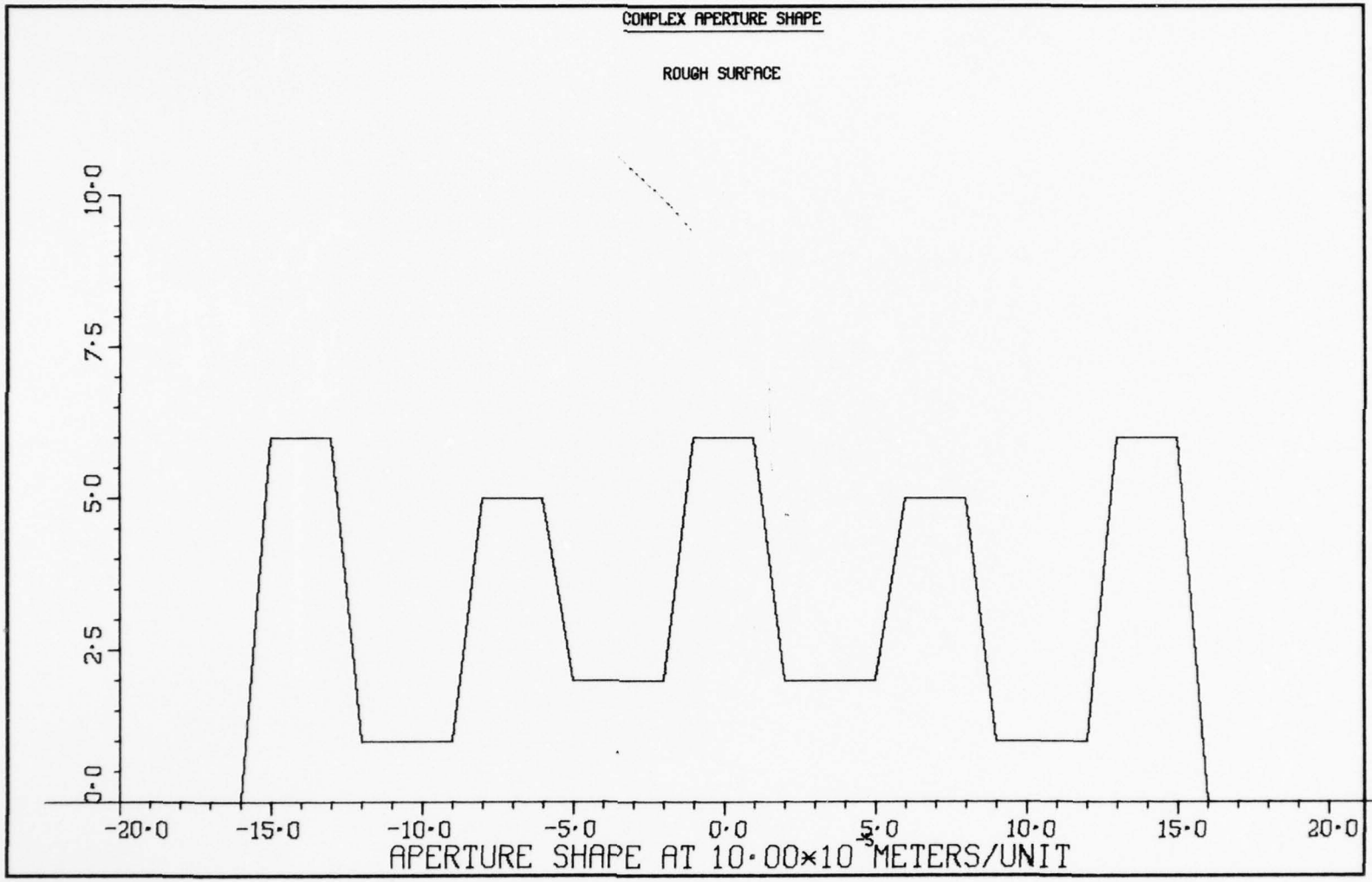

Fig. 58 One Dimensional Cut Through Fig. 57

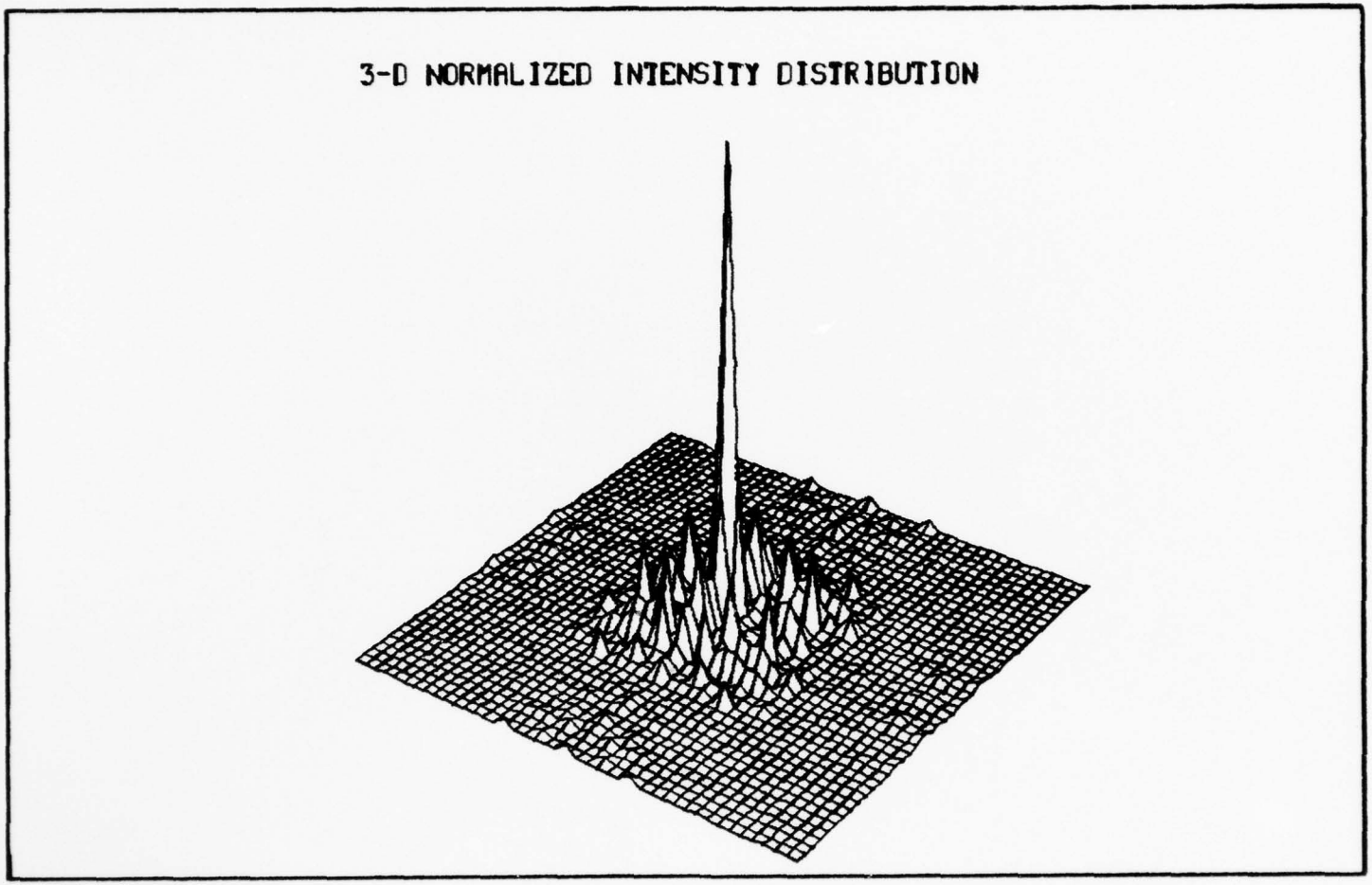

Fig. 59 Three Dimensional Perspective of Speckle Pattern

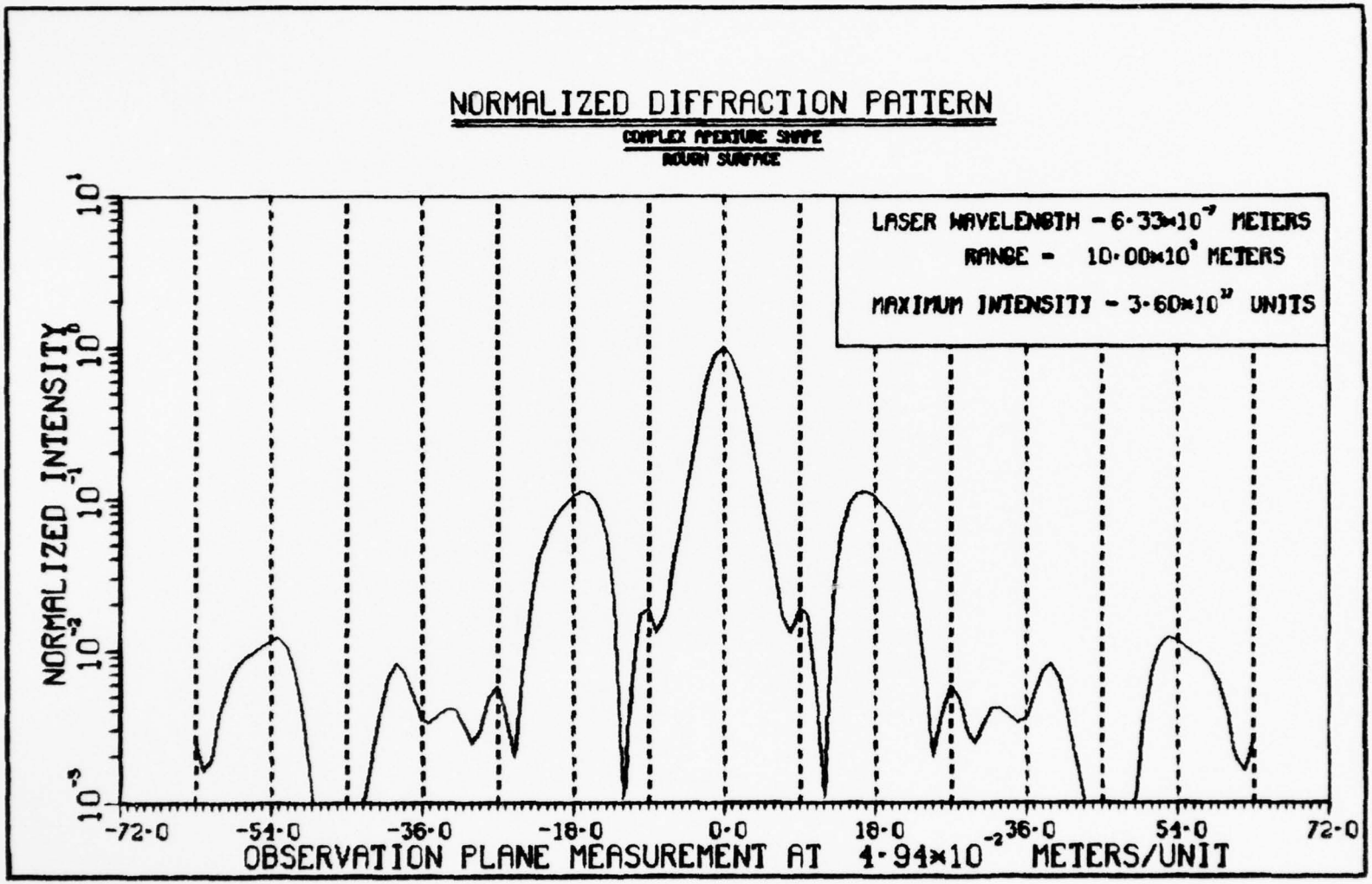

Fig. 60 One Dimensional Cut Through Speckle Pattern

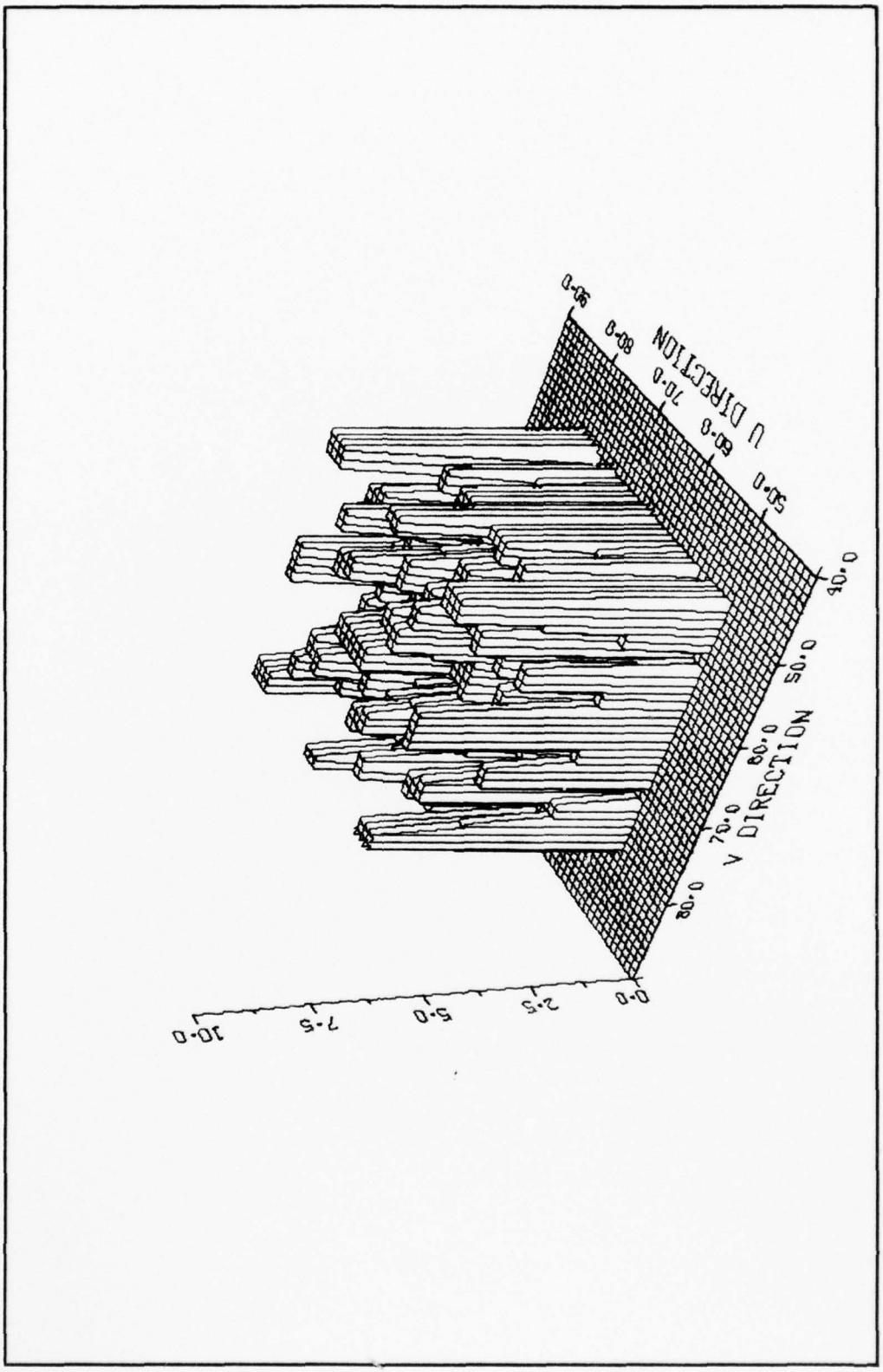

Fig. 61 Normalized Surface Height Distribution

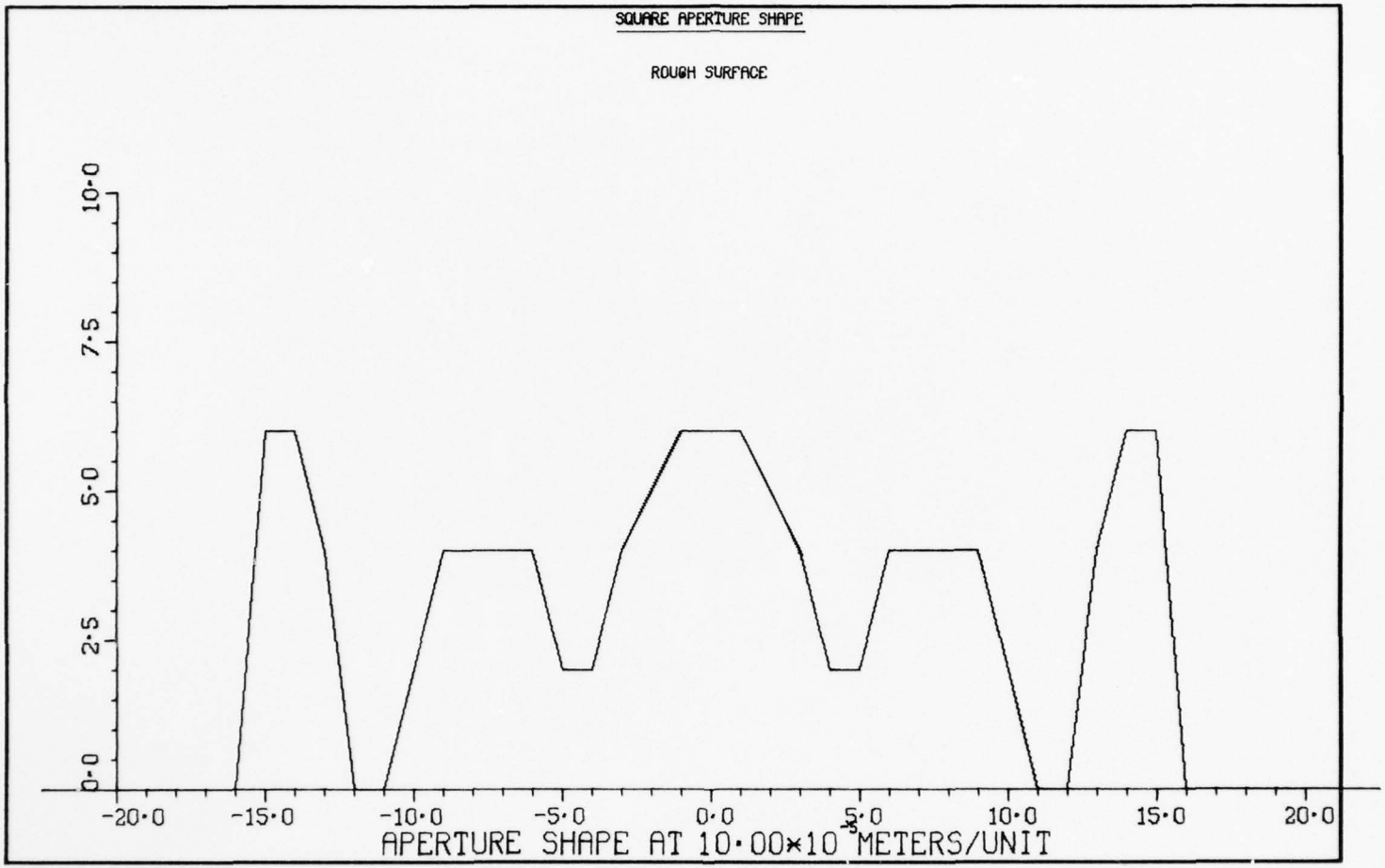

Fig. 62 One Dimensional Cut Through Fig. 61

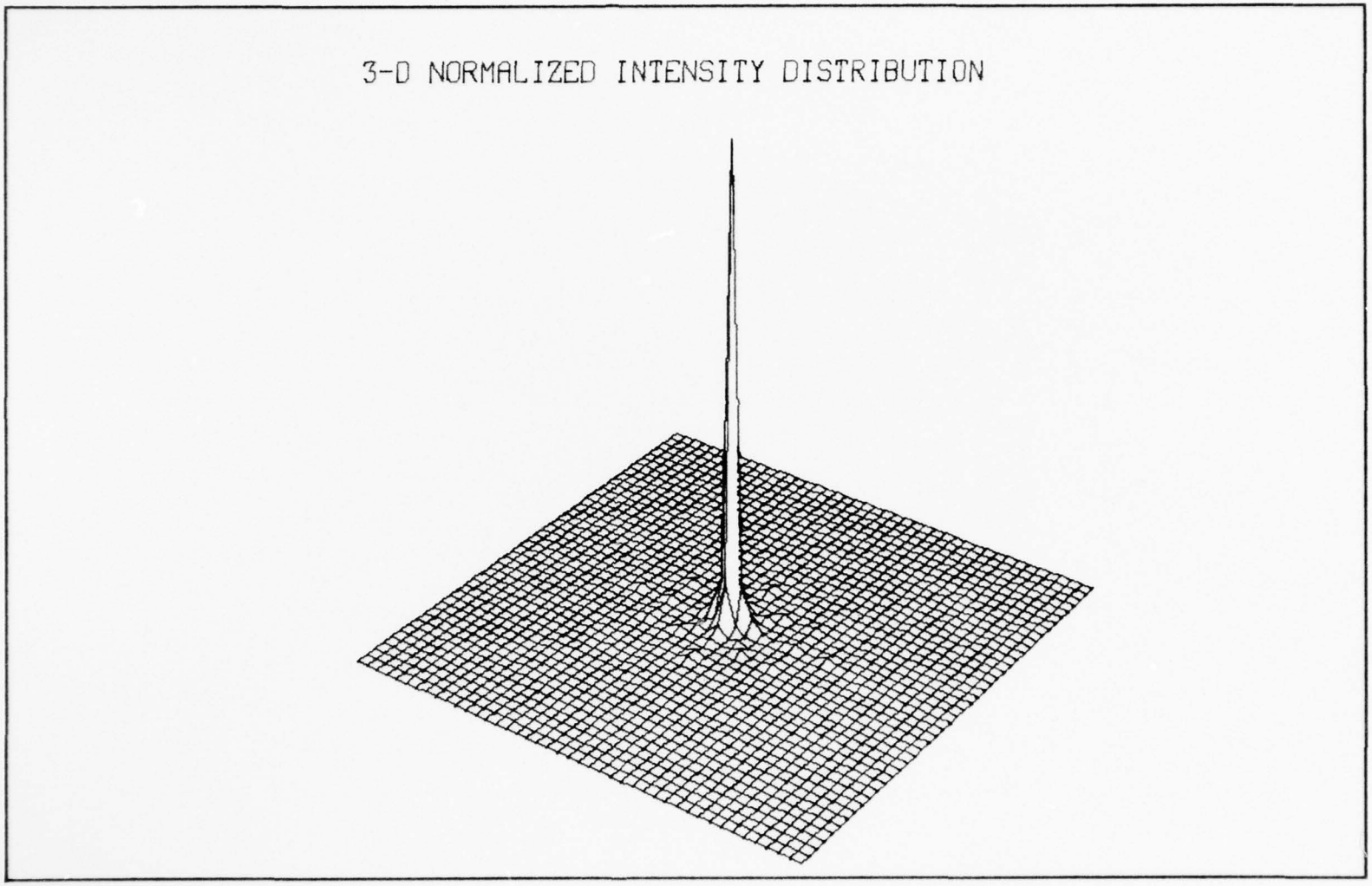

Fig. 63 Three Dimensional Perspective of Speckle Pattern

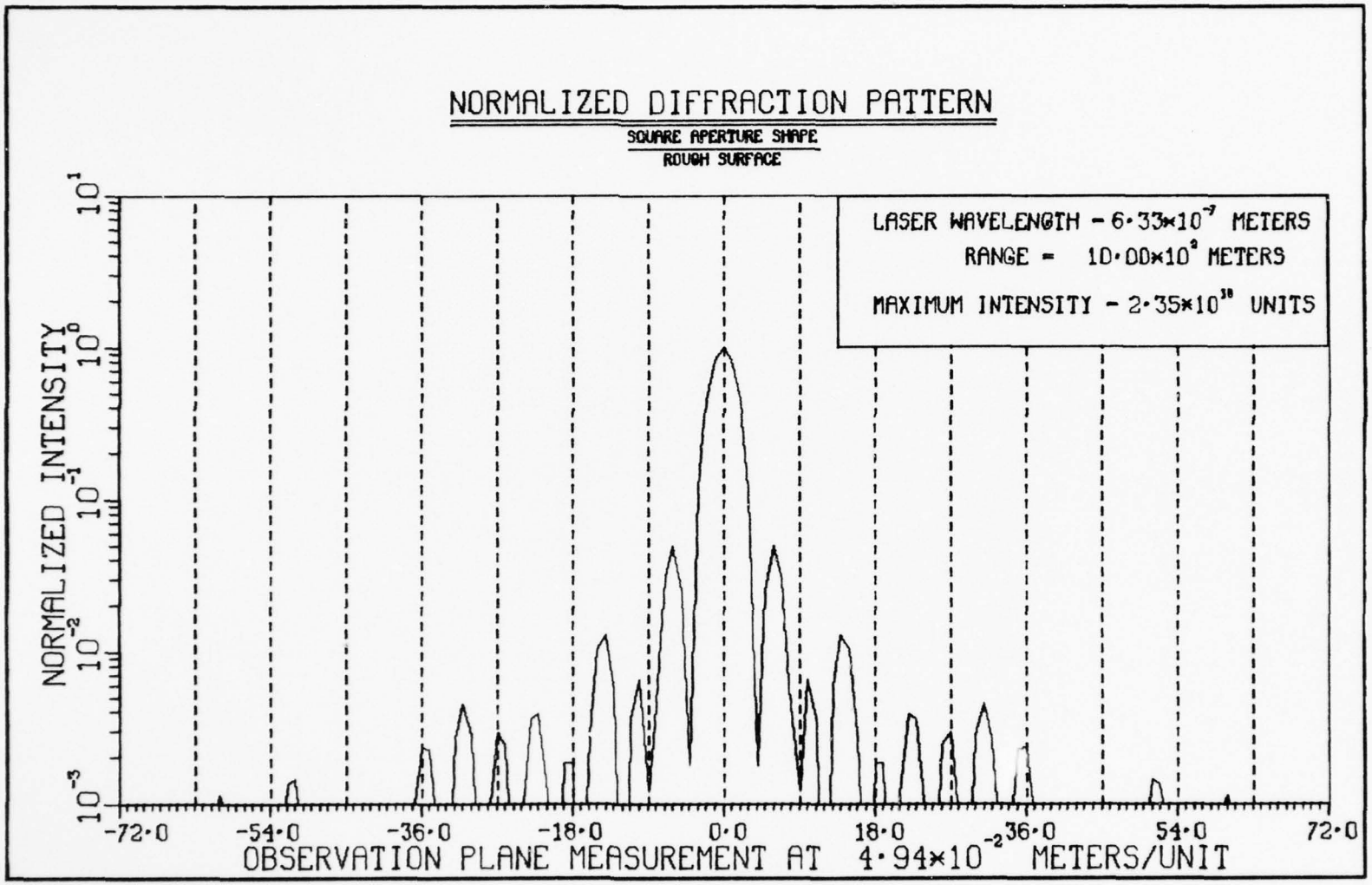

Fig. 64 One Dimensional Cut Through Speckle Pattern

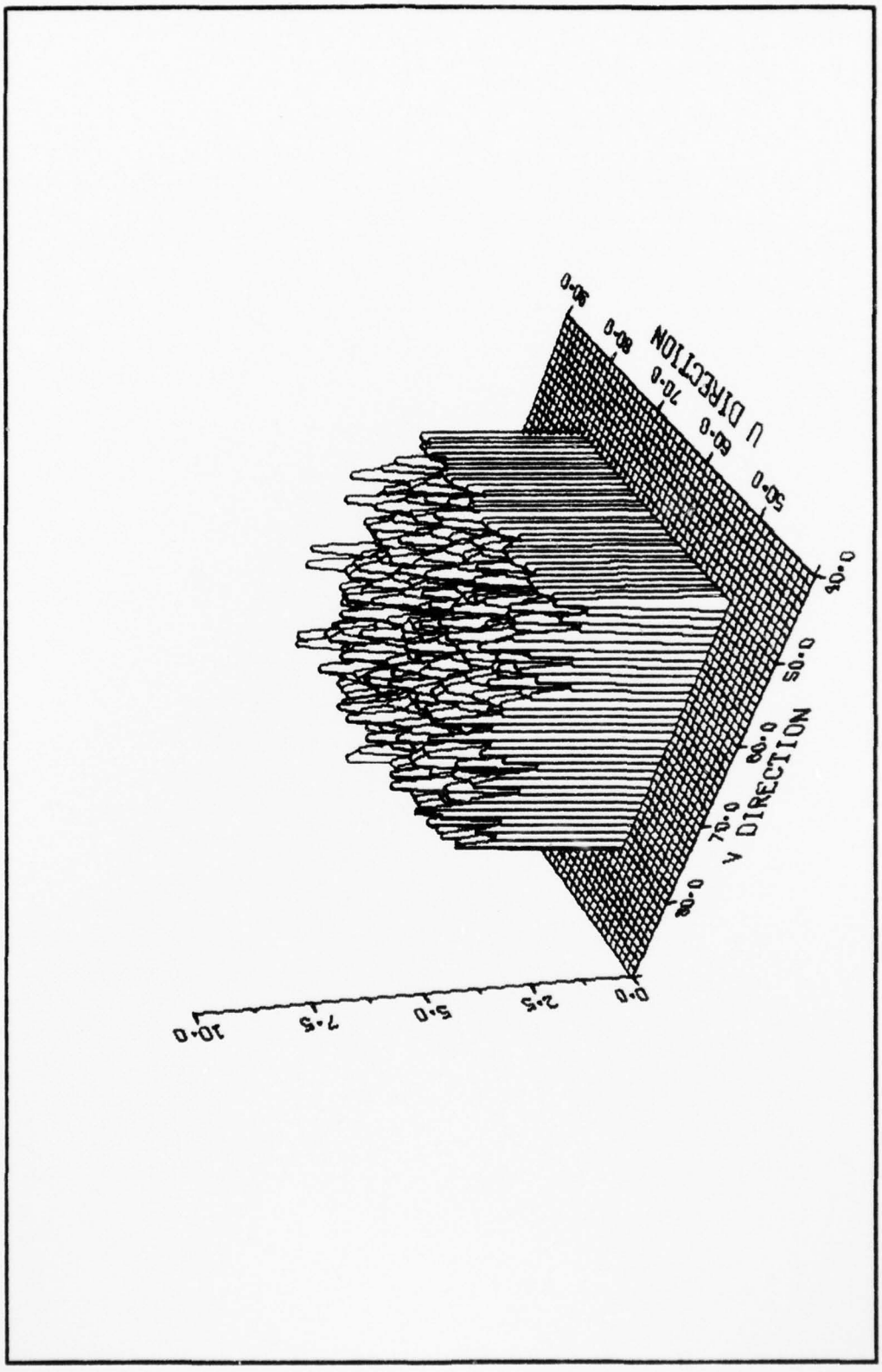

Fig. 65 Normalized Surface Height Distribution

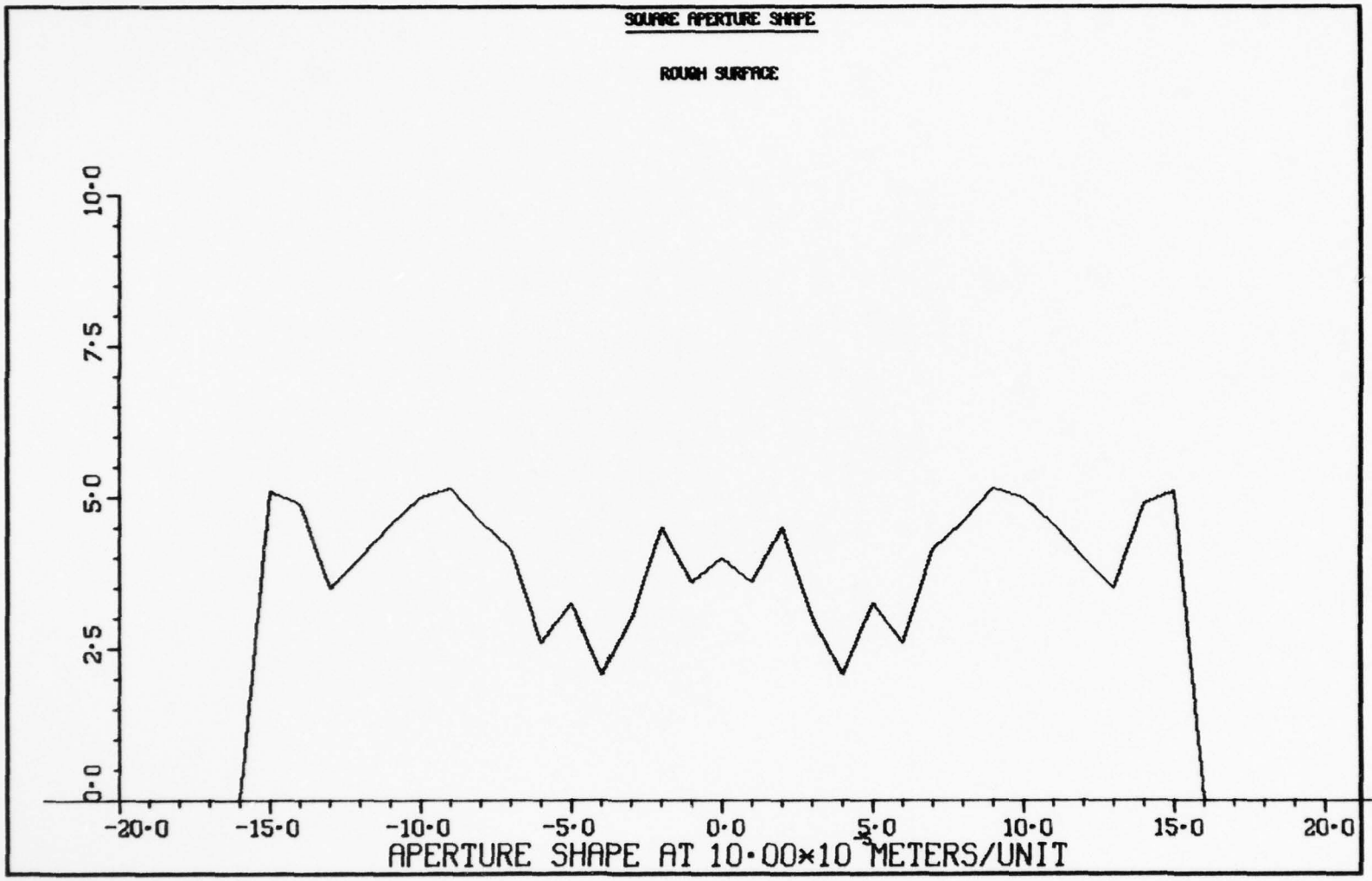

Fig. 66 One Dimensional Cut Through Fig. 65

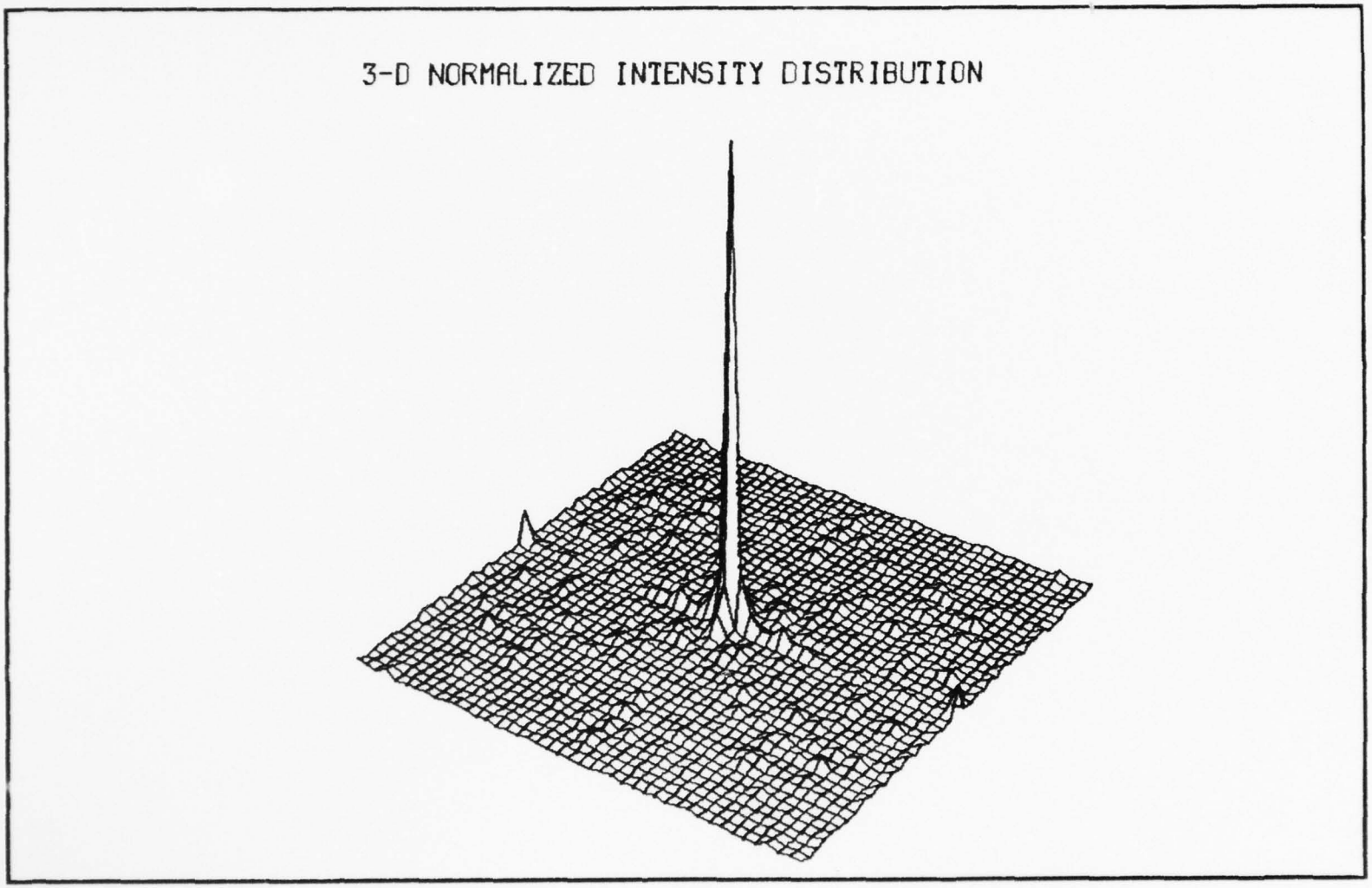

Fig. 67 Three Dimensional Perspective of Speckle Pattern

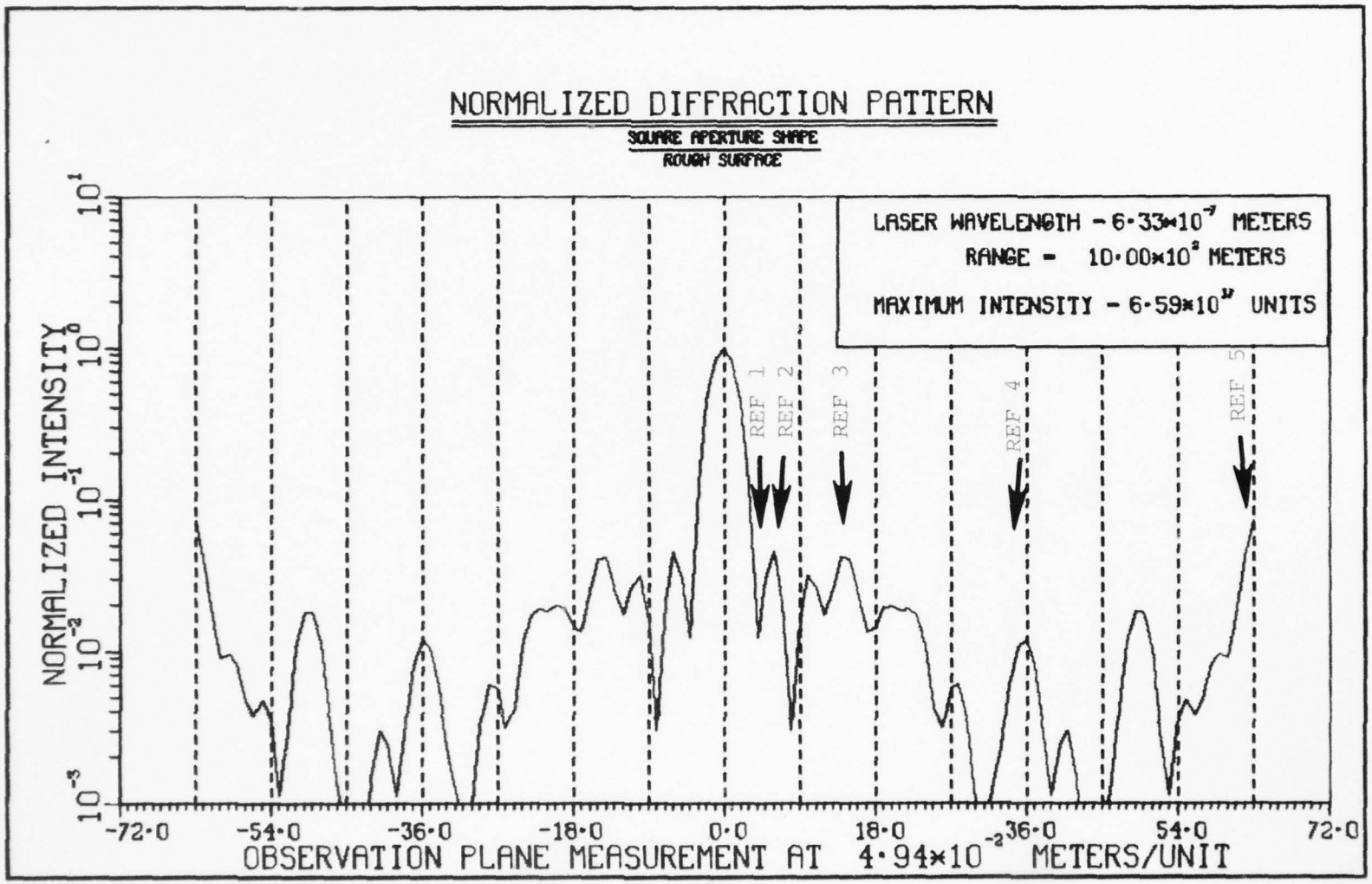

Fig. 68 One Dimensional Cut Through Speckle Pattern

AD-A039 696 AIR FORCE INST OF TECH WRIGHT-PATTERSON AFB OHIO SCH--ETC F/G 20/5
MODEL FOR PREDICTING LASER SPECKLE PATTERNS RESULTING FROM ROUG--ETC(U)
MAR 77 W E LANDIS

UNCLASSIFIED AFIT/GEO/EE/77-1 NL

3 OF 3
AD
A039696

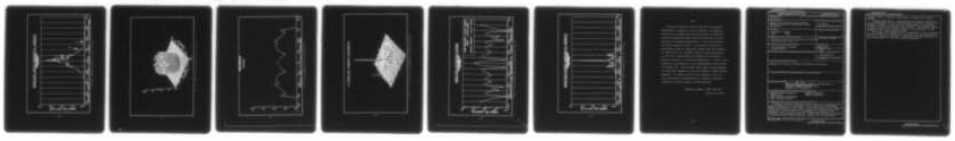

END

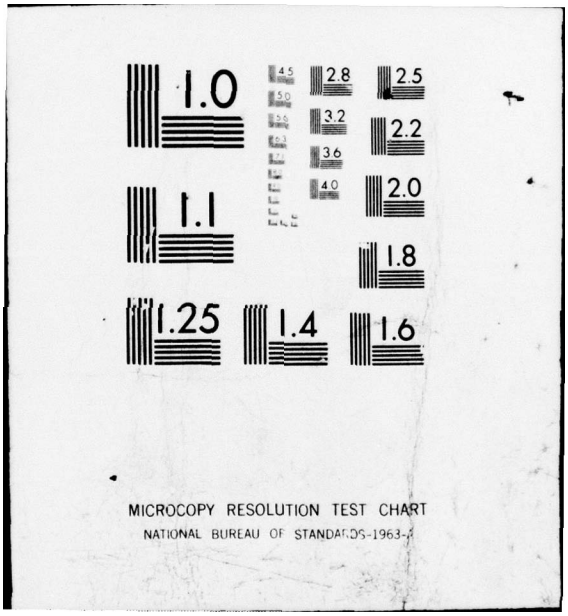
1.0
1.1
1.25
1.4
1.6
1.8
2.0
2.2
2.5
2.8
3.2
3.6
4.0
4.5
5.0
5.6
MICROCOPY RESOLUTION TEST CHART
NATIONAL BUREAU OF STANDARDS-1963-A

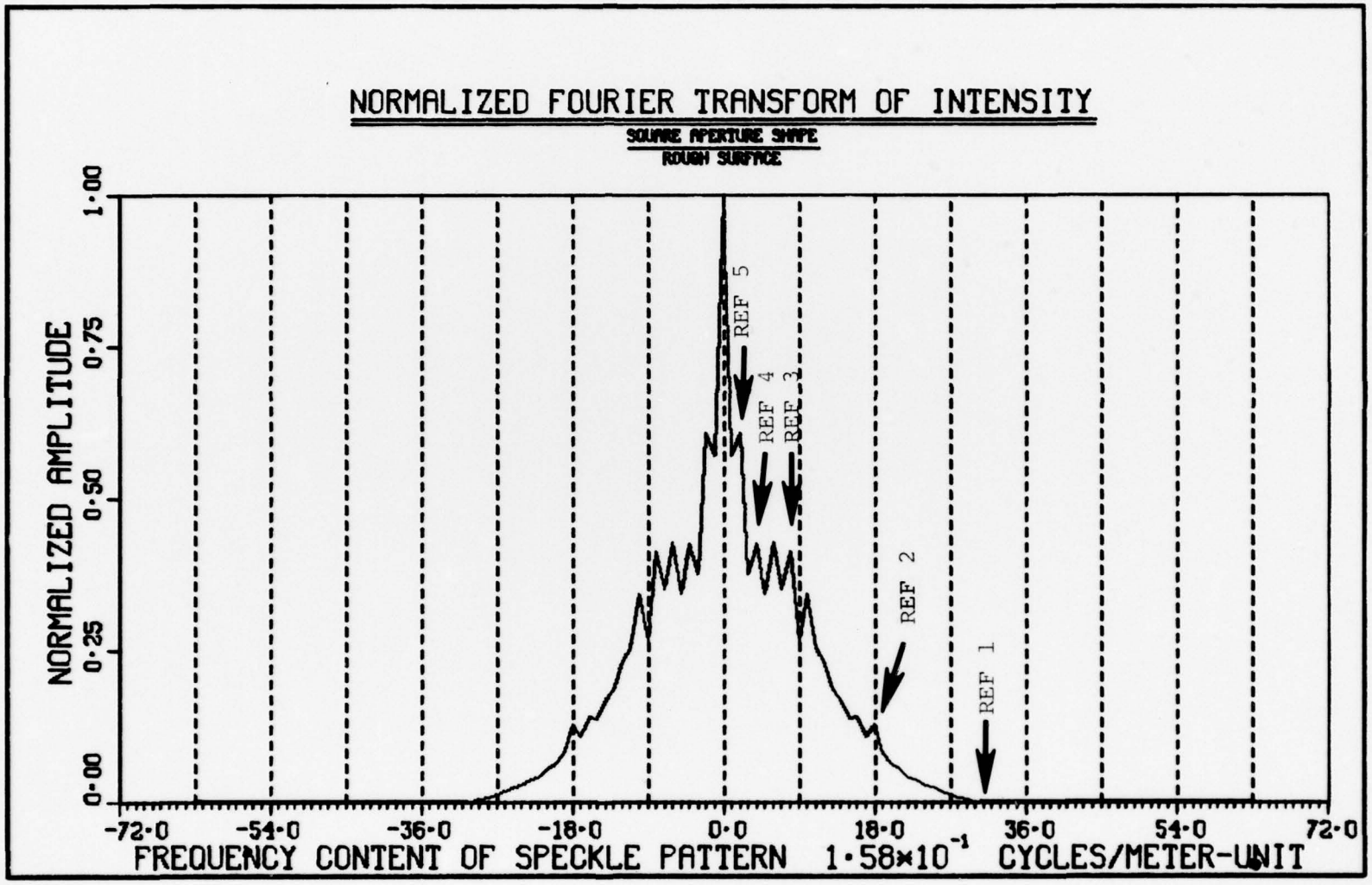

Fig. 69 Fourier Transform of Fig. 68 Data

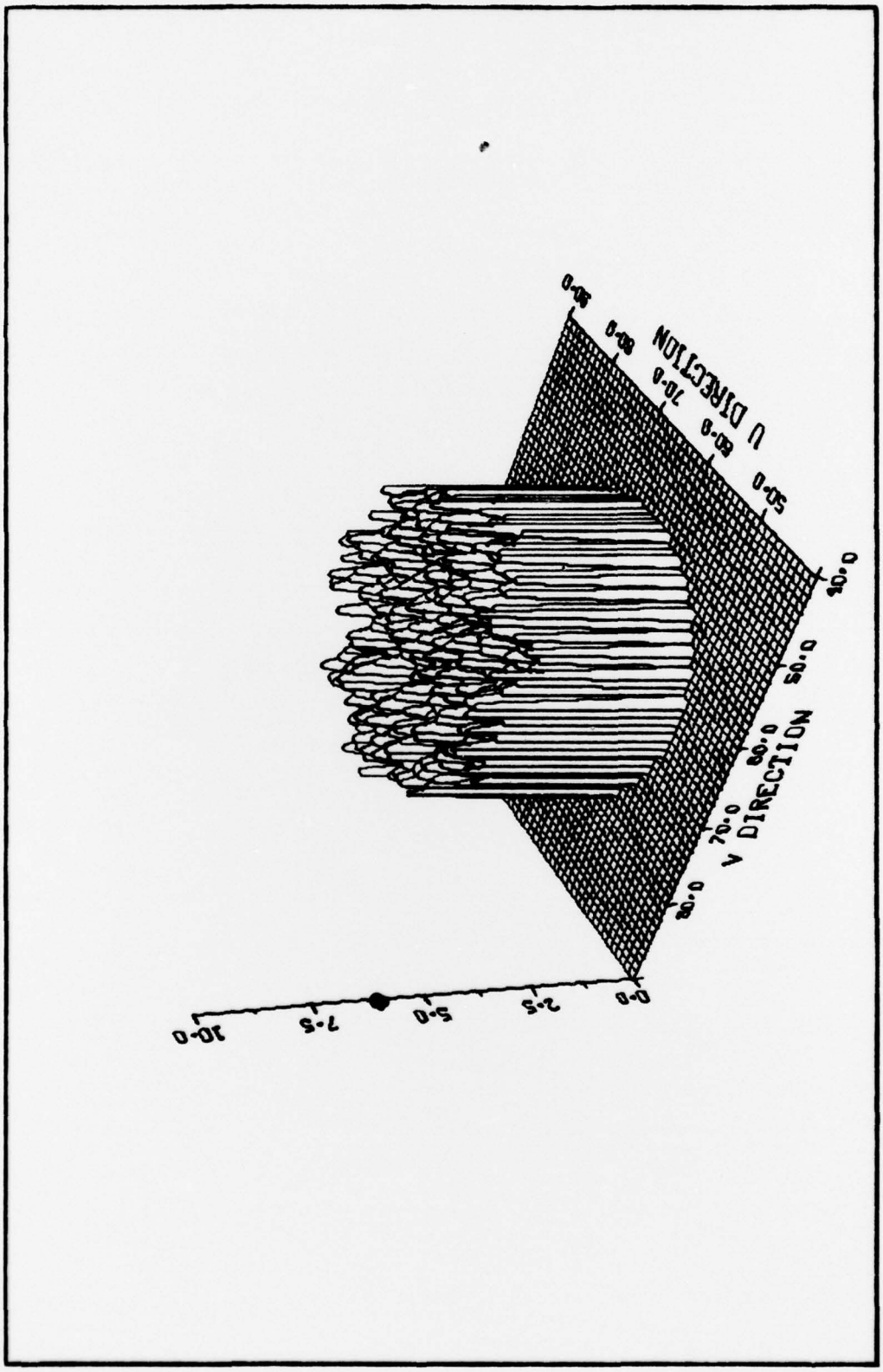

Fig. 70 Normalized Surface Height Distribution

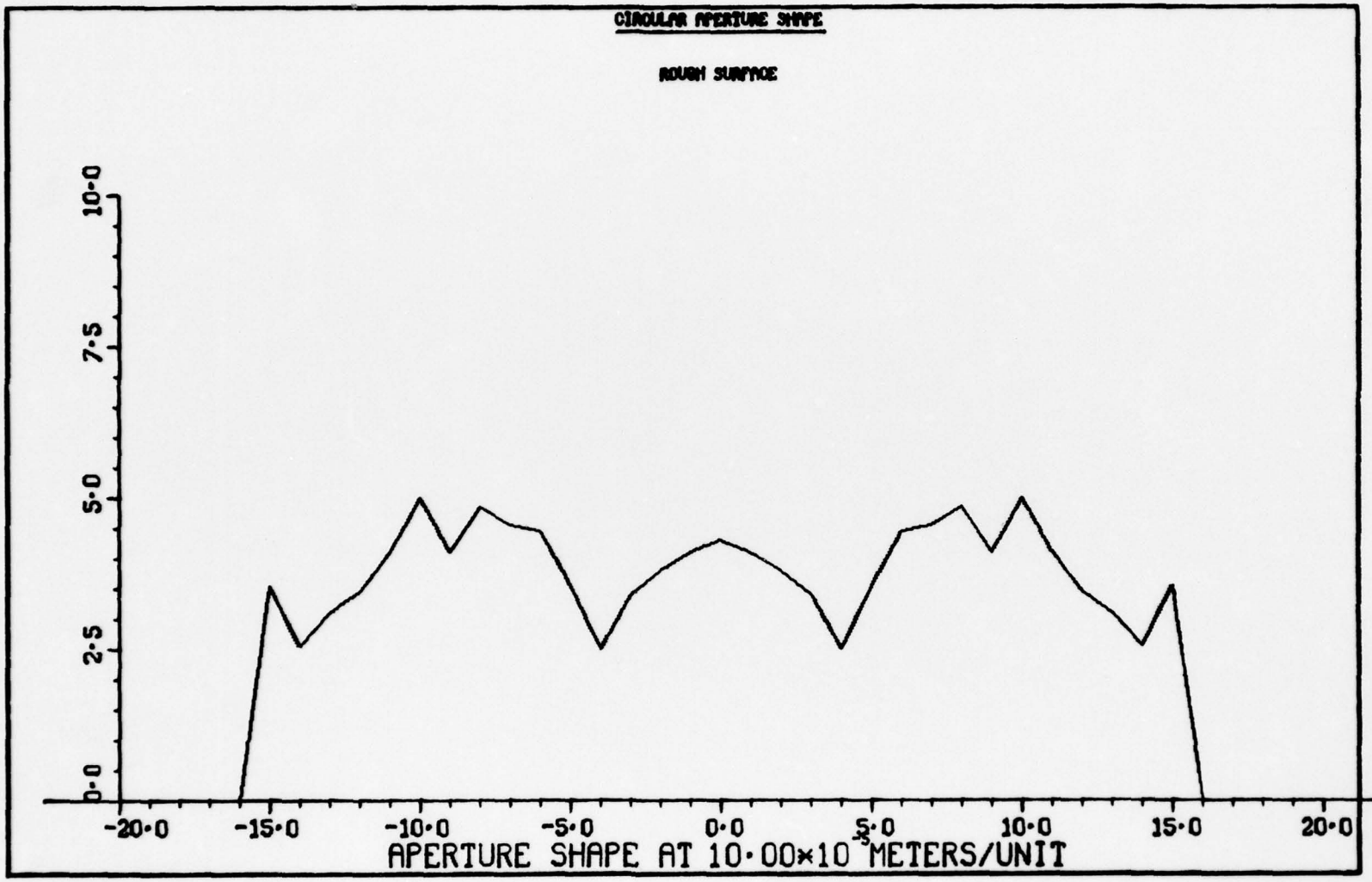

Fig. 71 One Dimensional Cut Through Fig. 70

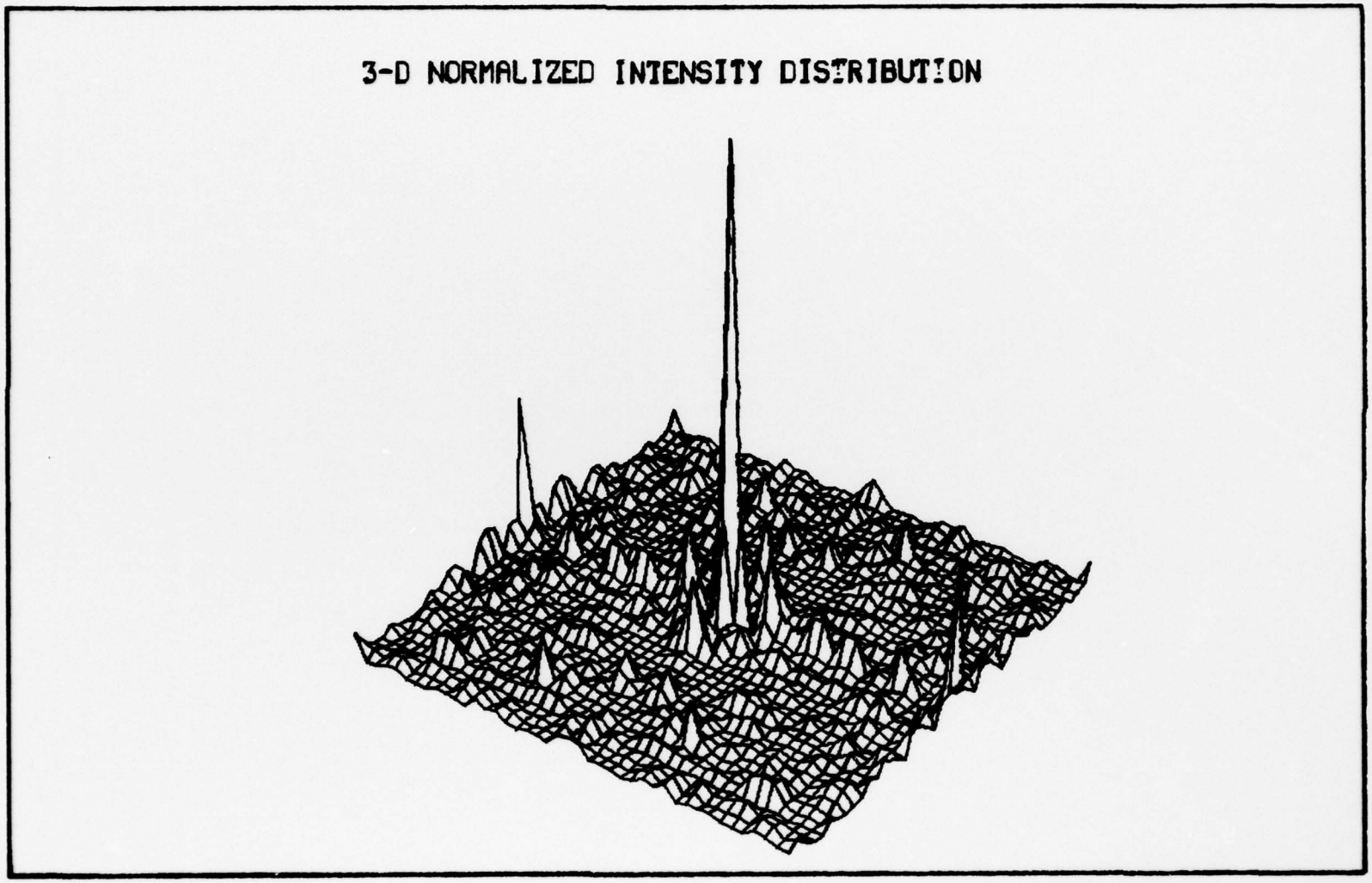

Fig. 72 Three Dimensional Perspective of Speckle Pattern

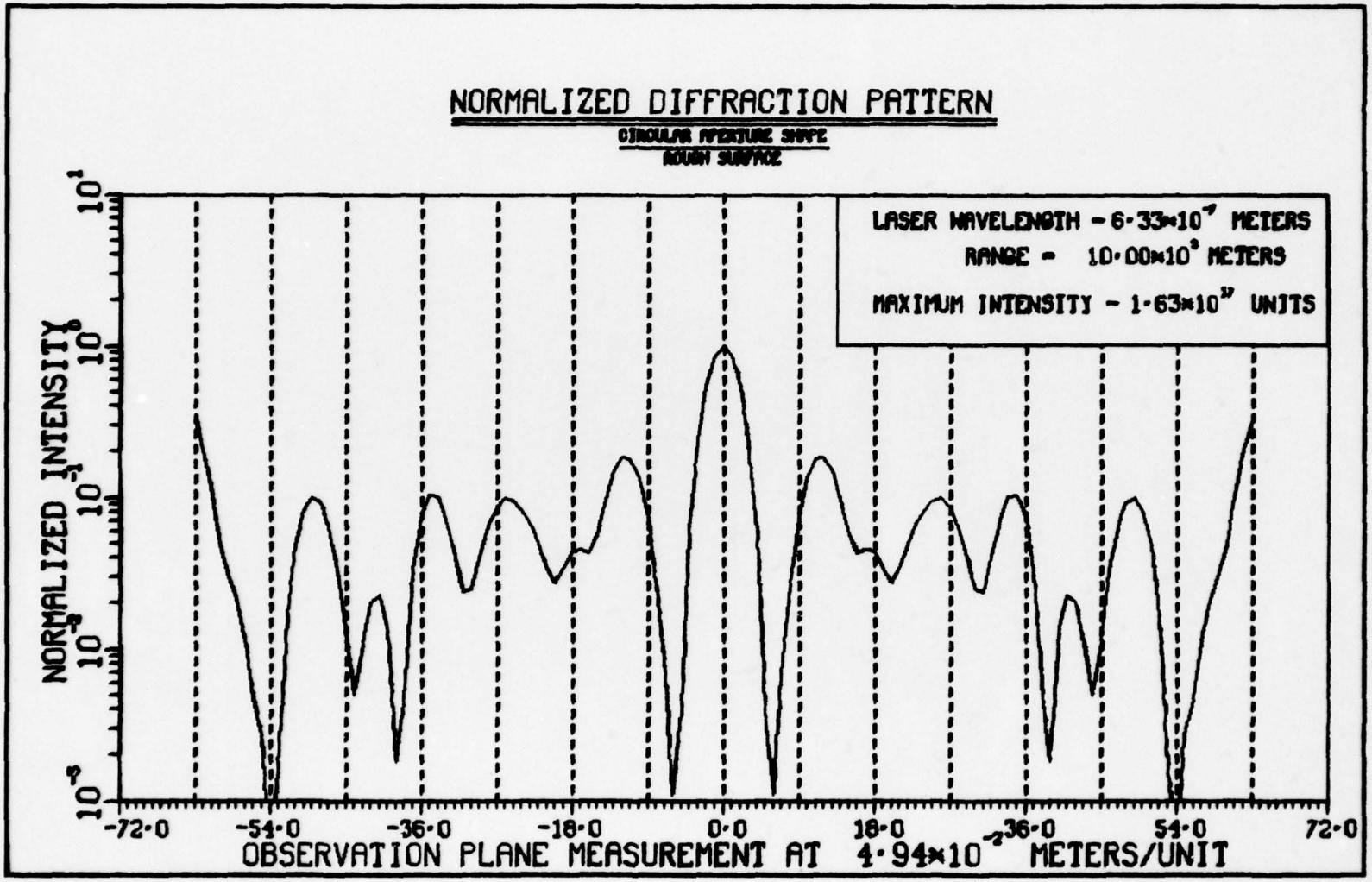

Fig. 73 One Dimensional Cut Through Speckle Pattern

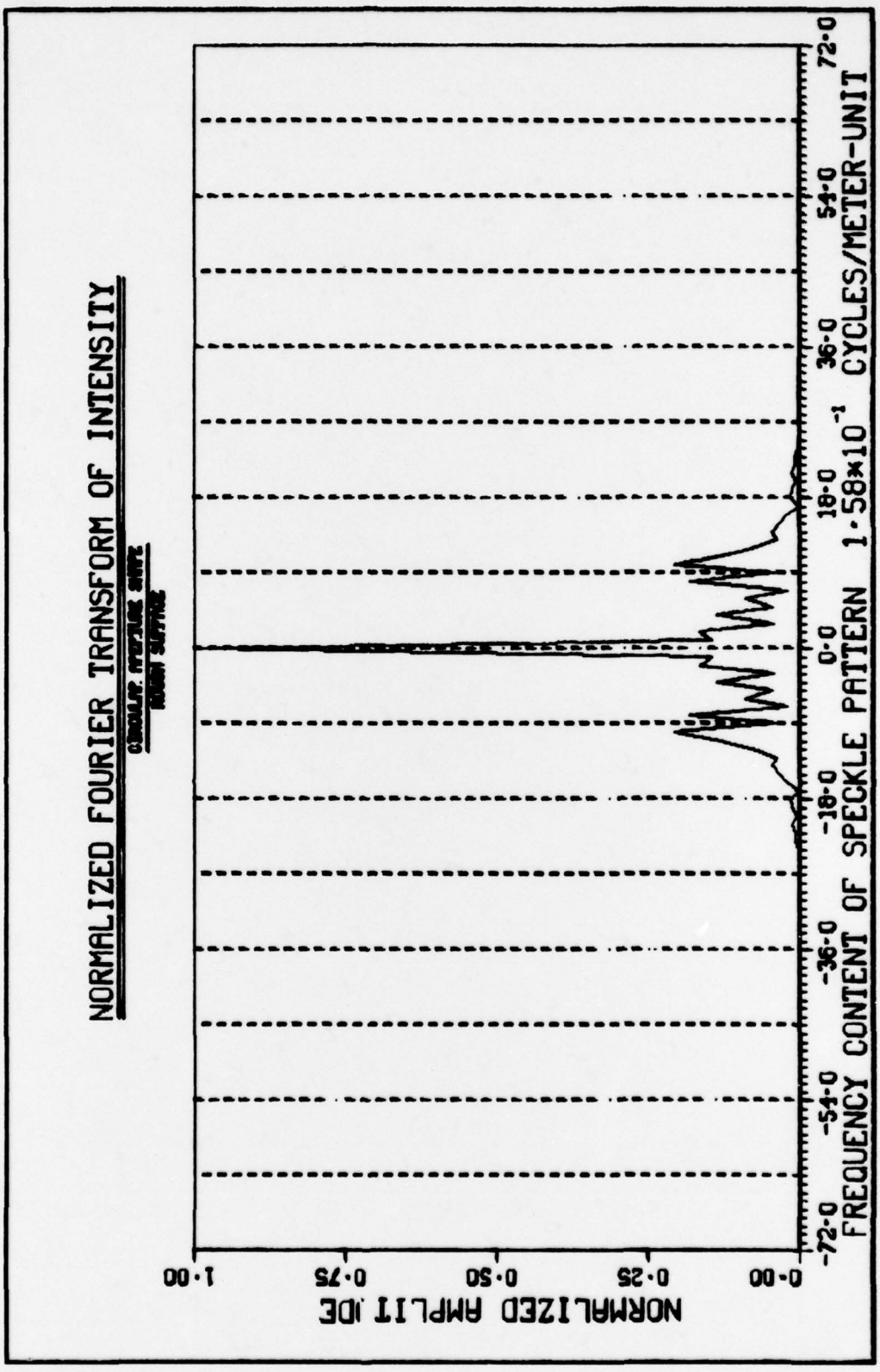

Fig. 74 Fourier Transform of Fig. 73 Data

Vita

William E. Landis was born 28 May 1945 in Somerset, Pennsylvania to Edward M. and Etta Landis. He graduated from Berlin Brothersvalley Joint High School in 1963 and attended Pennsylvania State University from 1963 to 1967, majoring in Aerospace Engineering. In 1967 he enlisted in the United States Air Force. He graduated from Special Electronics School at Lowry AFB, Colorado and was assigned to 1155th Tech. Ops. Squadron, McClellan AFB, California. In June 1970, through AECP he attended the University of Missouri, majoring in Electrical Engineering. In 1972, after graduating from Missouri, he was commissioned a 2nd Lieutenant through OTS. The following three years he was assigned to Offutt AFB, Nebraska in the 544th ARTW as a Radar Systems Engineer. In August of 1975 he was assigned to the Air Force Institute of Technology and is currently working on a Masters of Science Degree in Electro-Optics.

Permanent address: RD#4, Box 180
Berlin, PA 15530

Unclassified

SECURITY CLASSIFICATION OF THIS PAGE (When Data Entered)

REPORT DOCUMENTATION PAGE		READ INSTRUCTIONS BEFORE COMPLETING FORM
1. REPORT NUMBER GEO/EE/77-1 ✓	2. GOVT ACCESSION NO.	3. RECIPIENT'S CATALOG NUMBER
4. TITLE (and Subtitle) Model for Predicting Laser Speckle Patterns Resulting from Rough Surface Scattering		5. TYPE OF REPORT & PERIOD COVERED MS Thesis 6. PERFORMING ORG. REPORT NUMBER
7. AUTHOR(s) William E Landis Capt. USAF		8. CONTRACT OR GRANT NUMBER(s)
9. PERFORMING ORGANIZATION NAME AND ADDRESS Air Force Institute of Technology (AFIT/EN) Wright-Patterson AFB, OH		10. PROGRAM ELEMENT, PROJECT, TASK AREA & WORK UNIT NUMBERS
11. CONTROLLING OFFICE NAME AND ADDRESS Air Force Weapons Laboratory Kirtland AFB NM		12. REPORT DATE March 1977 13. NUMBER OF PAGES 187
14. MONITORING AGENCY NAME & ADDRESS(if different from Controlling Office)		15. SECURITY CLASS. (of this report) Unclassified 15a. DECLASSIFICATION/DOWNGRADING SCHEDULE

16. DISTRIBUTION STATEMENT (of this Report)

Approved for public release; distribution unlimited.

17. DISTRIBUTION STATEMENT (of the abstract entered in Block 20, if different from Report)

18. SUPPLEMENTARY NOTES

Approved for public release; IAW AFR 190-17
Jerral F. Guess, Captain, USAF
Director of Information

19. KEY WORDS (Continue on reverse side if necessary and identify by block number)

Huygens-Fresnel Equation
Diffraction
Rough Surface Scattering
Laser Speckle Pattern
Speckle Patterns
Laser Propagation

20. ABSTRACT (Continue on reverse side if necessary and identify by block number)

Speckle patterns produced by laser radiation scattering from rough surfaces can be calculated and plotted using the SPECKLE program developed in this report. The scattering surface characteristics that are required by the program are; surface height measurements, surface reflection coefficient distribution, and incident laser radiation profile. These three inputs are required to calculate the complex aperture function at the scattering

DD FORM 1 JAN 73 1473 EDITION OF 1 NOV 65 IS OBSOLETE

Unclassified

SECURITY CLASSIFICATION OF THIS PAGE (When Data Entered)

surface, which is Fourier transformed to produce the speckle pattern.

Through experimental investigation and program verification it was determined that the typical speckle width in a pattern is directly related to range and laser wavelength, and inversely related to scattering surface cross section. The highest spatial frequency present in a speckle pattern is proportional to the inverse of the typical speckle width.

The report also showed that the randomness of the scattering surface reflection coefficient also effects the speckle pattern. This is an important concept in camouflage and very important in the investigation of the ALOT system performance.